IL
NUOVO CIMENTO
ORGANO DELLA SOCIETÀ ITALIANA DI FISICA
SOTTO GLI AUSPICI DEL CONSIGLIO NAZIONALE DELLE RICERCHE

VOL. V, N. 3 *Serie decima* 1° Marzo 1957

The Masses of Light Mesons, K-Mesons and Hyperons in 1956 (*).

K. M. CROWE (+)

High-Energy Physics Laboratory, Stanford University - Stanford, Cal.

(ricevuto il 10 Settembre 1956)

Summary. — A number of independent accurate measurements of the masses of light mesons are critically reviewed. Assuming the positive- and negative-charged mesons to have equal masses, best values for the pion and muon masses can be calculated. It is found that the negative π- and μ-mesic X-ray energies measured by K absorption edges can be combined with the mass difference between the positive pion and muon to give a result with a standard deviation approximately one third of the assigned errors of the best previous measurement. All the results are in satisfactory agreement and can be combined in the usual way. The mass results are as follows: $M_\mu = (206.86 \pm 0.11)\, m_e$; $M_\pi = (273.27 \pm 0.11)\, m_e$. Experimental data on the mean lives, spins, parities, and decay modes are also reviewed and the results are given. The measurements of the masses of the various K-mesons are obtained in several ways: $M_{K\pi 2} = (966.0 \pm 1.5)\, m_e$; $M_{K\mu 2} = (965.3 \pm 1.9)\, m_e$; $M_\tau = (966.8 \pm 0.4)\, m_e$. There is at present no evidence for a difference in the masses to a precision of $1 \div 2\, m_e$. Results on the $K^+_{\pi 2}$ and τ^+ masses and lifetimes and the analysis of τ^+ decay are discussed. At present the experimental equality of these particles seems to be contradictory to assigning a spin of less than 2. The cosmic-ray data on the θ^0 lifetime are reviewed and recent results on artificially-produced θ^0's are discussed. The hyperon mass data are reviewed. $M_{\Lambda^0} = (2\,181.74 \pm 0.35)\, m_e$; $M_{\Sigma^0} = (2\,327.4 \pm 1.0)\, m_e$. The latest data on a $\Sigma^+ - \Sigma^-$ mass difference and their mean lives are presented.

(*) Supported by the joint program of the U. S. Office of Naval Research and the U. S. Atomic Energy Commission. Presented at the Turin Conference, 11-th–16-th September 1956.

(+) Now at the University of California Radiation Laboratory, Berkeley, California.

(°) The data used in this review are based on a survey completed in July 1956.

1. – Introduction.

The masses of the unstable particles are measured by several independent methods. The first set of direct determinations is crudely analogous to the methods of the mass spectroscopist: A pair of easily-measured properties is observed simultaneously for each particle. For example, the electromagnetic properties—energy loss, range, curvature in a magnetic field, or multiple-scattering angle—have different functional dependence on the charge, mass, and velocity; and, if the charge is known, the observation of any pair is sufficient to eliminate the velocity and determine the mass. The conservation of charge in all reactions assures that the specific charge of these particles will be an exact multiple of the electronic charge. The velocity can be found directly by, for example, measurement of the time of flight over a known path or determination of the angle of Čerenkov radiation while passing through a medium with a known index of refraction. Combinations of these properties are commonly used to identify a particle, and in a few cases to provide precise mass measurements, even though the total number of these unstable particles that have been observed may be very small.

The second set of mass data is obtained by the study of the kinematics of the decay processes and other reactions that the particle undergo. The Q-value mass determinations are important for the heavier particles, the hyperons.

The third set of mass data is obtained by the study of mesic X-rays. The measurement of the energies of μ- and π-mesic X-rays provides an accurate set of mass limits for the two light mesons.

2. – The Light Mesons.

The mass of the positive pion has been measured in an experiment by Barkas, Birnbaum and Smith [1]. Pions produced by the Berkeley 184 inch synchrocyclotron were analyzed in the cyclotron's magnetic field and came to rest in nuclear emulsions. Their ranges in the emulsion and their momenta were determined accurately from the geometry of the orbits and the magnetic-field intensity. To eliminate the errors arising from the uncertainty of the range-velocity relation in the emulsions, a calibrating bombardment of inelastic protons was scattered into the plates from a second target. The target positions were chosen such that the pions and protons would have the same velocity as they entered the nuclear plates. One can show that to a very good

(1) W. H. Barkas, W. Birnbaum and F. M. Smith: *Phys. Rev.*, **101**, 778 (1956).

approximation,

$$R_p/M_p = R_\pi/M_\pi\,, \quad \text{if} \quad P_\pi/M_\pi = P_p/M_p\,, \tag{2.1}$$

where the R, P and M terms are the mean ranges, momenta, and masses of the proton and pion, respectively (*). By a series of successive approximations, the momentum ratio can be adjusted to the previously estimated mass ratio. The ratio of ranges gives a better mass ratio. The convergence is rapid in practice; only a few trials are necessary. When the correct ratio is approached the dependence on the range-velocity relation vanishes. The absolute magnetic field intensity also cancels to first order. Only the ratio of momenta appears in (2.1). The main limitation on the accuracy of this method comes from the fluctuations in the energy loss that cause the ranges of the particles to straggle about the mean value given by (2.1). The range straggling can be calculated and has been measured for the samples used in this mass measurement: the pions have a measured range straggling standard deviation of $(3.7 \pm 0.4)\%$ and a calculated standard deviation of 3.7%; the proton ranges have a measured standard deviation of $(1.5 \pm 0.3)\%$ and a calculated standard deviation of 1.42%. The final data consisted of 368 positive pions and 60 protons, which yielded a pion mass (+)

$$M_{\pi^+} = (273.34 \pm 0.33)\ \mathrm{m_e}\,. \tag{2.2}$$

(*) To a very good approximation the energy loss in condensed materials is a function of the velocity of a particle. For a particle of velocity $v = \beta c$ and with charge Ze,

$$\mathrm{d}E/\mathrm{d}x = -\,Z^2 f(\beta)\,,$$

where the energy $E = T + Mc^2 = \gamma Mc^2$, and $\gamma = (1-\beta^2)^{-\frac{1}{2}}$. By integrating the energy-loss relation to find the range R for the particle that has an initial energy E, one has

$$R = \int_{Mc^2}^{E} \frac{\mathrm{d}E}{Z^2 f(\beta)} = \frac{Mc^2}{Z^2} \int_0^{\beta} \frac{\gamma^3 \beta\, \mathrm{d}\beta}{f(\beta)} = \frac{M}{Z^2}\, G(\beta)\,.$$

It follows that the quantity R/M is also a function of velocity only, so that for unit charges if $P_\pi/P_\mathrm{n} = M_\pi/M_\mathrm{n}$,

$$\frac{R_p}{M_p} = G(\beta_p) = g\left(\frac{P_p}{M_p}\right) = g\left(\frac{P_\pi}{M_\pi}\right) = \frac{R_\pi}{M_\pi}\,.$$

It therefore follows that if one chooses the momentum ratio in proportion to the estimated mass ratio, one obtains successively better estimates from the ratio of the ranges.

(+) The mass values quoted throughout this article are expressed in electron mass units $\mathrm{m_e}$, since the proton-electron mass ratio is known accurately. Quoted errors are standard deviations wherever possible.

The negative pion was measured relative to the proton:

$$M_{\pi^-} = (272.8 \pm 0.45)\ m_e\ ; \tag{2.3}$$

also, the ratio of the π^+ to π^- masses:

$$M_{\pi^+}/M_{\pi^-} = 1.002\,1 \pm 0.002\,7\ . \tag{2.4}$$

This value, which has already been corrected for the slight difference in stopping power between the positively- and negatively-charged particles, should be quite insensitive to systematic errors. The masses of positive and negative pions are equal within the experimental errors.

The π^+/μ^+ mass ratio has been measured by the method described above to be

$$M_{\pi^+}/M_{\mu^+} = 1.321 \pm 0.003\ . \tag{2.5}$$

The decay at rest of the π^+ meson,

$$\pi^+ \to \mu^+ + \nu\ , \tag{2.6}$$

has also been studied by BARKAS *et al.* [1] by measuring the resulting monoenergetic muons. If one bombards a single target, one observes pions that decay directly into muons in the emulsions. There are also some muons from pions that have stopped in the production target; the muons lose energy leaving the target and their momenta are determined by the cyclotron magnetic field; these muons enter the emulsions and come to rest, and can be selected over a velocity range approaching the velocity of muons from pion decays in the emulsions. The range can be restricted to minimize the error introduced by the uncertainty of the range-velocity relation used. The magnetic field intensity necessary to determine the muon momentum was measured with a nuclear-resonance technique. The final result for the mass difference between the π^+ and μ^+ obtained by this group is

$$M_{\pi^+} - M_{\mu^+} = (66.41 \pm 0.10)\ m_e\ . \tag{2.7}$$

Combining the mass difference (2.7) with the π^+ mass (2.2), one obtains a μ^+ mass value:

$$M_{\mu^+} = (206.93 \pm 0.35)\ m_e\ . \tag{2.8}$$

The π^- mass has been measured by determining the energy of the high-

energy monochromatic γ-ray produced when π^- mesons are captured from rest in hydrogen:

$$\pi^- + p \rightarrow n + \gamma \,. \tag{2.9}$$

The final experiment was an outgrowth of work by PANOFSKY, AAMODT and HADLEY ([2]) on the various capture reactions, and involved the use of a 130 MeV magnetic pair spectrometer. The multi-channel instrument used by CROWE and PHILLIPS ([3]) had a resolution of 1.6% full width at half-maximum. The energy scale was determined by extensive measurements of the magnetic field, including the inhomogeneous fringe field. The main electron and positron orbits were calculated by numerical methods, and the various aberrations due to the finite size of the target—multiple scattering, etc.—were calculated by perturbation methods using a differential analyzer. The π^- mass was found to be

$$M_{\pi^-} = (272.74 \pm 0.40)\, m_e \,. \tag{2.10}$$

The statistical uncertainty, the magnetic field intensity, calculations of orbits and the geometry of the counter array affect the total error approximately equally.

X-rays produced when negative mesons make transitions between various Bohr orbits in the mesic atom have been studied for several reasons. FITCH and RAINWATER ([4]) have studied μ-mesic X-rays in connection with the nuclear charge distribution, and STEARNS *et al.* ([5]), CAMAC *et al.* ([6]), and others have studied π-mesic X-rays to obtain information about the low-energy pion-nucleon interactions. There are a few transitions observed with sufficient intensity between orbits outside the nucleus and yet within the electron orbits, where the uncertainties in these effects—i.e., nuclear interaction, finite nuclear size, and electronic screening—are negligible. The X-rays are produced when a beam of mesons stops in a material, and are detected by a NaI crystal spectro-

([2]) W. K. H. PANOFSKY, R. L. AAMODT and J. HADLEY: *Phys. Rev.*, **81**, 565 (1951).

([3]) K. M. CROWE and R. H. PHILLIPS: *Phys. Rev.*, **96**, 470 (1954).

([4]) V. L. FITCH and J. RAINWATER: *Phys. Rev.*, **92**, 789 (1953).

([5]) M. STEARNS, M. B. STEARNS, S. DEBENEDETTI and L. LEIPUNER: *Phys. Rev.*, **97**, 240 (1955); **96**, 804 (1954); **95**, 1353 (1954); **93**, 1123 (1954); M. B. STEARNS and M. STEARNS: *Phys. Rev.*, **103**, 1534 (1956).

([6]) M. CAMAC, A. D. MCGUIRE, J. B. PLATT and H. J. SCHULTE: *Phys. Rev.*, **88**, 134 (1952); A. D. MCGUIRE, M. CAMAC, M. L. HALBERT and J. B. PLATT: *Phys. Rev.*, **95**, 625 (1954); M. CAMAC, A. D. MCGUIRE, J. B. PLATT and H. J. SCHULTE: *Phys. Rev.*, **99**, 897 (1955); M. CAMAC, H. L. HALBERT and J. B. PLATT: *Phys. Rev.*, **99**, 905 (1955).

meter that has a broad resolution. A series of absorbers is placed between the source and the detector to determine the energy, and a discontinuity of the absorption coefficient is observed. This break occurs as the X-ray energy passes over the K-absorption edge, and the X-ray energy is therefore between the K edges of those abbsorber elements where the break is seen.

TABLE I. – *Mesic X-ray upper and lower limits on the μ^--meson mass.*

Transition	K-absorption edges	Vacuum polarization	Mass limit
C: $2P$-$1S$	below Ir (76.123 ± 0.015) keV	+ 0.38 keV	$\leqslant$ (208.95 ± 0.04) m_e
P: $3D$-$2P$	above Pb (88.015 ± 0.002) keV	+ (0.325 ± 0.016) keV	$\geqslant$ (206.77 ± 0.04) m_e
Si: $4F$-$3D$	above Cd (26.713 ± 0.006) keV	+ 0.045 keV	$\geqslant$ (206.47 ± 0.04) m_e
$\therefore$ (206.77 ± 0.04) $m_e \leqslant M_{\mu^-} \leqslant$ (208.95 ± 0.04) m_e			

The X-rays from μ-mesic transitions in carbon, phosphorus, and silicon were studied by KOSLOV *et al.* [7], and are listed in Table I. The K-absorption edges have been measured accurately. Of most interest is the phosphorus $3D$-$2P$ transition which falls above the lead K edge. This K-absorption edge was measured directly by MACK and CORK [8] in 1927, with an error of ± 0.07%. In order to obtain a better value for this limit, the L edges and the K- lines can be combined to obtain the K-edge energy. The accuracy of the limit is improved over that published by KOSLOV *et al.* [7] and from the table it is seen that the main uncertainty comes from the 5% error conservatively assigned to the vacuum-polarization corrections, which have been calculated by MICKELWAIT and CORBEN [9] and others.

A similar series for pions has been studied by STEARNS *et al.* [5]; the limits they obtain are shown in Table II. In the pion X-ray measurements, all of the other corrections to the point-charge Klein-Gordon energy-level equation are calculated to be negligible. Of special interest are the aluminum and potassium transitions, which almost coincide.

---

(7) S. KOSLOV, V. FITCH and J. RAINWATER: *Phys. Rev.*, **95**, 291, 625 (1954).
(8) J. E. MACK and J. M. CORK: *Phys. Rev.*, **30**, 741 (1927).
(9) A. B. MICKELWAIT and H. C. CORBEN: *Phys. Rev.*, **96**, 1145 (1954).

These two sets of limits for the meson masses can be combined if it is assumed that for both the pion and muon the positively- and negatively-charged mesons have precisely equal masses. As stated before, this assumption is not contradicted by the other measurements. If this assumption is made

TABLE II. – *Mesic X-ray upper and lower limits on the π^--meson mass.*

Transition	*K*-absorption edges	Vacuum Polarization	Mass limit
P: $4F$-$3D$	above Ce (40.440 ± 0.006) keV	+ 0.100 keV	$\geqslant$ (272.2 ± 0.03) m_e
Al: $4F$-$3D$	below Sb (30.489 ± 0.004) keV	+ (0.065 ± 0.003) keV	$\leqslant$(273.51 ± 0.04) m_e
K: $4F$-$3D$	below Hf (65.347 ± 0.003) keV	+ (0.190 ± 0.010) keV	$\leqslant$(273.52 ± 0.04) m_e

$$\therefore\ (272.2 \pm 0.03)\ m_e \leqslant M_{\pi^-} \leqslant (273.51 \pm (0.04)\ m_e$$

TABLE III. – *Pion- and muon-mass summary. Limits obtained from mesic X-rays are compared with other measurements. The π-μ difference has been used to convert pion measurements to muon values, and vice-versa. All errors are standard deviations. Values are quoted in electron mass units* m_e.

π	μ	Method	Ref.
272.2 ±0.03 - 273.51±0.04	205.8 ±0.10 - 207.10±0.11	π-mesic X-rays	(10)
273.18±0.11 - 275.36±0.10	206.77±0.04 - 208.95±0.04	μ-mesic X-rays	(7)
$\therefore$ (273.18±0.11) $\leqslant M_\pi \leqslant$(273.51±0.04) (206.77±0.04) $\leqslant M_\mu \leqslant$(207.10±0.11)			
(π^+) 273.34±0.33	206.93±0.35	plate experiments	(1)
(π^-) 272.8 ±0.45	206.3 ±0.47	plate experiments	(1)
(π^-) 272.74±0.40	206.33±0.41	π^--capture spectrum	(3)
273.34±0.13	206.93±0.13	mesic X-rays (combined)	
273.27±0.11	206.86±0.11	Adopted values	

(10) M. STEARNS, M. B. STEARNS, S. DEBENEDETTI and L. LEIPUNER: *Phys. Rev.*, **95**, 1353 (1954).

and the measured $\pi^+ - \mu^+$ mass difference (2.7) is used, the combined values shown in Table III result. The π- and μ-mesic X-ray measurements are converted into limits for the pion and muon masses, respectively, using the mass difference. The closest limits for each are shown together with their errors. Similarly, the other pion mass measurements can be converted to muon-mass values as shown. The mean value and the standard deviation can be calculated for the mesic X-ray results. A grand average has been computed to obtain the best values of the light-meson masses:

$$M_\mu = (206.86 \pm 0.11)\ m_e\,, \tag{2.11}$$

$$M_\pi = (273.27 \pm 0.11)\ m_e\,. \tag{2.12}$$

The size of the standard deviation in these best values arises mainly from the separation between the mesic X-ray limits.

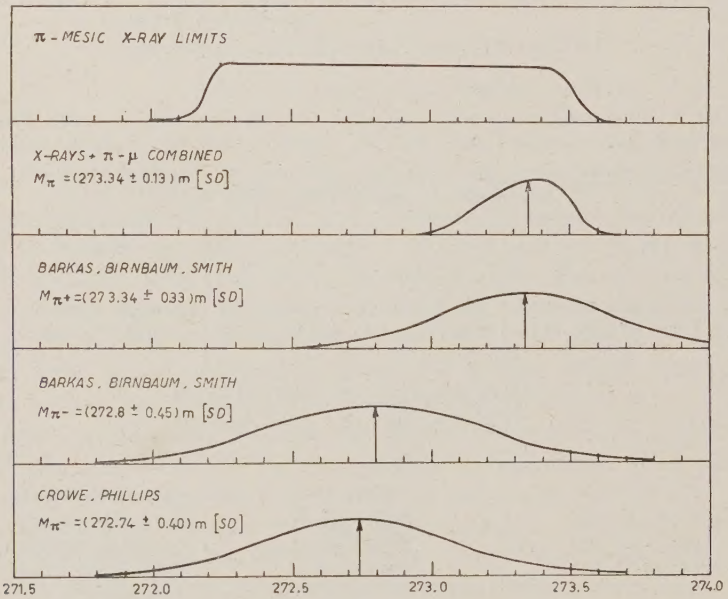

Fig. 1. – Graphical summary of data on the mass of the pion.

Fig. 1 summarizes graphically the pion-mass data. The π-mesic X-ray limits with their uncertainties are shown first. The μ-mesic X-ray limits, using the $\pi - \mu$ difference, appear next. The three other pion-mass measurements are seen to be in good agreement with the mesic X-ray results. To repeat,

however: the main assumption underlying this analysis is that of precise mass equality of positive and negative mesons.

The mass of the neutral pion has been obtained from the π^- capture from rest:

$$\pi^- + \mathrm{p} \to \pi^0 + \mathrm{n} \qquad (2.13)$$
$$\downarrow$$
$$2\gamma \ .$$

The kinetic energy of the π^0 is related to the mass difference between the π^- and π^0. PANOFSKY *et al.* [2] have measured the Doppler shift of the π^0 γ-rays. The mass difference they obtained is

$$M_{\pi^-} - M_{\pi^0} = (10.6 \pm 3.0)\ \mathrm{m_e} \ . \qquad (2.14)$$

CHINOWSKY and STEINBERGER [11] have measured the velocity of the π^0 by observing the angular aberration of the γ-rays. The mass difference they obtained is

$$M_{\pi^-} - M_{\pi^0} = (8.8 \pm 0.6)\ \mathrm{m_e} \ . \qquad (2.15)$$

Combining these two measurements with the best pion mass value (2.11) gives a π^0 mass value:

$$M_{\pi^0} = (264.37 \pm 0.60)\ \mathrm{m_e} \ . \qquad (2.16)$$

Measurements of the mean lives of the light mesons have been made by many experimenters. The most recent and accurate measurement of the mean life of the muon was made by BELL and HINCKS [12] using an electronic delayed-coincidence method recording the delay between a cosmic-ray muon and the decay positron:

$$\mu^+ \to \beta^+ + \nu + \nu \ . \qquad (2.17)$$

They obtained a mean life for the positive muon of

$$\tau_{\mu^+} = (2.22 \pm 0.02) \cdot 10^{-6}\ \mathrm{s} \ . \qquad (2.18)$$

The mean life of the negative muon depends on the material in which it stops due to the competition of the nuclear capture with the free decay. The free-

---

[11] W. CHINOWSKY and J. STEINBERGER: *Phys. Rev.*, **95**, 1561 (1954).
[12] W. E. BELL and E. P. HINCKS: *Phys. Rev.*, **84**, 1243 (1951).

decay rate of the μ^- is equal to the rate for the μ^+ within the error of measurement ($\sim 4\%$); this was also measured by BELL and HINCKS ([18]).

The more recent mean-life measurements for the π^+ and π^- mesons are

TABLE IV. – *Pion mean lifetime.*

Value ($\cdot 10^{-8}$ s)	Method	Ref.
$\tau_{\pi^+} = 1.65 \pm 0.33$ $\tau_{\pi^+} = 2.53 \pm 0.10$	Delayed coincidences; 57 events (preliminary) Differential data; 670 events	([14])
$\tau_{\pi^+} = 2.60 \pm 0.13$ $\tau_{\pi^+} = 2.56 \pm 0.14$	Delayed coincidences; 1277 pulses (integral data) Differential data; 557 pulses	([15])
$\tau_{\pi^+} = 2.54 \pm 0.11$	Delayed coincidences; 541 counts (background $\sim 20\%$ minimum)	([16])
$\tau_{\pi^-} = 2.72 \pm 0.25$ $\tau_{\pi^+} = 2.70 \pm 0.30$	Cloud chamber; ~ 188 events $\tau_{\pi^-}/\tau_{\pi^+} = 1.01 \pm 0.14$	([17])
$\tau_{\pi^-} = 2.55 \pm 0.19$ $\tau_{\pi^+} = 2.44 \pm 0.18$	Decay over variable path $\tau_{\pi^-}/\tau_{\pi^+} = 1.04 \pm 0.11$	([18])
$\tau_{\pi^\pm} = 2.56 \pm 0.05$	Average	

summarized in Table IV. The methods of measurement include electronic delayed coincidence, cloud-chamber observation of decays in flight, and experiments using counters. The earlier nuclear-plate results are not included because of the difficulty in evaluating the observer losses evidently present in the data. An average of the quoted measurements gives a mean life

$$\tau_{\pi^\pm} = (2.56 \pm 0.05) \cdot 10^{-8} \text{ s} . \tag{2.19}$$

Again, there is no evidence for any difference in the mean lives of the positive and negative pions.

([13]) W. E. BELL and E. P. HINCKS: *Phys. Rev.*, **88**, 1424 (1952).

([14]) W. L. KRAUSHAAR, J. E. THOMAS and V. P. HENRI: *Phys. Rev.*, **78**, 486 (1950); W. L. KRAUSHAAR: *Phys. Rev.*, **86**, 513 (1952).

([15]) O. CHAMBERLAIN, R. F. MOZLEY, J. STEINBERGER and C. E. WIEGAND: *Phys. Rev.*, **79**, 394 (1950); C. E. WIEGAND: *Phys. Rev.*, **83**, 1085 (1951).

([16]) M. JAKOBSON, A. SCHULZ and J. STEINBERGER: *Phys. Rev.*, **81**, 894 (1951).

([17]) L. LEDERMAN, E. T. BOOTH, H. BYFIELD and J. KESSLER: *Phys. Rev.*, **83**, 685 (1951).

([18]) R. P. DURBIN, H. H. LOAR and W. W. HAVENS: *Phys. Rev.*, **88**, 179 (1952).

The neutral pion decays $(1.45^{+0.80}_{-0.45})$ % of the time via the reaction

$$\pi^0 \to e^+ + e^- + \gamma \,. \tag{2.20}$$

as measured by LINDENFELD, SACHS and STEINBERGER [19]. By tracing narrow-angle pairs to their origin, ANAND [20] has measured the gaps between the parent star and the pair origin to obtain a distribution corresponding to a mean life as follows:

$$\tau_{\pi^0} = (5.0^{+5}_{-2}) \cdot 10^{-15} \text{ s} \,. \tag{2.21}$$

He calculated from the data that the probability of the π^0 mean life being zero is less than 0.1%.

3. – The Heavy Mesons.

The τ-meson (tauon) decays into three pions by the reaction

$$\tau^{\pm} \to \pi^{\pm} + \pi^+ + \pi^- \,. \tag{3.1}$$

The τ mass can be found accurately by measuring the Q-value of the τ decay from rest. The nuclear-emulsion results are obtained by measuring the ranges of the three pions when they come to rest within the stack of stripped emulsions. The stack exposed to the $K^{\pm}$ beam of the Bevatron can be carefully controlled; the density, moisture content, and shrinkage are known accurately, and the range-velocity relation has been measured accurately over the range of energies occurring in the decay. Results of HADDOCK [21] and of BARKAS *et al.* [22] can be combined to give

$$Q_{\tau^+} = (75.11 \pm 0.14) \text{ MeV} \,. \tag{3.2}$$

Using the best pion-mass value (2.12), this Q-value gives a τ^+ mass:

$$M_{\tau^+} = (966.80 \pm 0.43)\, m_e \,. \tag{3.3}$$

---

[19] P. LINDENFELD, A. SACHS and J. STEINBERGER: *Phys. Rev.*, **89**, 531 (1953).
[20] B. M. ANAND: *Proc. Roy. Soc.* (*London*), A **220**, 183 (1953).
[21] R. P. HADDOCK: *Nuovo Cimento.*, **4**, 240 (1956).
[22] W. H. BARKAS, H. H. HECKMAN and F. M. SMITH: *Bull. Am. Phys. Soc.*, Ser. II, **1**, 184 (1956); H. H. HECKMAN, F. M. SMITH and W. H. BARKAS: *University of California Radiation Laboratory Report No. UCRL-3291*, to be published in *Nuovo Cimento*.

The τ^+ decay is of interest also because the distribution of energy between the pions and the angular correlations can be analyzed to yield the spin and parity of the tauon ([23]). The θ or χ meson decays into two pions, so that the spin and parity assignment of the θ-meson is restricted to $0+$, $1-$, $2+$, $3-$, etc. From the analysis of the tauon decay ([21]), the relative probabilities of various assignments are summed up as follows: $0+$ is forbidden since the pion is known to be a pseudoscalar: $1-$ and $2+$ are extremely improbable; and even $3-$ and $4+$ are relatively unlikely. Of the states that cannot decay into two pions, $0-$ is likely, $1+$ is unlikely; whereas $2-$ and $3+$ and higher states are satisfactory. Therefore, if the spin of the tauon is less than 4, the τ and K_{π_2} cannot decay from the same state; if the spin is less than 2, the tauon is a pseudoscalar ($0-$) (*).

The masses of the other K^+ mesons have been compared to that of the tauon in a range-momentum analysis similar to that used for the pion-mass ratios discussed at the beginning of Sect. 2. The Q-values of the K_{π_2} and K_{μ_2} decays have been measured accurately. Table V is a summary of work done on the mass differences of the various K-mesons. The results are combined, and the K_{π_2} and K_{μ_2} masses are seen to be equal to the tauon mass within the error of $\sim 2\ m_e$.

The K^- mesons have been compared to the K^+ mesons. WEBB *et al.* ([25]) have obtained the ratio

$$M_{K^-}/M_{K^+} = (0.998 \pm 0.013)\,. \tag{3.4}$$

The neutral K-meson, the θ^0, has been observed to decay into two pions with a Q-value measured by THOMPSON ([26]) to be (+)

$$Q_{\theta^0} = (214.0 \pm 2.5)\ \text{MeV}\,, \tag{3.5}$$

([23]) R. H. DALITZ: *Phil. Mag.*, **44**, 1068 (1953); *Phys. Rev.*, **94**, 1046 (1954); E. FABRI: *Nuovo Cimento*, **11**, 479 (1954); E. FABRI and B. F. TOUSCHEK: *Nuovo Cimento*, **11**, 96 (1954).

([24]) See references ([21]) and ([22]), and D. M. RITSON, A. ODIAN, B. T. FELD and A. WATTENBERG: *Phys. Rev.*, **100**, 1263 (1955); J. OREAR, G. HARRIS and S. TAYLOR: *Phys. Rev.*, **102**, 1676 (1956); G. COSTA and L. TAFFARA: *Nuovo Cimento*, **3**, 169 (1956); R. H. DALITZ: *Proceedings of the Sixth Rochester Conference* New York, (1956), and private communication.

(*) The analysis of the decay energy and angular distributions is based on a phase-space calculation, and only the presence of excessively large pion-pion interactions would alter the conclusions.

([25]) F. H. WEBB, W. W. CHUPP, G. GOLDHABER and S. GOLDHABER: *Phys. Rev.*, **101**, 1212 (1956).

([26]) R. W. THOMSPON, J. R. BURWELL and R. W. HUGGETT: to be published.

(+) The error here is the measured external standard deviation and the known systematic uncertainties; the probable error quoted by THOMPSON is ± 5.0, which includes a conservative estimate of the unknown systematic errors.

corresponding to a mass value:

$$M_{\theta^0} = (965.1 \pm 5.0)\, m_e \; ; \tag{3.6}$$

this value is equal to the mass value of the charged K-mesons within its error.

TABLE V. – *Masses of* K *particles relative to the tauon mass. Values shown are* $M_K - M_\tau$ *Standard deviations are given.*

Particle	From Q-values	Ref.	From range-momentum	Ref.	Combined
K_{μ_2}	-4.0 ± 6.0	(27)	$+1.2 \pm 2.9$	(28)	
	-2.0 ± 3.4	(28)			
	-4.0 ± 6.1	(29)	$+1.8 \pm 5.9$	(31)	
	-11.8 ± 4.8	(30)			
Average	-4.6 ± 2.9		$+1.1 \pm 2.6$		-1.45 ± 1.9
K_{π_2}	$+1.5 \pm 4.0$	(27)	$+0.2 \pm 2.8$	(28)	
	-2.6 ± 2.3	(28)			
	-4.1 ± 4.0	(29)	$+0.0 \pm 7.9$	(31)	
	$+4.3 \pm 4.5$	(30)			
Average	-1.5 ± 2.2		$+0.2 \pm 2.7$		-0.83 ± 1.7
τ'	. . . . .		-4.4 ± 15.6	(31)	. . . . .
K_{μ_2}	. . . . .		$+1.0 \pm 5.8$	(28)	-1.2 ± 5.2
			-11.8 ± 15.6	(31)	
K_{β_2}	. . . . .		-3.3 ± 10	(28)	-8.7 ± 6.4
			-14.9 ± 8.5	(31)	

(27) G-STACK-COLLABORATION: *Nuovo Cimento*, **2**, 1063 (1955).

(28) R. W. BIRGE, R. P. HADDOCK, L. T. KERTH, J. R. PETERSON, J. SANDWEISS, D. H. STORK and M. N. WHITEHEAD: *Phys. Rev.*, **99**, 329 (1955); R. W. BIRGE, J. R. PETERSON, D. H. STORK and M. N. WHITEHEAD: *Phys. Rev.*, **100**, 430 (1955); M. N. WHITEHEAD *et al.*: *Bull. Am. Phys. Soc.*, Ser. II, **1**, 184 (1956); R. W. BIRGE, M. N. PERKINS, J. R. PETERSON, D. H. STORK and M. N. WHITEHEAD: *Nuovo Cimento*, **4**, 834 (1956).

(29) S. FUNG, A. PEVSNER, D. RITSON and N. MOHLER: *Phys. Rev.*, **101**, 493 (1956); D. RITSON, A. PEVSNER, S. FUNG, M. WIDGOFF, G. T. ZORN, S. GOLDHABER and G. GOLDHABER: *Phys. Rev.*, **101**, 1085 (1956).

(30) J. CRUSSARD, V. FOUCHÉ, J. HENNESSY, G. KAYAS, L. LEPRINCE-RINGUET, D. MORELLET and F. RENARD: *Nuovo Cimento*, **3**, 731 (1956).

(31) H. H. HECKMAN, F. M. SMITH and W. H. BARKAS: *Nuovo Cimento*, **3**, 85 (1956); *Phys. Rev.*, **100**, 1802, 1803 (1956).

TABLE VI. – K-*meson lifetimes-accelerator measurements.*

Particle	Mean life $\cdot 10^{-9}$ s	Method	Ref.
$K^+_{\pi_2}$	13 ± 2	Electronic	(32)
$K^+_{\mu_2}$	14 ± 2	Electronic	(32)
$K^+_{\mu_2}$	$11.7^{+0.8}_{-0.7}$	Electronic	(33)
$K^+_{\pi_2}$	$12.1^{+1.1}_{-1.0}$	Electronic	(33)
τ^+	$12.7^{+1.2}_{-2.0}$	Electronic	(34)
K^-	$9.5^{+3.6}_{-2.5}$	Plates, decay in flight	(35)
K^+	$10.1^{+3.3}_{-2.1}$	Plates, decay in flight	(36)

The mean lives of the various charged K-mesons have been measured to be equal within the error of 10-20%, as shown in Table VI. The mean life of the neutral K-meson has been measured in several cloud-chamber studies:

TABLE VII. – θ^0 *lifetime—cloud-chamber measurements.*

Number of events	Mean life $\cdot 10^{-10}$ s	Method	Ref.
6	$0.9^{+1.6}_{-0.3}$	Cosmic rays	(37)
8	$0.6^{+0.4}_{-0.2}$	Cosmic rays	(38, 39)
14	$0.7^{+0.3}_{-0.2}$	Cosmic rays	(40)
29	$0.8^{+0.3}_{-0.2}$	Cosmotron	(41)
52	0.6 ± 0.1	Cosmic rays	(42)
Average	$0.66^{+0.11}_{-0.07}$		

(32) L. W. ALVAREZ, F. S. CRAWFORD, M. L. GOOD and M. L. STEVENSON: *Phys. Rev.*, **101**, 503 (1956); **100**, 1264 (1955).

(33) V. FITCH and R. MOTLEY: *Phys. Rev.*, **101**, 496 (1956).

(34) V. L. FITCH: *Bull. Am. Phys. Soc.*, Ser. II, **1**, 52 (1956); *Proceedings of the Sixth Annual Rochester Conference* (1956), *op. cit.*

(35) E. L. ILOFF *et al.*: *Phys. Rev.*, **102**, 927 (1956).

(36) E. L. ILOFF, W. W. CHUPP, G. GOLDHABER, S. GOLDHABER, J. L. LANNUTTI, A. PEVSNER and D. RITSON: *Phys. Rev.*, **99**, 1617 (1955).

(37) H. S. BRIDGE, C. PEYROU, B. ROSSI and R. SAFFORD: *Phys. Rev.*, **91**, 362 (1953).

(38) D. B. GAYTHER: *Phil. Mag.*, **45**, 570 (1954).

(39) D. B. GAYTHER: *Phil. Mag.*, **46**, 1362 (1955).

(40) D. I. PAGE: *Phil. Mag.*, **46**, 103 (1955).

(41) H. BLUMENFELD, E. T. BOOTH, L. M. LEDERMAN and W. CHINOWSKY: *Phys. Rev.*, **102**, 1184 (1956).

(42) I. C. GUPTA, A. L. SNYDER and W. Y. CHANG: *Bull. Am. Phys. Soc.*, Ser. II, **1**, 186 (1956).

the recent data are summarized in Table VII (*). The average value of the mean lifetimes obtained here is considerably shorter than the value quotes previously ([39]). The result relies mainly on the PURDUE result ([42]) (+). The results of accelerator studies obtained with counters are not complete at this time.

The present status of K-meson studies can be summarized as follows: The masses of the τ and the K_{τ_2} are equal within a few parts in a thousand. The mean lives are also equal within $\pm 15\%$. The tauon decay indicates that if the spin of the τ is less than 4, the K_{τ_2} cannot be an alternate mode of decay of the τ. The various theories or schemes proposed to explain this paradoxical situation will not be discussed here ([43]) (×). The data for the less frequent K-meson decay modes are increasing rapidly, and already data on the interaction of K-mesons with nuclei are accumulating.

4. – Hyperons.

The Λ^0 decay has been observed many times in cloud chambers and nuclear emulsions:

$$\Lambda^0 \to p + \pi^- . \tag{4.1}$$

The data on the Q-values for this decays from the chamber measurements ([44])

(*) The earlier data have been omitted due to possible observational bias. The errors quoted are almost entirely statistical.

(+) Recent results by BUDDE, LEITNER, SAMIOS, SCHWARTZ and STEINBERGER (to be published) and counter results by RIDGWAY, BERLEY and COLLINS (to be published) and J. E. OSHER (to be published) do not confirm this mean lifetime. Likewise, the results of LANDE, BOOTH, IMPEDUGLIA, LEDERMAN and CHINOWSKY (to be published) and FITCH and PANOFSKY (to be published) indicate a complex decay of the neutral θ. Thus this average lifetime must be regarded cautiously.

([43]) S. A. BLUDMAN: *Phys. Rev.*, **102**, 1420 (1956); T. D. LEE and C. N. YANG: *Phys. Rev.*, **102**, 290 (1956); J. SCHWINGER: *Phys. Rev.*, **104**, 1164 (1956).

(×) LEE and YANG [*Phys. Rev.*, **104**, 254 (1956), and to be published] have suggested that one explanation of the τ-θ paradox might well be that parity is *not* conserved in the decay. Recent experimental results by WU, AMBLER, HAYWARD, HOPPES and HUDSON (to be published) on β-decay of ^{60}Co, and of GARWIN, LEDERMAN and WEINRICH (to be published) on π-μ-β decay show that parity is not conserved in these reactions.

([44]) W. B. FRETTER, M. M. MAY and M. P. NAKADA: *Phys. Rev.*, **89**, 168 (1953); W. H. ARNOLD JR., W. MARTIN and H. W. WYLD: *Phys. Rev.*, **100**, 1545 (1955); R. W. THOMPSON, A. V. BUSKIRK, L. R. ETTER, C. J. KARZMARK and R. H. REDIKER: *Phys. Rev.*, **90**, 329 (1953); R. ARMENTEROS, K. H. BARKER, C. C. BUTLER, M. S. COATES and M. G. SOWERBY: *Phil. Mag.*, **44**, 861 (1953); E. W. COWAN, quoted by R. W. THOM-

and the emulsion studies ([45]) are in good agreement, and have been combined to give a best value,

$$Q_{\Lambda^0} = (36.97 \pm 0.16)\ \text{MeV}\,, \tag{4.2}$$

and a corresponding best mass value,

$$M_{\Lambda^0} = (2\,181.74 \pm 0.35)\ \text{m}_e\,. \tag{4.3}$$

Table VIII summarizes the Λ^0 mean-life data, which have been combined to yield an average value

$$\tau_{\Lambda^0} = (3.4 \pm 0.3)\cdot 10^{-10}\ \text{s}\,. \tag{4.4}$$

The Σ^- mesons decay into π^- mesons and a neutron. The Σ^+ also decays

TABLE VIII. – *Lifetime measurements of the* Λ^0.

Number of events	Mean life $\cdot 10^{-10}$ s	Ref.
37 ($0 < Q < 50$ MeV)	2.9 ± 0.8	([46])
21	3.5 ± 1.2	([37])
22	$4.8\ ^{+2.6}_{-1.3}$	([47])
21	$4.0\ ^{+3.7}_{-1.2}$	([38])
26	$3.7\ ^{+3.9}_{-1.3}$	([48])
23	$3.6\ ^{+1.1}_{-0.7}$	([49])
65	$2.8\ ^{+0.5}_{-0.4}$	([41])
52	$3.6\ ^{+0.8}_{-0.5}$	([42])
Average	3.4 ± 0.3	

PSON: *Summary of Section A on the Properties of the Heavy Unstable Particles, International Conference on Elementary Particles, Pisa* (1955); W. A. VAN LINT, G. H. TRILLING, R. B. LEIGHTON and C. D. ANDERSON: *Phys. Rev.*, **95**, 295 (1954); see also references ([37]) and ([41]).

([45]) M. W. FRIEDLANDER: *Proceedings of the Sixth Annual Rochester Conference op. cit.*; R. R. DANIEL and D. LAL: *Proc. Indian Acad. Sci.*, **41**, 15 (1955); M. W. FRIEDLANDER, D. KEEFE, M. G. K. MENON and M. MERLIN: *Phil. Mag.*, **45**, 533 (1954).

([46]) R. B. LEIGHTON and W. L. ALFORD: *Phys. Rev.*, **92**, 540 (1953); **90**, 622 (1953).

([47]) M. DEUTSCHMANN, quoted by GAYTHER ([39]).

([48]) D. I. PAGE and J. A. NEWTH: *Phil. Mag.*, **45**, 38 (1954).

([49]) D. I. PAGE: *Phil. Mag.*, **45**, 863 (1954).

via the reaction

$$\Sigma^+ \to p + \pi^0 . \tag{4.5}$$

By measuring the proton range in nuclear emulsions, FRY ([50]) has been able to obtain an accurate measure of the Q for the reaction:

$$Q_{\Sigma^+(p,\pi^0)} = (116.08 \pm 0.47)\ \text{MeV} ; \tag{4.6}$$

from this the Σ^+ mass is found to be

$$M_{\Sigma^+} = (2327.4 \pm 1.0)\ m_e . \tag{4.7}$$

The Σ^- hyperon has been produced by K^- mesons on hydrogen:

$$K^- + p \to \Sigma^\pm + \pi^\mp . \tag{4.8}$$

CHUPP *et al.* ([51]) have observed in nuclear emulsions several such events produced by K^- mesons which are, from the colinearity, probably captured at rest on hydrogen. Assuming the K^- mass to be the same as the τ^+ mass, the Σ^- mass can be calculated to be

$$M_{\Sigma^-} = (2338 \pm 4)\ m_e . \tag{4.9}$$

STEINBERGER *et al.* ([52]) report a Σ^- mass measurement for a Σ hyperon produced in a π^--meson beam of well-defined energy, via the reaction

$$\pi^- + p \to \Sigma^- + K^+ . \tag{4.10}$$

The event was observed in a propane bubble chamber (no magnetic field). The Σ^- decayed in flight and the π^- stopped. The angles and ranges were measured, and the Q-value can be calculated to be

$$Q_{\Sigma^-(\pi^-,n)} = (118 \pm 2.6)\ \text{MeV} ; \tag{4.11}$$

([50]) W. F. FRY, J. SCHNEPS, G. A. SNOW and M. S. SWAMI: *Phys. Rev.*, **103**, 226 (1956).

([51]) W. W. CHUPP, G. GOLDHABER, S. GOLDHABER and F. H. WEBB: to be published in *Suppl. Nuovo Cimento*.

([52]) M. CHRÉTIEN, J. LEITNER, N. SAMIOS, M. SCHWARTZ and J. STEINBERGER: *Bull. Am. Phys. Soc.*, Ser. II, **1**, 185, 186 (1956); *Proceedings of the Sixth Annual Rochester Conference* (1956), *op. cit.*.

this Q-value gives a Σ^- mass:

$$M_{\Sigma^-} = (2\,343 \pm 5.2)\ m_e\ . \tag{4.12}$$

These two measurements indicate a mass difference between the Σ and Σ' hyperons from entirely different and independent assumptions. The values have been combined to give a best mass value for the Σ^- (*):

$$M_{\Sigma^-} = (2\,340 \pm 3.2)\ m_e\ . \tag{4.13}$$

The lifetime data obtained in emulsion studies on the Σ particles are complicated since in the mesonic decay the charge of the Σ hyperon is seldom known because of the long range of the pion. A mean life for an unknown mixture of Σ^+ and Σ' hyperons decaying in flight has been reported by FRY ([53]):

$$\tau_{\Sigma(+\text{ and }-)} = (0.34^{+0.14}_{-0.08})\cdot 10^{-10}\ \text{s}\ . \tag{4.14}$$

The Σ particles observed in the bubble-chamber study ([52]) are believed to consist of Σ^-'s only, since according to the tentative theory, the $(\Sigma^+ + K^-)$ process would be a violation of a « strangeness » selection rule. This selection rule has been successful in predicting a number of observed reactions, and no exceptions have been found. The mean life of these Σ hyperons is

$$\tau_{\Sigma^-} = (1.4^{+1.6}_{-0.5})\cdot 10^{-10}\ \text{s}\ . \tag{4.15}$$

It is seen that the mean-life measurements differ significantly, and this is interpreted as indicating that the Σ^+ and Σ^- lifetimes differ by at least three. The actual mean-life value of the Σ^+ will depend on the mixture ratio of Σ^+'s and Σ''s, which is not known (+). It is difficult to estimate the extent

(*) Recent results by BARKAS *et al.* (to be published), GILBERT, VIOLET and WHITE (private communication), CHUPP, GOLDHABER, GOLDHABER and WEBB (to be published), and FREDEN and TICHO (private communication), when combined, give Σ masses:

$$M_{\Sigma^+} = (2\,328.3 \pm 0.5)\ m_e\ ,$$

$$M_{\Sigma^-} = (2\,341.9 \pm 0.7)\ m_e\ .$$

([53]) W. F. FRY, J. SCHNEPS, G. A. SNOW, M. S. SWAMI: *Phys. Rev.*, **100**, 950 (1955); W. F. FRY: *Proceedings of the Sixth Annual Rochester Conference, op. cit.*,; W. F. FRY: private communication.

(+) The mean life obtained if it is assumed that decay-in-flight events are all Σ' hyperons and including the Σ^+ decays at rest (the Σ^- is always captured at rest) is

$$\tau_{\Sigma(+\,?)} = (0.76^{+0.2}_{-0.15})\cdot 10^{-10}\ \text{s}\ .$$

of selection bias with the very small number of events involved in these measurements (*).

The cascade particle Ξ^- decays as follows:

$$\Xi^- \to \Lambda^0 + \pi^- . \tag{4.16}$$

TABLE IX. – *Q-value measurements of Ξ^- cascade particles.*

Q – MeV	Method	Ref.
$15 < Q < 60$	Cloud chamber	(54)
60 ± 15	Cloud chamber	(55)
75 ± 15	Cloud chamber	(55)
67 ± 12	Cloud chamber	(56)
66 ± 6	Cloud chamber	(57)
63 ± 9	Cloud chamber	(58)
59 ± 11	Emulsions	(59)
63 ± 27	Emulsions	(60)
72 ± 20	Emulsions	(61)
71 ± 5	Emulsions	(62)
66.6 ± 3.0	Average	

(*) Recent results by ALVAREZ, BRADNER, FALK-VAIRANT, GOW, ROSENFELD, SOLMITZ and TRIPP [*University of California Radiation Laboratory Report No. UCRL-3583* (to be published)] give

$$\tau_{\Sigma^+} = (0.86 \pm 0.17) \cdot 10^{-10} \text{ s} ,$$

$$\tau_{\Sigma^-} = (1.86 \pm 0.26) \cdot 10^{-10} \text{ s} .$$

(54) R. ARMENTEROS, K. H. BARKER, C. C. BUTLER, A. CACHON, C. M. YORK, jr.: *Phil. Mag.*, **43**, 597 (1952); R. ARMENTEROS, B. GREGORY, A. LAGARRIGUE, L. LEPRINCE-RINGUET, F. MULLER and C. PEYROU: *Suppl. Nuovo Cimento*, **12**, 327 (1954).

(55) C. D. ANDERSON, E. W. COWAN, R. H. LEIGHTON and V. A. VAN LINT: *Phys. Rev.*, **92**, 1089 (1953); J. D. SORRELS, R. H. LEIGHTON and C. D. ANDERSON: *Phys. Rev.*, **100**, 1457 (1955).

(56) E. W. COWAN: *Phys. Rev.*, **94**, 161 (1954).

(57) W. B. FRETTER and L. W. FRIESEN: *Phys. Rev.*, **96**, 853 (1954).

(58) W. H. ARNOLD, J. BALLAM, G. K. LINDEBERG and V. A. VAN LINT: *Phys. Rev.*, **98**, 838 (1955).

(59) M. W. FRIEDLANDER, D. KEEFE and M. G. K. MENON: *Nuovo Cimento*, **1**, 482 (1955).

(60) C. DAHANAYAKE, P. E. FRANÇOIS, Y. FUJIMOTO, P. IREDALE, C. J. WADDINGTON and M. YASIN: *Nuovo Cimento*, **1**, 888 (1955).

(61) P. H. BARRETT: *Phys. Rev.*, **94**, 1328 (1954).

(62) C. CASTAGNOLI, G. CORTINI and A. MANFREDINI: *Nuovo Cimento*, **2**, 565 (1955).

Table IX gives the Q-values obtained in cosmic-ray cloud-chamber pictures and emulsion events. The mean value of the Q is

$$Q_{\Xi^-} = (66.6 \pm 3.0)\ \text{MeV} ; \tag{4.17}$$

from this the Ξ^- mass is found to be

$$M_{\Xi^-} = (2585.0 \pm 5.9)\ m_e . \tag{4.18}$$

These observations imply that the mean life of the Ξ^- is $\sim 10^{-10}$ s ([54-58]).

The masses and mean lifetimes of the unstable particles are collected in Table X. In all probability, some unknown systematic errors may be present in the data. The errors given are standard deviations whenever possible, and in no sense should they be considered as limits of error.

TABLE X. – *Summary of the masses of the unstable particles.*

Particle	Mass (m_e)	Mean life (s)
μ	206.86 ± 0.11	$(2.22 \pm 0.02)\cdot 10^{-6}$
$\pi^{\pm}$	273.27 ± 0.11	$(2.56 \pm 0.05)\cdot 10^{-8}$
π^0	264.37 ± 0.60	$(5\ ^{+5}_{-2})\cdot 10^{-15}$
K_{μ_2} *a*)	965.3 ± 1.9	$(11.8\ ^{+0.8}_{-0.7})\cdot 10^{-9}$
K_{π_2} *a*)	966.0 ± 1.5	$(12.1\ ^{+1.1}_{-1.0})\cdot 10^{-9}$
τ	966.80 ± 0.43	$(12.7\ ^{+1.2}_{-2.0})\cdot 10^{-9}$
θ^0	965.1 ± 5.0	$(0.66\ ^{+0.11}_{-0.07})\cdot 10^{-10}$
p	1836.12 ± 0.02	stable: $> 3\cdot 10^{28}$ *b*)
n	1838.65 ± 0.02	$(1.12 \pm 0.32)\cdot 10^{3}$ *c*)
Λ^0	2181.74 ± 0.35	$(3.4 \pm 0.3)\cdot 10^{-10}$
Σ^+	2327.4 ± 1.0	$(0.34\ ^{+0.14}_{-0.08})\cdot 10^{-10}$
Σ^-	2340 ± 3.2	$(1.4\ ^{+1.6}_{-0.5})\cdot 10^{-10}$
Ξ^-	2585.0 ± 5.9	$\sim 10^{-10}$

a) Note that the masses of these K mesons, as well as of other types of K mesons not listed, are not significantly different from that of the tauon (see Table V).
b) See reference [63]. *c*) See reference [64].

([63]) F. REINES, C. L. COWAN and M. GOLDHABER: *Phys. Rev.*, **96**, 1157 (1954).
([64]) J. M. ROBSON: *Phys. Rev.*, **83**, 349 (1951).

RIASSUNTO (*)

Si passano criticamente in rassegna numerose accurate misure delle masse dei mesoni leggeri. Assumendo che i mesoni carichi positivi e negativi abbiano masse uguali, si possono calcolare i valori ottimi delle masse del pione e del muone. Si trova che le energie dei raggi X emessi da mesoni π e μ misurate per mezzo di assorbimento da parte dei K si possono combinare con le differenze di massa tra il pione e il muone positivo ottenendo un risultato con scostamento medio pari a circa $\frac{1}{3}$ degli errori assegnati alle migliori misure precedenti. Tutti i risultati sono in accordo soddisfacente e si possono combinare nel modo usuale. Per le masse si hanno i seguenti risultati: $M_\mu = (206.86 \pm 0.11)\, m_e$; $M_\pi = (273.27 \pm 0.11)\, m_e$. Si sono anche riveduti i dati sperimentali sulle vite medie, gli spin, le parità e i modi di decadimento e si danno i risultati della revisione. Le misure delle masse dei vari mesoni K si ottengono in vari modi: $M_{K\pi 2} = (966.0 \pm 1.5)\, m_e$; $M_{K\mu 2} = (965.3 \pm 1.9)\, m_e$; $M_\tau = (966.8 \pm 0.4)\, m_e$. Attualmente non si hanno prove che esista nelle masse una differenza esatta a meno di $1 \div 2\, m_e$. Si discutono i risultati ottenuti per le masse e le vite medie di $K^+_{\pi 2}$ e τ^+. Sembra al presente che l'eguaglianza sperimentale di queste masse sia in contraddizione con l'assegnazione di uno spin inferiore a 2. Si discutono i dati ottenuti dalla radiazione cosmica sulla vita media del θ^0 e i recenti risultati ricavati da θ^0 prodotti artificialmente. Si passano in rassegna i dati sulle masse degli iperoni. $M_{\Lambda^0} = (2\,181.74 \pm 0.35)\, m_e$; $M_{\Sigma^0} = (2\,327.4 \pm 1.0)\, m_e$. Si espongono i più recenti dati sulla differenza fra le masse del Σ^+ e del Σ^-.

(*) *Traduzione a cura della Redazione*

Sulla struttura della gliossima allo stato solido (*).

M. Milone e E. Borello

Istituto di Chimica Fisica dell'Università - Torino

(ricevuto l'11 Settembre 1956)

Riassunto. — Si riferisce sui primi dati ottenuti mediante l'analisi röntgenografica e la spettroscopia nell'infrarosso. Dall'esame degli spettri infrarossi allo stato solido risulta che le molecole della gliossima sono centrosimmetriche e piane ed appartengono al gruppo spaziale C_{2h}; inoltre le molecole sono associate per la presenza di legami idrogeno. Lo studio röntgenografico ha permesso di stabilire che i cristalli appartengono al sistema monoclino ed hanno le seguenti costanti cristallografiche: $\alpha=\gamma=90°$, $\beta=88°30'$, $a=3{,}88$ Å, $b=4.45$ Å, $c=11.08$ Å. La cella elementare contiene due molecole. L'esame sistematico delle riflessioni permette di scegliere il gruppo spaziale con certezza: C_{2h}^5. In tale gruppo spaziale le coordinate delle posizioni equivalenti sono: x, y, z; $\bar{x}, \bar{y}, \bar{z}$; $\bar{x}, \frac{1}{2}+y, \frac{1}{2}-z$; $x, \frac{1}{2}-y, \frac{1}{2}+z$. Poichè nella cella elementare le molecole sono due, ciascuna di esse dovrà occupare due posizioni equivalenti: la molecola deve essere pertanto centrosimmetrica. Il piano (100) è un piano di facile sfaldatura e poichè le molecole sono piane con ogni probabilità giaceranno sul piano degli assi y e z. Abbiamo esaminato in luce infrarossa polarizzata delle sottili lamine cristalline tagliate parallelamente al piano (100). Le bande d'assorbimento corrispondenti alle vibrazioni di valenza dell'OH e del C=N presentano dicroismo parallelo all'asse cristallografico b, mentre le vibrazioni di valenza del legame NO dicroismo perpendicolare. Con ogni probabilità quindi il legame C—C della gliossima è di poco inclinato rispetto all'asse c e le molecole formano lunghe catene parallelamente all'asse b per mezzo dei legami idrogeno. Ciò è confermato dal fatto che i piani (001) sono anch'essi piani di facile sfaldatura.

Come è stato ricordato in un precedente lavoro presentato al XIV Congresso Internazionale di Chimica a Zurigo [1], oltre ai tipi possibili di stereoisomeri nelle gliossime e nelle ossime in generale, è ancora in discussione, per questa

(*) Presentato al Congresso di Torino, 11-16 Settembre 1956.

[1] M. Milone e E. Borello: *XVI Congresso Internazionale di Chimica pura ed applicata*, Zurigo, 1955.

classe di composti, la struttura stessa del gruppo ossiminico, per il quale deve essere considerata, accanto alla formula ossiminica « vera » (I), anche una forma N-ossido iminica (II)

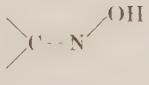

I

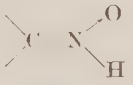

II

Se è vero che in soluzione è facile il passaggio dall'una all'altra di queste forme, come è dimostrato da numerose reazioni chimiche, quali ad esempio la formazione di N ed O eteri e la formazione dei sali complessi col Nichel e col Palladio, è altrettanto vero che allo stato solido, nel reticolo cristallino, deve essere stabile una forma soltanto.

Nelle gliossime poi, essendo presenti due gruppi ossiminici nella stessa molecola, è ancora possibile un terzo caso, in cui uno dei due gruppi ha la struttura (I) e l'altro la (II).

Questa non identità dei due gruppi ossiminici nelle gliossime è stata sostenuta dal Ponzio, con argomentazioni di carattere chimico, nel noto gruppo di circa 150 lavori usciti da questo Istituto tra il 1920 ed il 1940 [2].

Ci siamo quindi proposti uno studio della struttura delle gliossime allo stato solido ed abbiamo iniziato dalle forme *anti*, cioè da quelle che dànno il caratteristico sale complesso rosso col Nichel.

Nella letteratura esiste un unico lavoro strutturistico di Merritt e Lanterman [3] sulla dimetilgliossima allo stato solido: la molecola è centrosimmetrica e piana per quello che riguarda lo scheletro molecolare; si trova quindi nella forma *s-trans* rispetto al legame carbonio-carbonio centrale.

Le molecole sono poste sul piano degli assi *a* e *b* e formano delle lunghe catene nella direzione dell'asse *b* per mezzo di legami idrogeno.

Sulla base di questi dati abbiamo studiato lo spettro d'assorbimento nell'infrarosso della dimetilgliossima allo stato solido [4], il quale ha confermato per questo composto la struttura centrosimmetrica e per il gruppo ossiminico la struttura (I).

A quest'ultimo riguardo osserviamo che i dati cristallografici di Merrit e Lanterman non sono sufficienti a decidere con sicurezza.

L'assegnazione delle frequenze è stata fatta per mezzo della deuterazione all'ossidrile (deuterazione completa mediante un procedimento chimico ap-

[2] *Gazz. Chim. It.*, **50-70** (1920-1940).
[3] L. L. Merritt e E. Lanterman: *Acta Crystall.*, **5**, 811 (1952).
[4] E. Borello e L. Henry: *Compt. Rend.*, **241**, 1280 (1955).

positamente studiato (5)), la quale permette di individuare le frequenze ossidriliche, e per mezzo dell'esame in luce infrarossa polarizzata.

La dimetilgliossima infatti cristallizza nel sistema triclino con le seguenti costanti reticolari:

$$a = 6.10\ \text{Å} \qquad \alpha = 122°31'$$
$$b = 6.30\ \text{Å} \qquad \beta = 90º\ 6'$$
$$c = 4.48\ \text{Å} \qquad \gamma = 79º\ 1'.$$

Data la piccola inclinazione del legame carbonio-carbonio (6) centrale sull'asse a e dato il valore dell'angolo γ, le direzioni dei legami di valenza carbonio-azoto ed ossigeno-idrogeno sono all'incirca quelle dell'asse b: quindi se è possibile ottenere delle lamine cristalline sufficientemente sottili e di dimensioni adatte per l'orientamento davanti alla fenditura dello spettrofotometro, si dovrà avere un notevole effetto dicroico.

I piani delle molecole sono piani di facile sfaldabilità, poichè in essi le molecole sono legate le une alle altre da legami idrogeno; è quindi abbastanza facile ottenere lamine di dimensioni adatte, per cristallizzazione del composto dall'acetato di etile a caldo.

È possibile in tal modo individuare bene la banda dovuta alla vibrazione di valenza del C=N (di debole intensità nelle gliossime) per la sua polarizzazione parallela a quella di valenza dell'ossidrile e la vibrazione di valenza del gruppo N-O per la sua polarizzazione perpendicolare.

Riportiamo nella tabella seguente le frequenze osservate nella regione tra 1600 e 500 cm^{-1} per la dimetilgliossima e la dimetilgliossima deuterata, e la loro assegnazione.

Tabella I.

Dimetilgliossima	Dimetilgliossima deuterata	Assegnazione
711 F	690 F	OH fuori del piano
760 larga	557 larga	
905 F	897 F	
983 F	976 F	NO di valenza
1028 d	1031 d	
1152 m	1105 m	OH deformazione?
1369 f	1359 f	
1466 F	1460 F	CH_3 deformazione
1625 d	1625 d	C=N di valenza

(5) E. Borello e M. Colombo: *Ric. Scient.*, **25**, 2899 (1955).
(6) L. L. Merritt: *Anal. Chem.*, **25**, 718 (1953).

Lo spettro nella regione delle vibrazioni di valenza dell'ossidrile non è di facile interpretazione e non viene preso in considerazione in questa sede. La posizione e la forma delle bande d'assorbimento confermano però la presenza di legami idrogeno.

I risultati sull'assegnazione della vibrazione di valenza del gruppo NO alla banda a 983 cm $^{-1}$ sono in accordo con quelli ottenuti da altri autori sulle manossime ([7,8]).

Nelle Figure 1 e 2 sono riportate le curve di trasmissione della dimetilgliossima e della dimetilgliossima deuterata.

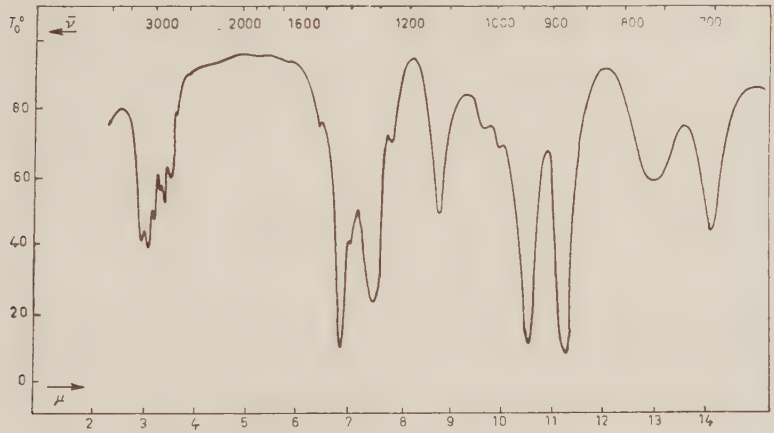

Fig. 1. - Curva di trasmissione della dimetilgliossima.

Assumendo anche per la gliossima allo stato solido una struttura centrosimmetrica e piana, e la struttura (I) per gli ossiminogruppi, è possibile interpretarne l'intero spettro d'assorbimento.

In tal caso infatti la molecola appartiene al gruppo di simmetria C_{2h} e presenta 12 vibrazioni attive in infrarosso: 8 del tipo B_u (simmetriche rispetto al piano ed antisimmetriche rispetto all'asse binario: quindi vibrazioni nel piano) e 4 del tipo A_u (antisimmetriche rispetto al piano e simmetriche rispetto all'asse binario: quindi vibrazioni fuori del piano). Dodici frequenze fondamentali sono riscontrabili sperimentalmente nello spettro (trascurando come già per la dimetilgliossima la struttura più complicata delle bande a maggior frequenza che può essere messa in evidenza con l'impiego di un prisma a fluo-

([7]) S. Califano e W. Lüttke: *Zeits. f. Phys. Chem.*, **6**, 83 (1956).
([8]) A. Palm e H. Werbin: *Can. Journ. Ch.*, **31**, 1004 (1953).

ruro di Litio: si tratta comunque delle vibrazioni di valenza dell'ossidrile e del CH).

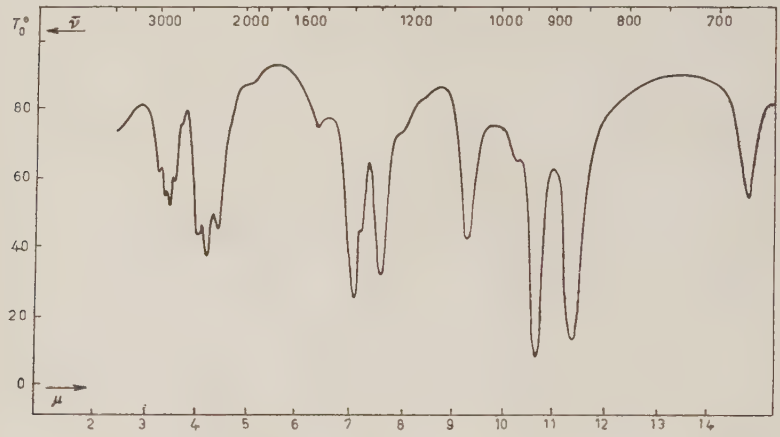

Fig. 2. – Curva di trasmissione della dimetilgliossima deuterata.

Nella Tabella II sono riportate le frequenze dei massimi d'assorbimento per la gliossima e per la gliossima deuterata nella regione spettrale tra 1600 e 500 cm^{-1}.

Tabella II.

Gliossima	Gliossima deuterata	Tipo di vibrazione	Assegnazione
655 m	648 m	Bu	C=NO deformazione
675 m	667 m	Bu	CCN deformazione?
767 f	554 f	Au	connesse
802 f	584 f	Ah	coll'OH
956 f	956 f	Au	connesse
974 f	966 f	Au	col CH
995 F	985 F	Bu	NO di valenza
1281 m	1072 m	Bu	OH deformazione
1432 f	1430 f	Bu	CH deformazione
1640 d	1640 d	Bu	C=N di valenza

Nelle Figure 3 e 4 sono riportate le curve di trasmissione della gliossima e della gliossima deuterata.

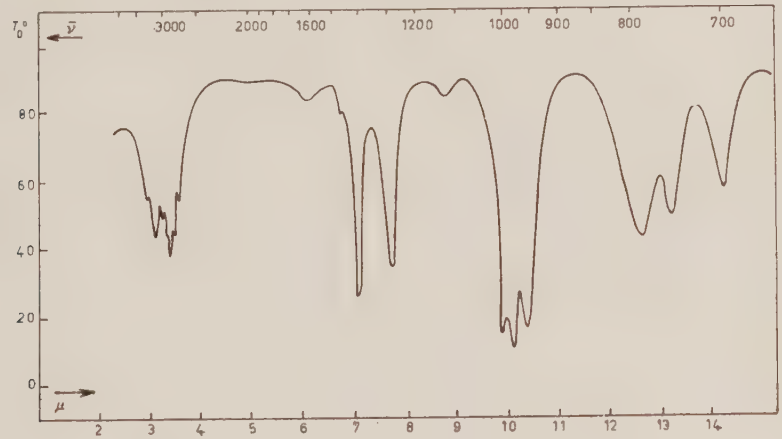

Fig. 3. - Curva di trasmissione della gliossima.

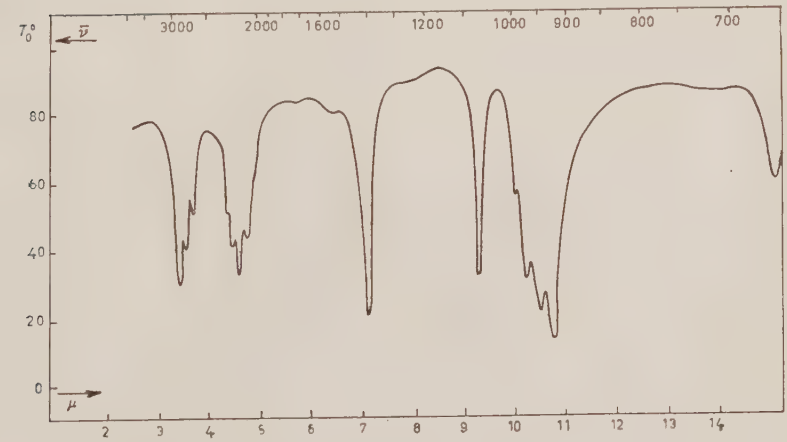

Fig. 4. – Curva di trasmissione della gliossima deuterata.

La conferma della struttura centrosimmetrica della molecola nel cristallo è stata inoltre ottenuta dai primi risultati dell'analisi roentgenografica, che abbiamo attualmente in corso. I fotogrammi di LAUE, quelli di BRAGG e di WEISSEMBERG ottenuti facendo ruotare il cristallo attorno alle direzioni dei

tre assi cristallografici, hanno permesso di stabilire che la gliossima cristallizza nel sistema monoclino, classe prismatica e che le costanti cristallografiche sono:

$$a = 3.88\ \text{Å} \qquad \alpha = \gamma = 90°$$
$$b = 4.45\ \text{Å} \qquad \beta = 88°30'$$
$$c = 11.08\ \text{Å}$$

assumendo la direzione della digira, normale al piano di simmetria, come asse y ed indicando con x ed y le direzioni parallele agli unici due spigoli presentati dal cristallo nel piano di simmetria. La densità della gliossima è 1.52: si calcola quindi che nella cella elementare sono contenute due molecole.

La sistematica delle estinzioni è la seguente:

per i piani	(hkl)	nessuna condizione
» »	$(h0l)$	$l = 2n$
» »	$(0k0)$	$k = 2n$

Questi piani individuano univocamente per la gliossima il gruppo spaziale C_{2h}^{5}.

Le coordinate delle posizioni equivalenti sono pertanto

$$x, y, z \qquad \bar{x}, y, \bar{z} \qquad \bar{x}, \tfrac{1}{2}+y, \tfrac{1}{2}-z \qquad x, \tfrac{1}{2}-y, \tfrac{1}{2}+z.$$

Poichè nella cella elementare le molecole sono due, ciascuna di esse dovrà occupare due posizioni equivalenti; la molecola deve essere pertanto centrosimmetrica.

Poichè abbiamo assunto, in base ai dati spettroscopici, che la molecola della gliossima è piana e centrosimmetrica, e quindi nella forma *s-trans* rispetto al legame carbonio-carbonio, e poichè è dimostrata la presenza di legami di idrogeno, avremo anche in questo caso, con la massima probabilità, lunghe catene di molecole tutte disposte sullo stesso piano.

I piani contenenti le molecole, come quelli a maggior densità e maggior coesione, dovranno essere quindi piani di facile sfaldabilità, il che si osserva in realtà per i piani (100). Le molecole giaceranno quindi sul piano degli assi y e z e le coordinate delle posizioni equivalenti saranno:

$$0, y, z \qquad 0, \bar{y}, z \qquad 0, \tfrac{1}{2}+y, \tfrac{1}{2}-z \qquad 0, \tfrac{1}{2}-y, \tfrac{1}{2}+z.$$

A conferma di queste supposizioni abbiamo studiato il dicroismo infrarosso

presentato da cristalli di gliossima orientati. Poichè i cristalli sono maggiormente sviluppati nella direzione dell'asse *b*, abbiamo orientato una sottile lamina cristallina, dello spessore di alcuni centesimi di millimetro, con tale asse parallelo alla fenditura d'ingresso dello spettrofotometro.

È stato osservato dicroismo parallelo:

per la banda OH a circa 3 100 cm^{-1}

» » CH » 2 800 cm^{-1}

» » C=N a 1 640 cm^{-1}

e piccolo dicroismo perpendicolare

per la banda NO a 995 cm^{-1}

Queste osservazioni, oltre a confermare l'esattezza dell'assegnazione fatta delle frequenze nell'infrarosso, permettono di dedurre che le molecole sono situate con la direzione dei legami C=N molto inclinata sull'asse cristallografico *b*, mentre la direzione del legame NO deve essere vicina ai 45° rispetto ai due assi, dato il suo piccolo dicroismo.

Esistono di conseguenza delle catene di molecole, unite da ponti di idrogeno, nella direzione dell'asse binario, il che è confermato dal fatto che anche il piano (010) è piano di facile sfaldatura, mentre il cristallo, non solo si sfalda parallelamente alla faccia (010), ma da nessun solvente cristallizza presentando la faccia (010).

Inoltre, se si assumono le molecole piane e giacenti sul piano (100) la distanza tra piani successivi di molecole è coincidente, a meno di 0,01 Å, alla distanza tra i piani delle molecole nella dimetilgliossima, composto che presenta notevoli analogie con la gliossima dal punto di vista spettroscopico.

Abbiamo ora in corso l'analisi Fourier-Patterson della gliossima; desideriamo però far notare quanto possa essere utile l'analisi spettrografica infrarossa, e soprattutto lo studio del dicroismo infrarosso, ai fini di avere indicazioni preliminari sulla posizione delle molecole nel cristallo.

Anche in soluzione le gliossime *anti* conservano la struttura piana; infatti lo studio degli spettri ultravioletti dimostra l'esistenza della coniugazione dei due doppi legami carbonio-azoto [9]. Ciò però non implica che sia impossibile la rotazione attorno al legame carbonio-carbonio centrale nè la tautomerizzazione del gruppo ossiminico dalla (I) alla (II).

Ciò è dimostrato dalla formazione dei sali complessi col Nichel, il cui mec-

---

[9] E. Borello e A. Catino: *Ann. Chim.*, **46**, 571 (1956).

canismo di formazione potrebbe essere il seguente:

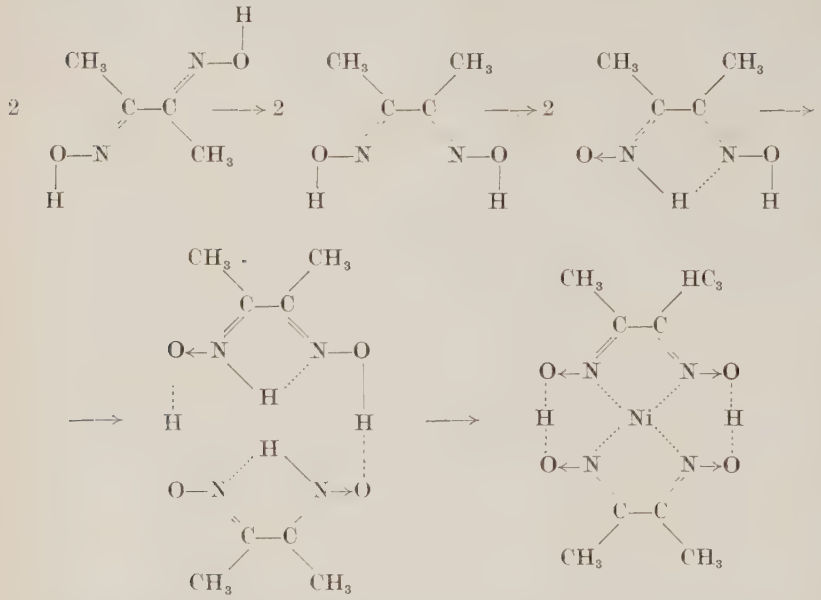

La gliossima è stata preparata dall'acetaldeide per bromurazione e successiva reazione con idrossilamina: la dimetilgliossima era quella del commercio purificata per successive cristallizzazioni.

La dimetilgliossima cristallizza bene ed in grossi cristalli dall'acetato di etile a caldo; la gliossima da una soluzione acquoso-alcolica.

Le lamine cristalline delle dimensioni utili per l'esame in luce polarizzata vennero ottenute conglobando adatti cristalli in paraffina e tagliandoli successivamente con un microtomo.

Gli spettri allo stato solido vennero registrati, con la tecnica delle pastiglie di bromuro potassico, mediante uno spettrofotometro Perkin-Elmer 12 C ed uno spettrofotometro Beckman IR 2 con ottica di bromuro potassico per la regione fino a 500 cm^{-1}.

SUMMARY

Preliminary results from X-rays analysis and infrared spectroscopy are reported. The study of the infrared spectra in the solid state suggests a centrosymmetrical structure for the glyoxime and the symmetry group C_{2h}. Hydrogen bonds are present.

Glyoxime crystallizes with the following crystallographic constants: $\alpha = \gamma = 90°$, $\beta = 88° 30'$, $a = 3.88$ Å, $b = 4.45$ Å, $c = 11.08$ Å, and two molecules in the unit cell. From the systematics of the reflections we can conclude that the glyoxime crystallizes in the spatial group C_{2h}^5 with $x, y, z; \overline{x}, \overline{y}, \overline{z}; x, \frac{1}{2} + y, \frac{1}{2} - z; x, \frac{1}{2} - y, \frac{1}{2} + z$, as coordinates of the equivalent positions. Each molecule in the unit cell must, therefore, occupy two equivalent positions and is then centrosymmetric. (100) is a cleavage plane and then the molecules lie in the y, z plane. We examined with polarized infrared radiations thin crystalline blades, cut parallel to (100) and we observed parallel dichroism for the OH and C = N stretching vibrations and perpendicular dichroism for the NO stretching vibration. Probably the C—C bond in glyoxime presents only a little beding on the crystallographic axis c and the molecules form long chains parallel to the axis b.

Sull'età dell'Universo (*).

M. Pierucci

Istituto di Fisica dell'Università - Modena

(ricevuto il 18 Settembre 1956)

Riassunto. — In una sua precedente nota l'A. aveva sottolineato una grave discrepanza messa già in evidenza dallo stesso Einstein: l'età dell'Universo, dedotta dalla sua espansione, risultava assai minore dell'età della crosta terrestre, dedotta dallo studio dei minerali radioattivi. L'A. aveva già individuato la causa di ciò in un errato procedimento nel calcolo dell'età dell'Universo, procedimento in cui si faceva ricorso ad una tautologia; ed aveva cercato di girare l'ostacolo, servendosi di invarianti della relatività ristretta, nonchè di formule approssimate di relatività generale. Per una precisa determinazione dell'età dell'Universo occorreva però conoscere la « densità iniziale », della quale, invece, non possiamo avere una conoscenza sicura. Ora, valendosi di una considerazione di natura astronomica, l'A. riesce a fare a meno di tale conoscenza. E la suddetta discrepanza risulta perfettamente sanata.

---

1. – Riassumo brevemente, per comprensione del lettore, una mia Nota precedente [1]. In essa ricordavo l'introduzione, fatta da Polvani [2], di un « *tempo assoluto entropico* »; e mostravo che questo tempo coincide col « *tempo di espansione* »; indicavo poi la possibilità di una misura, almeno concettuale, di quest'ultimo, mediante la determinazione della densità elettrica (istantanea) media-quadratica dell'Universo.

Passavo quindi ad osservare come esistesse allora una grave discrepanza, messa già in rilievo dallo stesso Einstein, fra l'età dell'Universo dedotta dal tempo di espansione e quella che occorrerebbe ascrivergli, affinchè essa potesse

---

(*) Presentato al Congresso di Torino, 11-16 Settembre 1956.

(1) M. Pierucci: *Atti Acc. Sc., Lett. Arti Modena* (1951).

(2) G. Polvani: *Il concetto di traccia di una trasformazione e il secondo principio della termodinamica*, Sem. Mat. Fis. di Milano, 1947; *Il divenire del mondo fisico*, in *Scienza e mistero* (Roma, 1948).

contenere in sè l'età della crosta terrestre (dedotta dallo studio dei minerali radioattivi), nonchè l'età delle stelle più vecchie (dedotta in base alle teorie sulle evoluzioni stellari). Mi domandavo, infine, se non fosse possibile sanare una tale discrepanza.

Notavo a tale proposito come nella comune maniera di calcolare l'età dell'Universo, ricavandola dall'espansione (*effetto Hubble*), si cada in una tautologia; in quanto che il tempo che si vuol misurare lo si introduce già, esplicitamente od implicitamente, con la relazione:

$$\frac{\mathrm{d}t}{T_0} = \frac{\mathrm{d}l}{l_0}, \tag{1}$$

(dove T_0 è la costante dell'effetto Hubble e dove è chiaro il significato degli altri simboli). E dicevo: «Ma che cosa significa che un intervallo di tempo si mantiene costante nel fluire del tempo stesso? E come possono confrontarsi fra di loro intervalli di tempo successivi? È possibile girare l'ostacolo? ».

Appunto per girare l'ostacolo introducevo allora nel problema la considerazione degli invarianti relativistici; e precisamente, con trattazione, che chiamavo di « *relatività ristretto-generale* », postulavo che: « *andando a ritroso nel tempo l'ipervolume rimane pressochè invariato* » [3]. Arrivavo così alla formula:

$$\frac{\mathrm{d}t}{T_0} = -\frac{3}{\alpha}\frac{\mathrm{d}l}{l_0}, \tag{2}$$

essendo α la *contrazione*.

A considerazioni analoghe giungevo adoperando, sia pure con qualche arbitrarietà, sanata però dai risultati, la formula di relatività generale:

$$(\Delta t)_1 = \left(1 + \frac{\varkappa}{8\pi}\int\frac{\varrho}{r}\,\mathrm{d}\tau_0\right)\cdot(\Delta t)_0\,, \tag{3}$$

dove $(\Delta t)_1$ è l'intervallo di tempo « dilatato » all'atto dell'inizio della espansione; ossia è la misura, rispetto ai nostri attuali riferimenti, lontani da masse, dello stesso intervallo di tempo, la cui misura attuale è $(\Delta t)_0$; σ è la densità, τ_0 il volume « lontano da campi », r la misura del raggio vettore, e $\varkappa$ è la solita

[3] Si fa dunque una transazione fra la relatività ristretta, in cui l'ipervolume è rigorosamente invariante, e la relatività generale, nella quale non risulta più invariante l'ipervolume, bensì la formazione:

$$\sqrt{g}\cdot\Delta\tau_3\cdot\Delta t\,,$$

dove g è il determinante delle g_{ik} (g_{ik}=componenti del tensore fondamentale).

costante einsteiniana, legata alla costante K di Newton dalla nota relazione

$$(4) \qquad \varkappa = \frac{8\pi K}{c^2}.$$

Per applicare praticamente questo metodo occorreva, però, una ipotesi supplementare: quella della densità iniziale dell'Universo. Ciò appunto impediva di sfruttare in pratica un metodo, che teoricamente sembrava ineccepibile. Nella Nota precedente tentavo di calcolare l'età « probabile » dell'universo facendo varie ipotesi sulla densità iniziale; e giungevo sempre a valori molto elevati. Così, ad esempio, assumendo per valore della densità iniziale quello di Alpher, Bethe e Gamow (1), trovavo: 300 miliardi di anni; cioè una età certamente molto superiore a quella presumibile.

2. – Una semplice osservazione di natura astronomica mi ha dato ora modo di sbarazzarmi di ogni ipotesi sulla densità iniziale dell'Universo; mentre essa ci fa giungere ad un resultato unico, indipendente da quella che può essere stata la densità iniziale (anche quella, ad esempio, di Alpher, Bethe e Gamow). Ecco l'osservazione. Noi sappiamo che l'espansione dell'Universo può anche ricavarsi trattando l'insieme dell'universo come un gas di particelle, che spontaneamente si diffonda (5). Sottolineiamo adesso il fatto astronomico che: si può parlare di un gas stellare dentro ogni galassia, e di un gas di galassie nell'Universo; meglio: *di un gas stellare* (e di un gas di particelle interstellari) *dentro ogni ammasso globulare* (6) *di stelle*; *di un gas di ammassi globulari* (e di un gas di particelle galattiche) *dentro ogni galassia*; *di un gas di galassie* (e di un gas di particelle intragalattiche) *dentro ogni ammasso di galassie*; *di un gas di ammassi galattici* (e di un gas di particelle interclusters) *dentro l'Universo* (7). Le velocità medie dei « costituenti » di tali gas vanno crescendo, passando da un gas al successivo nell'ordine su elencato. E ciò è in relazione col crescere delle dimensioni dell'*ambiente* (8) in cui il gas

(4) Vedi R. Alpher e R. C. Herman: *Phys. Rev.*, **84**, 61 (1951).

(5) E. A. Milne: *Nature*: **130**, 9 (1932).

(6) Non considero gli ammassi aperti, formati da un numero relativamente piccolo di stelle e dotati di debole individualità fisica.

(7) Non mi sembra assurdo il pensare che possano esservi anche dei raggruppamenti di ammassi galattici. (A tale esistenza farebbe pensare, a mio parere, il valore del rapporto fra densità degli ammassi galattici e densità dell'Universo, calcolato nelle due diverse maniere; valore assai più alto dei valori degli altri rapporti fra densità di gas contigui). In tal caso avremmo un gas di ammassi galattici dentro ogni raggruppamento di ammassi galattici, ed un gas di raggruppamenti dentro l'Universo.

(8) Questo *ambiente* può riguardarsi come l'*accidens* spaziale dei fotoni; l'insieme dei quali gioca, nella S_4 spazio-temporale einsteiniana, quella stessa parte che prima di Einstein giocava, nella S_3 spaziale, l'etere [v. M. Pierucci: *Alcune ardite considerazioni sulle particelle e sui campi*. Nota II, *Atti Acc. Modena* (1954)].

si espande. Ora la considerazione essenziale per il nostro calcolo è questa: che, mentre si espande il gas stellare in un ammasso globulare di stelle, si espande il gas di ammassi stellari dentro ogni galassia; e, contemporaneamente ancora, si espande il gas di galassie dentro ogni ammasso galattico; e così via.

Per calcolare l'età dell'Universo ci basterà dunque sapere quale sarebbe la densità dell'Universo, qualora tutti gli ammassi galattici (9) fossero costipati a costipazione massima; od anche: quale sarebbe la densità degli ammassi galattici, se tutte le galassie fossero costipate a costipazione massima: e così via. Insomma: per densità finale ed iniziale basta mettere, nei nostri calcoli, due numeri che stiano fra di loro come le densità medie di due classi contigue (seguente e precedente) nell'ordine segnato sopra. Noi, per la ragione espressa in nota (7), escluderemo il rapporto fra densità dell'Universo e densità media degli ammassi galattici. Ed escluderemo tale rapporto, anche perchè non sapremmo bene quale valore scegliere per la densità dell'Universo: se, cioè, quello d_u dato dalla relazione $d_u = 3r_\tau^2/8\pi G$ (dove r_τ è la velocità di recessione e G la costante di gravitazione), cioè: $1.5 \cdot 10^{-28}$ g cm^{-3}, oppure il valore 10^{-29} g cm^{-3}, calcolato dalla densità media del numero di galassie (v. ALLEN, *Astrophysical Quantities*, Londra 1955). Sceglieremo dunque il rapporto fra densità media degli ammassi di galassie e densità media di ogni galassia, valendoci di recenti dati dell'Allen (v.l.c.). Osserviamo, in ogni modo, che, siccome l'età dell'Universo, calcolata per questa strada, dipende, come vedremo, dalla potenza $\frac{1}{6}$ di detto rapporto, così lo spostamento che si ottiene nel valore di detta età è piccolo, anche quando si sposti assai il valore di tale rapporto. Detto ciò, riprendiamo i calcoli della mia Nota precedente.

3. – Osserviamo che la (2), integrata dal tempo iniziale a quello attuale, ci dà

$$T = \frac{3}{\alpha_m} \frac{l_0}{l_0 - l_i} T_0,$$

od anche

$$T = \frac{3}{\alpha_m} \left(1 - \frac{l_i}{l_0}\right) T_0;$$

ed assumendo per α_m il valore dato dalla:

$$\alpha_m = \sqrt[3]{\frac{l_i}{l_0}}, \tag{5}$$

si ha, con buona approssimazione, indicando con D_0 e con D_i le densità attuale

(9) O tutti i raggruppamenti di ammassi, secondo quanto è detto a nota (7).

ed iniziale.

$$T = 3\left(\frac{D_i}{D_0}\right)^{\frac{1}{2}} \cdot \left[1 - \left(\frac{D_0}{D_i}\right)^{\frac{1}{3}}\right] \cdot T_0 \,. \tag{6}$$

Ponendo, ora, come si è detto, per D_0 e D_i le densità medie degli ammassi di galassie e, rispettivamente, delle galassie, cioè i valori ([10]): $2.8 \cdot 10^{-25}$ e 7.10^{-24} (g.cm^{-3}), per T_0 il valore: $3.4 \cdot 10^9$ anni ([11]), si ottiene:

$$T = 1.1 \cdot 10^{10} \text{ anni circa.}$$

L'età dell'Universo risulta, quindi, approssimativamente, di *undici miliardi di anni.*

4. – Abbiamo trovato così un valore abbastanza plausibile, doppio di quello dato recentemente per l'età della Terra ($5.5 \cdot 10^9$ anni) da Alpher ed Herman ([12]) con metodi radioattivi.

Vero è che alcuni vorrebbero estendere a tutto l'Universo quel limite superiore di $6 \cdot 10^9$ anni trovato per il sistema solare ([13]). Ma, come giustamente osserva l'Houtermans ([13]), è prudente considerare questo limite superiore come valevole soltanto per il sistema solare. E ciò per una recente osservazione fatta sulle stelle *M*. Infatti, mentre vi sono valide ragioni per ritenere ([14]) che non si possano avere, in natura, isotopi stabili del tecnezio (del quale è stato isolato recentemente, in milligrammi, l'isotopo radioattivo a lunga vita media $^{99}_{43}$Tc), tale elemento è stato trovato nelle stelle della classe *M* ([15]). Ciò fa appunto sospettare che, mentre in nessuna parte del nostro sistema planetario esistono condizioni che possano cambiare l'andamento delle disintegrazioni degli elementi radioattivi, tali condizioni possono invece presentarsi al di fuori del sistema solare stesso.

In ogni modo si può osservare che:

1) l'età dell'Universo, calcolata (secondo questo mio metodo) dalla teoria della Relatività, risulta effettivamente, come auspicava Einstein ([16]), supe-

([10]) Vedi C. W. Allen: l. c. e G. Cecchini: *Il Cielo* (Torino, 1952).

([11]) Vedi C. W. Allen: l. cit., p. 244.

([12]) R. A. Alpher e R. C. Herman: *Phys. Rev.*, **84**, 1111 (1951).

([13]) F. G. Houtermans: *Suppl. Nuovo Cimento*, **12**, 17 (1954).

([14]) C. W. Allen *et al.*: *The Sc. and Rng. of Nuclear Power*, Vol. II (Cambridge, Mass., 1949).

([15]) P. W. Merrill: *Conferenza alla National Academy of Science* (1952).

([16]) « Last and not least: The age of the universe, in the sense used here, must certainly exceed that of the firm crust of the earth as found from the radioactive minerals. Since determination of age of these minerals in reliable in every respect, the cosmology

riore all'età della Terra, quale si ricava dallo studio delle trasforamzioni radioattive;

2) l'età dell'Universo, così calcolata, diviene dello stesso ordine di grandezza dell'età della Terra e di quella del sistema solare, ricavate dalle trasformazioni radioattive ([17]).

Sicchè, concludendo, si può dire che il resultato raggiunto è del tutto soddisfacente ([18,19]).

theory here presented would be disproved if it were found to contradict any such results. In this case I see no reasonable solution » (A. EINSTEIN: *The Meaning of Relativity* (Princeton, 1950)).

([17]) Vedi F. G. HOUTERMANS: l. c.

([18]) Come ho già sopra accennato, anche spostando sensibilmente i valori della densità media « iniziale », il risultato si sposta di pochissimo.

([19]) Tutti i dati astronomici, compresa la velocità di recessione, sono accordati con la « nuova scala delle distanze ». E si noti che, mentre con questi dati l'età dell'Universo, calcolata col vecchio metodo, cresce, essa resta tuttavia ancora minore, e non di poco, dell'età della Terra calcolata secondo i metodi radioattivi più recenti. Sicchè la discrepanza da sanare esisteva tuttora; donde la necessità della presente Nota, giustificata, anche, del resto, dalla arbitrarietà del comune metodo di calcolo per la determinazione dell'età dell'Universo.

SUMMARY

Five years ago the author began again to think of the conception of « absolute time » compatible with the Relativity, once introduced by POLVANI under the form of « entropic time »; he proved the entropic time coincided with the « expansion time »; then he calculated, in this absolute time, the age of the Universe. The author then pointed out a great discrepance existed at that time, which had already been evinced by EINSTEIN, between the age of the Earth, that was deduced from radioactive transformations, and the age of the Universe, deduced from the expansion; because the latter was shorter than the former. He intended then to abolish such a discrepancy; and he succeeded, by using, in a first approximation, the invariantive quantities of restricted Relativity, and by using, moreover, approximate formulas derived from the general Relativity. The method requested a supplementary hypothesis: that is the density of the Universe at the beginning of the expansion. That made the result very insecure; the author arrived in fact, with some hypotheses about the primitive density, to values which were very different from each other and all of them very high. The author now resumes the problem, using an observation of astronomical nature, that allows him to advance, even without knowing the first density of the Universe, and,

at the same time, modifies the practical development of the method. As is known, the expansion of the Universe can also be obtained theoretically (Milne) considering the Universe as a gas of particles, that dilates spontaneously. Now astronomical observations inform us that it is necessary to speak about a stellar gas (and about an interstellar particles gas) within every star-cluster, about a gas of star-clusters (and about a galactic particles gas) within every galaxy, about a gas of galaxies (and about an intergalactic particles gas) within every galaxy-cluster, about a gas of galaxy-clusters (and about an intercluster particles gas) within the Universe, all these expanding at the same time. As a quotient between the primitive density and the actual density of the Universe it is enough to put so, in the calculations, the quotient between the actual middle densities of two successive orders, in the disposition that was put before. We arrive, in such a way, at an age of the Universe of about eleven milliards of years, and we are able to show at last that such an age (about twice the age that has been recently given for the Earth) agrees very well with the recent results obtained from radioactive transformations.

Relazioni tra la struttura della blenda e il contenuto in gallio e indio (*).

G. Rigault

Istituto di Mineralogia e Petrografia dell'Università - Torino
Centro di studio per la Mineralogia e Petrografia delle Alpi Occidentali del C.N.R.

(ricevuto il 25 Settembre 1956)

Riassunto. — In base a precedenti risultati sperimentali, che consentirono di stabilire l'abbondanza e diffusione di gallio e indio in numerose blende appartenenti a giacimenti geneticamente differenti, si è cercato di mettere in correlazione temperatura di genesi della blenda e meccanismo di vicarianza di gallio e indio con lo zinco mediante considerazioni sulla struttura della blenda stessa. Uno dei risultati più notevoli per tal via conseguiti è la spiegazione del diverso comportamento di gallio e indio nei riguardi della blenda. Viene infine discussa la possibile genesi dell'indio *in loco* grazie a trasformazioni nucleari.

In miei recenti studi [1] condotti usando una particolare tecnica spettrografica e diretti a stabilire l'abbondanza e diffusione di gallio e indio, quali costituenti minori, in numerose blende appartenenti a giacimenti geneticamente differenti, sono giunto alla conclusione che non esiste parallelismo tra il contenuto di questi due elementi nella blenda, nonostante l'analogia del loro comportamento chimico.

In base poi ai risultati ottenuti nell'analisi di numerosi campioni provenienti da uno stesso giacimento, in cui esistono notevoli variazioni nel contenuto in gallio e indio, sono riuscito altresì a mettere in evidenza come il tenore in questi due elementi sia molto sensibile non soltanto alle variazioni delle concentrazioni di essi nelle soluzioni a contatto con la superficie del cristallo in via di formazione, ma in particolar modo alle variazioni, anche non molto elevate, delle condizioni termodinamiche dell'ambiente di genesi.

Per spiegare questi fatti e nell'insieme allo scopo di meglio inquadrare i

(*) Presentato al Congresso di Torino, 11-16 Settembre 1956.
(1) G. Rigault: *Periodico di Mineralogia*, **25**, 43 (1956).

risultati analitici ottenuti in una più ampia visione dal punto di vista geochimico, ho ritenuto opportuno prendere in esame la struttura della blenda, poichè evidentemente soltanto con il considerare gli eventuali meccanismi di sostituzione nel reticolo cristallino della blenda stessa è possibile identificare le ragioni ultime del complesso e delicato fenomeno.

In precedenza alcuni autori avevano preso in esame tale questione, nel tentativo di giustificare in qualche modo la presenza di questi due elementi nella blenda.

E precisamente Goldschmidt e Peters ([2]) avanzarono l'ipotesi che la presenza del gallio nella blenda, piuttosto che in altri solfuri, fosse da collegarsi al fatto che questo elemento poteva essere presente sotto forma di arseniuro, dato che GaAs ha la tipica struttura della blenda e costanti reticolari assai prossime (GaAs a_0 = 5.63 Å; ZnS a_0 = 5.41 Å). E poichè anche GaSb e GaP hanno struttura tipo blenda (GaSb a_0 = 6.09 Å; GaP a_0 = 5.43 Å) fu altresì prospettata la possibilità della presenza del gallio come antimoniuro e fosfuro.

Successivamente queste ipotesi vennero prese in esame da Morris e Brewer ([3]), i quali si proposero di indagare se, e fino a che punto, tali ipotesi potevano accordarsi con i risultati sperimentali di ricerche da loro *ad hoc* istituite. Essi misero in evidenza infatti come in linea generale campioni di blenda con contenuto in gallio superiore allo 0.02 % non mostrassero all'analisi spettrografica la riga Sb 2877.9 Å, sebbene il limite di sensibilità di essa corrispondesse allo 0.01 % di Sb. Tale fatto e l'esito di alcune esperienze sulla possibile coprecipitazione del gallio e dello zinco anche in assenza dell'arsenico portarono gli autori, sulle orme di Graton e Harcourt ([4]), alla conclusione che le ipotesi di Goldschmidt e Peters fossero da ritenersi inesatte, e che la presenza del gallio nella blenda trovasse più verosimile giustificazione nella considerazione che ZnS e Ga_2S_3 presentano lo stesso tipo di struttura, con costanti reticolari assai prossime (ZnS a_0 = 5.41 Å; Ga_2S_3 a_0 = 5.18 Å, per la fase stabile sotto 550°). Morris e Brewer ammisero perciò una sostituzione isomorfa Zn^{2+}-Ga^{3+} con la contemporanea formazione di posizioni reticolari libere, come d'altronde era già stato suggerito anche da Einecke ([5]).

Graton e Harcourt ipotizzarono invece che l'indio fosse presente nella blenda come ione bivalente, mentre Erämetsä ([6]), per spiegarne la presenza, ammise che si verificasse la sostituzione isomorfa coniugata tra le coppie Zn^{2+}-Zn^{2+} e Cu^{+}-In^{3+}, in modo da mantenere l'elettroneutralità.

([2]) V. M. Goldschmidt e C. Peters: *Nachr. Ges. Wiss. Göttingen, Math.-Phys. Klasse*, III, IV, 165 (1931).

([3]) D. F. C. Morris e F. M. Brewer: *Geochim. et Cosmochim. Acta*, **5**, 134 (1954).

([4]) L. C. Graton e G. A. Harcourt: *Econ. Geol.*, **30**, 800 (1935).

([5]) E. Einecke: *Das Gallium. Eine kritische Würdigung der Erkenntnisse mit experimentellen Beiträgen* (Leipzig, 1937).

([6]) O. Erämetsä: *Ann. Acad. Sci. Fennicae*, Ser. A, **51**, 1 (1938).

Indubbiamente in tutte le analisi da me eseguite il rame venne riscontrato in quantità superiori a quelle dell'indio e quindi tale fatto potrebbe essere interpretato come una conferma dell'ipotesi avanzata da ERÄMETSÄ, relativa alla sostituzione isomorfa coniugata. Rimane però sempre da rilevare che non ho constatato alcun parallelismo fra le quantità dei due costituenti minori e che in ogni caso sarebbe necessario ammettere un ambiente riducente tale da consentire la presenza di ioni Cu^+.

Infine ANDERSON (7), nelle sue osservazioni sulla geochimica dell'indio, prese in esame dettagliato la concentrazione di questo elemento in vari solfuri, tentando di mettere in evidenza una possibile relazione tra concentrazione e coordinazione tetraedrica, tipica in alcuni di questi minerali.

Allo scopo di chiarire il meccanismo della sostituzione indio-zinco e gallio-zinco, ritengo sia opportuno confrontare la struttura della blenda con quella, recentemente determinata da HAHN e KLINGLER (8), del In_2S_3 e riprendere in esame più dettagliato la struttura del Ga_2S_3 per poter istituire utili raffronti.

Il solfuro di gallio Ga_2S_3 ha la tipica struttura della blenda con $a_0 = 5.18$ Å e la distanza interatomica tra Ga e S è uguale a 2.24 Å; naturalmente affinchè nel reticolo cristallino sia mantenuta la elettroneutralità è necessario che le posizioni corrispondenti a quelle dello zinco nella blenda non siano tutte occupate dal gallio, ma ve ne sia sempre una libera in ogni cella elementare ed una ancora ogni tre celle elementari; HAHN e KLINGLER (9) hanno osservato che queste posizioni reticolari libere sono disposte in modo del tutto disordinato. PAULING e HUGGINS (10) determinarono per il raggio di coordinazione tetraedrica del gallio un valore di 1.26 Å molto prossimo al raggio di coordinazione tetraedrica dello zinco (1.31 Å): non è quindi difficile ammettere la possibilità di una sostituzione isomorfa Ga^{3+}-Zn^{2+} a condizione però che ogni due Ga^{3+} che entrano nel reticolo si formi una posizione libera, affinchè venga mantenuta la neutralità elettrica.

Il solfuro d'indio In_2S_3, nella fase stabile sotto 300°, presenta una struttura cubica, differente da quella della blenda, con $a_0 = 5.37$ Å ed è isotipico invece con $\gamma'Al_2O_3$; gli atomi di S sono anche qui in assestamento cubico compatto, formano cioè un reticolo cubico a facce centrate, mentre gli atomi di indio sono in due posizioni diverse: precisamente, per circa il 70%, occupano posizioni a coordinazione ottaedrica e, per il rimanente, posizioni a coordinazione tetraedrica; il tutto in modo disordinato (8).

PAULING (11) riporta come raggio di coordinazione tetraedrica per l'indio

(7) J. S. ANDERSON: *Geochim. et Cosmochim. Acta*, **4**, 225 (1953).
(8) H. HAHN e W. KLINGLER: *Zeits. anorg. Chem.*, **260**, 97 (1949).
(9) H. HAHN e W. KLINGLER: *Zeits. anorg. Chem.*, **259**, 135 (1949).
(10) L. PAULING e M. L. HUGGINS: *Zeits. f. Krist.*, **87**, 205 (1934).
(11) L. PAULING: *La natura del legame chimico* (Roma, 1949).

un valore di 1.44 Å, valore che presenta già una differenza sensibile da quello dello zinco. Ora nell'assestamento cubico compatto di atomi di S, che hanno raggio di 1.04 Å, quando $a_0 = 5.41$ Å nelle « buche tetraedriche » è disponibile uno spazio per una sfera di raggio di azione fino a 1.30 Å; qualora in tale posizione dovesse entrare una sfera con raggio maggiore comparirebbero necessariamente sensibili effetti di deformazioni reticolari.

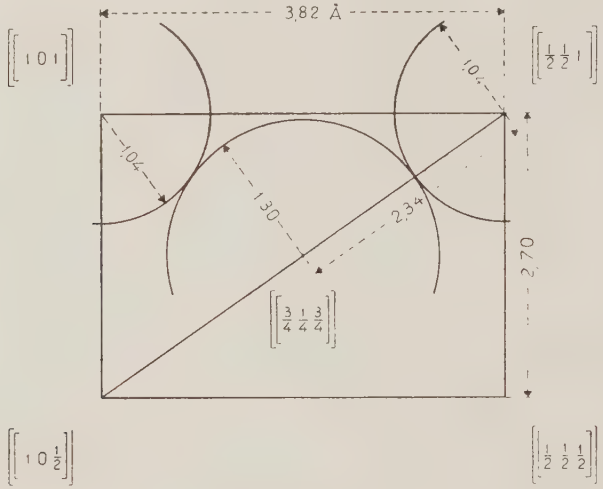

Fig. 1. – Sezione (110), con i raggi delle sfere d'azione e loro posizioni reticolari.

Per meglio chiarire questi fatti, ho ritenuto opportuno schematizzare graficamente nella figura 1 la sezione relativa al piano (110) della blenda, dimostrante appunto le dimensioni delle « sfere d'azione » dei vari atomi, con le loro posizioni relative e le dimensioni della « buca tetraedrica ». È facile rilevare dall'esame del disegno della figura 1 che la sostituzione dello zinco con l'indio nella posizione $[[\frac{3}{4}\ \frac{1}{4}\ \frac{3}{4}]]$ porta come effetto una certa distorsione nel reticolo, dati i valori dei raggi di coordinazione tetraedrica non più molto prossimi. Per spiegare quindi la presenza dell'indio nella blenda bisogna ammettere che gli atomi di questo elemento possano anche andare nelle « buche ottaedriche » dell'assestamento cubico compatto degli atomi di S, dove lo spazio disponibile è molto maggiore e tale da permettere l'entrata del leptone estraneo senza provocare alcuna distorsione. Ciò è facilmente osservabile nel disegno relativo alla sezione (100) che ho ritenuto opportuno riportare in figura 2 per mettere in evidenza la buca ottaedrica in $[[\frac{1}{2}\ \frac{1}{2}\ \frac{1}{2}]]$ e le sue dimensioni, con uno spazio disponibile per una sfera di raggio sino a 1.66 Å. Queste deduzioni sono in stretto

accordo con la tipica struttura presentata da In_2S_3, nel cui reticolo sono presenti per il 70% atomi di indio a coordinazione ottaedrica.

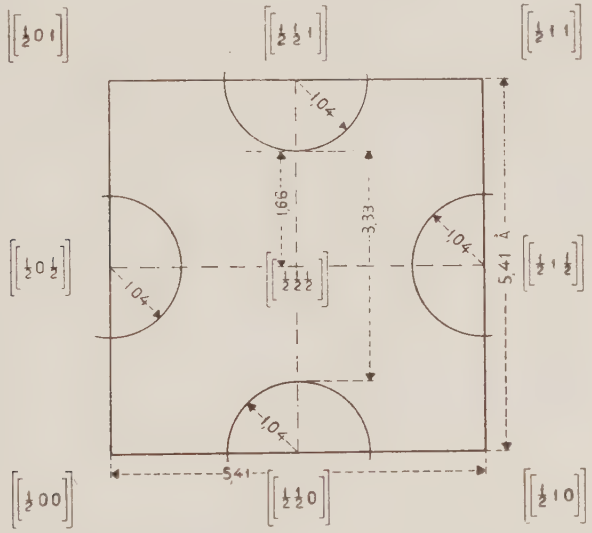

Fig. 2. – Sezione (100), con i raggi delle sfere d'azione e loro posizioni reticolari.

Inutile aggiungere che anche in questo caso, come per il gallio, l'entrata di due ioni In^{3+} nel reticolo della blenda, in qualunque posizione essi vadano a finire, sia ottaedrica che tetraedrica, implica sempre la formazioni di posizioni reticolari libere. E precisamente comparirà una buca tetraedrica se i due In vanno ambedue in posizioni prima occupate da due Zn, mentre, se ambedue vanno ad occupare una buca ottaedrica, tre dovranno essere le posizioni reticolari libere formatesi contemporaneamente. Se infine un In s'introduce in una buca ottaedrica e l'altro in una tetraedrica a sostituire Zn, due dovranno essere le posizioni reticolari libere che in definitiva verranno a formarsi.

Dal confronto dei due tipi di meccanismi, relativi alla sostituzione gallio-zinco e indio-zinco, risulta evidente l'esistenza di una notevole differenza fra di essi; è logico quindi cercare proprio in questa differenza la giustificazione del diverso comportamento di gallio e indio come costituenti minori nei confronti della blenda, come abbiamo già avuto occasione di notare.

Infatti, l'entità di una sostituzione isomorfa è funzione di vari fattori: fra questi la concentrazione dell'elemento vicariante nella soluzione a contatto con il cristallo in via di formazione, la temperatura e la pressione dell'ambiente. Ma bisogna inoltre tener conto di un altro fattore di notevole impor-

tanza e cioè del contributo all'energia reticolare portato dall'entrata di un elemento estraneo in un determinato reticolo cristallino. Questo contributo indica la maggiore o minor facilità di una certa sostituzione e venne indicato con E da WICKMAN ([12]), che introdusse nella geochimica questo concetto, riprendendo e precisando un'idea di FERSMAN. In altri termini quanto più elevato sarà E in valore assoluto tanto maggiore sarà la facilità della sostituzione.

Ora, se per due diversi costituenti minori, differenti sono questi valori di E nei riguardi di uno stesso reticolo, ne viene di conseguenza che differente dovrà essere la temperatura in cui si hanno i massimi di concentrazione degli elementi vicarianti, senza parallelismo tra le loro quantità.

Quindi, essendo diverso per gallio e indio il meccanismo di sostituzione e conseguentemente il contributo all'energia reticolare portato dai due elementi, risulta spiegato il non parallelismo osservato nei tenori di essi nelle blende di differenti condizioni genetiche. E quindi rimane altresì spiegata la dipendenza, con funzioni a diverso andamento, di tali valori delle concentrazioni dalle condizioni termodinamiche.

Rimane infine da prendere in considerazione un'altra possibilità, basata su eventuali trasformazioni nucleari, per spiegare la presenza dell'indio nella blenda.

Infatti l'indio possiede due isotopi naturali stabili e precisamente ^{113}In e ^{115}In con abbondanze percentuali rispettivamente di 4.23% e di 95.77% ([13]). Ambedue questi isotopi sono rispettivamente membri di coppie di isobari adiacenti ^{113}Cd-^{113}In e ^{115}In-^{115}Sn: ma l'esistenza di queste coppie sarebbe a rigore esclusa dalla regola di MATTAUCH, la quale stabilisce l'impossibilità di esistenza per coppie di isobari che differiscono per una unità nel numero di protoni. Di conseguenza, se tale regola avesse validità generale, nel caso ora in esame sarebbe necessario ammettere che uno dei nuclei in ciascuna coppia sia instabile e quindi presenti un decadimento radioattivo. In questo senso vari autori hanno cercato di accertare le relazioni di stabilità esistenti nell'ambito di tali coppie di isobari e di individuare in quale verso avvenga la trasformazione nucleare.

A questo riguardo le opinioni sono notevolmente contrastanti in quanto taluni, in base a considerazioni di abbondanza relativa, sostengono che abbia luogo la trasformazione $^{115}In \rightarrow {}^{115}Sn$, mentre altri ritengono, in relazione a determinazioni di massa e di stabilità nucleare, che ^{115}Sn sia il nucleo instabile e decada in ^{115}In per cattura di un elettrone.

In riferimento a questa incertezza, appariva notevolmente interessante l'osservazione dell'eventuale presenza di indio in minerali contenenti stagno e di un'eventuale variazione del rapporto In/Sn, in funzione del tempo.

([12]) F. E. WICKMAN: *Geol. För. Stockholm Förh.*, **65**, 371 (1943).
([13]) K. RANKAMA: *Isotope Geology* (London, 1954).

A tale proposito, dato che lo stagno è molte volte presente quale costituente minore della blenda, lo ricercai in un numero notevole di campioni di essa, in cui avevo in antecedenza dosato l'indio, e lo rintracciai in parecchi di essi: ebbi perciò agio, in base a questi risultati ed a quelli ottenuti nella determinazione dell'indio, di cercare un possibile legame tra il contenuto dei due elementi in questione. L'esito fu completamente negativo e fui quindi indotto a concludere che non esisteva assolutamente alcun parallelismo, nè regolarità di sorta nel contenuto in questi due elementi. Tale mia conclusione bene si accorda con le deduzioni di Itzikson e Rusanov [14], Ahrens [15], Ahrens e Liebenberg [16], i quali misero in evidenza come, in generale, minerali di stagno anche di formazione molto antica non rivelassero altro che tracce di indio, tali cioè da non giustificare un'eventuale genesi di ^{115}In per decadimento radioattivo.

Le conclusioni dei predetti autori, in pieno accordo con le mie, abbondantemente documentate sperimentalmente, vengono poi a trovarsi in netto contrasto con le idee di Eastman [17], che ammetteva l'esistenza di una relazione genetica tra i due nuclei a causa dell'erronea presunzione di un parallelismo tra i tenori di In e Sn.

Certamente, qualunque sia il verso della trasformazione, questa deve avvenire con una velocità di decadimento molto piccola (periodo di semitrasformazione dell'ordine di grandezza di 10^{12}-10^{14} anni), e quindi, in ogni caso, difficilmente considerazioni di carattere puramente geochimico potranno risolvere la delicata questione in un senso o nell'altro. E questo sia per l'esiguità delle quantità dei nuclei originati anche in tempi molto grandi, sia per l'analogia di comportamento geochimico esistente, in certe condizioni, tra i due elementi, analogia che può provocare un parallelismo tra il contenuto dei due elementi nella blenda in maniera del tutto indipendente da fenomeni di trasformazioni nucleari.

Per quel che riguarda poi l'altra coppia di isobari ^{113}Cd-^{113}In si potrebbero fare considerazioni analoghe alle precedenti, poichè anche in questo caso non si è riusciti a stabilire quale sia il nucleo instabile.

Ad ogni modo, nelle blende analizzate, ho cercato un possibile legame tra il contenuto in indio e quello in cadmio, ma non sono riuscito, nonostante il numero notevole di casi esaminati, a stabilire alcun parallelismo, e sarei perciò propenso a concludere che fra i due elementi non debba esistere rapporto alcuno di interdipendenza genetica.

([14]) M. I. Itzikson e A. K. Rusanov: *Compt. Rend. Acad. Sci. U.R.S.S.*, **53**, 631 (1946).

([15]) L. H. Ahrens: *Nature*, **162**, 413 (1948).

([16]) L. H. Ahrens e W. R. Liebenberg: *Amer. Min.*, **35**, 571 (1950).

([17]) E. D. Eastman: *Phys. Rev.*, **52**, 1226 (1937).

Ora, poichè anche il cadmio può essere un costituente minore della blenda, soltanto la determinazione della costituzione isotopica del cadmio e dell'indio in blende di differenti età e l'eventuale variazione delle abbondanze percentuali del ^{113}Cd e del ^{113}In potrà dare la chiave di volta per la soluzione del delicato problema.

SUMMARY

From the experimental results previously obtained on the abundance and diffusion of gallium and indium in samples of sphalerite with different modes of occurrence, it has been possible to relate the temperature of genesis to the diadochy of gallium, indium, and zinc in sphalerite. This correlation has been derived from structural considerations. One of the most important results obtained is an explanation of the dissimilar behaviour of gallium and indium with respect to sphalerite. Finally, a discussion of the possibility of the genesis of indium *in loco* through nuclear transformations is included.

Calcolo quantomeccanico della barriera di potenziale per la inversione della molecola di fosfina.

M. Simonetta e A. Vaciago

Istituto di Chimica Industriale, Laboratorio di Chimica Fisica e Fisica Tecnica Università di Milano

(ricevuto il 22 Ottobre 1956)

Riassunto. — È stato calcolato mediante la teoria degli orbitali molecolari nella consueta approssimazione L.C.A.O. l'andamento della barriera di potenziale per l'inversione della molecola di fosfina. Sono stati quindi discussi gli effetti di questa barriera sugli spettri di rotazione e di vibrazione.

Recentemente è stato eseguito da Wheland e Chen [1] un calcolo quantomeccanico, nella consueta forma M.O.-L.C.A.O. e in due diverse approssimazioni dimostratesi equivalenti, dell'altezza della barriera di potenziale per l'inversione della molecola di ammoniaca. In tale calcolo entrano due parametri empirici: i loro valori sono stati determinati in modo che, esprimendo l'energia della molecola in funzione dell'angolo $\varphi = \widehat{HNH}$, tale energia risultasse minima per $\varphi_0 = 107^\circ$ (valore sperimentale [2]) e che l'altezza della barriera di potenziale riproducesse il valore determinato in base ai dati spettroscopici [3,4], di circa 6 kcal/mole. D'altra parte l'attendibilità del metodo di calcolo proposto è suffragata dal fatto che non solo l'altezza della barriera di potenziale, ma l'intero andamento della curva dell'energia in funzione dell'angolo φ coincide con il dato ricavato dall'esperienza e che è pure riprodotto con

---

[1] G. W. Wheland e P. S. K. Chen: *Journ. Chem. Phys.*, **24**, 67 (1956).

[2] G. Herzberg: *Molecular Spectra and Molecular Structure*. Vol. II: *Infrared and Raman Spectra of Polyatomic Molecules* (New York, 1945), p. 439.

[3] D. M. Dennison e G. E. Uhlenbeck: *Phys. Rev.*, **41**, 313 (1932).

[4] M. F. Manning: *Journ. Chem. Phys.*, **3**, 136 (1935).

sufficiente precisione il salto di energia tra gli stati trivalenti dell'atomo di azoto con configurazione $2s^2 2p^3$ e $2s^1 2p^4$.

Abbiamo pertanto ritenuto interessante applicare alla fosfina un metodo di calcolo analogo, però nella sola approssimazione in cui gli integrali di sovrapposizione S_{ij} sono posti uguali a zero per $i \neq j$ quando compaiono moltiplicati per i valori w_n dell'energia. Infatti gli spettri di rotazione e di vibrazione della fosfina, anche con le alte risoluzioni oggi raggiungibili, non solo non permettono di poter ricavare un valore sperimentale dell'altezza della barriera di potenziale per l'inversione, ma nemmeno di decidere se tale inversione sia possibile ([5,6]).

La geometria adottata per la molecola è la seguente ([7]): P — H = 1.421 Å; $\widehat{HPH} = \varphi_0 = 93°27'$; gruppo di simmetria C_{3v}.

L'energia del sistema è risultata espressa dalla formula:

$$W = 8\alpha + 2kf(\varepsilon, \delta, \varphi)\,, \tag{1}$$

dove α è l'integrale di Coulomb per l'orbitale $1s$ dell'atomo di idrogeno, k il rapporto, considerato costante, tra gli integrali di scambio e i corrispondenti integrali di sovrapposizione, ε è la differenza, misurata in unità k, tra l'integrale di Coulomb per un orbitale $3p$ dell'atomo di fosforo e α, mentre δ è la differenza, sempre in unità k, tra l'integrale di Coulomb per un orbitale $3s$ dell'atomo di fosforo e α. In Appendice è riportata l'espressione analitica della funzione f.

Poichè l'altezza della barriera di potenziale ΔW è data dalla differenza tra i valori di W per $\varphi = 120°$ e $\varphi = \varphi_0$, dove φ_0 è l'angolo di equilibrio, e poichè è $\varepsilon = 69.50/k$ e $\delta = -1.4245\varepsilon$ (*), si vede come questa grandezza dipenda unicamente dal valore assegnato a k.

Un primo calcolo eseguito assumendo per k il valore di -259 kcal/mole, ottenuto da Wheland e Chen per l'ammoniaca, e ricavando il valore di $\varphi = \varphi_0$ per cui l'energia del sistema fosse minima, ha portato ai seguenti risultati:

$$\varphi_0 = 101°39'\,, \qquad \Delta W = 20.33 \text{ kcal/mole} = 7\,110 \text{ cm}^{-1}.$$

L'andamento della barriera di potenziale in funzione di φ è rappresentato

---

([5]) C. C. Loomis e M. W. P. Strandberg: *Phys. Rev.*, **81**, 798 (1951).

([6]) M. E. Sirvetz e R. E. Weston: *Journ. Chem. Phys.*, **21**, 898 (1953).

([7]) C. H. Townes e A. L. Schawlow: *Microwave Spectroscopy* (New York, 1955), p. 53.

(*) Le differenze tra gli integrali di Coulomb dei vari atomi sono state considerate come approssimativamente eguali alle differenze tra gli opportuni potenziali di ionizzazione, prendendo questi dalle tabelle di Skinner e Pritchard ([8]).

([8]) H. A. Skinner e H. O. Pritchard: *Trans. Faraday Soc.*, **49**, 1254 (1953).

dalla curva 1 di fig. 1, dove sull'asse delle ordinate V rappresenta il potenziale definito da $V(\varphi) - W(\varphi) - W(\varphi_0)$, mentre sull'asse delle ascisse è riportata l'altezza h della piramide, il cui valore è legato a quello di φ da una semplice relazione geometrica.

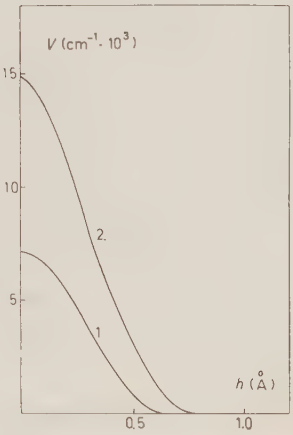

Fig. 1. - Barriera di potenziale per la inversione della molecola di fosfina.

Con questa barriera di potenziale abbiamo calcolato (*) lo sdoppiamento dei livelli energetici vibrazionali (per la vibrazione $\nu_2 = 991$ cm^{-1}, che regola l'inversione ([10])) dello stato fondamentale e del primo stato eccitato, rispettivamente Δ_0 e Δ_1. I risultati sono:

$$\Delta_0 = 5.27 \cdot 10^{-9} \text{ cm}^{-1},$$

$$\Delta_1 = 6.71 \cdot 10^{-7} \text{ cm}^{-1}.$$

Il tempo d'inversione τ, definito come $\tau = (1/2)(1/\Delta_0 c)$, dove Δ_0 è espresso in cm^{-1} e c in cm$\cdot$s^{-1}, risulta essere di $3.16 \cdot 10^{-3}$ s.

Lo sdoppiamento delle righe dello spettro vibrazionale è $\Delta\nu_v = \Delta_0 + \Delta_1$ e quello delle righe dello spettro rotazionale puro è $\Delta\nu_r = 2\Delta_0$.

Un calcolo dell'altezza e dell'andamento della barriera di potenziale nelle molecole NH_3, PH_3, e AsH_3 basato sulle costanti di forza vibrazionali è stato eseguito da COSTAIN e SUTHERLAND ([11]). Per la fosfina questi autori hanno ottenuto un valore di ΔW di 17.45 kcal/mole o 6085 cm^{-1}, non molto lontano dal nostro. L'accordo tra i due risultati è per altro più apparente che reale. Innanzi tutto COSTAIN e SUTHERLAND hanno adottato una geometria della molecola basata su vecchi dati ([12]): P — H 1.46 Å e $\widehat{HPH} = 100°30'$. Adot-

---

(*) Il metodo di calcolo da noi seguito è essenzialmente quello di DENNISON e UHLENBECK ([3]), riportato anche da TOWNES e SCHAWLOW ([9]). Per la massa ridotta abbiamo adottato l'espressione, valida per P — H costante, $\mu = \dfrac{3m(M + 3m\cos^2\vartheta_0)}{3m + M}$, dove m e M sono rispettivamente le masse atomiche dell'idrogeno e del fosforo e ϑ_0 è l'angolo, all'equilibrio, tra un legame P — H e l'asse di simmetria ternaria della molecola. L'energia di punto zero è stata grossolanamente valutata dai valori osservati delle frequenze di vibrazione.

([9]) C. H. TOWNES e A. L. SCHAWLOW: loc. cit., cap. 12.

([10]) G. HERZBERG: loc. cit., pag. 110 e 223.

([11]) C. C. COSTAIN e G. B. B. M. SUTHERLAND: *Journ. Phys. Chem.*, **56**, 321 (1952).

([12]) G. B. B. M. SUTHERLAND, E. LEE e CHENG-KAI WU: *Trans. Faraday Soc.*, **35**, 1373 (1939).

tando invece la geometria da noi accettata, una valutazione approssimativa dell'altezza della barriera di potenziale con il metodo di questi autori porta a un valore di 9400 cm^{-1}. Inoltre i valori calcolati con questo procedimento dipendono in modo assai sensibile dai valori delle costanti di forza ([6]), e mentre nel caso dell'ammoniaca questi ultimi sono stati determinati dalle frequenze normali corrette per l'anarmonicità, nel caso della fosfina sono state usate le frequenze osservate.

Poichè il metodo con il quale Wheland e Chen hanno determinato k per l'ammoniaca comporta che nel valore di questo parametro si accumulino gli effetti delle varie approssimazioni insite nel calcolo, e poichè per orbitali di diverso numero quantico principale i coefficienti di proporzionalità tra integrale di scambio e integrale di sovrapposizione non hanno necessariamente valori all'incirca eguali, ci è sembrato più attendibile il procedimento di adottare per k il valore che rendesse minima l'energia del sistema per $\varphi_0 = \varphi_{0sp}$. In questo modo risulta:

$$k = -166.3 \text{ kcal/mole}, \qquad \Delta W = 42.48 \text{ kcal/mole} = 14\,866 \text{ cm}^{-1}.$$

La nuova curva $V = V(h)$ è pure riportata in fig. 1 (curva 2). È risultato inoltre:

$$\Delta_0 = 1.94 \cdot 10^{-16} \text{ cm}^{-1}, \qquad \Delta_1 = 1.33 \cdot 10^{-14} \text{ cm}^{-1},$$

$$\tau \doteq 1 \text{ giorno}.$$

I risultati ottenuti indicherebbero come non sia possibile rilevare sdoppiamento di righe sia nello spettro di vibrazione, sia in quello di rotazione della fosfina.

Infatti lo spettro di rotazione pura dato da Wright e Randall ([13]) non presenta alcuno sdoppiamento, come non lo presentano le più recenti determinazioni in microonde ([5,6]): il potere risolutivo degli strumenti usati in queste ultime misure permette di affermare che in ogni caso il valore di Δ_0 è inferiore a 0.5 MHz $= 1.67 \cdot 10^{-5}$ cm $^{-1}$, mentre le esperienze di Wright e Randall permettevano solo di affermare che il valore di Δ_0 era inferiore a 0.4 cm^{-1}. Nello spettro di vbrazione riportato da Lee e Wu ([14]) era stato rilevato uno sdoppiamento, proprio per la frequenza ν_2 che regola l'inversione (la frequenza ν_3 di questi autori corrisponde alla nostra ν_2), ma questo sdoppiamento è stato successivamente riconosciuto spurio ([15]).

I nostri risultati sembrano indicare la possibilità di ottenimento di isomeri

---

([13]) N. Wright e H. M. Randall: *Phys. Rev.*, **44**, 391 (1933).
([14]) E. Lee e Cheng-Kai Wu: *Trans. Faraday Soc.*, **35**, 1366 (1939).
([15]) H. H. Nielsen: *Discussions Faraday Soc.*, **9**, 85 (1950).

otticamente attivi del tipo $PR'R''R'''$, soprattutto con gruppi R notevolmente pesanti.

Riteniamo opportuno sottolineare il carattere semiempirico dei valori riportati nel presente lavoro. Un più accurato calcolo per l'ammoniaca è stato recentemente pubblicato da Cohan e Coulson [16] e potrebbe forse essere utilmente esteso alla molecola di fosfina. Inoltre, poichè spesso l'atomo di fosforo usa nella formazione di legami covalenti orbitali ibridi di tipo *spd* [17], si può pensare che in una più accurata trattazione del problema si dovrebbe includere il contributo degli orbitali *3d* dell'atomo di fosforo: l'uso di soli orbtali leganti tipo *sp*, fatto nel presente lavoro, è però basato anche sui risultati ottenuti da Muller, Lanterbur e Goldenson [18] con misure di risonanza magnetica nucleare sulla fosfina e su altri composti di tipo PX_3.

Appendice

L'espressione analitica della $f = f(\varepsilon, \delta, \varphi)$ che compare nella (1), tenuto conto della relazione $\delta = -1.4245\varepsilon$, è la seguente:

$$f(\varepsilon, \varphi) = 2\{C + A^{-1} \sin (60^\circ - \tfrac{1}{3} \arcsin \tfrac{1}{2} A^3 F) + b\} ,$$

dove:

$$C = \{\varepsilon^2/4 + 0.2689(1 - \cos\varphi)\}^{\frac{1}{2}} ,$$

$$A = \{\tfrac{1}{3}(1.0370 + 1.4846\varepsilon^2 + 0.5379 \cos\varphi)\}^{-\frac{1}{2}} ,$$

$$F = -\varepsilon(0{,}2072\varepsilon^2 - 0.6901 \cos\varphi + 0.5317) ,$$

$$b = 0.3585\varepsilon .$$

---

[16] N. V. Cohan e C. A. Coulson: *Trans. Faraday Soc.*, **52**, 1163 (1956).

[17] L. Pauling e M. Simonetta: *Journ. Chem. Phys.*, **20**, 29 (1952).

[18] N. Muller, P. C. Lanterbur e J. Goldenson: *Journ. Am. Chem. Soc.*, **78**. 3557 (1956).

SUMMARY

A quantum-mechanical calculation of the potential barrier restricting inversion in phosphine is given, and the related doubling effects are discussed.

On the Cosmic Ray Penetrating Showers Underground (*).

S. Higashi, T. Oshio, H. Shibata, K. Watanabe and Y. Watase

Osaka City University - Osaka, Japan

(ricevuto l'8 Novembre 1956)

Summary. — In 218.5 h of receptive time, 13 penetrating showers were obtained with a large multiplate cloud chamber, at the depth 50 m w.e. from the top of the atmosphere. Five of these showers were produced in lead plates in the chamber. The rate of the number of penetrating showers produced by secondary rays (probably π-mesons) to that by primary rays (probably μ-mesons) is turned out to be $\frac{2}{3} \sim \frac{1}{1}$. Therefore it seems impossible to neglect the contributions of secondary particles to the production of penetrating showers underground. The apparent cross section of μ-mesons for the penetrating shower production is estimated as $(0.5 \pm 0.3) \cdot 10^{-30}$ cm^2/nucleon and the interaction mean free path of secondaries is (157 ± 90) g/cm^2.

Preliminary results are summarized on the study of cosmic ray penetrating showers underground with a multiplate cloud chamber. Nuclear interactions underground have so far been studied by means of nuclear emulsions [1] and counter hodoscopes [2,3]. Only a few cloud chamber studies have been reported on the penetrating showers [5,6] which were obtained along with other

(*) This work has been supported in part by a Grant from the Aid for Fundamental Scientific Research (Institutional Research) from the Ministry of Education.

(1) E. P. George and J. Evans: *Proc. Phys. Soc.* (*Lond.*), A **63**, 1248 (1950); A **68**, 829 (1955).

(2) P. E. Argan, A. Gigli and S. Sciuti: *Nuovo Cimento*, **11**, 530 (1954).

(3) D. Kessler and R. Maze: *Physica*, **22**, 69 (1956).

(4) S. Higashi, I. Higashino, M. Oda, T. Oshio, H. Shibata, K. Watanabe and Y. Watase: *Journ. Phys. Soc., Japan*, **11**, 1021 (1956).

(5) A. Lovati, A. Mura, C. Succi and G. Tagliaferri: *Nuovo Cimento*, **10**, 1201 (1953).

(6) H. J. J. Braddick and B. Leontic: *Phil. Mag.*, **45**, 1287 (1954).

phenomena, for instance A.P.P. (7). The « penetrating showers » are defined to be such events from which two or more penetrating particles originated, where penetrating particles are those that penetrate two or more lead plates (1 cm thick) in the cloud chamber without both multiplication and remarkable scattering and produce minimum ionizing tracks in the chamber. They are being observed at the depth of 50 m w.e. from the top of the atmosphere (in the Isohama Tunnel, Yaizu), the mean energy and the median energy of μ-mesons at this depth being 16.5 GeV and 7.4 GeV respectively (*).

The experimental arrangement is shown schematically in Fig. 1. The cloud chamber has a sensitive volume of $80 \times 70 \times 40$ cm^3 and contains 15 lead plates, each having the thickness of 1 cm, and the total amount of lead is about one geometrical m.f.p. The cloud chamber was triggered by coincidences « $(A \geqslant 1) \cdot (B \geqslant 2) \cdot (C \geqslant 2) \cdot (D \geqslant 2)$ ». All counters were « hodoscoped » and cloud chamber photographs were taken stereoscopically with two cameras. A lead layer of 10 cm thickness was set over the chamber.

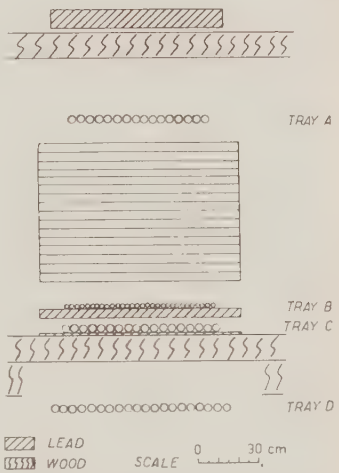

Fig. 1. – Schematic arrangement of the cloud chamber, the counter trays and the lead layers. The cloud chamber involves 15 lead plates, each of which having the thickness of 1 cm. The illuminated region of the chamber is $80 \times 70 \times 40$ cm^3. The thick lead layer on top is of $80 \times 10 \times 40$ cm^3 and is employed as a producer of penetrating showers. The sizes and the number of counters used in each tray are as follows:

Tray	Size	No. of counters
A	4 cm $\Phi \times$ 40 cm	16
B	2 cm $\Phi \times$ 50 cm	30
C	4 cm $\Phi \times$ 40 cm	18
D	4 cm $\Phi \times$ 120 cm	20

(7) See for example, V. Appapillai, A. W. Mailvaganam and A. W. Wolfendale: *Phil. Mag.*, **45**, 1059 (1954).

(*) These values were estimated from the Depth-Intensity relation, cited in the E. P. George's title (in the *Progress in Cosmic Ray Physics*, **1** (Amsterdam, 1952)) with the range-energy relation of μ-mesons in rock ($Z = 10$ and $A = 20$). Here it must be remarked that the μ-meson spectrum is represented by a decreasing function of the energy and the energy dependence of cross section of a μ-meson for nuclear interaction has been unknown.

In 218.5 hours of receptive time, 13 penetrating showers were obtained. They were classified in Table I according to the number of penetrating particles which simultaneously entered into the chamber. Five of these showers were produced in lead plates in the chamber, and details of them are listed in Table II.

Three cases of them are produced by single penetrating particles which may be recognized as single μ-mesons considering the geometrical conditions of the experiment as well as the contribution of shower secondaries to the reproduction of penetrating showers described below. Two of them are shown

TABLE I. – *Number of incident particles which appear in a picture and of their occurrence.*

No. of incident p.p.s.	No. of pictures	Items	
		Penetrating showers (1)	Stars (2)
0	218	1 (3)	0
1	315	4+1 Fe (4)	0
2	31	1+1 (5)	1
3	4	2+1 (Pb) (6)	0
4	1	0	0
5	1	0	0
6	2	0	2
7	1	0	0
8	0	0	0
9	1	0	0
≥ 10	0	0	0

(1) No. of pictures which include some nuclear interactions having two or more secondary penetrating particles.

(2) No. of pictures which include some stars having less than two penetrating particles and some heavily ionizing tracks.

(3) The origin of the shower was on the boundary of the illuminated region, so that the primary could not possibly appear in the illuminated region.

(4) A penetrating shower was produced in the iron ceiling of the cloud chamber.

(5) There were produced three cascade showers, each being a photon-initiated one, as well as a secondary penetrating particle in a nuclear interaction, which may be considered as the production of neutral π-mesons.

(6) Secondaries of a penetrating shower produced in the lead layer over the cloud chamber.

in Photo's 1 and 2. Photo 1 shows three cascade showers produced together with the penetrating secondaries. Concerning the two of these cascade showers farthest to the right, their energies and the angle between their axes are estimated to be about 400 MeV, 200 MeV and about 29 degrees, which satisfies the expected relation between two cascade showers resulting from the decay photons of a neutral π-meson. Therefore, the phenomenon

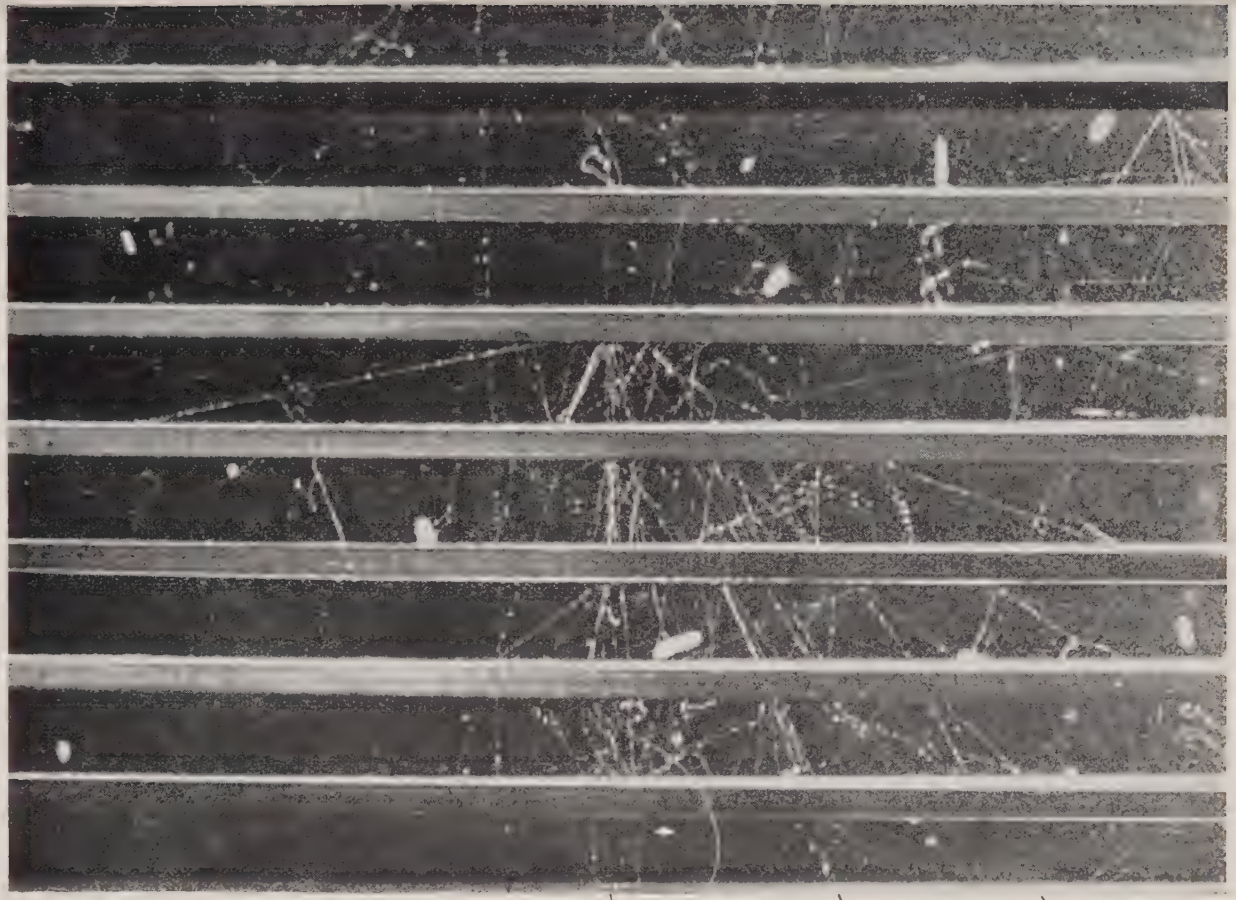

Photo 1. A penetrating shower underground produced by a single penetrating particle. Cascade showers 1, 2 and 3 have energies of about 600, 400 and 200 MeV respectively, the two most to the right of which indicate the existence of neutral π-meson (see the text). One of the secondary charged particles gives rise to a star after the traversal of a lead plate. Track 4 corresponds to such particles as have entered into the chamber before the incidence of the parent of the shower.

Photo 2. – A penetrating shower underground produced by a single incident particle (cf. Table II).

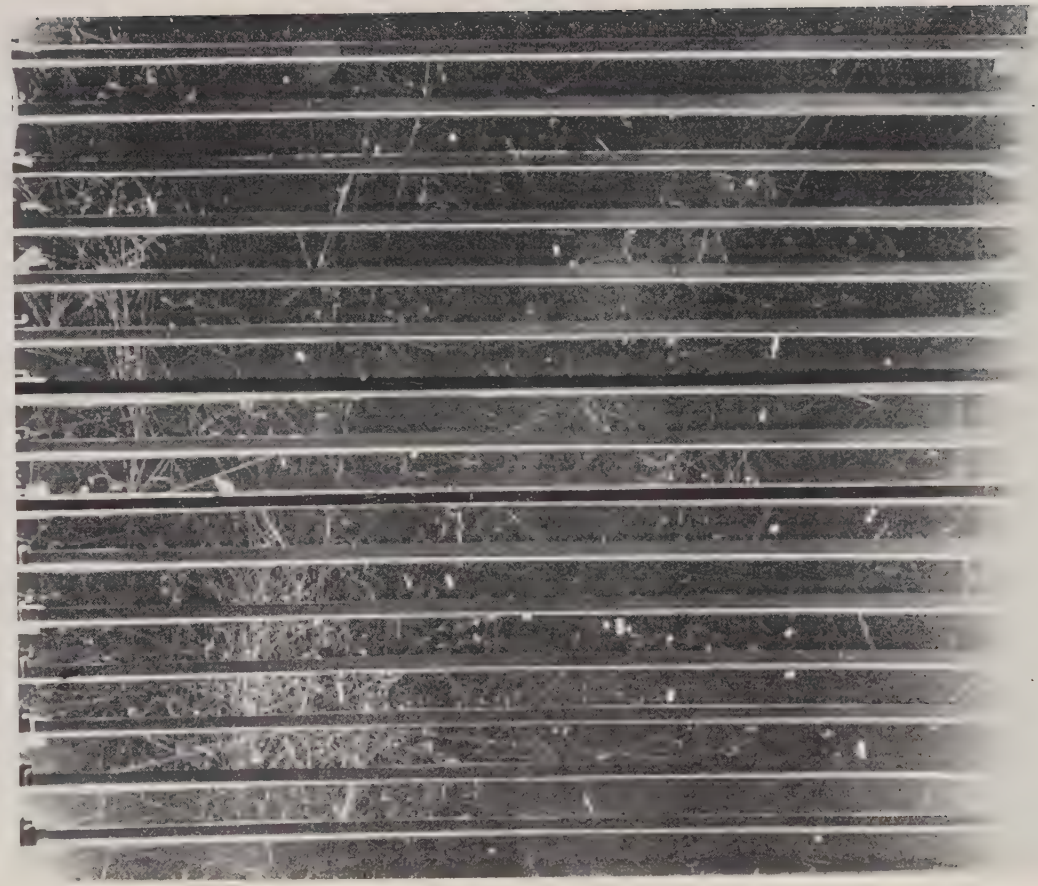

Photo 3. An event showing two cascade showers and three penetrating showers produced by the secondaries of a penetrating shower occurring in the overlaying rock (see the text).

Photo 4. – A penetrating shower produced by an incident penetrating particle which associated with the other two penetrating particles (cf. Table II).

TABLE II. *Details of five penetrating showers produced in the lead plates of the chamber.*

No. of incident p.p.s.	No. of secondaries			Secondary interactions	References
	Thin	Heavy	Cascade showers		
1	7	1	3	1 star 1 stopping (+)	Photo 1 (*)
1	6	0	1	1 stopping	Photo 2
1	4	0	1		
$\geqslant 3$	14	2	2	2 stars	Photo 3 (*)
3	4	1	0		Photo 4

(*) See the text.

(+) Such a event that a penetrating particle producing a minimum ionizing track entered into a lead plate without coming out.

suggests the fact that μ-mesons also produce neutral π-mesons besides charged ones.

For the other two cases, shown in Photo's 3 and 4, their parents are accompanied with a number of penetrating particles. Photo 3 shows two cascade showers (of about 2 GeV energy and about 0.6 GeV energy) and more than such three penetrating particles simultaneously falling onto the chamber as produce three secondary penetrating showers ($2+14$p, $2+3$p and $1+3$n) (*). Probably these cases provide examples of successive penetrating shower production by secondary particles of penetrating showers produced in the overlaying rock above the chamber.

The ratio of the number of penetrating showers produced by secondary rays to those produced by single rays (probably μ-mesons) is tentatively obtained to be $\frac{2}{3} \sim \frac{1}{1}$ from these experimental data. Therefore it seems impossible to neglect the contributions of secondary particles to the production of penetrating showers underground, as suggested by KITAMURA and ODA [8], whereas it has so far been assumed that almost all sources of penetrating showers underground are μ-mesons.

The apparent cross-section of μ-mesons for the penetrating shower production is estimated as $(0.5 \pm 0.3) \cdot 10^{-30}$ cm^2/nucleon from the events due to the single incident particles without association of penetrating particles as described above.

The interaction m.f.p. of secondaries of penetrating showers produced by

(*) Here is used the nomenclature of the emulsion work.

(8) T. KITAMURA and M. ODA: *Prog. Theor. Phys.*, **16**, 250 (1956).

single penetrating particles is 157 $\pm$ 90 g/cm^2 (*), and it is not inconsistent with the geometrical interaction m.f.p. in lead.

* * *

The authors wish to express their appreciation to the Shizuoka Railway Operating Divisional Office for permitting them to make the observations in the Isohama Tunnel. The authors also wish to thank the Institute for Food Chemistry for the financial aid.

(*) This value was obtained from the following data. Total shower secondaries of minimum ionizing tracks have penetrated 42 lead plates of 1 cm thickness. Along with them there have been observed one star production and two stoppings of the minimum ionizing secondaries incident into lead plates without coming out.

RIASSUNTO (*)

In una grande camera a nebbia munita di numerosi setti, in 218.5 h di funzionamento effettivo sono stati ottenuti 13 sciami penetranti alla profondità di 50 m a.e. dalla sommità dell'atmosfera. 5 di tali sciami furono prodotti nelle piastre di piombo della camera. Il rapporto del numero degli sciami penetranti prodotti dai secondari (probabilmente mesoni π) a quello degli sciami prodotti dai primari (probabilmente mesoni μ) risulta essere $\frac{2}{3} \div \frac{1}{1}$. Sembra pertanto impossibile trascurare il contributo delle particelle secondarie alla generazione degli sciami penetranti sotto la superficie del suolo. La sezione d'urto apparente dei mesoni μ per la produzione di sciami penetranti è stimata in $(0.5 \pm 0.3) \cdot 10^{-30}$ cm^2/nucleone e il cammino libero medio d'interazione dei secondari è (157 ± 90) g/cm^2.

(*) *Traduzione a cura della Redazione.*

On the Multiple Penetrating Particles Underground (*).

S. Higashi, T. Oshio, H. Shibata, K. Watanabe and Y. Watase

Osaka City University - Osaka, Japan

(ricevuto l'8 Novembre 1956)

Summary. — Penetrating showers have been observed at the depth of 50 m w.e. from the top of the atmosphere by means of a large multiplate cloud chamber, the sensitive volume of which is $80\times70\times40$ cm^3 and which contains 15 lead plates of the thickness of 1 cm each. In 218.5 hours of receptive time, four events each involving from 4 to 9 parallel penetrating particles falling onto the cloud chamber simultaneously were observed in addition to a number of penetrating showers. The parallel penetrating particles show neither nuclear interaction with lead nuclei nor appreciable scattering in the lead plates. It is considered that these events consist of μ-mesons having energies higher than 0.5 GeV at this depth. They were named the « Multiple Penetrating Particles » (M.P.P.), about which following conclusions were obtained: i) If they are the secondary particles of large penetrating showers produced in the overlaying rock over the apparatus, the statistical hypothesis that the origin of the shower is within 6 m over the apparatus can be abandoned with a significant level smaller than 0.01. The multiplicity of π-mesons produced in such a shower would be more than 300, even if all the secondaries, undergoing absorption with a mean free path $\lambda=145$ g/cm^2 ($=2\lambda_{gr}$, λ_{gr}: geometrical interaction mean free path in rock), decayed into μ-mesons. ii) If they belong to the penetrating component of air showers which traverse the earth down to this depth, the size and the frequency of those events cannot be interpreted on the assumption of the flat structure function of the penetrating component as usually employed.

1. – Introduction.

Almost all of the investigations on the cosmic-ray penetrating showers underground have been carried out with nuclear emulsions (1) or counter hodo-

(*) This work has been supported in part by a Grant from the Aid for Fundamental Scientific Research (Institutional Research) from the Ministry of Education.

(1) E. P. George and J. Evans: *Proc. Phys. Soc. (Lond.)*, A **63**, 1248 (1950); A **68**, 829 (1955).

scopes ([2-4]). Cloud chamber have been adopted by various authours for the observations of the anomalous large angle scattering ([5]) and the associated penetrating particles ([6]). Cloud chamber photographs of penetrating showers have been taken in the course of these observations ([6,7]). The total number of these photographs so far obtained is not very great because of the small cross-section for the production of these showers.

A large multiplate cloud chamber has been constructed in order to increase the statistics of the events concerned and to observe the whole features of events. The observation was carried out from November to December, 1955, at the depth of 50 m w.e. from the top of the atmosphere in the disused Isohama Tunnel of Government Railway, Yaizu, Shizuoka Prefecture, Japan, geomagnetic latitude 25° N, 15 m above sea level.

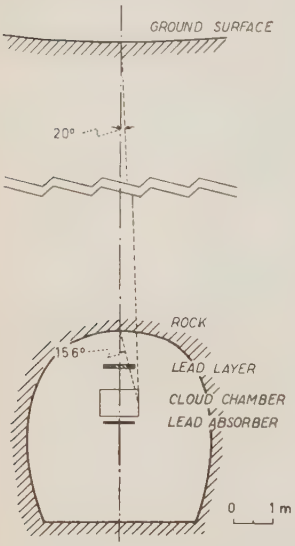

Fig. 1. – Situation of the cloud chamber in the tunnel.

In the course of the observation of 218.5 hours, there were observed four events each of which showed from 4 to 9 parallel penetrating particles falling simultaneously onto the chamber besides 13 nuclear interactions (*). These events named « Multiple Penetrating Particles » (M.P.P.) are analyzed in this paper.

2. – Apparatus (+) and Experimental Procedure.

The geometrical condition of the apparatus is shown in Fig. 1. The apparatus was located at the depth of 15 m rock (50 m w.e. from the top

([2]) P. E. Argan, A. Gigli and S. Sciuti: *Nuovo Cimento*, **11**, 530 (1954).

([3]) D. Kessler and R. Maze: *Physica*, **22**, 69 (1956).

([4]) S. Higashi, I. Higashino, M. Oda, T. Oshio, H. Shibata, K. Watanabe and Y. Watase: *Journ. Phys. Soc. Japan*, **11**, 1021 (1956).

([5]) See, for example, J. L. Lloyd and A. W. Wolfendale: *Proc. Phys. Soc. (Lond.)*, A **68**, 1045 (1955).

([6]) See, for example, H. J. J. Braddick and B. Leontic: *Phil. Mag.*, **45**, 1287 (1954).

([7]) A. Lovati, A. Mura, C. Succi and G. Tagliaferri: *Nuovo Cimento*, **10**, 1201 (1953).

(*) The results obtained on the penetrating showers will soon be published.

( ) The details on the construction of the cloud chamber and on the preliminary experiments will be published in *Journal of the Institute of Polytechnics, Osaka City University*.

of the atmosphere). In reference to the spectrum of μ-mesons at this depth, the median energy and the mean energy of μ-mesons were estimated (*) as 7.4 GeV and 16.5 GeV respectively. The minimum energy of μ-mesons capable of arriving at this depth in the vertical direction is about 10 GeV when they enter the ground. The experimental set-up consists of a cloud chamber and four trays of G.M. counters, as schematically shown in Fig. 2 Each counter is connected to a neon bulb whose resolving time for lighting is about 150 μs. The cloud chamber is triggered by coincidences « $(A \geqslant 1)\cdot(B \geqslant 2)\cdot(C \geqslant 2)\cdot$ $\cdot(D \geqslant 2)$ », the resolving time being about 15 μs.

The cloud chamber is of a pressure type and is filled with 1.5 atmospheric pressure of argon gas, which is saturated with the vapor of mixture of equal percentage of ethyl alcohol and iso-propil alcohol. It has a volume of $100 \times 70 \times 60$ cm^3 (sensitive volume: $80 \times 70 \times 40$ cm^3) and contains 15 nickel plated lead plates each of which has the thickness of 1 cm and is supported by an iron frame so that the bending is diminished. The sweeping voltage imposed alternatively upon the plates brings about the sweeping field of, on an average, 10 V/cm.

Two automatic operation cameras of 6×6 cm^2 size were mounted stereoscopically 2.3 metres apart from the front end of the chamber and the stereoscopic angle was 23.5°. Each lens has a focal length of 13.5 cm and an aperture of f 4.5, so that the de-

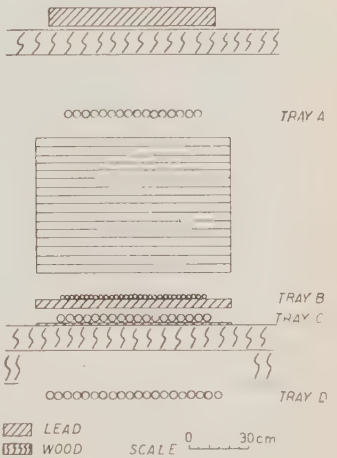

Fig. 2. – Schematic arrangement of the cloud chamber, the counter trays and the lead layers. The cloud chamber contains 15 lead plates, each of which is of 1 cm thickness. The illuminated region of the cloud chamber is $80 \times 70 \times 40$ cm^3. The thick lead layer on top is $80 \times 10 \times 40$ cm^3 and serves as a producer of penetrating showers.

The sizes and the number of counters used in each tray are as follows:

Tray	Size of a counter	No. of counters
A	4 cm $\Phi \times$ 40 cm	16
B	2 cm $\Phi \times$ 50 cm	30
C	4 cm $\Phi \times$ 40 cm	16
D	4 cm $\Phi \times 120$ cm	20

(*) Those values were estimated from the Depth-Intensity relation, cited in the E. P. George's title (in the *Progress in Cosmic Ray Physics*, **1** (Amsterdam, 1952)) with the range-energy relation of μ-mesons in rock ($Z = 10$ and $A = 20$).

magnification was about 17. They were operated with f 6.3 and photographs were taken with FUJI Neopan SS Film.

Accuracies of the measurement of direction angles were $\pm 1.0°$ and $\pm 2.5°$ for the front view and side view respectively. These accuracies are satisfactory for the present analysis.

The distortion of the track in the cloud chamber has been measured to be smaller than 0.5°. The momenta of penetrating particles are estimated from the multiple scattering which the particle undergoes in its traversal through lead plates in the chamber. Present accuracy of the scattering angle, $\pm 0.5°$, corresponds to the highest measurable momentum of 1.6 GeV/c.

The root mean square projected angle of multiple scattering of a particle after the passage through the scattering materials—lead (10 cm), lead (1 cm) and iron (1 cm)—vs. the energy of the particles after the traversal is shown in Fig. 3.

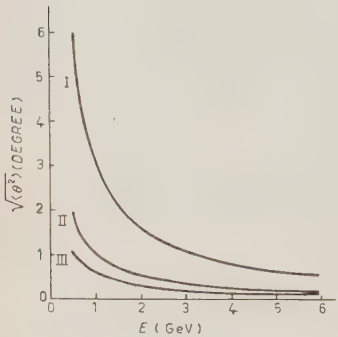

Fig. 3. – Curves I, II, and III illustrate the root mean square projected angles, $\sqrt{\langle\theta^2\rangle}$, of multiple scattering which a μ-meson undergoes during its passage through the lead scatterers having the thickness of 10 cm and 1 cm, and the iron one of 1 cm respectively. The abscissa, E, represents the energy of the μ-meson measured after the passage through the scatterer.

3. – Experimental Results.

574 pairs of photographs were obtained in receptive time of 218.5 hours. They are classified according to the number of penetrating particles which simultaneously enter into the chamber and are listed in Table I. Six cases show simultaneous incidences of four or more penetrating particles.

Two of these six cases in Table II are composed mainly of particles which have smaller energies than 0.5 GeV, and each of them is associated with a star. One case shows a diverging appearance of incidence of particles, that is, these particles have such dispositions as if being ejected from an origin. The other case associates with a cascade shower of more than 1 GeV energy which may result from one of the decay photons of a neutral π-meson in the shower secondaries. Thus both of them may be considered to be the secondary particles of the penetrating showers produced in the overlaying rock.

Features of the other four events, listed in Table III, are no association with the nuclear interaction and mainly involve higher energy particles than

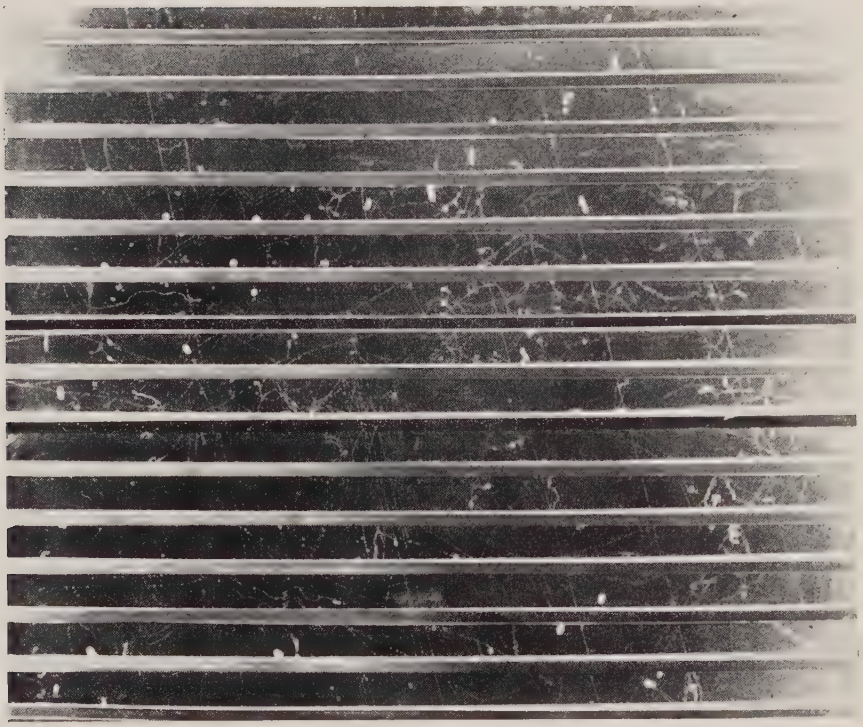

Photo 1. An example of the multiple penetrating particles (M.P.P.). Seven penetrating particles entered in the cloud chamber simultaneously being parallel with one another (cf. Table III D)).

TABLE I. – *Number of incident particles which appear in a photograph and of their occurrence.*

No. of incident P.P.S.	No. of photographs	Items	
		Penetrating showers (1)	Stars (2)
0	218	1 (3)	0
1	315	4+1 (Fe) (4)	0
2	31	1+1 (5)	1
3	4	2+1 (Pb) (6)	0
4	1	0	0
5	1	0	0
6	2	0	2
7	1	0	0
8	0	0	0
9	1	0	0
$\geqslant 10$	0	0	0

(1) No. of photographs which include some nuclear interactions having two or more secondary penetrating particles.

(2) No. of photographs which include some stars having less than two penetrating particles and some heavily ionizing tracks.

(3) The origin of the shower was on the boundary of the illuminated region, so that the primary did not possibly appear in the illuminated region.

(4) A penetrating shower was produced in the iron ceiling of the cloud chamber.

(5) There were produced three cascade showers, each being a photon-initiated one, as well as a secondary penetrating particle in a nuclear interaction, which may be considered as the production of neutral π-mesons.

(6) Secondaries of a penetrating shower produced in the lead layer over the cloud chamber.

TABLE II. – *Features of two cases which are regarded as the secondaries of the penetrating shower produced in the rock.*

No. of incident P.P.s			Total No. of traversals of lead plates	No. of associated stars
$\leqslant 0.5$ GeV	> 0.5 GeV	Total		
4	2	6	54	2
3	2	5	54	1

0.5 GeV. Photo 1 represents an example of these events. Fig. 4 shows the projected zenith angle distribution of incidence of these penetrating particles, and there was no diverging shaped correlation of the angular distribution of the individual tracks with their disposition. Among them three events 4(*A*), 4(*C*) and 4(*D*) consist of 4, 5 and 7 parallel penetrating particles respectively within the allowance of $\pm 2°$. If these parallel penetrating particles come from the atmosphere these angular distributions may be considered as those due to multiple scattering in the course of their traversing the rock, and their

TABLE III. – *Features of M.P.P.*

	No. of incident P.P. s			Total No. of traversals of lead plates	Zenith angle of incidence	Distribution of the incidence angles
	$\leqslant 0.5$ GeV	> 0.5 GeV	Total			
a)	1 ? (*)	3	4	38 (31) (+)	46°	cf. Fig. 4(*A*)
b)	3 ?	6	9	27 (25)	55°	cf. Fig. 4(*B*)
c)	1 ?	4	5	26 (24)	25°	cf. Fig. 4(*C*)
d)	0	7	7	75 (75)	23°	cf. Fig. 4(*D*)

(*) ? means the number of particles which have escaped from the illuminated region before they traverse four plates of lead.

(+) Numbers closed in the brackets are that of P.P. s having energies higher than 0.5 GeV.

relative scattering, as shown in Figs. 4(*A*), 4(*C*) and 4(*D*), corresponds to that of particles of energies smaller than 30 GeV. Then it is concluded that the dominant part of these penetrating particles have energies smaller than 30 GeV. The event 4(*B*) consists of 9 penetrating particles and has an angular spread of $\pm 5°$.

From a preliminary experiment, the upper limit of probabilities of chance coincidences (*) for one penetrating particle was obtained to be (0.077 ± 0.018) p.p.s/picture. Hence the probability for one spurious penetrating particle to appear in four pictures by chance coincidence

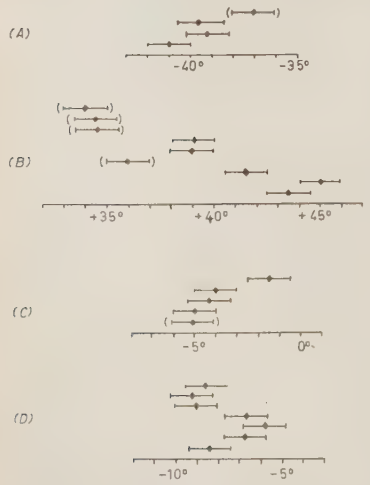

Fig. 4. – Distribution of the incident projected angles of the tracks in each event of M.P.P. The abscissa represents the clockwise projected angle between the downward vertical and the incident track measured on the front plane of the chamber. The errors added show the maximum ones derived from the accuracy of the measurements of angles with the present cloud chamber. The representatives of tracks closed in the brackets correspond to ones having traversed less than three plates in the chamber. The ordinate conveniently indicates the order of tracks. The upper side corresponds to the track in the chamber farthest to the left.

(*) The probability of chance coincidence for one penetrating particle means the probability for one penetrating particle to appear independently of its direction in a cloud chamber photograph taken by random expansion.

due to the statistical fluctuation is 0.22, and that for two or more penetrating particles is 0.03. As the above values of the chance coincidence are concerned with arbitrary directions of incidence of penetrating particles, it is very hard to consider that even one particle may intermingle with penetrating particles of these four pictures having such a sharp distribution of incident angles. Thus one may affirm that the effect of chance coincidence is negligible in the pictures of these four cases which are named the « Multiple Penetrating Particles » M.P.P.).

4. – Discussions and Conclusions.

M.P.P. events are most probably considered as the secondaries of the penetrating showers though their origins are either in the overlaying rock or in the atmosphere.

When one assumes that M.P.P.'s are the secondaries of the showers concurring in the rock above the apparatus, there are some probabilities that these secondaries undergo multiple scattering through the rock and give an appearance of parallel particles in the cloud chamber. One may compute the probabilities of appearance of these events taking the fluctuation into consideration (see Appendix). Then in these cases of 4(A), 4(C) and 4(D), such a statistical hypothesis can be abandoned with a significant level ([8]) smaller than 0.01 that the origin of the shower is within 6 m apart over the apparatus under the present condition of experiment. It is the case of 4(B) that the lower limit of the distance which is allowed for the same significant level is 2.7 m.

If the shower origin is situated at 2.7 m apart from the apparatus (case 4(B)), the surviving of five mesons requires that at least 750 π-mesons of about 2 GeV or more energies have been produced at the origin. (In this estimate, the nature of showers underground is assumed to be similar to that of the showers produced in N-N collisions, and the absorption mean free path of π-mesons to be twice as large as the geometrical interaction mean free path.) Even if the estimated multiplicity decreases owing to the fluctuation, 340 π-mesons may be required with the significant level of 0.02. Yet this multiplicity is still surprisingly large. The farther the origins of showers separate as the cases of 4(A), 4(C) and 4(D), the larger the multiplicities of the shower secondaries my be required.

As the total path length of M.P.P. in lead was 1860 g/cm^2 ($= 11.7\ \lambda_{gl}$, λ_{gl}: geometrical interaction mean free path in lead) and no visible nuclear

([8]) See, for example, P. G. Hoel: *Introduction to Mathematical Statistics* (London, 1947).

interaction was observed, almost all of the tracks are considered as μ-mesons. When one considers that the absence of the nuclear interaction would come from the fluctuation, the whole 20 penetrating particles, that is, the total sum of such penetrating particles of four cases as penetrate more than three sheets of lead, could not be attributed to more than 8 π-mesons and less than 12 μ-mesons with the significant level of 0.02. Thus it can be excluded that the shower origin approaches closer than 3.5 m from the apparatus (cf. Fig. 5).

Therefore, if M.P.P.'s are secondaries of penetrating showers underground, one must assume such a new-type interaction that a μ-meson produced directly μ-mesons in collision with a rock nucleus underground.

On the contrary, as a limiting case, one may assume M.P.P.'s to be the tails of air showers which penetrate the overlaying rock and reach the depth of the observation. Considering that incident angles of penetrating particles in three out of the four cases distribute within 2°, this interpretation is most probable.

There has been an experiment on air showers observed at a depth of 60 m w.e. underground by GEORGE *et al.* [9]. The authors of this experiment have concluded that their results on the decoherence behavior of the coincidence with two or more penetrating particle monitors are consistent with the assumption that the penetrating components in an air shower have a uniform density over a circle of about 60 m radius. When one adopts the above assumption, M.P.P. can hardly be interpreted because of their high density and high frequency, that is, the flat lateral structure function obtained by the above authors, having $\Delta_\mu = 1 \div 3$ p.p.s/m², is

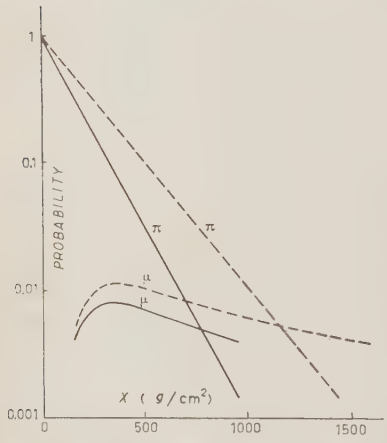

Fig. 5. – When a π-meson has been ejected as a shower secondary at a distance of x g/cm² (rock) over the chamber, the probability of being observed as it is (π) and that of being observed after decay into a μ-meson (μ) are shown. The solid (dotted) lines correspond to the assumption that the absorption mean free path of a π-meson is twice (three times) as long as the geometrical interaction mean free path. The energy of the particle is assumed to be 0.5 GeV at the point of observation.

---

[9] E. P. GEORGE, J. W. MACANUFF and J. W. STURGESS: *Proc. Phys. Soc.* (*Lond.*), A **66**, 346 (1952).

too small to account for these M.P.P.'s. In order to give a consistent interpretation of the decoherence behavior and M.P.P.'s, it may be necessary to assume that the structure function is altered to be, say, inversely proportional to the distance from the core of the air shower and it is applied down to about 1 m. But this assumption hardly agrees with the present air shower theory ([10,11]) which is based on the Fermi-Landau theory of the nucleon-nucleon collision. In this theory the energies of the shower secondaries and their ejected angles are correlated, so that the lateral spread of nuclear cascade is predicted to be larger than the observation. In order to account for the small lateral spread of penetrating particles, such a small inelasticity is required as could not account for the transition phenomena about cosmic rays in the atmosphere.

Further there may be considered the possibilities of such interpretations that the M.P.P.'s were members of air showers produced by heavy primaries ([12]), and that the M.P.P.'s where produced by air showers owing to the fluctuation (*) about them. The former of these interpretations might have a disagreement with the experimental results that the dominant part of the M.M.P. have energies smaller than 30 GeV. With regard to the latter interpretation, the fluctuation problem about air showers has not been resolved experimentally, so that unfortunately it cannot be decided if air showers give rise to M.P.P.'s owing to the fluctuation about air showers.

At the present it is of great importance to decide experimentally whether M.P.P.'s come from the penetrating showers produced in the rock or in the atmosphere, for which the observation has been performed concurrently for the determination of the lateral distribution of the M.P.P.

* * *

The authors wish to thank Professor M. Oda of the Tokyo University for many valuable suggestions and discussions, and Professor S. Hayakawa of the Kyoto University for helpful discussions. The authors also with to express their appreciation to the Shizuoka Railway Operating Divisional Office for permitting them to make the observations in the Isohama Tunnel. It is a pleasure to thank the Institute for Food Chemistry for the financial aid.

([10]) E. Amaldi, L. Mezzetti and G. Stoppini: *Nuovo Cimento*, **10**, 803 (1953).
([11]) M. Oda: *Nuovo Cimento*, **5**, 615 (1957).
([12]) S. Hayakawa: *Nuovo Cimento*, **5**, 608 (1957).
(*) This suggestion owes to Prof. S. Miyake of Osaka City University.

APPENDIX

Such a parallelism of penetrating particles as M.P.P. could be interpreted in terms that the secondaries of the shower occurring in the overlaying rock suffer the multiple scattering in the course of traversing the rock.

Suppose that the shower, the axis of which is in the downward directed vertical and runs just through the center of the chamber, is produced in the overlaying rock. Then some secondaries of the shower may pass through the rock and come out of it parallel with the shower axis or with convergent angles, after undergoing multiple scattering. The probability for such cases to occur is particularly sensitive to the distance between the shower axis and the secondaries coming out, measured on the level immediately under the rock. In the case of M.P.P., this distance may be taken to be about 25 cm, equal to a quarter of the width of the cloud chamber; because penetrating particles in each case of these M.P.P.'s were distributed over a half or more width of the cloud chamber, this value of 25 cm is to give an upper limit of the probability discussed here. Under these assumptions the probability for a shower secondary to come out in the directions above mentioned can be estimated to be shown in Fig. 6, as a function of the distance between the origin of the shower and the lower surface of rock, x g/cm^2. In this estimate the space between the rock and the cloud chamber has been neglected from the consideration.

According to the result in Fig. 6 the statistical hypothesis that the origin of the shower is within 2.3 m from the apparatus could be abandoned with the significant level of 0.05 taking into account in each picture only the particle farthest to the right, assumed to have an energy of 0.05 GeV. If one takes into account both the particles farthest to the right and to the left in the M.P.P. and the parallelism of all particles, with the significant level of 0.01 such a hypothesis could be abandoned for the case of 4(B) that the origin of the shower is within 2.7 m from the apparatus. With the same value of significant level the corresponding distance is 6 m for the cases of 1(A), 4(C) and 4(D).

The probability estimated about is the upper limit of those for the secondaries to become parallel with one another. If the significant

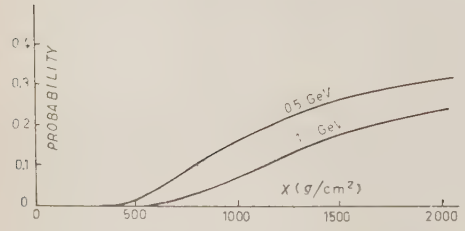

Fig. 6. – Suppose that an origin of a shower is at a distance of x g/cm^2 (abscissa) over the point of observation with its axis in the vertical, and one of the secondaries appears at a point 25 cm apart from the shower axis on the observation level. The ordinate represents the probability for this secondary to come out in a direction parallel to the shower axis or in convergent direction after undergoing multiple scattering in rock. The value close to each curve shows the energy of the secondary on the observation level (see the text).

level is fixed, the smaller becomes the estimated probability the larger becomes the corresponding distance between the origin of the shower and the apparatus, and so the larger is required the multiplicity of the shower as described in the text.

The showers, occurred in the rock, have hitherto been intended to be interpreted as usual ones as possible considering the upper limit of the probability, and it was found that the showers must have a surprisingly great multiplicity (see the text).

RIASSUNTO (*)

Per mezzo di una grande camera a nebbia del volume utile di $80 \times 70 \times 40$ cm^3 contenente 15 setti di piombo dello spessore singolo di 1 cm si sono osservati degli sciami penetranti alla profondità di 50 m a.e. dalla sommità dell'atmosfera. In 218.5 ore di attività utile si sono osservati 4 eventi interessanti singolarmente da 4 a 9 particelle penetranti parallele cadute simultaneamente sulla camera, oltre a numerosi sciami penetranti. Le particelle penetranti parallele non dimostrano nè interazione nucleare con nuclei di piombo nè scattering apprezzabile nei setti di piombo. Si assume che tali eventi siano prodotti da mesoni μ di energie superiori a 0.5 GeV a questa profondità. Si sono chiamate « Particelle Penetranti Multiple » (M.P.P.) sulle quali si sono raggiunte le seguenti conclusioni: i) se sono i secondari di grossi sciami penetranti prodotti nella roccia sovrastante l'apparecchiatura, l'ipotesi statistica che l'origine dello sciame si trovi 6 m al disopra dell'apparecchiatura stessa deve essere abbandonata avendo probabilità inferiore a 0.01. La molteplicità dei mesoni π prodotti in un tale sciame sarebbe superiore a 300 anche se tutti i secondari, restando assorbiti con un cammino libero medio $\lambda = 145$ g/cm^2 ($= 2\lambda_{gr}$, λ_{gr}: cammino libero medio d'interazione geometrica in roccia), decadessero in mesoni μ; ii) se appartengono alla componente penetrante degli sciami dell'aria che traversano la terra fino a questa profondità, la mole e la frequenza di questi eventi non può essere interpretata con l'ipotesi della funzione di struttura piana della componente penetrante normalmente invocata.

(*) *Traduzione a cura della Redazione.*

IL NUOVO CIMENTO Vol. V, N. 3 1° Marzo 1957

A Possible Interpretation of the Multiple Penetrating Particles.

S. Hayakawa

Research Institute for Fundamental Physics, Kyoto University - Kyoto, Japan

(ricevuto l'8 Novembre 1956)

Summary. — Some of the multiple penetrating particles observed by Higashi *et al.* are regarded as a bundle of μ-mesons produced in the atmosphere. It is suggested to interpret this observation in terms of the heavy primary nucleus that is split into nucleons by the collision with an air nucleus, each of the split nucleons producing multiple π-mesons which subsequently decay into μ-mesons of high energies.

1. – Introduction.

As shown in the preceding paper, cited as A, Higashi *et al.* [1] observed the multiple penetrating particles (M.P.P.) with their cloud chamber underground. At least three cases of the M.P.P.'s are interpreted as due to parallel μ-mesons produced in the atmosphere, because of their small angles of divergence and the lack in their interactions with lead plates inside the cloud chamber. On account of that several such μ-mesons are concentrated in a small area, approximately 0.3 m^2, the above authors regarded these μ-mesons as different from the general μ-mesons contained in extensive air showers; the lateral distribution of the latter is rather flat, while that of the former should be highly concentrated towards the core, perhaps within one metre from the axis.

Comparing this experiment with the lateral distribution of penetrating particles observed by Barrett *et al.* [2] at the depth of 1600 m w.e., the following features may be worth noticing. In the latter work the penetrating

---

[1] S. Higashi, T. Oshio, H. Shibata, K. Watanabe and Y. Watase: *Nuovo Cimento* **5**, 592 (1957).

[2] P. H. Barrett, L. H. Bollinger, G. Cocconi, Y. Eisenbeg and K. Greisen: *Rev. Mod. Phys.*, **24**, 133 (1952).

particles are attributed to the tail of extensive showers and the average lateral spread of the particles is estimated as 13 m. The energy of μ-mesons capable to reach the depth of 1600 m w.e. is larger than $7 \cdot 10^{11}$ eV and the average multiplicity is of the order of unity. On the other hand, in A, the average lateral spread seems to be of the order of 1 m and the multiplicity is of the order of ten. Although the spread is hardly observed, such a high density should not continue farther from the axis, because, otherwise, the number of μ-mesons either at sea level or far underground would become too large.

Such a high concentration may be understood if one takes account of a characteristic feature of the pion production at extremely high energies. NISHIMURA ([3,4]) has analyzed a number of examples obtained with photographic plates as well as with extensive air showers and found that the transverse momenta of produced pions lie between 0.1 and 1 GeV/c almost independent of primary energies ($10^3 \div 10^6$ GeV). If the μ-mesons observed in A are of very high energies, say $10^3 \div 10^4$ GeV, the small lateral spread can naturally be expected.

Based on this idea we shall analyze the experimental result of A, in order to ask what will be the primary particle of producing the multiple μ-mesons. For this purpose we refer to the intensity of primary cosmic rays and features of the multiple pion production which are known from other sources at least qualitatively. On account of the lack in the quantitative knowledge of materials we use, we restrict ourselves to the order of magnitude theory and refer only to average values. The materials which we refer to are summarized first and then they are applied to the analysis of the events under consideration.

The analysis is begun with qualitative considerations, showing that a single primary proton can hardly account for the events of interest. The single proton is supposed to give rise to μ-mesons with a flat lateral distribution, observed as a bulk of μ-mesons contained in an air shower. They are mainly produced in later generations of a N-cascade with large angular divergences. Indeed, the μ-mesons even from the second generation are found to have too large a lateral distribution. If their density is increased to the observed one, the primary energy will turn out to be too high and the frequency to be too low. The μ-mesons from the first generation are well concentrated near the shower axis, but their number is too few. Thus a possibility is suggested that the events are due to heavy primaries. Then both the number of μ-mesons and the frequency of the events are consistently explained. In order to check our hypothesis by observations, the expected multiplicity spectrum of the μ-mesons is derived.

([3]) J. NISHIMURA: private communication.

([4]) See also Z. KOBA: *Prog. Theor. Phys.*, **15**, 461 (1956).

2. – Basic Assumptions and Observed Facts.

2·1. *The frequency of the events.* – Let the energy of primary cosmic rays responsible for the events of interest be greater than E_0 per nucleon. The intensity of such primary rays is given, taking account of the angular distribution of high energy μ-mesons, by (*)

$$I(>E_0) = gE_0^{-\frac{3}{2}} \text{ cm}^{-2} \text{ s}^{-1} , \tag{1}$$

for E_0 around 10^6 GeV (†). g indicates the relative abundance of a certain species of primary rays: $g=1$ for protons. A primary particle produces n_μ μ-mesons as a result of the processes discussed below and they have the lateral spread of r. Hence n_μ μ-mesons cover an area of πr^2. Thus the primary particles falling on this area at the top of the atmosphere are responsible for the events concerned. Since HIGASHI *et al.* operated the cloud chamber for 218.5 hours, approximately 10^6 s, the total number of primary particles which we have to consider is

$$J(>E_0) \simeq 10^6 \, I(>E_0)\pi r^2 \simeq 10^6 \, gE_0^{-\frac{3}{2}}\pi r^2 . \tag{2}$$

It is quite likely that the effective area of the cloud chamber, $S \simeq 3 \cdot 10^3$ cm^2, is not larger than πr^2. Then the number of parallel μ-mesons observed is

$$N \simeq (S/\pi r^2) n_\mu \lesssim n_\mu . \tag{3}$$

They have observed at least three events of $N=4$, 5 and 7 and possibly another of $N=9$. With these figures (2) and (3) result in

$$NJ(>E_0) \simeq 10^6 \, gE_{0_0}^{-\frac{3}{2}} S n_\mu \simeq 3 \cdot 10^9 \, gE_0^{-\frac{3}{2}} n_\mu \simeq 20 . \tag{4}$$

From this, we have

$$E_0 \simeq 3 \cdot 10^5 \, g^{\frac{2}{3}} n_\mu^{\frac{2}{3}} . \tag{5}$$

Since $n_\mu \gtrsim 10$, (4) gives us the lower limit of E_0 as

$$n_\mu \simeq 7 \cdot 10^{-9} \, g^{-1} E_0^{\frac{3}{2}} \gtrsim 10 ,$$

(*) Although the energy spectrum in this energy region is based on air shower experiments, in which the total energy but not the energy per nucleon is observed, we use the form extrapolated from the one at low energies.

(†) In this paper energy and momentum are expressed in units of GeV and GeV/c respectively.

or

$$E_0 \gtrsim 1.3 g^{\frac{3}{5}} \cdot 10^6 \text{ GeV} .$$

Thus the primary energy is found to be considerably high.

2·2. *The π-μ decay.* – The average momentum of the μ-mesons under consideration can be estimated as

$$P_\mu \simeq (h/r) P_T , \tag{6}$$

where h is the height at which their parent π-mesons are produced, $h \sim 10 \div 20$ km. Since the transverse momentum P_T is $0.1 \div 1$ GeV c, P_μ is presumed to be higher than 10^3 GeV c, which is far above the characteristic momentum for the π-μ decay, $b \simeq 10^2$ GeV c. Hence only a fraction, b/P_μ, of π-mesons can decay into μ-mesons; the average number of charged π-mesons is given by (*)

$$n_\pi \simeq (P_\mu/b) n_\mu . \tag{7}$$

The average energy of the parent π-mesons is

$$E_\pi \simeq (m_\pi/m_\mu) P_\mu c \simeq 1.3 P_\mu c , \tag{8}$$

where m_π and m_μ are the masses of π- and μ-mesons.

2·3. *The multiple meson production.* – We assume that n_π π-mesons are produced by n_N N-particles whose average energy is E_N. The well known multiplicity law is

$$n_\pi \simeq n_N k E_N^{\frac{1}{4}} , \tag{9}$$

where k is a constant of the order of unity. If a fraction, $f \simeq \frac{1}{4}$, of the incident energy is transferred to charged π-mesons, there holds

$$f E_N \simeq (n_\pi/n_N) E_\pi . \tag{10}$$

Eliminating n_π from (9) and (10), we get

$$E_\pi \simeq (f/k) E_N^{\frac{3}{4}} . \tag{11}$$

(*) μ-mesons coming from heavy mesons and hyperons are about one tenth of those from π-mesons, so that the formers are neglected.

As n_μ is rather directly related to the observed quantity, we express n_μ as a function of E_N and n_N with the aid of (7)–(11).

$$n_\mu \simeq (b/P_\mu) n_\pi \simeq (m_\pi/m_\mu)(k^2 f)(bc/E_N^{\frac{1}{2}}) n_N \,. \tag{12}$$

3. – Analysis of the Experiment.

3·1. *Contribution from the first generation of a* N*-cascade caused by a primary proton.* – In this case $n_N = 1$ and E_N can be equated to the average energy of primary protons with energies greater than E_0, that is qE_0, where $q \simeq 3$. Substituting n_μ of (12) in (5) we find $E_0 \simeq 2 \cdot 10^5$ GeV or $E_N \simeq 6 \cdot 10^5$ GeV. However, this value of E_N results in $n_\mu < 1$, in definite disagreement with the observation. Thus we can rule out the possibility that the single primary proton produces the μ-mesons at the first nuclear collision in the atmosphere.

3·2. *Contribution from the second generation.* – Next we consider the case where n_N N-particles are produced by a single primary proton; namely, we are observing the μ-mesons from the second generation of a nuclear cascade in the atmosphere. Then we eliminate E_N and n_N in (12) by means of (9) and 10):

$$n_\mu \simeq (m_\pi/m_\mu)(k^{\frac{7}{2}}/f^{\frac{3}{2}}) bc (qE_0)^{-\frac{1}{2}} \,. \tag{13}$$

Substituting (13) in (5) E_0 is found to be about $5 \cdot 10^5$ GeV. Hence $n_N \simeq 35$ and $E_N \simeq 10^4$ GeV, so that the number of the μ-mesons coming from the μ-mesons of the first generation is negligibly small. For those from the second generation $n_\mu \simeq 2 \cdot 10^2$, but E_μ is only about $2 \cdot 10^2$ GeV. Therefore, the lateral spread turns out to be quite large, $r > 10$ m. This will correspond to the μ-mesons observed by BARRETT *et al.* [2], because only a small fraction of the μ-mesons with relatively high energies that can penetrate the earth of 1 600 m w.e. will be observable with such a small multiplicity as they found.

The contribution from later generations increases n_μ, but the lateral spread becomes so large that only extremely high energy protons can give rise to the events of interest with too low a frequency.

3·3. *Contribution from heavy primaries.* – Now there remains a possibility that the events under consideration are due to heavy primaries. When a heavy nucleus collides with an air nucleus, a part of the nucleus suffers a violent collision and produces π-mesons in much the same way as a proton hits the nucleus. But the remaining part is excited rather weakly and is splitted into small fragments mainly consisting of nucleons. As these fragments emerge with very small divergence, they can produce mesons in a narrow angle even

in the subsequent collision. The energy loss in the course of the fragmentation may be negligible, so that E_N can be equated to qE_0, the average primary energy per nucleon.

Hence we are allowed to substitute (12) in (5) with E_N replaced by qE_0. Thus we obtain

$$E_N \simeq qE_0 \simeq 1.3 \cdot 10^4 (m_\pi/m_\mu)^{\frac{1}{2}} (k/f^{\frac{1}{2}})(bc)^{\frac{1}{2}} q^{\frac{3}{2}} (gn_N)^{\frac{1}{2}} \simeq 6 \cdot 10^5 (gn_N)^{\frac{1}{2}} \tag{14}$$

and

$$n_\mu \simeq 0.9 \cdot 10^{-2} (m_\pi/m_\mu)^{\frac{3}{2}} (k^{\frac{3}{2}}/f^{\frac{3}{2}})(bc)^{\frac{3}{4}} q^{-\frac{3}{2}} n_N/(gn_N)^{\frac{1}{4}} \simeq n_N^{\frac{3}{4}} g^{-\frac{1}{4}} . \tag{15}$$

If n_N is assumed as a half of the mass number of a heavy primary, as an example, $gn_N \simeq 0.2$ for helium and $\simeq 3 \cdot 10^{-2}$ for respective groups of $Z = 6 \div 10$ and $Z > 10$. Consequently, n_μ is too small for helium but is a right order of magnitude for nuclei of $Z \gtrsim 6$. In the latter case $E_N \simeq 10^5$ GeV and $P_\mu \simeq 10^3$ GeV/c. If the transverse momentum is about 0.1 GeV/c, the lateral spread is of the order of 1 m. Thus the heavy primary seems to be responsible for the events, observed by HIGASHI *et al.*

3·4. *Multiplicity spectrum of μ-mesons* (*). – Now we see that the heavy primary seems to be only a possible source of the parallel μ-mesons. On this basis our discussions can be specified to derive the multiplicity spectrum and the n_N-dependence, because the height of the pion production, h, may be regarded as constant, about 15 km.

In reference to (6)–(12), πr^2 is eliminated and the integral multiplicity spectrum is obtained, for the period of observation of 10^6 s, as

$$J(>E_0(N)) \simeq 10^6 g q^{\frac{3}{2}} (m_\mu/m_\pi)(k^2/f^5)(b^3/P_\pi^{\frac{3}{2}})(S^3/(\pi h^2)^2) n_N^3 N^{-3} \simeq \tag{16}$$

$$\simeq 10^3 \, g (0.1/P_\pi)^{\frac{3}{2}} n_N^3 N^{-3} .$$

As an example, we give numerical values

$$J \simeq 10^2 \, g , \tag{17}$$

for $P_\pi \simeq 0.2$ GeV/c, $n_N = 10$ and $N = 5$. Therefore, $g \simeq 10^{-2}$ is good enough to account for the observed frequency and the lateral spread of $r \simeq 1$ m.

As (16) is proportional to n_N^3, the observed frequency seems to rule out too large a value of n_N. Before drawing the conclusion that too heavy primary particles are absent at high energies, one has to study the correlation between n_N and the mass number of a heavy primary nucleus.

(*) This point is kindly remarked by Professor FUJIMOTO.

4. – Implications of the Experiment.

If the interpretation described above is correct, the existence of heavy primaries at such high energies will bring about an important consequence on the origin of cosmic rays. Since the cross section for heavy nuclei to collide with galactic hydrogen is larger than that for protons and a high energy is attained by a long period of acceleration, according to the Fermi mechanism of gradual acceleration, the abundance of heavy primaries would decrease in comparison with that of protons with increasing energy, if the nuclear collision were essential to determine the lifetime of cosmic rays in our galaxy. The relative abundance of heavy nuclei at about 10^5 GeV as many as at 10 GeV indicates that the average path length traversed in the galaxy is not larger than 1 g cm^{-2}, which is expected from the abundance of Li, Be and B ([5]). Before going to this problem in more detail, however, we have to wait for more quantitative experimental information and its analysis than we have now. At present we only emphasize the extreme importance of the experiment concerned and hope further progress of the experiment and its analysis.

* * *

In conclusion I would like to mention that the authors of the experimental work A have kindly made constant contact with me. I enjoyed stimulating discussions with these authors and also with Professors FUJIMOTO, NISHIMURA and ODA. Without their help this work would not have been performed.

([5]) S. HAYAKAWA: *Prog. Theor. Phys.*, **15**, 111 (1956).

RIASSUNTO (*)

Alcune delle particelle penetranti multiple osservate da HIGASHI *et al.* si considerano come un fascio di mesoni μ prodotti nell'atmosfera. Si propone di interpretare tale osservazione in termini del nucleo primario pesante spezzato in nucleoni dalla collisione con un nucleo dell'aria; ogni nucleone prodotto produrrebbe a sua volta mesoni π multipli successivamente decadenti in mesoni μ di alta energia.

(*) *Traduzione a cura della Redazione.*

IL NUOVO CIMENTO Vol. V, N. 3 1° Marzo 1957

A Calculation on the Structure of the Nucleonic Cascade in the Atmosphere.

M. Oda

Institute for Nuclear Study, University of Tokyo - Tokyo

(ricevuto l'8 Novembre 1956)

Summary. — Hypothetical models of the nucleonic cascade were used for interpreting cosmic ray air showers. Numerical calculations were made on energy and angular distributions of π-mesons and μ-mesons produced at each generation of the nucleonic cascade. The number of electrons and μ-mesons at sea level and their lateral distribution are also derived. Assumptions on the nucleon-nucleus interaction are adjusted so that results of the calculation agree with experimental results on the air showers.

1. – Introduction.

It is well approved that the basic structure of the cosmic ray air showers is the nucleonic cascade which starts from a primary particle of extremely high energy near the top of the atmosphere. As the cascade proceeds, the number of particles increases and the average energy of the particles decreases. The cascade continues itself until the energy of the particle becomes too small to make further nuclear interactions. Essentially all of the neutral π-mesons produced in the cascade decay into photons which start electron cascade showers. Many charged π-mesons of low energy produced in later stages of the cascade decay into μ-mesons.

Part of the features of the air shower thus strongly depend upon the feature of the nuclear interaction in the cascade; i.e. relation of the number of produced π-mesons and incident energy of the interaction, energy and angular distribution of the produced π-mesons, inelasticity of the interaction etc.

Thus the investigation of the air shower may be utilized as means of studying the nuclear interaction of extremely high energy. Because of the complexity caused by the cascade process, however, it is very hard to derive directly unique conclusions on the nuclear interaction from the knowledge of the air shower. If a model of the nucleonic cascade is constructed on a combination of assumed characters of the nuclear interaction and is compared with experimental results on the air shower, one may check the assumptions and may understand how the characters must be. Several proposals ([1-5]) of theories on the meson production have been made from a theoretical point of view on the nucleon-nucleon collision at extremely high energy. Attempts ([6-9]) have been made to construct the model of the air shower on one of those theories and compare it with experiments concluding that Fermi's and Heisenberg's theories are not inconsistent with experiments. Conclusions, however, were not definite enough to let one distinguish a theory and further systematic treatments of the problem from the above mentioned view-point seem to be required.

Numerical calculations have been made, based on assumptions described in the following section, on the development of the nucleonic cascade which starts from protons of various energies at the top of the atmosphere. One of the assumptions essentially is in accord with Fermi's theory of meson production and another assumption involves stronger concentration of emitted energy in the foreward direction so that it more or less simulates a Landau-type theory of meson production. The calculation was done successively from a generation to the next generation of the nucleonic cascade. The energy distribution of produced π-mesons in each generation of the cascade will be presented. Also the energy distribution of μ-mesons produced by the decay of π-mesons will be given. The lateral distribution of μ-mesons of various energies and the distribution of axes of composite electron cascade showers in an air shower result from the calculation. It will be shown that the electron component of the air shower at sea level is mostly contributed by neutral π-mesons of very early stages of the cascade, and hence, regarding the electronic component results of the calculation is not much different from that based on a

---

([1]) H. W. Lewis, J. R. Oppenheimer and S. A. Wouthuysen: *Phys. Rev.*, **73**, 127 (1948).

([2]) H. Fukuda and G. Takeda: *Prog. Theor. Phys.*, **5**, 957 (1950).

([3]) W. Heisenberg: *Zeits. f. Phys.*, **113**, 61 (1939); **126**, 569 (1949); **133**, 64 (1952).

([4]) E. Fermi: *Prog. Theor. Phys.*, **5**, 570 (1950); *Phys. Rev.*, **81**, 683 (1951).

([5]) L. D. Landau: *Izv. Acad. Nauk USSR*, **17**, 51 (1953).

([6]) W. E. Hazen, R. W. William and C. A. Randall: *Phys. Rev.*, **93**, 538 (1954).

([7]) E. Amaldi, L. Mezzetti and G. Stoppini: *Nuovo Cimento*, **10**, 803 (1955).

([8]) P. Budini and G. Moliére: *Kosmische Strahlung*, II. Ed. (Berlin-Göttingen-Heidelberg, 1953).

([9]) U. Haber-Schaim: *Phys. Rev.*, **84**, 1199 (1951).

single cascade model of the air shower except the lateral distribution at the very center of the shower. Thus the electron component of the air shower may not be useful in distinguishing the assumptions on the nuclear interaction. Experimental information on the energy distribution or the lateral distribution of μ-meson component of the air shower is given by experimental works underground and it is of interest to compare them with the present calculation.

2. – Assumptions.

Although there are many nucleons in a large air shower, they are perhaps not the essential component in developing the nucleonic cascade and only the effect of the π-meson component will be considered here neglecting possible roles of nucleon pairs or unstable particles other than π-mesons in the air shower.

The number of the produced π-mesons is approximately given as a function of the incident energy of the interaction as follows:

$$n = 1.3 W^{\frac{1}{4}} , \tag{1}$$

where n = number of produced π-mesons,
W = incident energy in the laboratory system in GeV.

The angular distribution in the center of mass system (c.m.s.) of produced π-mesons is assumed as follows:

$$g(\eta)\,\mathrm{d}\eta \simeq f(0.96\eta)\,\mathrm{d}\eta . \tag{2}$$

η is $\cos\theta'$ and θ' is the angle of production with respect to the direction of the incident particle, and

$$\begin{cases} f(x) = \dfrac{2}{x^2(1-x^2)} \cdot \dfrac{1}{x^3} \log \dfrac{1+x}{1-x} \\ \qquad \text{or approximately (2) is:} \\ g(\eta)\mathrm{d}\eta \simeq 3.1\,|\eta|^{8.6} + 0.17 . \end{cases} \tag{3}$$

We make two alternative assumptions on the energy distribution of the produced π-meson; (i) the total available energy of the interaction in the c.m.s. is assumed to be equally divided among the produced π-mesons so that the energy distribution of the π-meson in the c.m.s. is a line spectrum and that in the laboratory system is uniquely determined by the angular distribution in the c.m.s. (Assumption I); (ii) the total energy of the produced

π-mesons in the c.m.s. is assumed to be represented by the following expression.

$$U_\pi \simeq a + b\eta^{2x} \tag{4}$$

(Assumption II). Assumption I combined with (2) corresponds to Haber-Schaim's theory [9] based on Fermi's theory [4]. Assumption II shows the concentration of emitted energy in the foreward and backward directions in addition to the collimation of produced π-mesons expressed by (2). a and b in (4) are to be determined by the following formula:

$$2n\int_0^1 f(0.96\eta)(a + b\eta^{2x})\,\mathrm{d}\eta = \text{total available energy in the interaction} = (2W)^{\frac{1}{2}}\,. \tag{5}$$

There is a possible reason to believe that the transverse momentum of the produced π-mesons is about constant and is perhaps around 1 GeV [10]. The transverse momentum calculated from (4) and (5) is nearly consistent with this requirement if we take about a few GeV for a and $x \geqslant 3$.

The energy of the π-meson in the laboratory system, E_π, and that in the c.m.s., E'_π, are related by $E_\pi = E'_\pi \cdot \gamma \cdot (1+\eta)$ where γ is $(W/2)^{\frac{1}{2}}$.

The angle of production in the laboratory system, θ, is related with η and W by

$$\theta \simeq (2/W)^{\frac{1}{2}}\big((1-\eta)/(1+\eta)\big)^{\frac{1}{2}}\,. \tag{6}$$

As W' is approximately equal to $(2W)^{\frac{1}{2}}$,where W is the total energy of the incident particle and $E'_\pi = W'\eta$ for Assumption I, η is expressed as follows:

$$\begin{cases} \eta = (1.3E_\pi/W^{\frac{3}{4}}) - 1 \quad \text{or} \\ \quad = (0.93E_\pi/W^{\frac{1}{2}}\cdot\gamma) - 1\,. \end{cases} \tag{7}$$

From (6) and (7) the following relation is derived,

$$E_\pi/\gamma \simeq 2.18W^{\frac{1}{2}}/\big(1 + (\gamma\theta)^2\big)\,. \tag{8}$$

For the Assumption II the following relation is obtained,

$$E_\pi/\gamma = 2\,\frac{a\big(1 + (\gamma\theta)^2\big)^{2x} + b\big(1 - (\gamma\theta)^2\big)^{2x}}{\big(1 + (\gamma\theta)^2\big)^{2x+1}}\,. \tag{9}$$

---

[10] J. Nishimura: Private communication.

These relations between E_π, θ and W for Assumptions I and II are shown in Fig. 1.

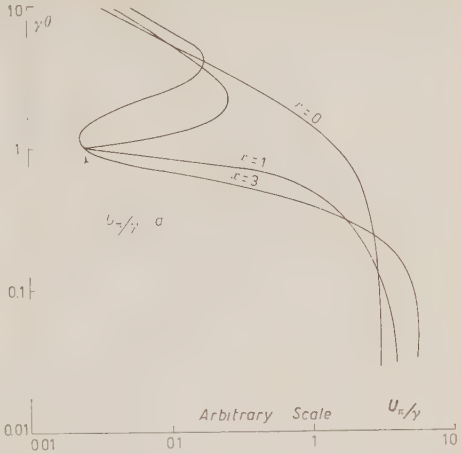

Fig. 1. – Examples of relations between the energy of produced π-mesons and the angle of production with respect to the direction of the colliding particle. γ is the Lorentz factor. r is a parameter which represents the degree of collimation of energy in the foreward direction as is given in (4). The scale of abscissae is arbitrary. Maximum value of U_π/γ is $2(a+b)$ which is calculated with (5).

3. – Nucleonic Cascade in the Atmosphere.

Using (1), (2), (6) and either of (8) or (9) we may proceed to calculate the number of produced π-mesons, $p_i(E_{\pi,i})\,\mathrm{d}E_{\pi,i}$, for the i-th generation of the nucleonic cascade from that of the former generation as follows:

$$(10)\quad p_{i+1}(E_{\pi,i+1})\mathrm{d}E_{\pi,i+1}\cdot\mathrm{d}\theta_{i+1} = \\ = p_i(E_{\pi,i})\cdot\frac{\partial E_{\pi,i}}{\partial\theta_{i+1}}\cdot\mathrm{d}\theta_{i+1}\cdot(1-w(E_{\pi,i}))\cdot n(E_{\pi,i})g(\eta)\cdot\frac{\partial\eta}{\partial E_{\pi,i+1}}\cdot\mathrm{d}E_{\pi,i+1}\,.$$

Suffixes in the formula are put to indicate the generation. $n(E_{\pi,i})$ is about $1.3\cdot E_{\pi,i}^{\frac{1}{4}}$ according to (1). $\partial E_{\pi,i}/\partial\theta_{i+1}$ and $\partial\eta/\partial E_{\pi,i+1}$ in the formula are obtained from (8) or (9) and (6) replacing W by $E_{\pi,i}$, E_π by $E_{\pi,i+1}$ and θ by θ_{i+1}. $w(E_{\pi,i})$ is the decay probability of the π-meson and is expressed by

$$(11)\quad \simeq\left(1-\exp\left[-\lambda\mu c^2/\tau c E_{\pi,i}\right]\right),$$

where τ: the life-time of the π-meson,

λ: the mean free path for the nuclear interaction in cm,

μc^2: the mass energy of the π-meson expressed by the unit of the of the proton mass,

c: light velocity in cm/s.

For the practice of the calculation of (10) it is convenient to use a diagram of $\log\theta$ vs. $\log E_{\pi}$ plotting points each of which represents a π-meson and proceed from one generation to the next with the aid of Fig. 1. An example of those diagrams is presented in Fig. 2. The example is for Assumption I

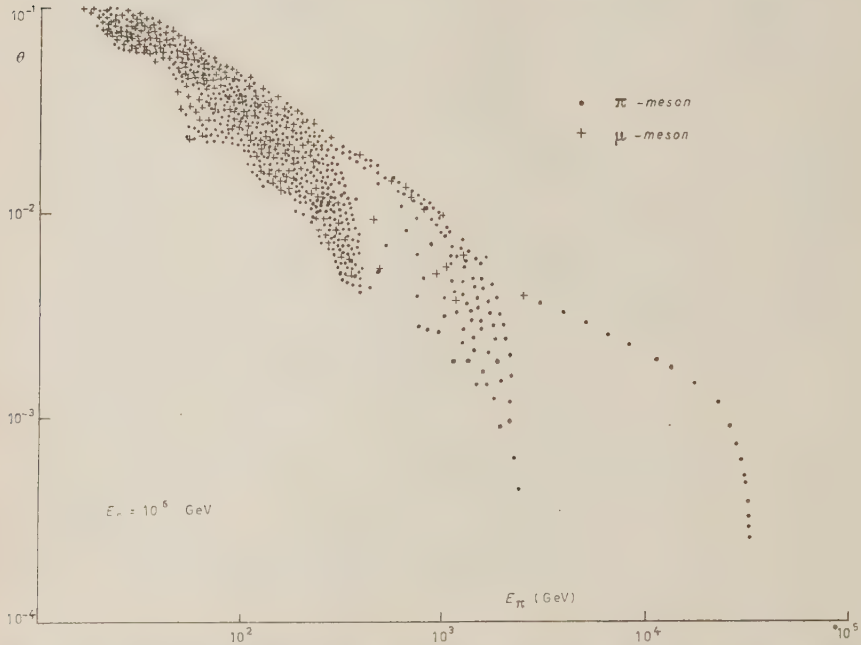

Fig. 2. An example of energies and angles of production, with respect to the axis of the shower, of mesons produced in 1-st to 3-rd generation of the nucleonic cascade of 10^6 GeV. Points and crosses correspond to π-mesons and μ-mesons respectively. Assumption I is used for the calculation.

and for the primary energy of 10^6 GeV and λ assumed as 70 g/cm^2. Each point of the diagram represents a π-meson which is produced by that of the former generation and which contributes to the next generation. Crosses represent μ-mesons which are the decay products of π-mesons. θ is now the angle of production of the meson with respect to the original axis of the nucleonic cascade. θ_{i+1} is usually much larger than θ_i except for very small θ_{i+1}, so that θ_{i+1} is regarded to be equal to θ. For very small θ_i, $\theta^2 \sim \theta_{i+1}^2 + \theta_i^2$. The projection of those points in the diagram on the energy co-ordinate gives the energy distributions of π-mesons and μ-mesons for each generation. Energy distributions of π-mesons and μ-mesons for primary energies of 10^6 GeV and

10^8 GeV were obtained and shown in Figs. 3 and 4 corresponding to Assumptions I and II respectively.

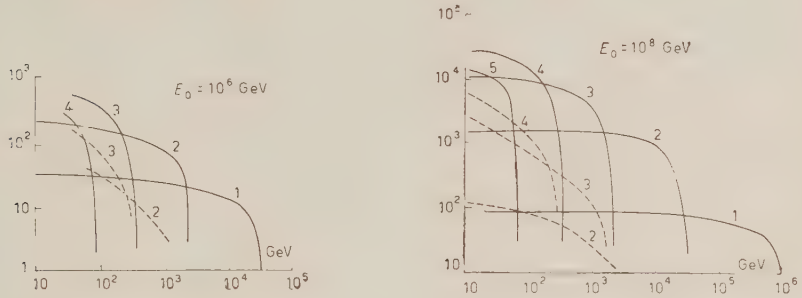

Fig. 3. – Integral energy spectrum of π-mesons and μ-mesons in each generation of the nucleonic cascade which starts from protons of 10^6 and 10^8 GeV. Dashed lines represent the curves for μ-mesons. Ordinates give the number of particles. Numbers of generations are given. Assumption I is adopted.

The figure leads to the conclusion that the μ-meson components of more than a few hundred GeV and a few tens of GeV are mostly contributed by

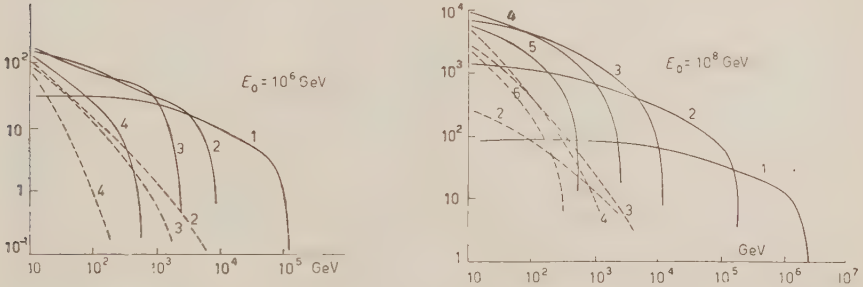

Fig. 4. – Same as Fig. 3 with Assumption II.

the 3-rd generation and the 3-rd $\sim$ 4-th generation of the nucleonic cascade respectively. μ-mesons of less than 10 GeV depend upon rather detailed features of assumptions of the model and will not be discussed here.

4. – Electron Components at Sea Level.

One third of π-mesons are supposed to be neutral π-mesons which decay into pairs of photons and cause electron cascade showers. The electron com-

ponent of the air shower is the superposition of those electron cascade showers. Using the conventional cascade theory (B approximation) and the energy spectrum of π-mesons which is given in the prevoius section, one obtains the expected total number of electrons at sea level as a function of the primary energy of the air showers. By a simple consideration (*) one may conclude that this function is like that derived for the single cascade model of the air shower except the constant factor which depends on the model of the air shower. The calculation, based on Assumption I and on the assumption that $g(\eta)$ is a δ-function for $\eta = 1$, gives a relation between the number of electrons and the primary energy shown in Fig. 5. The relations are given for various zenith angles of the air shower axes. The relation is expressed as follows:

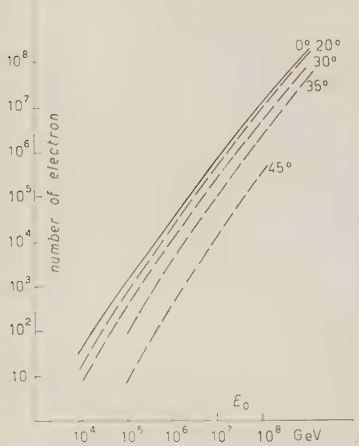

Fig. 5. The number of electrons involved in an air shower at sea level as the function of the primary energy and the zenith angle.

$$(12) \qquad E_0 \approx k \cdot N^{0.8} \cdot \sec^{4\sim 6}\varphi\,, \qquad \varphi < 30^\circ;\ 10^5 \lesssim N \lesssim 10^8,$$

where N is the number of electrons and φ is the zenith angle. k is a constant which depends on the model of the air shower and is usually of the order of hundred.

Most of the electron component in the air showers is perhaps contributed by the first few generations of the nucleonic cascade and the first generation is probably enough for a rough consideration of the electron component of the air showers. The π-meson energy is expressed as the function of the angle of production with respect to the direction of the primary particle, θ, according to either (8) or (9). From (2) and (6) we obtain the angular distribution of the produced π-mesons in the laboratory system as follows:

$$(13) \qquad h(\theta)\,\mathrm{d}\theta = g(\eta(\theta))\,\frac{\mathrm{d}\eta}{\mathrm{d}\theta}\cdot \mathrm{d}\theta \simeq f(0.96\,\eta)\,\frac{1-\eta(\theta)^2}{\theta}\,\mathrm{d}\theta\,.$$

Thus, $E_\pi^{1.3}(\theta)\cdot h(\theta)\,\mathrm{d}\theta$ will approximately represent the contribution to the number of electrons at the ground of a neutral π-meson which is produced

(*) Suppose that the number of electrons in a single electron cascade shower is expressed by a x-th power of the primary energy E_0. If E_0 is to be divided into n electronic cascades, the total number of electrons is roughly proportional to $n(E_0/n)^x$ or $n^{1-x}E_0^x$ where x is about 1.3 and n is proportional to, say, $E_0^{\frac{1}{2}}$ resulting $n^{1-x} \sim E_0^{0.075}$.

at an angle θ. As θ increases, this function increases rapidly at first, reaches its maximum at $\sim 0.13(2/W)^{\frac{1}{2}}$, if we take (8), and then decreases. Integration shows that more than fifty percent of electrons at the ground come from neutral π-mesons produced in angles $< 0.3(2/W)^{\frac{1}{2}}$; angles less than $5\cdot10^{-5}$ and $5\cdot10^{-4}$ radian for $W = 10^8$ and 10^6 GeV respectively. And, if we suppose that the first generation of the nucleonic cascade has about 15 km altitude, most of the axes of the component electronic cascades of large contribution hit the ground in circles of about 0.5 and 5 meters radius correspondingly. This distribution of axes of component cascade showers around the main axis of the air shower may cause a flattening of the lateral distribution of the electron in these circles even if the lateral distribution of each component shower were quite sharp. There has been no clear evidence that the lateral distribution of the air shower has a flat part as far as several meters from the center or any so-called multi-core and that the distribution is not flat around the centre. Above results of the consideration based on Assumption I do not contradict with experimental results so far but are not supported especially. Thus experimental results on the electron component of the air shower give no particular restriction on the model mentioned above.

5. – μ-Meson Component at Sea Level.

One may deduce the lateral distribution of the μ-meson component from the projection of points of μ-mesons in Fig. 2 to the θ axis taking into account the difference of altitudes of the production for different generations. Densities of the μ-meson component the energy of which is more than 10 GeV and those the energy of which is more than 600 GeV are given in Figs. 6 and 7 as functions of the distance from the core for primary energies of 10^6 and 10^7 GeV. Lowest energies of μ-mesons concerned are expressed by

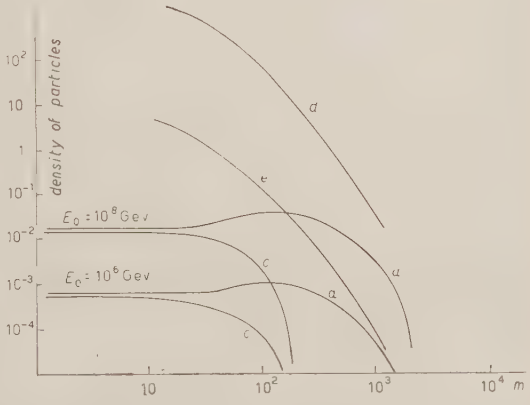

Fig. 6. – Lateral distributions of μ-mesons the energy of which is larger than E_m for assumption I. E_0 is the primary energy of the shower. a and c correspond to $E_m \approx 10$ and 600 GeV respectively and d and e represent lateral distributions of electrons on the ground for each E_0.

E_m. The lateral distributions of the electron component according to NISHIMURA and KAMATA [11] and assumption I is also given in the figures. As is seen in the figure the lateral distribution of μ-mesons has a flat shape around the center and sharp decrease at a certain distance from the center which increases by decreasing E_m and is insensitive to the change of the primary energy or the size of the air shower. Thus, we may be allowed to use a simplified model of the lateral distribution as follows; the density, Δ, is a constant in a circle of radius R, where Δ only depends upon the primary energy of the air shower being rather insensitive to E_m, and R is a function of only E_m. By this simplification the above results of the calculation on the expected lateral distribution of high energy μ-mesons are summarized in the following.

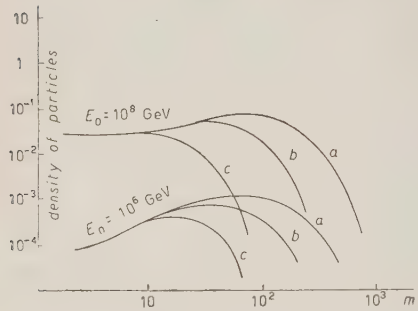

Fig. 7. – Same as Fig. 6 for assumption II. *b* represents the case of $E_m \approx 60$ GeV.

$$(14) \qquad \begin{cases} \text{(Assumption I)} & \Delta \simeq 2 \cdot 10^{-8} E_0^{0.75} \\ \text{(Assumption II)} & \Delta \simeq 2 \cdot 10^{-7} E_0^{0.65} \end{cases}$$

E_0 is the primary energy of the air shower and R for various E_m are given as:

E_m (GeV)	600	60	10
Assumption I	60 m	340 m	840 m
Assumption II	24 m	150 m	370 m.

We may express the primary energy spectrum of the cosmic ray, which was derived by BARRETT *et al.* [12], at the energy region of the air showers as:

$$(15) \qquad F(E_0)\,\mathrm{d}E_0 \simeq 4 \cdot 10^4 \cdot E_0^{-2.6 \sim 2.7}\,\mathrm{d}E_0 \text{ GeV, m}^2 \text{ s sr}.$$

Since the total number of μ-mesons, M, is roughly given by $2\pi R \cdot \Delta$ and, hence, is proportional to $E_0^{0.75}$ or $E_0^{0.65}$ according to (14), the above energy spectrum leads to the conclusion that the frequency of showers which contain M μ-mesons is proportional to $M^{-3.2 \sim 3.6}$

[11] J. NISHIMURA and K. KAMATA: *Prog. Theor. Phys.*, **5**, 899 (1950).

[12] P. H. BARRET, M. L. BOLLINGER, G. COCCONI, Y. EISENBERG and K. GREISEN: *Rev. Mod. Phys.*, **24**, 133 (1952).

The probability of two μ-mesons coming simultaneously into the detector of area S is about $\mathrm{d}p \approx A^2 \cdot S^2 \cdot 2\pi r \cdot \mathrm{d}r$ for an air shower whose center hits a point as far as r, $r + \mathrm{d}r$ from the detector if l is small. Integrating $\mathrm{d}p \cdot F(E_0)\,\mathrm{d}E_0$ with regard to r and using (14) and (15) we obtain

$$(16) \qquad \begin{cases} 5 \cdot 10^{-11} \cdot S^2 \cdot R^2 \cdot E_0^{-1.1 \sim 1.2} \cdot \mathrm{d}E_0 & \text{(Assumption I)} \\ \text{or} \\ 5 \cdot 10^{-9} \cdot S^2 \cdot R^2 \cdot E_0^{-1.3 \sim 1.4} \cdot \mathrm{d}E_0 & \text{(Assumption II)}. \end{cases}$$

If we take, for example, $S = 1600\ \mathrm{cm}^2$ and $R =$ several hundred meters corresponding to $E_m \sim 10\ \mathrm{GeV}$ which is the lowest μ-meson energy on the ground capable of penetrating about 30 m w.e. integrating (16) we obtain the total expected frequency of the above events as the order of magnitude of 10^{-6}/s sr, that is about once per 10 days.

These results of calculations are to be compared with experimental results on μ-mesons underground. When an air shower strikes the ground, electron component and other strongly interacting particles are rapidly absorbed in a few metres of the earth leaving the μ-meson component as the skeleton of the air shower. This is observed underground as penetrating particles coming simultaneously. There have been a few investigations on these events, which give following knowledge on the event. First of all BARRET *et al.* [12] have obtained the decoherence curve of the shower of penetrating particles at 1600 m w.e. underground. The curve is consistent with a flat lateral distribution which extends about ten metres from the axis. The rate of coincidence of two detectors, C_{12}, was about once per 100 hours where S is about 0.8 m^2. The differential number spectrum of the penetrating particles in the shower was concluded to go as $M^{-3.4 \pm 0.1}$. GEORGE *et al.* [13] have observed the showers at 60 m w.e. underground. From the decoherence curve obtained, assuming the lateral distribution to be flat out to a certain distance R from the core and zero thereafter, they concluded $R \approx 60$ m. The differential number spectrum of the shower was proportional to $M^{-3.2 \pm 0.2}$. HIGASHI *et al.* [14] have observed two or more penetrating particles entering a counter hodoscope set at 32 m w.e. underground. Its effective area was 0.160 m^2. A part of the events were concluded to be produced in the earth and the rest had a correspondence with the air shower on the ground. The correspondence was confirmed by the discharge of the air shower counter tray on the ground.

---

[13] E. P. GEORGE, J. W. MCANUFF and J. W. STURGESS: *Proc. Phys. Soc.*, A **66**, 346 (1953).

[14] S. HIGASHI, I. HIGASHINO, M. ODA, T. OSHIO, H. SHIBATA, K. WATANABE and Y. WATASE: *Journ. Phys. Soc. Jap.*, **11**, 1021 (1956).

Most of the events correspond to the electron densities of $10 \div 50$ m^2 on the ground above the detector underground. The frequency was about twice per a hundred hours. At 200 m w.e. the frequency was about one tenth of the former.

The comparison of lateral distributions with the above calculations shows that the model based on Assumption I gives too diffuse lateral distribution and even stronger collimation of emitted energy in the foreward direction than Assumption II may be required to explain the experiments. Taking $S=0.17$ m^2 for 32 m w.e., that is $E_m \approx 10$ GeV, and for 200 m e.w., that is $E_m \approx$ several ten GeV, and $S = 0.8$ m^2 for 100 m w.e., that is $E_m \approx 600$ GeV, and taking R given for Assumption II, relative figures of C_{12} calculated for 32, 200 and 1600 m w.e. are roughly consistent with that found experimentally. Integrating (16) we get the expected figures of C_{12} i. e. once per 800 hours for the experimental condition of BARRET *et al.* and once per 200 hours for that at 32 m w.e. The experimental figures are once per 100 hours and once per 50 hours respectively. These discrepancies result in the discrepancy of A by a factor of about two. We may say that the results are consistent with experiments if we consider ambiguities involved in the integration of (16) or in the simplification of the lateral distribution. The differential number spectrum of the penetrating particles seems to check well. Thus, the comparisons seem to show that the present model based on Assumption II may explain the air shower in the present accuracy of experiments and calculations except that the lateral distribution of high energy μ-mesons seems to be a little sharper than that obtained with the model. This may, perhaps, be explained by either the model of a little stronger collimation of energy in the foreward direction than that in Assumption II or the elasticity of the nuclear interaction.

Very recently HIGASHI *et al.* ([15]) suggested a possible existence of dense μ-meson showers underground which may be correlated with the air showers on the ground. They have observed several penetrating particles entering a multiplate cloud chamber simultaneously almost in parallel with each other by a rate of about once per hundred hours. It seems to be hard to interprete this rate of the events with the above model, although the event of two penetrating particles has been explained. A expected in the model is too small to give the present rate of the phenomena. Although results of the present calculation are by no means definite because of various ambiguities in assumptions on the nuclear interaction, it is very improbable that A is as big as to be able to explain the rate of the events unless radically different assumptions are to be adopted. Thus, it may be supposed that these events are different phenomena from those which can be explained by the conventional picture

([15]) S. HIGASHI, T. OSHIO, H. SHIBATA, K. WATANABE and Y. WATASE: Accompanying article.

of the air shower whereas the majority of the events of smaller density are explained as the tail of usual air showers.

* * *

The author wishes to express his gratitude to Prof. Y. WATASE of Osaka City University for his encouragement on this work. He is also indebted to Profs. S. HAYAKAWA and J. NISHIMURA and those who attended the Symposium of High Energy Phenomena held at Kyoto for valuable discussions on the subject. The author owes much to Prof. B. ROSSI and members of the cosmic ray group of the Massachusetts Institute of Technology who suggested this work and helpful discussions on the same.

RIASSUNTO (*)

Per l'interpretazione degli sciami dell'aria dei raggi cosmici si sono impiegati modelli ipotetici della cascata nucleonica. Si sono eseguiti calcoli numerici sulle distribuzioni d'energia e angolare dei mesoni π e μ prodotti in ogni generazione della cascata nucleonica. Si deducono anche il numero degli elettroni e dei mesoni μ al livello del mare e la loro distribuzione laterale. Le ipotesi sull'interazione nucleone-nucleo si adattano in modo che i risultati del calcolo siano in accordo coi risultati sperimentali sugli sciami dell'aria.

(*) *Traduzione a cura della Redazione.*

IL NUOVO CIMENTO Vol. V, N. 3 1° Marzo 1957

Quantum Fluid as a Common Model for Superfluidity and Superconductivity.

N. Mikoshiba

Physical Institute, Nagoya University - Nagoya, Japan

(ricevuto il 21 Novembre 1956)

Summary. — Some dynamical properties of quantum fluid as a simple common model for superfluidity and superconductivity are studied. Comparison with another common model i.e. an ideal Bose gas is made. The connection theorem proved by Schafroth in the case of many particle systems is proved also in the case of quantum fluid. By the theorem Landau's equation of superfluidity and London's equation of superconductivity can be verified for quantum fluid.

1. – Introduction.

There have been various discussions about the close connection between superfluidity and superconductivity. Recently the common models for two phenomena have been found. One of them is an ideal Bose gas (hereafter called IBG) proposed by Schafroth [1] and the other is quantum fluid (hereafter called QF) proposed by the present author [2] and Nakajima [3]. We shall compare the two models.

1·1. *Ideal Bose Gas.*

(*a*) Superfluidity. – Thermostatic properties of IBG were studied by F. London [4], who found the qualitative agreement of these properties with

[1] M. R. Schafroth: *Phys. Rev.*, **96**, 1149 (1954); **100**, 463 (1955).
[2] N. Mikoshiba: *Prog. Theor. Phys.*, **13**, 627 (1955).
[3] S. Nakajima: *Busseiron Kenkyu*, **85**, 17 (1955).
[4] F. London: *Phys. Rev.*, **54**, 947 (1938).

those of liquid helium. On the other hand, superfluidity of IBG was examined recently by BLATT and BUTLER (5). When a cylinder containing IBG is rotating around the symmetrical axis, its moment of inertia I becomes smaller than the classical value I_0 in the limit of the vanishing angular velocity.

(*b*) Superconductivity. – SCHAFROTH (1) pointed out that the diamagnetism of a charged ideal Bose gas obeys London's equation below its transition temperature. Moreover he proved the connection theorem (6) between superfluidity and superconductivity in the case of many particle systems. The theorem is a mathematical expression for the close connection between superfluidity and superconductivity of IBG.

1·2. *Quantum Fluid.*

(*a*) Superfluidity. – The QF model was proposed by LANDAU (7), who showed that not only thermostatic properties but superfluidity of QF were in good agreement with those of liquid helium II. He proved the inequality $I/I_0 < 1$. Later KRONIG and THELLUNG (8) reformulated Landau's idea by quantizing the hydrodynamic equation, but they did not discuss dynamical properties in detail.

(*b*) Superconductivity. – From the phenomenological point of view, the present author (2) suggested that the hydrodynamical description might be possible also for superconductivity. In fact, NAKAJIMA (3) proved that the non-viscous fluid obeys London's equation if it is quantized.

The purpose of the present paper is to study some dynamical properties of QF as a common model for superfluidity and superconductivity. In Sect. **2** we shall prove the connection theorem in the case of quantum fluid by means of Schafroth's method (6). The theorem will clarify the characteristics of QF as a common model. We shall show in Sect. **3** that some dynamical properties of QF can be derived by the same method as that used by BLATT, BUTLER and SCHAFROTH (9). QF in a rotating cylinder will be discussed in Sect. **4**.

2. – The Connection Theorem.

First, we shall prove the connection theorem in the case of QF. The Lagrangian density (2) of a charged non-viscous fluid in a magnetic field is

(5) J. M. BLATT and S. T. BUTLER: *Phys. Rev.*, **100**, 476 (1955).
(6) M. R. SCHAFROTH: *Phys. Rev.*, **100**, 502 (1955).
(7) L. LANDAU: *Journ. Phys. U.S.S.R.*, **5**, 71 (1941).
(8) R. KRONIG and A. THELLUNG: *Physica*, **18**, 749 (1952); G. R. ALLCOCK and C. G. KUPER: *Proc. Roy. Soc.*, A **231**, 226 (1955).
(9) J. M. BLATT, S. T. BUTLER and M. R. SCHAFROTH: *Phys. Rev.*, **100**, 481 (1955).

given by

$$L(\boldsymbol{r}) = \varrho(\boldsymbol{r})\left\{\frac{\partial}{\partial t}\varphi(\boldsymbol{r}) - \chi(\boldsymbol{r})\frac{\partial}{\partial t}\psi(\boldsymbol{r}) - \frac{1}{2}\boldsymbol{V}^2(\boldsymbol{r}) - W(\varrho(\boldsymbol{r}))\right\}, \tag{2.1}$$

where $\varrho(\boldsymbol{r})$ and $\varrho(\boldsymbol{r})\cdot W(\varrho(\boldsymbol{r}))$ are respectively the mass density and compressional energy density. The velocity $\boldsymbol{V}(\boldsymbol{r})$ is connected with Clebsch potentials $\varrho(\boldsymbol{r})$, $\chi(\boldsymbol{r})$, $\psi(\boldsymbol{r})$ and vector potential $\boldsymbol{A}(\boldsymbol{r})$ through

$$\boldsymbol{V}(\boldsymbol{r}) = -\nabla\cdot\varphi(\boldsymbol{r}) - \chi(\boldsymbol{r})\nabla\cdot\psi(\boldsymbol{r}) - \frac{e}{mc}\boldsymbol{A}(\boldsymbol{r}). \tag{2.2}$$

Since the canonical conjugates of $\varphi(\boldsymbol{r})$ and $\psi(\boldsymbol{r})$ are respectively $\varrho(\boldsymbol{r})$ and $\varrho(\boldsymbol{r})\cdot\chi(\boldsymbol{r})$, the Hamiltonian density becomes

$$H(\boldsymbol{r}) = \tfrac{1}{2}\varrho(\boldsymbol{r})\boldsymbol{V}^2(\boldsymbol{r}) + \varrho(\boldsymbol{r})W(\varrho(\boldsymbol{r})). \tag{2.3}$$

This expression can be transformed to

$$H(\boldsymbol{r}) = \frac{1}{2\varrho(\boldsymbol{r})}(\boldsymbol{G}(\boldsymbol{r}) - \varrho(\boldsymbol{r})\cdot\boldsymbol{\omega}\times\boldsymbol{r})^2 + \varrho(\boldsymbol{r})W(\varrho(\boldsymbol{r})), \tag{2.4}$$

where $\boldsymbol{G}(\boldsymbol{r})$ is the momentum density:

$$\boldsymbol{G}(\boldsymbol{r}) = -\varrho(\boldsymbol{r})\nabla\cdot\varphi(\boldsymbol{r}) - \varrho(\boldsymbol{r})\chi(\boldsymbol{r})\nabla\cdot\psi(\boldsymbol{r}), \tag{2.5}$$

and $\boldsymbol{A}(\boldsymbol{r}) = \boldsymbol{B}\times\boldsymbol{r}/2$, $\boldsymbol{\omega} = e\boldsymbol{B}/2mc$.

Then we shall define the « magnetic moment density » as

$$\boldsymbol{\mu}(\boldsymbol{r}) = -\frac{\partial H(\boldsymbol{r})}{\partial \boldsymbol{B}} = \frac{e}{2mc}\boldsymbol{r}\times(\boldsymbol{G}(\boldsymbol{r}) - \varrho(\boldsymbol{r})\cdot\boldsymbol{\omega}\times\boldsymbol{r}). \tag{2.6}$$

Using (2.4) and (2.6), the expectation value of the total magnetic moment in thermal equilibrium becomes

$$\langle\boldsymbol{M}\rangle_\beta = \frac{e}{2mc}\cdot\frac{\mathrm{Trace}\,\{[\int(\boldsymbol{r}\times\boldsymbol{G}(\boldsymbol{r}))\,\mathrm{d}\tau]\exp[-\beta\mathcal{H}]\}}{\mathrm{Trace}\,\{\exp[-\beta\mathcal{H}]\}} - \frac{e}{2mc}\cdot\frac{\mathrm{Trace}\,\{[\int\boldsymbol{r}\times(\varrho(\boldsymbol{r})\cdot\boldsymbol{\omega}\times\boldsymbol{r})\,\mathrm{d}\tau]\exp[-\beta\mathcal{H}^0]\}}{\mathrm{Trace}\,\{\exp[-\beta\mathcal{H}^0]\}}, \tag{2.7}$$

where the terms higher than ω^2 have been neglected and $\mathcal{H} = \int H(\boldsymbol{r})\,\mathrm{d}\tau$, $\mathcal{H}^0 = \mathcal{H}_{\omega=0}$.

We shall now consider a non-viscous fluid in a cylinder. In terms of the

cylindrical co-ordinates the Lagrangian and Hamiltonian densities are given by

$$(2.8)\qquad L(\boldsymbol{r}) = \varrho(\boldsymbol{r})\left\{\frac{\hat{c}}{\partial t}\varphi(\boldsymbol{r}) + \chi(\boldsymbol{r})\frac{\hat{c}}{\partial t}\psi(\boldsymbol{r}) - \frac{1}{2}\left[\left(\frac{\hat{c}}{\partial r}\varphi(\boldsymbol{r}) + \chi(\boldsymbol{r})\frac{\hat{c}}{\partial r}\psi(\boldsymbol{r})\right)^2 + \right.\right.$$

$$\left.\left. + \frac{1}{r^2}\left(\frac{\partial}{\partial\theta}\varphi(\boldsymbol{r}) + \chi(\boldsymbol{r})\frac{\partial}{\partial\theta}\psi(\boldsymbol{r})\right)^2 + \left(\frac{\partial}{\partial Z}\varphi(\boldsymbol{r}) + \chi(\boldsymbol{r})\frac{\partial}{\partial Z}\psi(\boldsymbol{r})\right)^2\right] - W(\varrho(\boldsymbol{r}))\right\},$$

$$(2.9)\qquad H(\boldsymbol{r}) = \frac{1}{2\varrho(\boldsymbol{r})}\left[G_r^2(\boldsymbol{r}) + \frac{1}{r^2}G_\theta^2(\boldsymbol{r}) + G_z^2(\boldsymbol{r})\right] + \varrho(\boldsymbol{r})W(\varrho(\boldsymbol{r}))\,,$$

where $G_r(\boldsymbol{r})$, $G_\theta(\boldsymbol{r})$ and $G_z(\boldsymbol{r})$ are respectively the r, θ and Z components of the momentum density.

Our purpose is to calculate the expectation value of the total angular momentum in thermal equilibrium when the cylinder is rotating around the Z axis with a constant angular velocity ω. Transform the co-ordinate system to the rotating system:

$$(2.10)\qquad \theta' = \theta - \omega t\,, \quad r' = r\,, \quad Z' = Z\,; \quad t' = t\,.$$

Then,

$$(2.11)\qquad L(\boldsymbol{r}) = L(\boldsymbol{r}') =$$

$$= \varrho(\boldsymbol{r}')\left\{\frac{\hat{c}}{\partial t'}\varphi(\boldsymbol{r}') + \chi(\boldsymbol{r}')\frac{\partial}{\partial t'}\psi(\boldsymbol{r}') - \omega\left(\frac{\partial}{\partial\theta'}\varphi(\boldsymbol{r}') + \chi(\boldsymbol{r}')\frac{\partial}{\partial\theta'}\psi(\boldsymbol{r}')\right) - \right.$$

$$- \frac{1}{2}\left[\left(\frac{\partial}{\partial r'}\varphi(\boldsymbol{r}') + \chi(\boldsymbol{r}')\frac{\partial}{\partial r'}\psi(\boldsymbol{r}')\right)^2 + \frac{1}{r'^2}\left(\frac{\partial}{\partial\theta'}\varphi(\boldsymbol{r}') + \chi(\boldsymbol{r}')\frac{\partial}{\partial\theta'}\psi(\boldsymbol{r}')\right)^2 + \right.$$

$$\left.\left. + \left(\frac{\hat{c}}{\partial Z'}\varphi(\boldsymbol{r}') + \chi(\boldsymbol{r}')\frac{\hat{c}}{\partial Z'}\psi(\boldsymbol{r}')\right)^2\right] - W(\varrho(\boldsymbol{r}'))\right\}.$$

From (2.11) the transformed Hamiltonian density is reduced to

$$(2.12)\qquad H'(\boldsymbol{r}') = H'(\boldsymbol{r}) = \frac{1}{2\varrho(\boldsymbol{r})}\left[G_r^2(\boldsymbol{r}) + \frac{1}{r^2}(G_\theta - \varrho(\boldsymbol{r})\cdot r^2\omega)^2 + G_z^2(\boldsymbol{r})\right] -$$

$$- \frac{1}{2}\varrho(\boldsymbol{r})\cdot r^2\omega^2 + \varrho(\boldsymbol{r})\,W(\varrho(\boldsymbol{r}))\,.$$

When the direction of $\boldsymbol{\omega}$ is arbitrary, (2.12) is generalized as follows:

$$(2.13)\qquad H'(\boldsymbol{r}) = \frac{1}{2\varrho(\boldsymbol{r})}(\boldsymbol{G}(\boldsymbol{r}) - \varrho(\boldsymbol{r})\cdot\boldsymbol{\omega}\times\boldsymbol{r})^2 - \frac{1}{2}\varrho(\boldsymbol{r})(\boldsymbol{\omega}\times\boldsymbol{r})^2 + \varrho(\boldsymbol{r})W(\varrho(\boldsymbol{r}))\,.$$

Therefore, $H'(\boldsymbol{r})$ is equivalent to $H(\boldsymbol{r})$ of (2.4) if the ω^2 term is neglected.

The angular momentum density referred to the rest system is written as $\boldsymbol{l}(\boldsymbol{r}) = \boldsymbol{r} \times \boldsymbol{G}(\boldsymbol{r})$. Thus the expectation value of the total angular momentum is given by

$$\langle \boldsymbol{L} \rangle_\beta = \frac{\mathrm{Trace}\,\{[\int (\boldsymbol{r} \times \boldsymbol{G}(\boldsymbol{r}))\,\mathrm{d}\tau]\,\exp[-\beta\mathscr{H}]\}}{\mathrm{Trace}\,\{\exp[-\beta\mathscr{H}]\}}\,, \tag{2.14}$$

where the ω^2 term has been neglected. We shall assume that the fluid is nearly incompressible. Then $\varrho(\boldsymbol{r})$ in the integrand of (2.7) is approximately replaced by its average value ϱ_0. Comparing (2.7) with (2.14), we get

$$\langle M \rangle_\beta = \frac{c}{2mc} \langle L \rangle_\beta - \frac{e\varrho_0 V}{2mc} \langle x^2 + y^2 \rangle_\beta \cdot \omega\,. \tag{2.15}$$

If we define the « moment of inertia » and the « magnetic susceptibility » ([6]) by

$$I = [\partial \langle L \rangle_\beta / \partial\omega]_{\omega=0}\,, \quad X = \frac{1}{V}[\partial \langle M \rangle_\beta / \partial B]_{B=0}\,, \tag{2.16}$$

respectively, we can derive the connection theorem:

$$\frac{I}{I_0} = 1 + \frac{4Xm^2c^2}{\varrho_0 \langle x^2 + y^2 \rangle_\beta \cdot e^2}\,, \tag{2.17}$$

where $I_0 = \varrho_0 V \langle x^2 + y^2 \rangle_\beta$ is the classical value of the moment of inertia.

Now we shall discuss the application of (2.17) to QF. In the system which obeys London's equation, $-\Lambda c\,\mathrm{curl}\,\boldsymbol{J} = \boldsymbol{B}$, we have

$$X = -\frac{1}{4\Lambda c^2} \langle x^2 + y^2 \rangle_\beta\,, \tag{2.18}$$

as was proved by SCHAFROTH ([6]). As was pointed out in the previous paper ([2]), for a charged non-viscous classical fluid London's equation is valid if the density fluctuation and the vortex motion are forbidden. In this case $\Lambda = m^2/\varrho_0 e^2$. From (2.17) and (2.18) we get $I = 0$. On the other hand, for the incompressible QF

$$\Lambda = \frac{m^2}{[\varrho_0 - (\varrho_{\mathrm{ph}} + \varrho_{\mathrm{rot}})]e^2}\,, \tag{2.19}$$

at lower temperatures (NAKAJIMA ([3])). Thus we have

$$\frac{I}{I_0} = \frac{\varrho_{\mathrm{ph}} + \varrho_{\mathrm{rot}}}{\varrho_0}\,, \tag{2.20}$$

where

$$\varrho_{\text{ph}} = \frac{4}{3S^2V}\sum_k \hbar S k \frac{1}{\exp(\beta\hbar S k) - 1}, \tag{2.21}$$

$$\varrho_{\text{rot}} = \frac{m^*}{V}\sum_{\boldsymbol{q}} \frac{1}{\exp[\beta(\Delta + (\hbar^2/2m^*)\boldsymbol{q}^2)] - 1}. \tag{2.22}$$

The equation (2.20) is Landau's equation of superfluidity which so far has not been proved rigorously.

3. – Superfluidity of Quantum Fluid.

In this section we shall discuss some dynamical properties of QF. We first recall two methods of measuring the viscosity of liquid helium II, which led to the two fluid theory; the oscillating disk ([10]) and the narrow tube ([11]) method. The two methods may be idealized as follows:

1) Put liquid helium II into a cylinder and rotate it around the symmetrical axis with a constant angular velocity. After the system has reached thermal equilibrium, measure the moment of inertia. It will be smaller than the classical value.

2) Pull the narrow tube containing liquid helium II with a constant velocity v and measure the momentum or the effective mass in thermal equilibrium, referred to the rest co-ordinate system. The effective mass $\mathfrak{M}$ will be smaller than the actual mass $\mathfrak{M}_0$.

We shall now discuss superfluidity of QF in the limit of vanishing ω or v. Recently Blatt, Butler and Schafroth ([9]) have developed statistical mechanics of a rotating bucket and Blatt and Butler ([5]) applied the method to IBG. Following them we define « superfluidity » as follows:

$$I < I_0 \qquad \text{or} \qquad \mathfrak{M} < \mathfrak{M}_0, \tag{3.1}$$

where

$$I = [\partial\langle L\rangle_\beta/\partial\omega]_{\omega=0}, \qquad \mathfrak{M} = [\partial\langle \mathfrak{G}\rangle_\beta/\partial v]_{v=0}, \tag{3.2}$$

($\mathfrak{G}$ is the total momentum). Since Landau's equation $I < I_0$ was proved for IBG and QF, we shall prove $\mathfrak{M} < \mathfrak{M}_0$.

Let us consider the narrow tube at rest containing a non-viscous fluid.

([10]) E. Andronikashvilli: *Journ. Phys. U.S.S.R.*, **10**, 201 (1946).
([11]) P. Kapitza: *Nature*, **141**, 74 (1938).

The Lagrangian and the Hamiltonian density are given by (2.1) and (2.3). If the tube is moving along the x axis with a constant velocity v, the transformation of the co-ordinate system:

$$x' = x - vt\,, \quad y' = y\,, \quad z' = z\,; \quad t' = t\,, \tag{3.3}$$

must be carried out to satisfy appropriate boundary conditions ([9]). Then the Lagrangian density is rewritten as

$$L(\boldsymbol{r}) - L(\boldsymbol{r}') = \varrho(\boldsymbol{r}')\left\{\frac{\partial}{\partial t'}\varphi(\boldsymbol{r}') + \chi(\boldsymbol{r}')\frac{\partial}{\partial t'}\psi(\boldsymbol{r}') - \right. \tag{3.4}$$

$$\left. - \frac{1}{2}[\nabla'\cdot\boldsymbol{q}(\boldsymbol{r}') + \chi(\boldsymbol{r}')\nabla'\cdot\psi(\boldsymbol{r}')]^2 - W(\varrho(\boldsymbol{r}')) - v\left[\frac{\partial}{\partial x'}\varphi(\boldsymbol{r}') + \chi(\boldsymbol{r}')\frac{\partial}{\partial x'}\psi(\boldsymbol{r}')\right]\right\}.$$

From (3.4) the transformed Hamiltonian density is reduced to

$$\begin{aligned} H'(\boldsymbol{r}') &= H'(\boldsymbol{r}) \\ &= H(\boldsymbol{r}) - v\mathfrak{G}_x(\boldsymbol{r})\,. \end{aligned} \tag{3.5}$$

Thus we have

$$\langle \mathfrak{G}_x \rangle_\beta = \frac{\mathrm{Trace}\,\{\mathfrak{G}_x \exp[-\beta(\mathscr{H} - v\mathfrak{G}_x)]\}}{\mathrm{Trace}\,\{\exp[-\beta(\mathscr{H} - v\mathfrak{G}_x)]\}}\,, \tag{3.6}$$

where $\mathfrak{G}_x$ is the x component of the total momentum referred to the rest co-ordinate system. To calculate (3.6) we shall carry out quantization in terms of Fourier transforms. According to ALLCOCK and KUPER ([8]), the Hamiltonian of a nearly incompressible fluid at lower temperatures is approximately given by the sum of the free phonon- and roton-Hamiltonians:

$$\begin{cases} \mathscr{H} \cong \mathscr{H}_{\mathrm{ph}} + \mathscr{H}_{\mathrm{rot}}\,, \\ \mathscr{H}_{\mathrm{ph}} = \hbar S \sum_{\boldsymbol{k}} k\left(N_{\boldsymbol{k}} + \frac{1}{2}\right), \qquad \mathscr{H}_{\mathrm{rot}} = \sum_{\boldsymbol{q}}\left(\Delta + \frac{\hbar^2}{2m^*}\boldsymbol{q}^2\right) N_{\boldsymbol{q}}\,, \end{cases} \tag{3.7}$$

where $N_{\boldsymbol{k}}$, $N_{\boldsymbol{q}}$ are numbers of renormalized phonons and rotons respectively. Quantization of $\mathfrak{G}_x$ is carried out in a similar manner:

$$\begin{cases} \mathfrak{G}_x = \mathfrak{G}_{x\,\mathrm{ph}} + \mathfrak{G}_{x\,\mathrm{rot}}\,, \\ \mathfrak{G}_{x\,\mathrm{ph}} = \hbar \sum_{\boldsymbol{k}} k_x N_{\boldsymbol{k}}\,, \qquad \mathfrak{G}_{x\,\mathrm{rot}} = \hbar \sum_{\boldsymbol{q}} q_x N_{\boldsymbol{q}}\,. \end{cases} \tag{3.8}$$

Therefore inserting (3.7) and (3.8) into (3.6), we get

$$(3.9)\qquad \begin{cases} \langle \mathfrak{G}_x \rangle_\beta = \langle \mathfrak{G}_{x\,\mathrm{ph}} \rangle_\beta + \langle \mathfrak{G}_{x\,\mathrm{rot}} \rangle_\beta , \\ \langle \mathfrak{G}_{x\,\mathrm{ph}} \rangle_\beta = \mathrm{trace}\left\{ \hbar k_x \dfrac{1}{\exp[\beta\hbar Sk - \beta\hbar v k_x] - 1} \right\}, \\ \langle \mathfrak{G}_{x\,\mathrm{rot}} \rangle_\beta = \mathrm{trace}\left\{ \hbar q_x \dfrac{1}{\exp[\beta(\Delta + (\hbar^2/2m^*)\boldsymbol{q}^2) - \beta\hbar v q_x] - 1} \right\}, \end{cases}$$

where the trace must be taken over one phonon or one roton states. If we consider the limiting case of $v \to 0$,

$$(3.10)\qquad \begin{cases} \langle \mathfrak{G}_{x\,\mathrm{ph}} \rangle_\beta = -\beta\hbar^2 v \sum_{\boldsymbol{k}} k_x^2 \dfrac{\partial f_{\mathrm{ph}}}{\partial(\beta\hbar Sk)} = \dfrac{4v}{3S^2} \sum_k (\hbar Sk) f_{\mathrm{ph}} , \\ \langle \mathfrak{G}_{x\,\mathrm{rot}} \rangle_\beta = m^* v \sum_{\boldsymbol{q}} f_{\mathrm{rot}} , \end{cases}$$

where

$$(3.11)\qquad f_{\mathrm{ph}} = 1/(\exp[\beta\hbar Sk] - 1) , \quad f_{\mathrm{rot}} = 1\Big/\left(\exp\left[\beta\left(\Delta + \frac{\hbar^2}{2m^*}\boldsymbol{q}^2\right)\right] - 1\right).$$

In terms of ϱ_{ph} and ϱ_{rot} in (2.21) and (2.22), we get

$$(3.12)\qquad \langle \mathfrak{G}_x \rangle_\beta = (\varrho_{\mathrm{ph}} + \varrho_{\mathrm{rot}}) V v$$

or

$$(3.13)\qquad \mathfrak{M} = (\varrho_{\mathrm{ph}} + \varrho_{\mathrm{rot}}) V ,$$

which satisfy the criterion for « superfluidity ». The equation (3.12) is the same result as LANDAU's [7]. Finally we shall discuss « superfluidity » of IBG. BLATT and BUTLER have proved for IBG that

$$(3.14)\qquad \frac{I}{I_0} = \frac{n_e}{n} ,$$

where n is the total number density and n_e is the number density of the excited particles. In the case of the narrow tube, we can prove $\mathfrak{M} < \mathfrak{M}_0$ by the same method as used for QF. Instead of (3.9) we have

$$(3.15)\qquad \langle P_x \rangle_\beta = \mathrm{trace}\left\{ p_x \frac{1}{\exp[\beta((1/2m)\boldsymbol{p}^2 - v p_x - \zeta)] - 1} \right\},$$

and

$$(3.16)\qquad \mathfrak{M} = m \sum_{\boldsymbol{p}} \left\{ \frac{1}{\exp[\beta((1/2m)\boldsymbol{p}^2 - \zeta)] - 1} \right\},$$

for IBG. Then if the length of the tube is finite so that $\boldsymbol{p}$ has discrete eigenvalues, the condensed particles ($\boldsymbol{p} = 0$) can not be excited to higher levels and do not contribute to the trace of (3.15) and (3.16) in the limiting case of $v \to 0$. Thus we get

$$\langle P_x \rangle_\beta = mn_i V v \tag{3.17}$$

or

$$\mathfrak{M} = mn_e V . \tag{3.18}$$

In the case of the infinite length, however, we can not prove « superfluidity » for IBG by the present method, as was discussed by ZILSEL ([12]).

4. – Quantum Fluid in a Rotating Cylinder.

In Sect. 2 we have proved Landau's equation by means of the connection theorem. We shall prove it more directly in this section. For this purpose we shall make use of a Fourier-Bessel type transformation ([13]). Field variables φ, ϱ, $\Psi = (\varrho\chi/\hbar)^{\frac{1}{2}} \cdot (\psi + i)$, and $\Psi^* = (\varrho\chi/\hbar)^{\frac{1}{2}} \cdot (\psi - i)$ are expanded as

$$\begin{cases} \varphi = \sum_{\varkappa\mu\nu} \left(\dfrac{S\hbar}{2\varrho_0 V}\right)^{\frac{1}{2}} \left(\dfrac{1}{\varkappa^2 - \nu^2}\right)^{\frac{1}{4}} (a_{\varkappa\mu\nu} + a^*_{-\varkappa-\mu-\nu}) S_\mu(\varkappa r) \exp[i(\mu\theta + \nu Z)] , \\ \varrho - \varrho_0 = i \sum_{\varkappa\mu\nu} \left(\dfrac{\varrho_0\hbar}{2SV}\right)^{\frac{1}{2}} \cdot (\varkappa^2 + \nu^2)^{\frac{1}{4}} \cdot (a^*_{\varkappa\mu\nu} - a_{-\varkappa-\mu-\nu}) S_\mu(\varkappa r) \exp[-i(\mu\theta + \nu Z)] , \\ \Psi = V^{-\frac{1}{2}} \sum_{\varkappa'\mu'\nu'} b_{\varkappa'\mu'\nu'} S_{\mu'}(\varkappa' r) \exp[i(\mu'\theta + \nu' Z)] , \\ \Psi^* = V^{-\frac{1}{2}} \sum_{\varkappa'\mu'\nu'} b^*_{\varkappa'\mu'\nu'} S_{\mu'}(\varkappa' r) \exp[-i(\mu'\theta + \nu' Z)] , \end{cases} \tag{4.1}$$

where

$$S_\mu(\varkappa r) = (\sqrt{2}/R)[J_{\mu+1}(\varkappa R)]^{-1} J_\mu(\varkappa r) \tag{4.2}$$

and

$$J_\mu(\varkappa R) = 0 , \tag{4.3}$$

$J_\mu(\varkappa r)$ is the Bessel function of the μ-th order and R is a radius of the cylinder. After the renormalization, the Hamiltonian and total angular momentum of

([12]) P. R. ZILSEL: *Phys. Rev.*, **92**, 1106 (1953).
([13]) J. M. ZIMAN: *Proc. Roy. Soc.*, A **219**, 257 (1953).

QF become

$$
(4.4)\qquad \begin{cases} \mathcal{H} \cong \mathcal{H}_{\text{ph}} + \mathcal{H}_{\text{rot}}\,, \\ \mathcal{H}_{\text{ph}} = \hbar S \sum_{\varkappa\mu\nu} (\varkappa^2 + \nu^2)^{\frac{1}{2}} \left(N_{\varkappa\mu\nu} + \frac{1}{2} \right), \\ \mathcal{H}_{\text{rot}} = \sum_{\varkappa'\mu'\nu'} \left(\Delta + \frac{\hbar^2}{2m^*} (\varkappa'^2 + \nu'^2) \right) N_{\varkappa'\mu'\nu'}\,, \\ \mathcal{G}_\theta = \mathcal{G}_{\theta\,\text{ph}} + \mathcal{G}_{\theta\,\text{rot}}\,, \\ \mathcal{G}_{\theta\,\text{ph}} = \hbar \sum_{\varkappa\mu\nu} \mu N_{\varkappa\mu\nu}\,, \\ \mathcal{G}_{\theta\,\text{rot}} = \hbar \sum_{\varkappa'\mu'\nu'} \mu' N_{\varkappa'\mu'\nu'}\,, \end{cases}
$$

where the interaction terms have been neglected.

Therefore in the same manner as (3.8), the expectation value of the total angular momentum is given by

$$
(4.5)\qquad \begin{cases} \langle \mathcal{G}_\theta \rangle_\beta = \langle \mathcal{G}_{\theta\,\text{ph}} \rangle_\beta + \langle \mathcal{G}_{\theta\,\text{rot}} \rangle_\beta\,, \\ \langle \mathcal{G}_{\theta\,\text{ph}} \rangle_\beta = \text{trace} \left\{ \hbar\mu \, \frac{1}{\exp\left[\beta\hbar S\sqrt{\varkappa^2 + \nu^2} - \beta\hbar\omega\mu\right] - 1} \right\}, \\ \langle \mathcal{G}_{\beta\,\text{rot}} \rangle_\beta = \text{trace} \left\{ \hbar\mu' \, \frac{1}{\exp\left[\beta(\Delta + (\hbar^2/2m^*)(\varkappa'^2 + \nu'^2)) - \beta\hbar\omega\mu'\right] - 1} \right\}. \end{cases}
$$

In the limit of $\omega \to 0$,

$$
(4.6)\qquad \begin{cases} \mathcal{G}_{\theta\,\text{ph}} \rangle_\beta = -\beta\hbar^2\omega \, \text{trace} \left\{ \mu^2 \, \frac{\partial f_{\text{ph}}}{\partial(\beta\hbar S\sqrt{\varkappa^2 + \nu^2})} \right\}, \\ \langle \mathcal{G}_{\theta\,\text{rot}} \rangle_\beta = -\beta\hbar^2\omega \, \text{trace} \left\{ \mu'^2 \, \frac{\partial f_{\text{rot}}}{\partial[\beta\Delta + (\beta\hbar^2/2m^*)(\varkappa'^2 + \nu'^2)]} \right\}, \end{cases}
$$

where f_{ph} and f_{rot} are equivalent to (3.11). To evaluate (4.6) we shall make use of $\boldsymbol{k}$-space instead of $(\varkappa, \mu, \nu)$-space. Thus we get

$$
(4.7)\qquad \begin{cases} \langle \mathcal{G}_{\theta\,\text{ph}} \rangle_\beta = \frac{4\omega}{3S^2} \langle x^2 + y^2 \rangle_\beta \sum_{\boldsymbol{k}} (\hbar S k) f_{\text{ph}}\,, \\ \langle \mathcal{G}_{\theta\,\text{rot}} \rangle_\beta = m^* \omega \langle x^2 + y^2 \rangle_\beta \sum_{\boldsymbol{q}} f_{\text{rot}}\,. \end{cases}
$$

Using (2.21), (2.22) and (3.2)

$$\frac{I}{I_0} = \frac{\varrho_{\rm ph} + \varrho_{\rm rot}}{\varrho_0}, \tag{4.8}$$

is obtained. This is a direct proof of Landau's equation for QF.

5. – Concluding Remarks.

Some dynamical properties of QF were investigated in this paper. To be easily seen, these results will be tabulated in the Table I with some other results obtained by Schafroth, Blatt, Butler and Nakajima.

Table I.

		IBG	*QF*
Connection Theorem		$\frac{I}{I_0} = 1 + \frac{4Xmc^2}{n\langle x^2+y^2\rangle_\beta \cdot e^2}$	$\frac{I}{I_0} = 1 + \frac{4Xm^2c^2}{\varrho_0\langle x^2+y^2\rangle_\beta \cdot e^2}$
Superfluidity	(*a*) Translation	$\left(\frac{\mathfrak{M}}{\mathfrak{M}_0} = \frac{n_e}{n}\right)^*$	$\frac{\mathfrak{M}}{\mathfrak{M}_0} = \frac{\varrho_{\rm ph} + \varrho_{\rm rot}}{\varrho_0}$
	(*b*) Rotation	$\frac{I}{I_0} = \frac{n_e}{n}$	$\frac{I}{I_0} = \frac{\varrho_{\rm ph} + \varrho_{\rm rot}}{\varrho_0}$
Superconductivity		$\Lambda = \frac{m}{(n-n_e)\cdot e^2}$	$\Lambda = \frac{m^*}{[\varrho_0 - (\varrho_{\rm ph} + \varrho_{\rm rot})]\cdot e^2}$

(*) This is verified only for a tube of finite length.

The QF model is not very realistic in the sense that it has not yet been based on the electron theory of metals. But it may suggest the importance of collective modes occurring in superconductors as well as in liquid helium. The collective motion in liquid helium II has been studied by various authors with many successful results, whereas the treatment of the collective motion in superconductors has not yet been successful. Perhaps some ingenious ideas will be required.

Ginzburg [14] has developed independently the theory on the basis of ideas similar to ours.

[14] V. L. Ginzburg: *Nuovo Cimento*, **2**, 1234 (1955); D. Shoenberg: *Suppl. Nuovo Cimento*, **10**, 459 (1953).

* * *

The author should express his sincere thanks to Prof. ARIYAMA for the encouragement. He also is deeply indebted to Dr. NAKAJIMA for valuable discussions.

RIASSUNTO (*)

Si esaminano alcune proprietà dinamiche di un fluido quantico preso come semplice modello comune per lo studio della superfluidità e della superconduttività. Si fa un confronto con un altro modello usuale, cioè con il gas ideale di Bose. Il teorema di connessione dimostrato da SCHAFROTH per il caso di sistemi di più particelle è dimostrato anche per il caso del fluido quantico. In virtù di tale teorema, si possono verificare per il fluido quantico l'equazione di Landau della superfluidità e quella di London della superconduttività.

(*) *Traduzione a cura della Redazione.*

Conformally Invariant Wave Equations for Non-Linear and Interacting Fields (*).

J. A. McLennan, Jr.

Department of Physics, Lehigh University - Bethlehem, Penn. U. S. A.

(ricevuto il 26 Novembre 1956)

Summary. — Non-linear conformally invariant wave equations for spinors of arbitrary rank are obtained. These include an equation recently proposed by Gürsey. In addition, conformally invariant equations for interacting fields are given.

Recently Gürsey [1] has proposed a conformally invariant spinor wave equation which resembles Heisenberg's [2] non-linear equation for a unitary field theory. Of course, the spirit of Heisenberg's theory requires that the wave equation involve a spinor of the first rank. However, it may be of interest that equations resembling Gürsey's can be obtained for spinors of arbitrary rank, as will be shown here; conformally invariant equations for interacting fields can be obtained similarly.

Gürsey's equation is

$$\gamma_j P_j \psi + \lambda(\overline{\psi}\psi)^{\frac{1}{2}}\psi = 0\,, \tag{1}$$

where λ is a dimensionless constant, γ_j are the Dirac matrices, and

$$P_j = \frac{\partial}{\partial x_j}\,.$$

(*) This research was supported by the United States Air Force under Contract No. AF 18 (600)-1462 monitored by the AF Office of Scientific Research of the Air Research and Development Command.

(1) F. Gürsey: *Nuovo Cimento*, **3**, 988 (1956).

(2) W. Heisenberg: *Zeits. f. Naturf.*, **10***a*, 425 (1955).

As shown by GÜRSEY, his equation is conformally invariant. This may also be seen by considering the Lagrangian

$$L = \bar{\psi}\gamma_j P_j \psi + \tfrac{3}{4}\lambda(\bar{\psi}\psi)^{\frac{4}{3}}, \tag{2}$$

which leads to equation (1). If we apply the inversion

$$x_j' = k^2 x_j/(x_i x_i), \tag{3}$$

then

$$P_j' = (1/k^2)[\delta_{jk} x_i x_i - 2x_j x_k] P_k,$$

and if ψ transforms according to

$$\psi' = (x_i x_i/k^3) x_j \gamma_j \psi \tag{4}$$

a simple calculation shows that

$$L' = (x_i x_i/k^2)^4 L.$$

Since the Jacobian determinant of the transformation (3) is given by

$$J = \left| \frac{\partial x_j'}{\partial x_k} \right| = -(k^2/x_i x_i)^4,$$

it follows that

$$L' \, \mathrm{d}^4 x' = -L \, \mathrm{d}^4 x.$$

Thus the variational principle

$$\delta \int L \, \mathrm{d}^4 x = 0,$$

and hence equation (1), is invariant under the inversion (3). All conformal transformations can be obtained by combining the inversions with the inhomogeneous Lorentz transformations [3]. Consequently equation (1) is conformally invariant. More precisely, it is invariant under the subgroup of the conformal group containing all transformations which do not reverse the di-

[3] S. LIE and F. ENGEL: *Theorie der Transformationsgruppen* (Leipzig, 1893), vol. III, p. 347 ff.

rection of time, since it is not invariant under the anti-chronous Lorentz transformations (under a time-like reflection, $\bar{\psi}\psi$ transforms into $-\bar{\psi}\psi$).

Now, conformally invariant equations for particles with zero rest mass are known for all spin values (4). To obtain non-linear equations similar to Gürsey's, it is only necessary to add to the Lagrangian for such equations a non-linear term with the correct transformation properties. As a first example, we consider the Lagrangian for a scalar field u

$$L_0 = \frac{1}{2}\frac{\partial \bar{u}}{\partial x_j}\frac{\partial u}{\partial x_j}, \tag{5}$$

where $\bar{u}$ is the complex conjugate of u. If, under the transformation (1), u transforms according to

$$u' = (x_i x_i/k^2)u\,, \tag{6}$$

one finds that

$$L_0' = (x_i x_i/k^2)^4\left[L_0 + \frac{\partial}{\partial x_j}\, x_j \bar{u}u/x_i x_i)\right].$$

The divergence term does not contribute to the equations of motion and may be neglected. Now, a term

$$L_1 = \tfrac{1}{4}\lambda(\bar{u}u)^2 \tag{7}$$

has the correct behaviour under the inversion, as is readily verified from (6). Thus the variational principle based on the Lagrangian

$$L = L_0 + L_1 \tag{8}$$

will be conformally invariant. The field equation obtained from this Lagrangian is

$$\Box u - \lambda(\bar{u}u)u = 0\,. \tag{9}$$

For spinors of higher even rank, let $q^{\alpha_1\alpha_2\ldots\alpha_m\dot{\beta}_1\ldots\dot{\beta}_m}$ be a symmetric spinor (5),

---

(4) J. A. MCLENNAN, jr.: *Nuovo Cimento*, **10**, 1360 (1956).

(5) The spinor notation used is that of O. LAPORTE and G. E. UHLENBECK: *Phys. Rev.*, **37**, 1380 (1931). s and $\dot{s}$ are operators which make a spinor symmetric where it is not already so, e.g.:

$$sp_{\dot{\beta}}^{\alpha_1} u^{\alpha_2\ldots\alpha_m} = p_{\dot{\beta}}^{\alpha_1} u^{\alpha_2\ldots\alpha_m} + p_{\dot{\beta}}^{\alpha_2} u^{\alpha_1\alpha_3\ldots\alpha_m} + \ldots + p_{\dot{\beta}}^{\alpha_m} u^{\alpha_2\ldots\alpha_{m-1}}.$$

with $m-1$ dotted and $m-1$ undotted indices. Considering the φ's as potentials, we define fields according to

$$(10)\qquad \begin{cases} u^{\alpha_2..\alpha_m\,\dot\beta_1..\dot\beta_m} = \dot s p^{\dot\beta_1}_{\alpha_2}\varphi^{\alpha_2..\alpha_m\,\dot\beta_2..\dot\beta_m}, \\ v^{\alpha_2..\alpha_m\,\dot\beta_2..\dot\beta_m} = s p^{\alpha_1}_{\dot\beta_2}\varphi^{\alpha_2..\alpha_m\,\dot\beta_2..\dot\beta_m}, \end{cases}$$

where

$$p^{\alpha\dot\beta} = \frac{\partial}{\partial x_{\alpha\dot\beta}}.$$

Then the Lagrangian

$$(11)\qquad L_0 = (1/2m)[u_{\alpha_2..\alpha_m\,\dot\beta_1..\dot\beta_m}u^{\alpha_2..\alpha_m\,\dot\beta_1..\dot\beta_m} + v_{\alpha_1..\alpha_m\,\dot\beta_2..\dot\beta_m}v^{\alpha_1..\alpha_m\,\dot\beta_2..\dot\beta_m}]$$

leads to the equation of motion

$$(12)\qquad s p^{\alpha_2}_{\dot\beta_1}u^{\alpha_2..\alpha_m\,\dot\beta_1..\dot\beta_m} + \dot s p^{\dot\beta_2}_{\alpha_2}v^{\alpha_1..\alpha_m\,\dot\beta_2..\dot\beta_m} = 0.$$

Now, under the inversion (3), we transform φ according to

$$(13)\qquad \varphi'^{\alpha_2..\alpha_m\,\dot\beta_2..\dot\beta_m} = (1/k^2)(x_ix_i)^{2-m}x^{\alpha_2}_{\dot\lambda_2}\cdots x^{\alpha_m}_{\dot\lambda_m}x^{\dot\beta_2}_{\varrho_2}\cdots x^{\dot\beta_m}_{\varrho_m}\varphi^{\varrho_2..\varrho_m\,\dot\lambda_2..\dot\lambda_m}.$$

Then, using the spinor identity

$$x_{\alpha\dot\beta}x^{\dot\beta\varrho} = -(x_ix_i)\delta^{\varrho}_{\alpha},$$

one may show that

$$(14)\qquad \begin{cases} u'^{\alpha_2..\alpha_m\,\dot\beta_1..\dot\beta_m} = -(1/k^4)(x_ix_i)^{3-m}x^{\alpha_2}_{\dot\lambda_2}\cdots x^{\alpha_m}_{\dot\lambda_m}x^{\dot\beta_1}_{\varrho_1}\cdots x^{\dot\beta_m}_{\varrho_m}v^{\varrho_1..\varrho_m\,\dot\lambda_2..\dot\lambda_m}, \\ v'^{\alpha_1..\alpha_m\,\dot\beta_2..\dot\beta_m} = -(1/k^4)(x_ix_i)^{3-m}x^{\alpha_1}_{\dot\lambda_1}\cdots x^{\alpha_m}_{\dot\lambda_m}x^{\dot\beta_2}_{\varrho_2}\cdots x^{\dot\beta_m}_{\varrho_m}u^{\varrho_2..\varrho_m\,\dot\lambda_1..\dot\lambda_m}. \end{cases}$$

From this [4] it follows that

$$(15)\qquad L_0' = (x_ix_i/k^2)^4 L_0.$$

If we introduce the abbreviation

$$\varphi\cdot\varphi = \varphi_{\alpha_2..\alpha_m\,\dot\beta_2..\dot\beta_m}\varphi^{\alpha_2..\alpha_m\,\dot\beta_2..\dot\beta_m},$$

it follows from (13) that

$$\varphi' \cdot \varphi' = (x_i x_i/k^2)^2 \varphi \cdot \varphi \,.$$

Thus

$$L_1 = \tfrac{1}{4}(\lambda/(m-1))(\varphi \cdot \varphi)^2 \tag{16}$$

has the required transformation properties.

The Lagrangian

$$L = L_0 + L_1 \tag{17}$$

then leads to the conformally invariant equations

$$sp^{\alpha_2}_{\dot\beta_1} u^{\alpha_2..\alpha_m \dot\beta_1..\dot\beta_m} + \dot s p^{\dot\beta_2}_{\alpha_1} v^{\alpha_1..\alpha_m \dot\beta_2..\dot\beta_m} - \lambda(\varphi\cdot\varphi)\varphi^{\alpha_2..\alpha_m \dot\beta_2..\dot\beta_m} = 0 \,. \tag{18}$$

The equations (18) for spinors of even rank can also be written in tensor notation. For example, if $m = 2$, equation (18) becomes

$$P_i F_{ij} + \tfrac{1}{2}\lambda A_i A_i A_j = 0 \,,$$

where

$$F_{ij} = P_i A_j - P_j A_i \,.$$

For spinors of odd rank, let the wave function be the two symmetric objects $u^{\alpha_1..\alpha_m \dot\beta_2..\dot\beta_m}$ and $v^{\alpha_2..\alpha_m \dot\beta_1..\dot\beta_m}$. One may then form the Lagrangian

$$L_0 = \overline{u}_{\alpha_2..\alpha_m \dot\beta_1..\dot\beta_m} \dot s p^{\dot\beta_1}_{\alpha_1} u^{\alpha_1..\alpha_m \dot\beta_2..\dot\beta_m} + \overline{v}_{\alpha_1..\alpha_m \dot\beta_2..\dot\beta_m} sp^{\alpha_1}_{\dot\beta_1} v^{\alpha_2..\alpha_m \dot\beta_1..\dot\beta_m} \,, \tag{19}$$

where $\overline{u}^{\alpha_2..\alpha_m \dot\beta_1..\dot\beta_m}$ and $\overline{v}^{\alpha_1..\alpha_m \dot\beta_2..\dot\beta_m}$ are the complex conjugates of $u^{\dot\alpha_2..\dot\alpha_m \beta_1..\beta_m}$ and $v^{\dot\alpha_1..\dot\alpha_m \beta_2..\beta_m}$ respectively. Then, if the wave function transforms according to

$$\begin{cases} u'^{\alpha_1..\alpha_m \dot\beta_2..\dot\beta_m} = (1/k^3)(x_i x_i)^{2-m} x^{\alpha_1}_{\dot\lambda_1} \dots x^{\alpha_m}_{\dot\lambda_m} x^{\dot\beta_2}_{\varrho_2} \dots x^{\dot\beta_m}_{\varrho_m} v^{\varrho_2..\varrho_m \dot\lambda_1..\dot\lambda_m} \,, \\ v'^{\alpha_2..\alpha_m \dot\beta_1..\dot\beta_m} = (1/k^3)(x_i x_i)^{2-m} x^{\alpha_2}_{\dot\lambda_2} \dots x^{\alpha_m}_{\dot\lambda_m} x^{\dot\beta_1}_{\varrho_1} \dots x^{\dot\beta_m}_{\varrho_m} u^{\varrho_1..\varrho_m \dot\lambda_2..\dot\lambda_m} \,, \end{cases} \tag{20}$$

it follows that [4]

$$\begin{cases} sp'^{\dot\beta_1}_{\alpha_1} u'^{\alpha_1..\alpha_m \dot\beta_2..\dot\beta_m} = -(1/k^5)(x_i x_i)^{3-m} x^{\alpha_2}_{\dot\lambda_2} \dots x^{\alpha_m}_{\dot\lambda_m} x^{\dot\beta_1}_{\varrho_1} \dots x^{\dot\beta_m}_{\varrho_m} sp^{\varrho_1}_{\dot\lambda_1} v^{\varrho_2..\varrho_m \dot\lambda_2..\dot\lambda_m} \,, \\ sp'^{\alpha_1}_{\dot\beta_1} v'^{\alpha_2..\alpha_m \dot\beta_1..\dot\beta_m} = -(1/k^5)(x_i x_i)^{3-m} x^{\alpha_2}_{\dot\lambda_1} \dots x^{\alpha_m}_{\dot\lambda_m} x^{\dot\beta_2}_{\varrho_2} \dots x^{\dot\beta_m}_{\varrho_m} sp^{\dot\lambda_1}_{\varrho_1} u^{\varrho_1..\varrho_m \dot\lambda_2..\dot\lambda_m} \,. \end{cases} \tag{21}$$

As a consequence, the Lagrangian (19) satisfies the transformation law (15). If further we define the quantities

$$u \cdot \overline{v} = u_{\alpha_1..\alpha_m \dot{\beta}_1..\dot{\beta}_m} \overline{v}^{\alpha_1..\alpha_m \dot{\beta}_1..\dot{\beta}_m} ,$$

$$\overline{u} \cdot v = \overline{u}_{\alpha_1..\alpha_m \dot{\beta}_1..\dot{\beta}_m} v^{\alpha_1..\alpha_m \dot{\beta}_1..\dot{\beta}_m} ,$$

then it may be verified that

$$u' \cdot \overline{v}' = (x_i x_i / k^2)^3 \overline{u} \cdot v ,$$

$$\overline{u}' \cdot v' = (x_i x_i / k^2)^3 u \cdot \overline{v} .$$

Thus the Lagrangian

$$L_1 = \tfrac{3}{4} \lambda [\overline{u} \cdot v - u \cdot \overline{v}]^{\frac{4}{3}} \tag{22}$$

has the required transformation properties. (It is necessary to include both $\overline{u} \cdot v$ and $u \cdot \overline{v}$ in order to provide for improper Lorentz transformations.) Then the Lagrangian

$$L = L_0 + L_1 \tag{23}$$

formed from (19) and (22) leads to the conformally invariant equations

$$\left\{ \begin{array}{l} \dot{s} p^{\dot{\beta}_1}_{\alpha_1} u^{\alpha_1..\alpha_m \dot{\beta}_2..\dot{\beta}_m} + \lambda [\overline{u} \cdot v - u \cdot \overline{v}]^{\frac{1}{3}} v^{\alpha_2..\alpha_m \dot{\beta}_1..\dot{\beta}_m} = 0 , \\ s p^{\alpha_1}_{\dot{\beta}_1} v^{\alpha_2..\alpha_m \dot{\beta}_1..\dot{\beta}_m} - \lambda [\overline{u} \cdot v - u \cdot \overline{v}]^{\frac{1}{3}} u^{\alpha_1..\alpha_m \dot{\beta}_2..\dot{\beta}_m} = 0 . \end{array} \right. \tag{24}$$

If in equation (22) a positive sign is used, so that

$$L_1 = \tfrac{3}{4} \lambda [\overline{u} \cdot v + u \cdot \overline{v}]^{\frac{4}{3}} ,$$

the resultant equation is invariant under time-like, but not space-like, reflections. It is also invariant under the infinitesimal conformal transformations but not the inversion (3). This corresponds to replacing Gürsey's equation (1) by

$$\gamma_j P_j \psi + \lambda (\overline{\psi} \gamma_5 \psi)^{\frac{1}{3}} \psi = 0 .$$

In addition to the equations given above for a single irreducible spinor, it is also possible to obtain conformally invariant equations for interacting

fields. Let A be a scalar formed from contraction of a product of $2N_f$ fermion (odd rank) spinors, N_b boson (even rank) potentials, and M_b boson fields, the fields and potentials being related by equation (10). The fermion spinors may appear in the combinations

$$\overline{s}p^{\beta_1}_{\alpha_1} u^{\alpha_1..\alpha_m}{}_{\dot\beta_2..\dot\beta_m}, \qquad \text{and} \qquad sp^{\alpha_1}_{\dot\beta_1} v^{\alpha_2..\alpha_m}{}_{\dot\beta_1..\dot\beta_m}\ ; \tag{25}$$

let the number of derivative operators appearing in such a way be N_d. We assume that A is invariant under the space-like reflections; this requires that u, v, and $\overline{u}$, $\overline{v}$ appear together as in (19) and (21). Then, on performing the transformation (3), it follows from the transformation laws (6), (13), (14), (20), and (21), that each pair of fermion wave functions contributes a factor $(x_i x_i/k^2)^3$, each boson potential a factor $(x_i x_i/k^2)$, and each boson field a factor $(x_i x_i/k^2)^2$ (the scalar u of equation (6) is counted as a boson potential for this purpose); each derivative operator appearing in the combination (25) contributes a factor $(x_i x_i/k^2)$. Thus the scalar A transforms according to

$$A' = (x_i x_i/k^2)^{3N_f+N_b+2M_b+N_d} A\ . \tag{26}$$

Consequently an interaction Lagrangian

$$L_{\text{int}} = gA^p\ , \tag{27}$$

where

$$p(3N_f + N_b + 2M_b + N_d) = 4\ , \tag{28}$$

has the proper transformation properties, and will, when combined with the Lagrangians for the non-interacting fields, lead to conformally invariant equations. Clearly, the requirement of conformal invariance restricts the form of interaction terms more than does Lorentz invariance. Any function of a scalar A will give a Lorentz invariant interaction, while for conformal invariance, the interaction is restricted to a linear combination of terms of the form (27).

As an example, we mention the usual interaction between the electron field and the electromagnetic field,

$$L_{\text{int}} = \exp[\overline{\psi}\gamma_j\psi A_j]\ .$$

However, the Pauli interaction [6]

$$L_{\text{int}} = \tfrac{1}{2}\, eF_{jk}\overline{\psi}\gamma_j\gamma_k\psi$$

[6] W. PAULI: *Rev. Mod. Phys.*, **13**, 203 (1941).

does not lead to a conformally invariant equation, since $3N_f+N_b+2M_b+N_d=5$. As another example, a β-type interaction (7) involving four fermions,

$$L_{\text{int}} = g[\overline{\psi}_p \Gamma \psi_n \overline{\psi}_e \Gamma \psi_\nu]^p ,$$

where Γ is any Dirac matrix, is invariant for $p = \frac{2}{3}$.

* * *

The author wishes to express his appreciation to Professor PETER HAVAS for his suggestions.

(7) By treating the conformal transformations of space-time as linear transformations in a six-dimensional space, R. J. FINKELSTEIN: *Nuovo Cimento*, **1**, 1104 (1955) has obtained some conformally invariant β-type interactions. However, these appear to be unrelated to the particular interactions given above, due to the dependence on six co-ordinates.

RIASSUNTO (*)

Si ottengono equazioni d'onda non lineari conformemente invarianti per spinori di ordine arbitrario. Tali equazioni ne includono una recentemente proposta da GÜRSEY. Si danno inoltre equazioni conformemente invarianti per campi interagenti.

(*) *Traduzione a cura della Redazione.*

Velocità delle onde elastiche e dissipazione interna nel metacrilato di polimetile.

L. Verdini

Istituto Nazionale di Ultracustica «O. M. Corbino» - Roma

(ricevuto il 5 Dicembre 1956)

Riassunto. — Servendosi di un metodo dinamico a vibrazioni flessionali, sono state misurate la velocità di propagazione delle onde estensionali e la dissipazione interna di energia elastica in sbarrette di metacrilato di polimetile, al variare della temperatura in un intervallo compreso tra 20 °C e 100 °C. È stato così possibile determinare la temperatura di transizione di tale polimero, tanto dalla variazione del coefficiente di temperatura della velocità, quanto dal flesso che la curva relativa al decremento logaritmico delle oscillazioni libere presenta in un intorno del punto di transizione. La temperatura di transizione varia tra 52 °C e 63 °C e dipende in modo essenziale dal trattamento termico precedentemente subito dal campione sottoposto ad esame. Sembra interessante notare che al disotto del punto di transizione, la dissipazione di energia elastica cresce con legge esponenziale all'aumentare della temperatura, analogamente a quanto è stato recentemente osservato anche nei metalli ed in alcune leghe. Questo fenomeno sembra inquadrarsi in una teoria esposta recentemente da W. P. Mason, secondo cui l'aumento della dissipazione con la temperatura è legato alla progressiva liberazione di un sempre maggior numero di dislocazioni, usualmente bloccate da atomi di impurità.

1. – Introduzione.

Le indagini sperimentali compiute in questi ultimi anni sulla dipendenza della velocità di propagazione delle onde elastiche dalla temperatura nel metacrilato di polimetile, hanno portato a risultati talora notevolmente diversi tra loro [1-4].

[1] T. F. Protzman: *Journ. Appl. Phys.*, **20**, 627 (1941).
[2] J. L. Melchor e A. A. Petrauskas: *Industr. Eng. Chem.*, **44**, 716 (1952).
[3] S. V. Subrahmanyam: *Journ. Chem. Phys.*, **22**, 1562 (1954).
[4] M. Krishnamurthi e G. Sivarama Sastry: *Nature*, **174**, 132 (1954).

Infatti mentre è stata accertata in ogni caso la presenza di una variazione abbastanza brusca del coefficiente di temperatura della velocità — variazione che è generalmente attribuita ad un fenomeno di transizione — i risultati relativi al valore della temperatura in cui si manifesta tale fenomeno sono tuttora piuttosto incerti.

Inoltre, dal lavoro di T. F. PROTZMAN [1] la temperatura in cui si nota la transizione risulta diminuire con l'aumentare della frequenza delle onde elastiche, in netto contrasto con le teorie del rilassamento che prevedono un aumento della temperatura di transizione con il crescere della frequenza. Tuttavia i più recenti risultati sperimentali indicano una netta indipendenza del punto di transizione dalla frequenza, almeno in un intervallo compreso tra 100 kHz e 10 MHz.

Recentemente P. HATFIELD [5], prendendo in esame i risultati sperimentali raccolti nella Fig. 1, ha affacciato l'ipotesi che la dipendenza dalla frequenza del punto di transizione notata da T. F. PROTZMAN, sia da attribuire ad una errata valutazione della temperatura del campione. Infatti, la notevole quantità di energia elastica impiegata in queste esperienze provocherebbe, all'interno del campione, un aumento della temperatura — il quale dipende in modo essenziale dalla frequenza della sollecitazione — alterando così i risultati sperimentali.

D'altra parte, le differenze riscontrate nella determinazione della temperatura di transizione da sperimentatori diversi potrebbero essere attribuite alla non identica natura dei campioni esaminati, dovuta sia ad un diverso processo di polimerizzazione, sia all'impiego di catalizzatori e di sostanze plastificanti differenti. Un notevole ruolo gioca anche il trattamento termico in quanto esso dà origine, in seno al polimero, a processi di natura irreversibile.

Prendendo le mosse dalle considerazioni di P. HATFIELD, ci è sembrato essenziale tener conto, nella presente indagine sperimen-

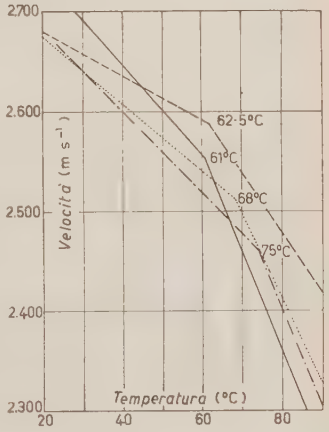

Fig. 1. – Velocità degli ultrasuoni nel metacrilato di polimetile in funzione della temperatura: ------ risultati di PROTZMAN a 3 MHz; ···· risultati di HATFIELD a 350÷750 kHz; -·-·- risultati di MELCHOR e PETRAUSKAS a 0.5÷10 MHz; ——— risultati di KRISHNAMURTHI e SASTRY a 1÷6 MHz (da P. HATFIELD [5]).

[5] P. HATFIELD: *Nature*, **174**, 1186 (1954).

tale, anche della storia termica di ciascun campione, completando inoltre i dati relativi alla dipendenza della velocità dalla temperatura con una determinazione sistematica della dissipazione interna, in funzione tanto della temperatura quanto del trattamento termico.

2. – Tecnica sperimentale.

Per la determinazione della velocità di propagazione delle onde elastiche estensionali, si è fatto uso di un metodo dinamico a vibrazioni flessionali, già più volte descritto e sul quale non è qui il caso di insistere ([6,7]).

Basterà solo ricordare che, tanto l'eccitazione elettrostatica della sbarretta in esame quanto la rivelazione della sua ampiezza di vibrazione, vengono fatte servendosi di un unico elettrodo.

Le frequenze di risonanza delle sbarrette utilizzate in questa ricerca sono comprese tra 580 Hz e 750 Hz, essendo i valori minori relativi alle temperature più elevate.

La precisione che è stata possibile ottenere in questa serie di misure di autofrequenze, si aggira intorno all'1 ‰, con un lieve aumento dell'imprecisione verso le temperature più elevate per le quali le difficoltà nella determinazione della frequenza di risonanza divengono notevolmente maggiori.

Come misura della dissipazione dell'energia elastica, è stato preso il reciproco del coefficiente di risonanza Q della sbarretta vibrante. Come è noto, Q^{-1} è legato al decremento logaritmico δ delle oscillazioni libere dalla relazione

$$\delta = \pi \cdot Q^{-1} . \tag{1}$$

La precisione raggiunta in queste misure è di qualche unità per cento: essa è da ritenersi soddisfacente quando si tenga conto del forte smorzamento di questo materiale, specialmente alle alte temperature, e delle notevoli difficoltà sperimentali.

Il metacrilato di polimetile, da cui sono stati ricavati i nostri campioni, è il polimero noto commercialmente con il nome di « Perspex », del tipo non plastificato, prodotto dalle Industrie inglesi I.C.I. Tutte le sbarrette adoperate nella presente ricerca sono state ricavate da una unica lastra dello spessore di circa 0.8 mm.

Per ragioni di brevità, riporteremo qui i dati sperimentali relativi a due soli campioni, che chiameremo « sbarretta A » e « sbarretta B », la cui storia termica è stata notevolmente diversa durante il periodo di misura.

([6]) I. Barducci e G. Pasqualini; *Nuovo Cimento*, **5**, 416 (1948).
([7]) P. G. Bordoni e M. Nuovo: *Ric. Scient.*, **24**, 560 (1954).

Le dimensioni dei due campioni, prima di qualsiasi trattamento termico, erano le seguenti:

$$A: \begin{cases} l = 50.00 \text{ mm} \\ h = 0.86 \text{ »} \end{cases} ; \quad B: \begin{cases} l = 49.78 \text{ mm} \\ h = 0.87 \text{ »} \end{cases}$$

ove con l si è indicata la lunghezza e con h lo spessore della sbarretta. È da tener presente che uno dei più importanti effetti del riscaldamento sul metacrilato di polimetile è la perdita di peso del campione, unita a fenomeni di contrazione; da ciò si comprende come sia stato necessario un continuo controllo delle dimensioni della sbarretta subito dopo ciascun trattamento termico.

Le due sbarrette A e B sono state via via sottoposte a trattamenti termici sempre più elevati, ma differenti nei due casi, come risulta dalla Tabella I.

TABELLA I. – *Trattamenti termici subiti dai due campioni.*

Sbarretta A		Sbarretta B	
Temperatura di ricottura (°C)	Tempo di ricottura (ore)	Temperatura di ricottura (°C)	Tempo di ricottura (ore)
40	5	—	—
60	6	—	—
—	—	70	7
80	14	—	—
—	—	90	20
100	15	—	—

Durante le successive serie di misure, il campione in esame veniva posto in un forno, la cui temperatura era automaticamente controllata entro ± 1 °C, mediante un termometro autoregolatore.

Le misure, tanto di velocità quanto di dissipazione, sono state eseguite su un intervallo di temperatura compreso tra 15 °C e 90 °C. La temperatura della sbarretta veniva determinata servendosi di un termometro immerso nell'ambiente circostante al campione, e di una termocoppia posta a diretto contatto.

La tecnica impiegata è la seguente: portato il campione ad una temperatura prefissata e raggiunto l'equilibrio termico, si seguivano le fasi di questo primo trattamento termico misurando di ora in ora l'autofrequenza fondamentale e lo smorzamento della sbarretta; quando non si rilevavano ulteriori differenze, si dava inizio alla serie di misure in temperatura decrescente, abbassando di volta in volta la temperatura di $2 \div 4$ °C. Si noti che per avere una misura corretta era opportuno attendere circa un'ora e mezza tra due misure

successive, e ciò anche a causa dell'elevato calore specifico (0.35 cal g^{-1} $°C^{-1}$) e della bassa conducibilità termica ($3.5 \cdot 10^{-4}$ unità c.g.s.) del metacrilato di polimetile.

Procedendo in questo modo è stato possibile determinare la temperatura del campione entro 2 o 3 decimi di grado.

Ripetendo la serie di misure, tanto a temperatura decrescente quanto a temperatura crescente, ma senza superare la temperatura dell'ultimo trattamento termico, si sono ottenuti risultati ripetibili, almeno entro i limiti degli errori sperimentali, anche a distanza di tempo.

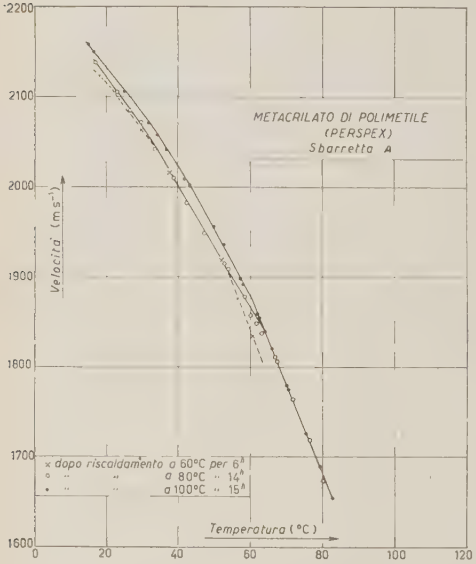

Fig. 2. – Velocità delle onde elastiche estensionali (580÷750 Hz) nella « sbarretta A » in funzione della temperatura e del trattamento termico.

3. – Risultati sperimentali.

Nella Fig. 2 sono riportati i risultati sperimentali delle misure di velocità relative alla sbarretta A, ottenuti dopo tre trattamenti termici differenti. Per semplicità non sono stati riportati i punti ricavati dopo il primo trattamento termico (5 ore a 40 °C), sia perchè non interessano la zona di transizione, sia perchè essi risultano perfettamente allineati.

In tutte e tre le curve qui riportate, si nota una netta variazione del coefficiente di temperatura, rispettivamente a 52 °C, 63 °C e 62 °C, corrispondenti alla temperatura di transizione del polimero.

I successivi trattamenti termici hanno provocato via via un aumento del valore della velocità ed uno spostamento del punto di transizione verso le temperature più elevate.

È interessante notare che, mentre per i trattamenti termici effettuati a temperature inferiori a 50 °C, l'andamento della velocità è sensibilmente lineare, dopo ricotture più spinte il diagramma, in corrispondenza alle temperature più basse, tende ad incurvarsi sempre di più e su un intervallo sempre più ampio.

La Fig. 3 riporta gli analoghi risultati relativi alla sbarretta B; su di essa si possono ripetere le considerazioni già fatte nel caso della sbarretta A. Anche

da queste due curve è facile determinare il punto di transizione, che si ha rispettivamente a 52.5 °C e 55 °C, in buon accordo con i dati ricavati dalla precedente figura.

Nella Tabella II sono raccolti, a titolo di confronto, i valori del coefficiente di temperatura della velocità, ricavati dalla letteratura, considerati immediatamente al disotto ed al disopra del punto di transizione T_0. Si è ritenuto utile completare questi dati riportando anche la frequenza ν delle vibrazioni elastiche.

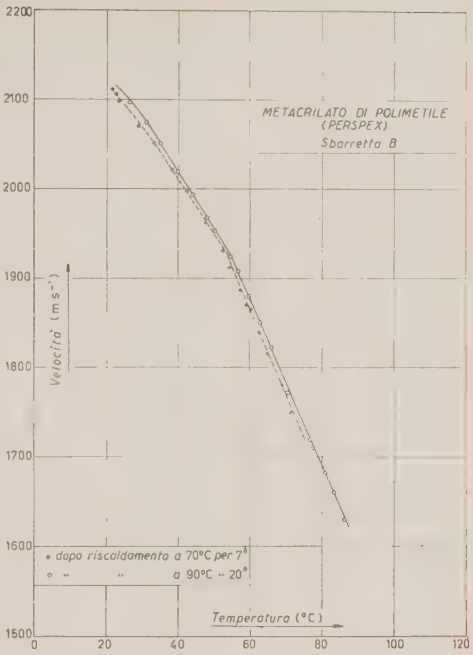

Fig. 3. – Velocità delle onde elastiche estensionali (580 ÷ 750 Hz) nella «sbarretta B» in funzione della temperatura e del trattamento termico.

TABELLA II. – *Coefficiente di temperatura della velocità* $\Delta v/\Delta T$.

Autori	ν	T_0	$\Delta v/\Delta T$ per $T < T_0$	$\Delta v/\Delta T$ per $T > T_0$
MELCHOR e PETRAUSKAS [2]	0.5 ÷ 10 MHz	75 °C	— 4.5 $ms^{-1}\,°C^{-1}$	— 9,1 $ms^{-1}\,°C^{-1}$
KRISHNAMURTHI e SASTRY [4]	1.0 ÷ 6 »	61 »	— 4.6 »	— 9.2 »
HATFIELD [5]	350 ÷ 750 kHz	68 »	— 3.35 »	— 8.3 »
SUBRAHMANYAM [3]	90 ÷ 100 »	61 »	— 4.9 »	— 8.6 »
Presente lavoro, sbarretta A	580 ÷ 750 Hz	62 »	— 6.7 »	— 9.9 »
Presente lavoro, sbarretta B	580 ÷ 750 Hz	55 »	— 6.4 »	— 9.2 »

Come si vede, l'accordo fra questi dati non è sempre soddisfacente, specialmente per temperature inferiori a T_0 e ciò potrebbe essere dovuto non solo

alla differente natura dei campioni, ma anche al tipo di vibrazione ed ai diversi valori della frequenza impiegata. In particolare, nel nostro caso venivano usate, come già si è detto, vibrazioni di tipo flessionale e di frequenza notevolmente più bassa di tutte quelle riportate nella Tabella II.

Nelle Fig. 4 e 5 è stato riportato, in funzione della temperatura, il reciproco del coefficiente di risonanza Q delle due sbarrette in esame, il cui valore, come si è detto, può essere preso a rappresentare la dissipazione di energia elastica nel campione. Da questi diagrammi risulta chiaro che i successivi trattamenti termici provocano solamente una piccola diminuzione della dissipazione interna, mentre l'andamento generale delle curve rimane sensibilmente invariato.

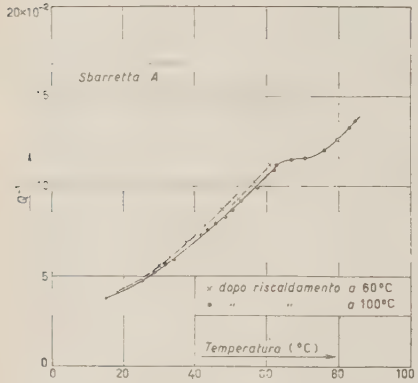

Fig. 4. – Dissipazione interna di energia elastica nella « sbarretta A » in funzione della temperatura e del trattamento termico.

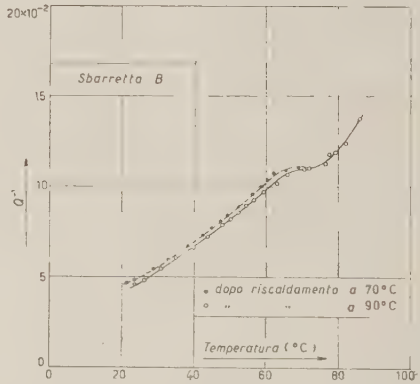

Fig. 5. – Dissipazione interna di energia elastica nella « sbarretta B » in funzione della temperatura e del trattamento termico.

La legge secondo cui la dissipazione interna cresce con la temperatura è dapprima esponenziale, ma subisce una brusca variazione in corrispondenza al punto di transizione T_0 già osservato nelle curve relative alla velocità. Al disopra di tale punto, l'aumento della dissipazione è appena sensibile in un intervallo compreso entro una decina di gradi, e riprende poi il suo andamento esponenziale per temperature ancora maggiori.

Allo scopo di verificare questo andamento esponenziale della dissipazione, abbiamo riportato nelle Fig. 6 e 7 il logaritmo del decremento δ in funzione del reciproco della temperatura assoluta T. I punti che così si ottengono, risultano disposti con buona approssimazione su di una retta, mentre la temperatura di transizione rimane caratterizzata da una netta discontinuità nella

pendenza della retta stessa. Il trattamento termico, d'altra parte, modifica solo lievemente il valore della pendenza.

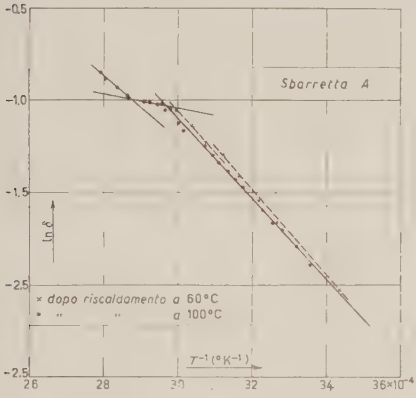

Fig. 6. – Logaritmo naturale del decremento delle oscillazioni libere in funzione del reciproco della temperatura assoluta.

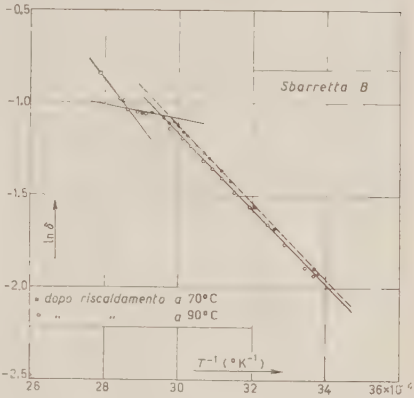

Fig. 7. – Logaritmo naturale del decremento delle oscillazioni libere in funzione del reciproco della temperatura assoluta.

Sembra pertanto giustificato scrivere per il decremento logaritmico δ, oppure per il coefficiente di risonanza Q, una formula del tipo:

$$\delta = \delta_0 \cdot \exp\left[-\frac{\Delta H}{RT}\right], \tag{2}$$

e

$$\frac{1}{Q} = c \cdot \exp\left[-\frac{\Delta H}{RT}\right], \tag{3}$$

ove ΔH rappresenta l'energia di attivazione del fenomeno legato all'aumento della dissipazione interna con la temperatura, T la temperatura assoluta, e R la costante dei gas.

Una legge di questo tipo è stata trovata anche nei metalli [8,9] e nelle leghe metalliche [10] da vari sperimentatori. W. P. Mason [11], ne ha recentemente data una spiegazione, proponendo una teoria strutturale secondo la

[8] T. S. Ké: *Phys. Rev.*, **71**, 533 (1947).
[9] P. G. Bordoni e M. Nuovo: *Nuovo Cimento*, **11**, 127 (1954).
[10] I. Barducci: *Ric. Scient.*, **22**, 1733 (1952).
[11] W. P. Mason: *Bell. Syst. Techn. Journ.*, **34**, 903 (1955).

quale l'aumento esponenziale della dissipazione elastica è da attribuirsi alla progressiva liberazione di un sempre maggior numero di dislocazioni — usualmente bloccate da atomi di impurità — in conseguenza dell'agitazione termica. Secondo questo schema, la dissipazione verrebbe ad essere indipendente dalla frequenza delle sollecitazioni, e pertanto quest'effetto è stato indicato da MASON con il nome di « isteresi meccanica attivata dalla temperatura ».

Applicando la sua teoria ai risultati sperimentali noti per alcuni metalli, MASON ha trovato valori di ΔH compresi tra 3 000 e 5 200 cal/mole circa. Con questo risultato si accordano i dati dedotti dalle nostre misure e raccolti nella Tabella III.

TABELLA III. – *Valori dell'energia di attivazione* ΔH *(cal/mole).*

Campione	Trattamento termico	$T < T_0$	$T_0 < T < T_A$	$T > T_A$
Sbarretta *A*	60 °C	4 250	—	—
	100 °C	4 150	750	3 500
Sbarretta *B*	70 °C	4 100	—	—
	90 °C	4 000	870	5 100

N. B. La temperatura T_A rappresenta il punto in cui la dissipazione riprende a crescere rapidamente.

Per la costante c della relazione (3) si sono trovati i seguenti valori:

$$\text{sbarretta } A \begin{cases} c = 70.5 & \text{dopo trattamento a } 60\ ^\circ\text{C} \\ c = 52.5 & \text{» » » } 100\ ^\circ\text{C} \end{cases}$$

$$\text{sbarretta } B \begin{cases} c = 48.5 & \text{» » » } 70\ ^\circ\text{C} \\ c = 40.0 & \text{» » » } 90\ ^\circ\text{C} \end{cases}$$

In questo schema teorico, trova immediata spiegazione la diminuzione della dissipazione interna e dell'energia ΔH per effetto dei trattamenti termici; basta pensare che questi provocano una progressiva eliminazione sia di difetti e di dislocazioni, sia di eventuali impurità ancora presenti in seno al polimero.

L'esistenza della singolarità osservata in un ristretto intervallo immediatamente superiore alla temperatura T_0, fa pensare che questo fenomeno di transizione non sia così brusco come apparirebbe dai diagrammi relativi alla velocità, pur non escludendo che tale fatto possa essere legato alla particolare frequenza impiegata.

Circa la dipendenza nel metacrilato di polimetile della dissipazione interna dalla frequenza, G. C. PARFITT [12] ha rilevato una lieve diminuzione di questo parametro in un intervallo compreso tra 5 kHz e 60 kHz. Estrapolando alle frequenze adoperate nelle nostre esperienze i dati riportati da G. C. PARFITT, si trova per il reciproco del coefficiente di risonanza a temperatura ambiente un valore di $4.8 \cdot 10^{-2}$, che è in buon accordo con i nostri dati sperimentali. L'esclusione di una forte dipendenza della dissipazione interna dalla frequenza si allinea con la teoria di Mason e trova una ulteriore conferma nei recenti risultati sperimentali di I. BARDUCCI [13], relativi ad alcune particolari leghe metalliche in cui l'attrito interno cresce esponenzialmente con la temperatura.

4. – Conclusioni.

I risultati ottenuti, confermano nel metacrilato di polimetile la presenza di un fenomeno di transizione, che si rivela con una discontinuità tanto nel coefficiente di temperatura della velocità, quanto nell'andamento della dissipazione interna di energia elastica.

Particolarmente interessante appare la dipendenza dei vari parametri qui considerati dalla storia termica dei campioni in esame.

I trattamenti termici via via più spinti, provocano un aumento della velocità ed una lieve diminuzione della dissipazione interna di energia elastica, mentre la temperatura di transizione si sposta verso valori più elevati e risulta compresa tra 52 °C e 63 °C.

Il fatto che i diagrammi sperimentali, in particolare quelli relativi alla dissipazione, siano ripetibili purchè non si superi la temperatura della ricottura precedente, consente di escludere la possibilità che le singolarità riscontrate, siano dovute a variazioni strutturali irreversibili.

In altri termini, i risultati di queste misure rivelano il reale effetto della temperatura sul parametro in esame e sulla struttura venutasi a determinare dopo l'ultimo trattamento termico, poichè la tecnica sperimentale qui adoperata permette di separare l'effetto permanente della ricottura da quello reversibile della temperatura.

Si è così verificato che la dissipazione interna cresce con la temperatura seguendo una legge esponenziale, analogamente a quanto è stato trovato in alcuni metalli e leghe metalliche.

I dati sperimentali ottenuti trovano una prima soddisfacente interpretazione nella teoria di Mason detta della « isteresi meccanica », secondo cui l'au-

[12] G. C. PARFITT: *Nature*, **164**, 489 (1949) (London).
[13] I. BARDUCCI: *Ric. Scient.*, **26**, 2159 (1956).

mento della dissipazione con la temperatura è legato al numero di dislocazioni via via liberate dall'agitazione termica.

Resta ancora da accertare se la singolarità presentata dalla dissipazione interna al disopra della temperatura di transizione sia legata o meno alla frequenza: solo nel secondo caso infatti è possibile escludere che tale singolarità sia semplicemente dovuta ad un fenomeno di rilassamento elastico.

* * *

Ci è particolarmente gradito ringraziare il prof. A. GIACOMINI, direttore dell'Istituto Nazionale di Ultracustica, ed il prof. I. BARDUCCI per i validi suggerimenti e per l'interesse con cui ha seguito la presente ricerca.

SUMMARY

By means of a dynamical method, the velocity of elastic extensional waves as well as internal friction, have been measured on polymethyl-metacrylate bars, in a temperature range from 20 °C to 100 °C. Bars of rectangular cross-section having a flexural natural frequency between 580 and 750 Hz have been employed. The transition temperature of the polymer has been detected from the velocity vs. temperature and damping vs. temperature curves. At the transition point, the damping curves show an anomalous horizontal behaviour and in the velocity curves a sudden change in the temperature coefficient is observed. The specimens under measurement have been annealed at different temperatures, and as a consequence of these heat treatements, a series of transition temperatures laying between 52 °C and 63 °C has been found. It may be observed that below the transition point, internal friction increases exponentially with temperature, in agreement with the results obtained in pure metals and alloys. This behaviour seems to agree with a theory due to W. P. MASON, who has shown that the exponential increase of internal friction in solids is due to the breakways of the dislocations from their impurity pinning points, as a consequence of thermal agitation.

On Scattering at Very High Energies (*).

K. Symanzik (+)

Enrico Fermi Institute for Nuclear Studies, University of Chicago

(ricevuto il 10 Dicembre 1956)

Summary. — The asymptotic behavior of the scattering amplitude at very high energies is discussed on the basis of the general dispersion relations and the unitarity requirement. The assumption that the tangent approximation fulfills the dispersion relation leads to the prediction that the total cross-section can asymptotically not increase as strongly as proportional to the laboratory energy. The relevance of this result is discussed.

1. – Introduction.

From the local character of the conventional field theory only the dispersion relations (1) as well as low-energy-limit theorems implied by them have as yet been derived. The property of the scattering amplitude that is expressed by the dispersion relation is most simply formulated if the scattering process is looked at in the center of mass system of the target particle in its initial and final state. In this system the target particle of mass M has momentum $-\Delta$ and $+\Delta$ before and after the collision, respectively, and the scattered particle of mass μ keeps its energy ω. Then, for neutral scalar particles, the scattering amplitude $T_{\omega,\Delta}$ possesses for fixed Δ (Δ an analytical continuation into the upper half complex ω-plane that is holomorphic there and increases in infinity absolutely not stronger than a finite power of $|\omega|$. By division

(*) This work was supported by a grant from the U.S. Atomic Energy Commission.

(+) At present at the University of Hamburg, Germany.

(1) N. N. Bogoliubov: *Phys. Rev.* (to appear). Reported at the *International Conference of Theoretical Physics, Seattle, Washington*, September 1956.

by a polynomial in ω of sufficiently high degree with no zeros in the upper half plane one forms out of the scattering amplitude a holomorphic function that vanishes for $|\omega| \to \infty$ such that between its real and imaginary part at the real ω-axis Hilbert's relation (2) holds. If the zeros of the polynomial are chosen at $\pm\omega_1 \ldots, \pm\omega_n$ infinitesimally below the real axis one obtains the dispersion relation

$$(1) \qquad \mathrm{Re}\, T_{\omega,\Delta} = \sum_{\nu=1}^{n} \mathrm{Re}\, T_{\omega_\nu,\Delta} \prod_{\lambda\neq\nu} \frac{\omega^2-\omega_\lambda^2}{\omega_\nu^2-\omega_\lambda^2} + \\ + \frac{1}{\pi}\prod_{\nu=1}^{n}(\omega^2-\omega_\nu^2) P\int_0^\infty \frac{2\omega'\,\mathrm{d}\omega'\,\mathrm{Im}\, T_{\omega',\Delta}}{(\omega'^2-\omega^2)-(\omega'^2-\omega_\nu^2)}.$$

The minimal number of auxiliary denominators in (1) depends on the strength of the singularity of the commutator of the meson field operator on the light cone and is not yet known. The introduction of such auxiliary denominators in (1) is also practically indispensable in order to secure a sufficiently rapid convergence of the integral if experimental data are to be inserted. Since, however, the theoretically unknown functions $\mathrm{Re}\, T_{\omega_\nu,\Delta}$ appear in the relation, it is of interest to know how many are unavoidable. This is synonymous with the practically significant question of how strong a convergence of the integral in (1) may be expected.

We shall present an argument in favour of the sufficiency of $n = 1$ in the dispersion relation (1). For we shall show that this follows if we assume that the tangent approximation (3) which seems to be appropriate at high energies fulfills (1) with any finite n. At the end the relevance of this result will be discussed.

2. – Derivation of Formula (8).

For total energy W and scattering angle ϑ in the ordinary center of mass system, we have

$$W^2 = 2\omega\sqrt{M^2+\Delta^2} + 2\Delta^2 + M^2 + \mu^2$$

and

$$\vartheta = 2\sin^{-1}\{2W\Delta[(W^2-(M+\mu)^2)(W^2-(M-\mu)^2)]^{-\frac{1}{2}}\}.$$

(2) E.g. E. C. Titchmarsh: *Theory of Fourier Integrals* (Oxford, 1937).

(3) This approximation has already been used in conjunction with the dispersion relation by H. A. Bethe and F. Rohrlich: *Phys. Rev.*, **86**, 10 (1952).

Furthermore

$$T_{\omega,\Delta} = T_W(\vartheta) = \frac{16\pi W^2}{[(W^2-(M+\mu)^2)(W^2-(M-\mu)^2)]^{\frac{1}{2}}} \sum_{l=0}^{\infty} (2l+1) c_{W,l} P_l(\cos\vartheta) ,$$

where

$$C_{W,l} = \sin\delta_{W,l} \exp[i\delta_{W,l}]$$

with

$$0 \leqslant \operatorname{Im} c_{W,l} - |c_{W,l}|^2 \leqslant (2l+1)^{-\frac{1}{2}} r(W) \tag{2}$$

for some $r(W)$.

In tangent approximation we get

$$W^2 \approx 2\omega\sqrt{M^2+\Delta^2} ,$$

$$\vartheta \approx 4\Delta W^{-1}$$

and

$$T_W(\vartheta) \approx 32\pi \int_0^{\infty} l\, \mathrm{d}l c_{W,l} J_0(4W^{-1}l\Delta) . \tag{3}$$

Inserting (3) into (1), multiplying by $J_0(4W^{-1}l_0\,l)\,l\,\mathrm{d}\,l$ and integrating from zero to infinity, we obtain

$$W^2 \operatorname{Re} c_{W,l_0} = \sum_{\nu=1}^{n} W_\nu^2 \operatorname{Re} c_{W_\nu,W^{-1}W_\nu l_0} \prod_{\lambda\neq\nu} \frac{W^4-W_\lambda^4}{W_\nu^4-W_\lambda^4} + \tag{4}$$

$$+ \frac{1}{\pi} \prod_{\nu=1}^{n} (W^4-W_\nu^4) P \int_0^{\infty} \frac{2W'^2\,\mathrm{d}W'^2 W'^2 \operatorname{Im} c_{W',W'^{-1}W'l_0}}{(W'^4-W^4)\prod(W'^4-W_\nu^4)} .$$

With $c_{W,l} \equiv c_{l/W}(W^2)$ and therefore

$$T_{\omega,\Delta} = T_W(4W_\Delta^{-1}) = 32\pi W^2 \int_0^{\infty} \alpha\,\mathrm{d}\alpha c_\alpha(W^2) J_0(4\alpha\Delta) . \tag{5}$$

Eq. (4) means that $zc_\alpha(z)$ possesses for fixed α a holomorphic continuation into the upper half z-plane. It increases for $z \to \infty$ not as strongly as z^{2n} and at the real z-axis the imaginary part of $zc_\alpha(z)$ is odd, the real part even. $c_\alpha(z)$ then has the same properties but even imaginary and odd real part. (Here $\alpha = W^{-1}l$ is half the impact parameter, and for the case of photon scattering the analytic property of $c_\alpha(z)$ has been concluded by BETHE and ROHRLICH [3] from an elementary consideration.) $d_\alpha(z) = 1 + 2ic_\alpha(z)$ then, as

a consequence of (2), satisfies $|d_\alpha(z)| \leqslant 1$ at the real axis and possesses a holomorphic continuation. According to the theorem of PHRAGMÉN and LINDELÖF [4] $d_\alpha(z)$, due to its moderate increase in infinity, satisfies $|d_\alpha(z)| \leqslant 1$ everywhere in the upper half plane. Therefore $c_\alpha(z)$ satisfies $|c_\alpha(z)| \leqslant 1$ and has non-negative imaginary part in the whole upper half plane. (If we, at the real axis, only demand $\operatorname{Im} c_{W,l} \geqslant \beta |c_{W,l}|^2$ with $\beta > 0$, we obtain $|c_\alpha(z)| \leqslant \beta^{-1}$ instead of < 1.) Due to its non-negative part $c_\alpha(z)$, according to the theorem of HERGLOTZ and RIESS [5], possesses the representation

$$c_\alpha(z) = A_\alpha + B_\alpha z + \dot{\int_{-\infty}^{+\infty}} \frac{1+tz}{t-z}\, \mathrm{d}\sigma_\alpha(t)\,,$$

with A_α, B_α, $\sigma_\alpha(t)$ real, $B_\alpha \geqslant 0$, $\sigma_\alpha(t)$ non decreasing.

Because of $|c_\alpha(z)| < 1$ the Stieltjes integral could be written as a Riemannian one. The symmetry character of $c_\alpha(z)$ leads to

$$c_\alpha(z) = B_\alpha z + z \dot{\int_{-\infty}^{+\infty}} \frac{1+t^2}{t^2-z^2}\, \mathrm{d}\sigma_\alpha(t). \tag{6}$$

Since the integral vanishes for $|z| \to \infty$, from $|c_\alpha(z)| \leqslant 1$ we conclude $B_\alpha = 0$. Furthermore

$$\dot{\int_{-\infty}^{\infty}} \mathrm{d}\sigma_\alpha(t) = \mathrm{i} c_\alpha(\mathrm{i}) < 1\,.$$

Inserting (6) with $B_\alpha = 0$ into (5), we infer from the finiteness of $T_W(4\Delta/W)$ and especially from $T_W(4W^{-1}\Delta)|_{W^2=\mathrm{i}} < \infty$ that the integrations can be interchanged and therefore

$$T_W(4W_\Delta^{-1}) = 32\pi W^4 \dot{\int_{-\infty}^{+\infty}} \frac{1+t^2}{t^2-W^4} \left[\int_0^\infty x\, \mathrm{d}x J_0(4x\sqrt{\Delta})\, \mathrm{d}\sigma_\alpha(t) \right] \quad W^4 \dot{\int_{-\infty}^{+\infty}} \frac{\mathrm{d}S(t,\Delta)}{t^2-W^4}\,, \tag{7}$$

with $S(t,0)$ non-decreasing and $|\mathrm{d}S(t,\Delta)| \leqslant \mathrm{d}S(t,0)$. Furthermore

$$|\operatorname{Im} W^{-2} T_W(4\Delta/W)| \leqslant \operatorname{Im} W^{-2} T_W(0)$$

and in the first W^2-quadrant even

$$|\operatorname{Im} W^{-4} T_W(4\Delta/W)| \leqslant \operatorname{Im} W^{-4} T_W(0)\,.$$

[4] E.g. E. C. TITCHMARSH: *Theory of Functions* (Oxford, 1939).
[5] E.g. R. NEVANLINNA: *Eindeutige analytische Funktionen* (Berlin, 1936).

Replacing W^2 by the asymptotically proportional ω and subtracting from (7) the equation for a fixed real ω_0, we obtain the universally valid formula

$$T_{z,\Delta} = \operatorname{Re} T_{\omega_0,\Delta} + (z^2 - \omega_0^2) \int_{-\infty}^{+\infty} \frac{\mathrm{d}\hat{S}(t, \Delta)}{t^2 - z^2} P \frac{1}{t^2 - \omega_0^2} \tag{8}$$

which is the aforementioned result. The total cross-section

$$\sigma_{tot}(\omega) = \tfrac{1}{2} M^{-1} (\omega^2 - \mu^2)^{-\frac{1}{2}} \operatorname{Im} T_{\omega,0}$$

has obviously the property

$$\int_{\mu}^{\infty} \frac{\sigma_{tot}(\omega)}{\omega^2} \mathrm{d}\omega < \infty . \tag{9}$$

If the present method is applied to the pseudoscalar symmetric meson theory, we obtain for the four amplitudes A_1, B_1, A_2, B_2 as defined by GOLDBERGER [6] (the subscripts 2 and 1 refer to isospin flip and non-flip, respectively; B, A to spin flip and non-flip, respectively, in the previously introduced coordinate system) the relations

$$\operatorname{Re} A_1(\omega, 1) - \operatorname{Re} A_1(\omega_0, 1) = \frac{(\omega^2 - \omega_0^2)}{\pi} P \int_0^{\infty} \frac{2\omega' \mathrm{d}\omega' \operatorname{Im} A_1(\omega', \Delta)}{(\omega'^2 - \omega^2)(\omega'^2 - \omega_0^2)} \tag{10}$$

$$\operatorname{Re} B_1(\omega, \Delta) = \frac{2\omega}{\pi} P \int_0^{\infty} \frac{\mathrm{d}\omega' \operatorname{Im} B_1(\omega', \Delta)}{\omega'^2 - \omega^2} , \tag{11}$$

$$\operatorname{Re} A_2(\omega, 1) = \frac{\omega}{\omega_0} \operatorname{Re} A_2(\omega_0, \Delta) + \frac{2\omega}{\pi} (\omega^2 - \omega_0^2) P \int_0^{\infty} \frac{\mathrm{d}\omega' \operatorname{Im} A_2(\omega', \Delta)}{(\omega'^2 - \omega^2)(\omega'^2 - \omega_0^2)} , \tag{12}$$

$$\operatorname{Re} B_2(\omega, 1) - \operatorname{Re} B_2(\omega_0, 1) = \frac{\omega^2 - \omega_0^2}{\pi} P \int_0^{\infty} \frac{2\omega' \mathrm{d}\omega' \operatorname{Im} B_2(\omega', \Delta)}{(\omega'^2 - \omega^2)(\omega'^2 - \omega_0^2)} , \tag{13}$$

where in addition

$$\int_0^{\infty} \frac{\operatorname{Im} A_2(\omega, \Delta) \omega \, \mathrm{d}\omega}{(\omega^2 + \omega_0^2)^2} < \infty , \qquad \int_0^{\infty} \frac{\operatorname{Im} B_2(\omega, \Delta) \, \mathrm{d}\omega}{\omega^2 + \omega_0^2} < \infty .$$

[6] M. L. GOLDBERGER: *Proceedings of the Sixth Annual Rochester Conference on High Nuclear Physics*, Rochester, 1956.

and therefore

$$\lim_{\omega|\to\infty} \left| \frac{A_1(\omega, \Delta)}{\omega^2} \right| = \lim \left| \frac{B_1(\omega, \Delta)}{\omega} \right| = \lim \left| \frac{A_2(\omega, \Delta)}{\omega^2} \right| = \lim \left| \frac{B_2(\omega, \Delta)}{\omega} \right| = 0 .$$

For the total cross-sections $\sigma^+_{\text{tot}}(\omega)$ and $\sigma^-_{\text{tot}}(\omega)$ again (9) is valid, and we have $\omega\sigma^-_{\text{tot}} \sim 3\sigma^-_{\text{tot}}$. The difference between (11) and the other relations stems from the weaker asymptotic increase of $B_1(\omega, \Delta)$ as compared with $A_2(\omega, \Delta)$ together with the different symmetry character as compared with $B_2(\omega, \Delta)$.

In the case of only one space dimension instead of three, the foregoing method (with a slight modification made necessary by the « bound state » pole in the scattering amplitude) applies rigorously and leads to the result that the transmission coefficient

$$D(\omega) \equiv 1 + \tfrac{1}{4} i M^{-1} (\omega^2 - \mu^2)^{-\frac{1}{2}} T(\omega) \tag{14}$$

can, in infinity, not increase as strongly as proportional to the « laboratory energy » ω.

Finally, it is interesting to observe that our method can be applied even if it is, in the beginning, only known that the scattering amplitude increases in infinity not as strongly as exponentially. But this knowledge we do have since an exponential increase would violate causality so that actually no further assumption is involved.

3. – Discussion.

Te above argument is, because of the rather speculative assumption of a strict analytic behavior of the tangent approximation, not very convincing, but we believe that it gives at least strong indication of incisive restrictions for the scattering amplitudes as a consequence of unitarity, and even expect formulae (8), etc., to be correct. We may add that our conclusion $n = 1$ is in agreement with the perturbation theoretical result.

The behavior of the experimental amplitudes A_1, B_1, A_2, B_2 in the until now accessible region $\omega \lesssim 2$ GeV seems to indicate [6,7] that in (10), (12) and (13) the limit $\omega_0 \to -\infty$ exists with only in (10) a term $\operatorname{Re} A_1(\infty, \Delta) \neq 0$ left over, but from such energies it is hardly justified to infer an asymptotic behavior. Finally, in view of the fact that the dispersion relations in their present form

(7) G. F. Chew: *Theory of Pion Scattering and Photoproduction*, in *Encyclopaedia of Physics* (Berlin, 1957).

may be expected to break down much earlier than an « asymptotic region » is attained, the « correct » asymptotic behavior is primarily of field theoretical interest.

* * *

The author has profited from a discussion with Dr. T. T. Wu on the mathematical character of dispersion relations.

Note added in proof:

We may mention the explicit result for the transmission coefficient $D(\omega)$ of (14): $D(\omega)$ fulfills $|D(\omega)| \leqslant 1$ for real « laboratory energy » $\omega \geqslant \mu$ and possesses the representation

$$D(\omega) \quad i \frac{g^2\mu^2\sqrt{\omega^2 - \mu^2}}{8M(1 - \mu^2/4M^2)(\omega^2 - \mu^4/4M^2)}$$

$$i \frac{\sqrt{\omega^2 - \mu^2}}{\pi} \int_{\mu}^{\infty} \frac{2\omega' \, d\omega' \, \mathrm{Re}\, D(\omega')}{\sqrt{\omega'^2 - \mu^2}(\omega'^2 - (\omega + i\varepsilon)^2)} \qquad (\varepsilon \to +0).$$

RIASSUNTO (*)

Sulla base delle relazioni generali della dispersione e dell'esigenza di unitarietà si discute il comportamento asintotico dell'ampiezza di scattering ad altissime energie. L'ipotesi che l'approssimazione tangenziale soddisfa le relazioni della dispersione conduce a predire che la sezione d'urto totale non può crescere asintoticamente tanto quanto cresce in proporzione dell'energia del laboratorio. Si discute l'importanza di questo risultato.

(*) *Traduzione a cura della Redazione.*

IL NUOVO CIMENTO Vol. V, N. 3 1° Marzo 1957

Non-Local Models of Pion-Nucleon, Pion-Hyperon Interactions.

P. Budini and L. Fonda

Istituto di Fisica dell'Università - Trieste
Istituto Nazionale di Fisica Nucleare - Gruppo di Trieste

(ricevuto il 25 Gennaio 1957)

Summary. — Starting from the hypothesis that the pion interacts with nucleons and hyperons only through intermediate fields, non-local covariant models of pion-nucleon, and pion-hyperon interactions can be obtained after formal elimination of the intermediate fields. First a simple mathematical model is discussed which admits exact solutions. This model has some formal features in common with the Pais-Uhlenbeck non-local theory but avoids the non definite energy difficulty. From this model a static nucleon-nucleon potential is obtained which exhibits a core effect in the central part and no divergence in the tensor part. Then a physical model is suggested in which the internal field is represented by a couple of K-mesons of opposite parity. A linear approximation of this model is equivalent to a non-local form factor theory of pion-nucleon pion-hyperon interactions of the Kristensen-Møller type in which the Fourier transform of the form factor is, however, of a class more general than that of the algebraic functions. A theory started from this form factor lagrangian exhibits general convergence features which are breafly discussed in appendix. In this linear approximation, relations between the K-nucleon-hyperon and pion-nucleon, pion-hyperon coupling constants, are obtained.

1. – Introduction.

Recent theoretical investigations [1], on the interpretation of pion-nucleon low energy phenomenology, as well as recent discussions on the self-consistency of the renormalization programme [2], seem to indicate that the

[1] G. C. Wick: *Rev. Mod. Phys.*, **27**, 339 (1955); G. F. Chew and E. F. Low: *Phys. Rev.*, **101**, 1570, 1579 (1956).

[2] T. D. Lee: *Phys. Rev.*, **95**, 1329 (1954); V. Haber-Schaim and W. Pauli: *Dan. Mat. Fys. Medd.*, **30**, No. 7 (1955); see also *Rochester Conference* (1956), Section III.

usual linear theory (*) of pion-nucleon interaction needs a cut-off at high momentum transfers of the interacting particles, thus suggesting the hypothesis of a non-local character of the interaction. Accepting this hypothesis as a starting point the problem arises if the non-local property of the interaction reflects a fundamental property of the space-time and, as such, is independent of the particular fields, and interactions, or if it is due to the inability of the local, linear pion-nucleon theory, to describe what happens when high momentum transfers are involved. In what follows we shall attempt to analize this second point of view and to see which consequences can be deduced from it without internal inconsistency and contradiction with experimental facts.

Experiments tell us that at high energy nuclear collisions, pions are multiply created and new mesons appear. These facts in themselves render the pion-nucleon linear, local interaction inadequate for the description of reality when high energy interactions are involved. It is possible, as suggested [3], that the matter-field possesses a fundamental non linear character which can explain both the multiple production of pions and the various possible states of masses of the field constituting the so called elementary particles. With the known mathematical instruments it is rather difficult to follow theories of this type. But it is to be hoped that, whichever will be the final form of the theory, one can attempt to formulate a linear approximation to it in which the masses of the particles are given a priori and the presence of some type of particles in virtual states furnish the physical explanation of the non-local character of the interaction of others.

A model for this line of thought could be furnished by the explanation of the electrodynamical properties of the nucleon through the theory of the photon-pion-nucleon interaction.

2. – A Mathematical Model.

It has already been suggested that the typical divergent features of field theories may be avoided taking into due account possible intimate relations between the so called elementary particles of various kinds. A typical attempt in this direction is represented by the theory of PAIS and UHLENBEK [4] which is based on a field equation of the following type:

$$F(\Box)\varphi = \varrho \,, \tag{1}$$

(*) By linear we mean that the interaction lagrangian is linear in the boson field and quadratic in the spinor fields.

(3) W. HEISENBERG: *Zeits. f. Naturf.*, **9***a*, 292 (1954).

(4) A. PAIS and G. E. UHLENBECK: *Phys. Rev.*, **79**, 145 (1950).

where φ represents an unspecified boson field; ϱ the source and

$$F(\Box) = \prod_{i=1}^{N} (\Box - \varkappa_i^2) . \tag{2}$$

The authors quoted show in fact that this formulation, representing an assembly of quanta of rest mass $\varkappa_i$ all bound with the same strength to the source ϱ, is useful in eliminating some at least (*) of the divergencies of the theory. On the other hand a new difficulty arises from the fact that the energy of the thus formed field is indefinite both classically and quantum mechanically. We think that in order to avoid this difficulty the P.U. theory may be reinterpreted introducing appropriate assumptions about the connection between the various elementary particles.

For the sake of simplicity we will limit ourselves to the case corresponding to the P.U. theory with $N=2$. Let us suppose then to have two boson fields of same parity, Φ and φ, whose masses (bare) are M and μ respectively. The lagrangian of the free fields will be:

$$L_0 = L_0^{\Phi} + L_0^{\varphi} \tag{3}$$

and the energy of the free fields will obviously be positive definite.

Let the Φ field be coupled with the source S with a certain strength g. We make now the assumption that the φ field can interact with the source S only through the field Φ (5). This implies an interaction between the fields φ and Φ, and quantum mechanically the possibility of a transition of matter from the state of a number of particles φ to a state of a number of particles Φ and viceversa (**). We shall thus add to the lagrangian (3) the interaction lagrangian:

$$L_I = -f\varphi\Phi - g\Phi S , \tag{4}$$

where it is understood that S has the same parity as the Φ field.

N.B. – Throughout the work we use the units in which $\hbar=1$ and $c=1$.

(*) In the electrodynamical example given by the authors the vacuum polarization divergence, in fact, is not eliminated.

(5) P. BUDINI: *Nuovo Cimento*, **3**, 1104 (1956).

(**) If the existence of the particles Φ can be connected with non-linear properties of the φ field these transitions could occur only where this field is very intense, that is in the vicinity of the source S. In a non-linear theory this fact would automatically follow from the mathematical formulation; in our linear model one should introduce an assumption *ad hoc*; the interaction, and thus the possibility of transitions, between the φ and Φ fields has to be zero very far from the source of the Φ field; thus at a large distance from the source the fields should be represented by the lagrangian (3). This situation could be easily represented with a model of the Lee type (see ref. (2)).

From the lagrangian (3+4) a classical field theory can then be deduced without difficulty, the field equations are

$$\begin{cases} (\Box - \mu^2)\varphi = f\Phi \\ (\Box - M^2)\Phi = f\varphi + gS\,, \end{cases} \tag{5}$$

from which, in presence of the source, that is if gS and f are different from zero, one gets the following equation for φ:

$$[(\Box - M^2)(\Box - \mu^2) - f^2]\varphi = fgS\,, \tag{6}$$

which can be put in the form:

$$(\Box - M_1^2)(\Box - \mu_1^2)\varphi_1 = fgS \tag{7}$$

with (*):

$$\begin{cases} \mu_1^2 = \tfrac{1}{2}[\mu^2 + M^2 - \sqrt{(M^2 - \mu^2)^2 + 4f^2}] \\ M_1^2 = \tfrac{1}{2}[\mu^2 + M^2 + \sqrt{(M^2 - \mu^2)^2 + 4f^2}] \end{cases} \tag{8}$$

(7) is of the type (1). Thus it could be taken as a starting point for a P.U. theory: in this case φ_1 should be replaced by a linear combination of fields both coupled directly to the source S and the linear combination would be such that some divergences would be eliminated from the theory, but the energy of the free boson fields of masses M_1 and μ_1, would be indefinite.

An equation for φ_1 can also be obtained from the system (5) by the following procedure. Let us put the second equation in the form

$$\Phi = \Phi_0 - \int \Delta_M^{\text{in}}(x - x')[f\varphi(x') + gS(x')]\,\mathrm{d}^4x'\,, \tag{9}$$

where Δ_M^{in} is a Green's function of the inhomogeneous Klein-Gordon equation:

$$(\Box - M^2)\,\Delta_M^{\text{in}}(x - x') = -\,\delta^4(x - x')\,, \tag{10}$$

Φ_0 represents a solution of the homogeneous equation.

We now put the condition that at $t \to -\infty$ and $t \to +\infty$, Φ has only negative and positive frequencies respectively, we exclude thus the homogeneous

---

(*) In the following we shall suppose $f^2 < M^2\mu^2$ in order that μ_1 be real.

solution Φ_0 and the possibility of incoming and outgoing free Φ waves. We obtain:

$$\Phi = -\int \Delta^c_M(x - x')[f\varphi(x') + gS(x')]\,\mathrm{d}^4x', \tag{11}$$

where $\Delta^c_M(x - x')$ is the causal Green's function satisfying the equation (10). Substituting this solution in the first equation of the system (5), we obtain:

$$(\Box - \mu^2)\varphi(x) = -\int \Delta^c_M(x - x')[f^2\varphi(x') + fgS(x')]\,\mathrm{d}^4x' , \tag{12}$$

the first term on the R.H.S. represents the self-energy of the field φ as well as the reaction of this field on Φ; writing the equation (12) in momentum space, we obtain:

$$[(k^2 + \mu^2)(k^2 + M^2 - i\varepsilon) - f^2]\,a(k) = fg\,S(k) , \tag{13}$$

where ε is an infinitesimal positive number; $a(k)$ and $S(k)$ are the Fourier transforms of φ and S respectively.

This equation can be written as:

$$(k^2 + \mu_1^2)(k^2 + M_1^2 - i\varepsilon\, b(k))\,a(k) = fg\,S(k) \tag{14}$$

where $b(k)$ is given by:

$$b(k) = \frac{k^2 + \mu^2}{k^2 + \mu_1^2} . \tag{15}$$

It is easily verified that this quantity is positive in the neighbourhood of the poles:

$$k_0 = \pm\sqrt{\boldsymbol{k}^2 + M_1^2} , \tag{16}$$

supposing that $M > \mu$. Going back to the ordinary space, the equation (12) can be put in the form (*):

$$(\Box - \mu_1^2)\varphi_1(x) = -fg\int \Delta^c_{M_1}(x - x')\,S(x')\,\mathrm{d}^4x' , \tag{17}$$

(*) M_1 and μ_1 are to be interpreted as the physical masses of the particles Φ and φ, when the interaction $f\varphi\Phi$ only is taken into account.

which can be deduced from the lagrangian:

$$L = L_0^{(1)} + fg \int \varphi_1(x)\, \Delta^{\circ}_{M_1}(x - x')\, S(x')\, \mathrm{d}^4x' , \tag{18}$$

which is a non-local form factor lagrangian. We note that φ_1, which in the P.U. theory represented a linear combination of the physical fields, in this model represents itself the physical field. The energy of the free field φ_1 is obviously positive definite and the non-localizability can eliminate some of the divergences from the theory which describes the interaction between φ_1 and the source S.

This model shows, by an example, how eliminating, from a theory describing mutually interacting fields, an internal field, the resulting interaction between the remaining fields becomes non-local. We think that this may be a possible physical explanation of the meaning of the form factors in linear theories that can be interpreted as representing the « ignorance » of internal physical situations.

In the physical hypothesis on which this model is grounded, however, the field Φ is interacting locally with the source, and consequently it implies divergent features in a theory which takes explicitly into account its interaction with the source. Thus in this interpretation the divergences are shifted over to the Φ field which, however, does not appear explicitly in the model. To shift the problem of the divergences to the Φ field means to shift it to the high energy region where any theory with the masses introduced a priori is anyway unsatisfactory.

This model, giving a non-local description of the interaction between the φ_1 field and the source S, can be compared with the extended source models [6] of the pion-nucleon interaction, and the extension of the source is determined by the characteristics of the ignored Φ_1 field. An attempt in this direction has been made (see ref. [5]) and it has been found that in order to reproduce the known results of the extended source models, one has to introduce for M, mass of the Φ field, a value about five times the mass of the pion.

In order to test this model on experimental facts it is also useful to calculate the nucleon-nucleon potential. For this computation we shall suppose φ and Φ isovector pseudoscalar fields and start from a PS-PV interaction lagrangian for the coupling between the field Φ and the nucleon current $S_\mu^{(1)}$:

$$L_I = - f\varphi_i \Phi_i - ig \frac{\partial \Phi_i}{\partial x_\mu} S_\mu^{(1)} . \tag{19}$$

it is understood that $S_\mu^{(1)}$ is a well defined 4-vector in ordinary space and a well defined 3-vector in isotopic space.

---

[6] G. F. Chew: *Phys. Rev.*, **95**, 1669 (1954).

Adding to the interaction lagrangian (19) the lagrangian for the free fields, one obtains, by the usual procedure, the field equations for the fields φ_i and Φ_i respectively. In this case too one can eliminate the field Φ_i from these equations, obtaining for φ_i the equation:

$$(\Box - \mu_1^2)\varphi_i(x) = ifg \int \dot{\Delta}^c_{M_1}(x - x') \frac{\partial S^{(i)}_\mu(x')}{\partial x'_\mu} \, \mathrm{d}^4x' \,, \tag{20}$$

which can be derived from the lagrangian:

$$L = L_0^{(1)} - ifg \int \varphi_i(x) \Delta^c_{M_1}(x - x') \frac{\partial S^{(i)}_\mu(x')}{\partial x'_\mu} \, \mathrm{d}^4x' \,. \tag{21}$$

In the static approximation, we write for the spatial part of the nucleon current $S^{(i)}_\mu$ the following expression:

$$\boldsymbol{S}^{(i)}(x') = -i \sum_A \tau_i^A \boldsymbol{\sigma}_A \, \delta^3(\boldsymbol{x}' - \boldsymbol{z}_A) \,, \tag{22}$$

where the sum $\sum_A$ is extended over the nucleons.

A static solution for the equation (20) is now easily obtained:

$$\varphi_i(\boldsymbol{x}) = \sum_A fg \frac{\tau_i^A}{4\pi(M_1^2 - \mu_1^2)} (\boldsymbol{\sigma}_A \boldsymbol{\nabla}_A) \cdot \cdot \left\{ \frac{\exp[-\mu_1 |\boldsymbol{x} - \boldsymbol{z}_A|] - \exp[-M_1 |\boldsymbol{x} - \boldsymbol{z}_A|]}{|\boldsymbol{x} - \boldsymbol{z}_A|} \right\} . \tag{23}$$

In the static approximation considered, in which all the sources are obviously external, the interaction hamiltonian, corresponding to the lagrangian density (21), can be defined without ambiguity:

$$H_I = \sum_A fg \int \mathrm{d}^3x \int \mathrm{d}^4x' \varphi_i(x) \Delta^c_{M_1}(x - x') \boldsymbol{\nabla}' \tau_i^A \boldsymbol{\sigma}_A \delta^3(\boldsymbol{x}' - \boldsymbol{z}_A) \,, \tag{24}$$

which can be calculated explicitly, by using the static solution (23) for φ_i, giving for the nucleon-nucleon potential the following expression:

$$V_{AB}(r) = \frac{f^2 g^2}{4\pi(M_1^2 - \mu_1^2)^2} (\boldsymbol{\tau}_A \boldsymbol{\tau}_B)(\boldsymbol{\sigma}_A \boldsymbol{\nabla})(\boldsymbol{\sigma}_B \boldsymbol{\nabla}) \cdot \cdot \left\{ \frac{\exp[-\mu_1 r] - \exp[-M_1 r]}{r} - \frac{M_1^2 - \mu_1^2}{2M_1} \exp[\quad M_1 r] \right\} , \quad r \quad \boldsymbol{z}_A - \boldsymbol{z}_B . \tag{25}$$

a straightforward calculation gives:

$$V_{AB}(r) = \quad ^c_{AB}(r) + S_{AB} V^t_{AB}(r) \,, \tag{26}$$

with

$$
(27)\quad \begin{cases}
V^c_{AB}(r) = \dfrac{f^2 g^2}{4\pi(M_1^2-\mu_1^2)^2}\dfrac{1}{3}(\boldsymbol{\tau}_A\boldsymbol{\tau}_B)(\boldsymbol{\sigma}_A\boldsymbol{\sigma}_B)\cdot \\
\qquad\qquad \cdot\left[\dfrac{\mu_1^2}{r}(\exp[-\mu_1 r]-\exp[-M_1 r]) + \dfrac{\mu_1^2-M_1^2}{2}M_1\exp[-M_1 r]\right] \\
V^t_{AB}(r) = \dfrac{f^2 g^2}{4\pi(M_1^2-\mu_1^2)^2}\dfrac{1}{3}(\boldsymbol{\tau}_A\boldsymbol{\tau}_B)\cdot\left[\dfrac{\mu_1^2-M_1^2}{2}\left(M_1-\dfrac{1}{r}\right)\exp[-M_1 r] + \right. \\
\qquad\qquad \left. + \left(\dfrac{3}{r^3}+\dfrac{3\mu_1}{r^2}+\dfrac{\mu_1^2}{r}\right)\exp[-\mu_1 r] - \left(\dfrac{3}{r^3}+\dfrac{3M_1}{r^2}+\dfrac{M_1^2}{r}\right)\exp[-M_1 r]\right] \\
S_{AB} = 3(\boldsymbol{\sigma}_A\cdot\boldsymbol{n})(\boldsymbol{\sigma}_B\cdot\boldsymbol{n}) - (\boldsymbol{\sigma}_A\cdot\boldsymbol{\sigma}_B); \qquad \boldsymbol{n} = \dfrac{\boldsymbol{r}}{r}.
\end{cases}
$$

At large distances this potential behaves like the ordinary static pseudovector potential of the local theory (7). At short distances the central part $V^c_{AB}(r)$ changes sign, exhibiting thus a core effect of the Levy's type. The change in sign happens at $r = r^*$, r^* being the solution of the equation:

$$
(28)\qquad \exp[(M_1-\mu_1)r] = r\,\frac{M_1^2-\mu_1^2}{2\mu_1^2}M_1 + 1\,.
$$

For $M_1 = 6\mu_1$, r^* turns out to be $\sim 0.91\ (\hbar c/\mu_1)$.

Finally we point out that the tensor part $V^t_{AB}(r)$ vanishes in the limit $r = 0$, the high singularity of the local pseudoscalar symmetric theory is thus completely removed (*).

We can say, in conclusion, that qualitatively the potential deduced from the proposed model exhibits features like those requested for the explanation of the low energy nucleon-nucleon phenomenology. It has to be investigated further to what degree of precision this potential or the one obtainable from the physical model of next paragraph, can reproduce the details of experimental data.

3. – A Physical Model.

The model sketched in the previous paragraph had only a mathematical character. It is obvious, in fact, that the quanta of the Φ_1 field should be able to be emitted in real states in high energy interactions. Now, if one

(7) W. Pauli: *Meson Theory of Nuclear Forces* (London, New York, 1948).

(*) A potential which exhibits similar features as the potential (25) has been discussed by E. Clementel and C. Villi: *Nuovo Cimento*, **4**, 935 (1956).

identifies the quantum of the φ_1 field with the pion, the Φ_1 field, for invariance requirements, should have the same parity and isotopic spin as the pion, and in order to account for the experimental facts it should have a mass comparable with that of the nucleon: there is however no evidence for the existence of such particles.

In high energy pion-nucleon and nucleon-nucleon collisions K-mesons are created, thus it is reasonable to inquire if they can constitute the internal field of the pion-nucleon interaction ([8]). Experimental evidence suggests ([9]) that these particles are isospinors, so that an interaction lagrangian linear in the pion field and invariant with respect to reflections and rotations in isotopic space, should be at least quadratic in the K fields. This means that inserting K-mesons in the model of the preceeding paragraph, between pion and nucleon two K-mesons should be exchanged (*). The most reasonable value for the ordinary spin of the K-mesons seems to be zero like that of the pion, but this particle is pseudoscalar, thus in order to get a Lorentz invariant interaction lagrangian linear in the pion field and quadratic in the K field, we should postulate different parities for the two K wave functions appearing in it. The possibility of different parity for the K-mesons seems in fact not to be excluded by reality ([10]).

The simplest invariant interaction lagrangian, compatible with experiments, to put as a basis for our model, is thus:

$$L_I^{(1)} = -g_\pi [\boldsymbol{\pi} K_s^{*\top} \boldsymbol{\tau} K_{ps} + \boldsymbol{\pi} K_{ps}^{*\top} \boldsymbol{\tau} K_s] , \tag{29}$$

where π, K_s and K_{ps} represent the pion, the scalar and pseudoscalar K fields and g_π a coupling constant to be determined; $\top$ means isospinorial transposition, $*$ conjugation of all the components.

To this lagrangian we have now to sum an interaction lagrangian of the K fields with the nucleon field. Experiments suggests that hyperons cannot be ignored in these interactions and that their role is well expressed by the Gell-Mann selection rules. We thus take for the K-nucleon-hyperon interaction' the following interaction lagrangian:

$$\begin{aligned} L_I^{(2)} = &- g_5 \widetilde{N}^{*\top} K_s \Lambda - i g_5' \widetilde{N}^{*\top} \gamma_5 K_{ps} \Lambda - g_6 \widetilde{N}^{*\top} \boldsymbol{\tau} \cdot \boldsymbol{\Sigma} K_s - \\ &- i g_6' \widetilde{N}^{*\top} \gamma_5 \boldsymbol{\tau} \cdot \boldsymbol{\Sigma} K_{ps} - g_7 K_s^{*\top} \tau_- \widetilde{\Xi}^* \Lambda - i g_7' K_{ps}^{*\top} \tau_- \widetilde{\Xi}^* \gamma_5 \Lambda - \\ &- g_8 K_s^{*\top} \boldsymbol{\tau} \tau_- \widetilde{\Xi}^* \boldsymbol{\Sigma} - i g_8' K_{ps}^{*\top} \boldsymbol{\tau} \tau_- \widetilde{\Xi}^* \gamma_5 \boldsymbol{\Sigma} + \text{c. c.} \end{aligned} \tag{30}$$

([8]) P. BUDINI and L. FONDA: *Nuovo Cimento* **5**, 306 (1957).

([9]) M. GELL-MANN: *Phys. Rev.*, **92**, 833 (1953).

(*) In consideration of the order of magnitude, this agrees with the cut-offs of the extended source theory which is about two K masses.

([10]) T. D. LEE and C. N. YANG: *Phys. Rev.*, **102**, 290 (1956).

where N, Λ, Σ and Ξ represent the nucleon and various hyperons which are isoscalar, isovector and isospinor respectively; $\sim$ denotes spinorial transposition and multiplication from the right by γ_4. This interaction lagrangian, as shown by B. D'ESPAGNAT and J. PRENTKI [11], is compatible with the Gell-Mann rules, it is invariant with respect to reflections and rotations in isotopic space and to Lorentz transformations in ordinary space (*).

Adding to the interaction lagrangian (29+30) the lagrangian for the free fields and supposing equal the masses of the K_s and K_{ps} particles, we obtain the following field equations for the pion and K fields:

$$
(31)\quad \begin{cases} (\Box - \mu_k^2)K_s = g_7\tau_2\widetilde{\Xi}^*\Lambda + g_8\boldsymbol{\tau}\tau_2\widetilde{\Xi}^*\boldsymbol{\Sigma} + g_5\widetilde{\Lambda}^*N + g_6\widetilde{\boldsymbol{\Sigma}}^*\boldsymbol{\tau}N + g_\pi\boldsymbol{\pi}\cdot\boldsymbol{\tau}K_{ps} \\ (\Box - \mu_k^2)K_{ps} = ig_7'\tau_2\widetilde{\Xi}^*\gamma_5\Lambda + ig_8'\boldsymbol{\tau}\tau_2\widetilde{\Xi}^*\gamma_5\boldsymbol{\Sigma} + ig_5'\widetilde{\Lambda}^*\gamma_5 N + ig_6'\widetilde{\boldsymbol{\Sigma}}^*\boldsymbol{\tau}\gamma_5 N + g_\pi\boldsymbol{\pi}\cdot\boldsymbol{\tau}K_s \\ (\Box - \mu_\pi^2)\pi_i = g_\pi K_s^{*\top}\tau_i K_{ps} + g_\pi K_{ps}^{*\top}\tau_i K_s \end{cases}
$$

and analogous equations for $K_s^{*\top}$ and $K_{ps}^{*\top}$.

The integral equations corresponding to the K fields, which take into account the boundary conditions that we have only negative and positive frequencies respectively in the limit $t \to -\infty$ and $t \to +\infty$, are the following:

$$
(32)\quad \begin{cases} K_s(x) = -\int \Delta_k^e(x-x')\{g_7\tau_2\widetilde{\Xi}^*\Lambda + g_8\boldsymbol{\tau}\tau_2\widetilde{\Xi}^*\boldsymbol{\Sigma} + \\ \qquad + g_5\widetilde{\Lambda}^*N + g_6\widetilde{\boldsymbol{\Sigma}}^*\boldsymbol{\tau}N + g_\pi\boldsymbol{\pi}\cdot\boldsymbol{\tau}K_{ps}\}(x')\,\mathrm{d}^4x' \\ K_{ps}(x) = -i\int \Delta_k^e(x-x')\Big\{g_7'\tau_2\widetilde{\Xi}^*\gamma_5\Lambda + g_8'\boldsymbol{\tau}\tau_2\widetilde{\Xi}^*\gamma_5\boldsymbol{\Sigma} + \\ \qquad + g_5'\widetilde{\Lambda}^*\gamma_5 N + g_6'\widetilde{\boldsymbol{\Sigma}}^*\boldsymbol{\tau}\gamma_5 N + \frac{1}{i}g_\pi\boldsymbol{\pi}\cdot\boldsymbol{\tau}K_s\Big\}(x')\,\mathrm{d}^4x' \end{cases}
$$

and analogous expressions for $K_s^{*\top}$ and $K_{ps}^{*\top}$.

Substituting now these expressions for K_s and K_{ps} in the equation for π, we obtain the following equation for the pion field:

$$
\begin{aligned}
(33)\qquad (\Box - \mu_\pi^2)\pi_i(x) = g_\pi \iint \mathrm{d}^4x'\mathrm{d}^4x''\,\Delta_k^e(x'-x)\Delta_k^e(x-x'')\cdot \\
\cdot\Big[(g_8\widetilde{\boldsymbol{\Sigma}}^*\Xi^\top\tau_2\boldsymbol{\tau} + g_7\widetilde{\Lambda}^*\Xi^\top\tau_2 + \widetilde{N}^{*\top}[g_5\Lambda + g_6\boldsymbol{\tau}\boldsymbol{\Sigma}] + \\
+ g_\pi K_{ps}^{*\top}\boldsymbol{\pi}\cdot\boldsymbol{\tau})(x')\tau_i\cdot i\Big(g_8'\boldsymbol{\tau}\tau_2\widetilde{\Xi}^*\gamma_5\boldsymbol{\Sigma} + g_7'\tau_2\widetilde{\Xi}^*\gamma_5\Lambda + \\
+ [g_5'\widetilde{\Lambda}^* + g_6'\widetilde{\boldsymbol{\Sigma}}^*\boldsymbol{\tau}]\gamma_5 N + \frac{1}{i}g_\pi\boldsymbol{\pi}\cdot\boldsymbol{\tau}K_s\Big)(x'') + \text{c. c.}\Big].
\end{aligned}
$$

---

[11] B. D'ESPAGNAT and J. PRENTKI: *Nuclear Physics*, **1**, 33 (1956).

(*) If the existence of pseudospinor hyperons is also admitted, then one should add to the lagrangian (30) terms with the position of γ_5 shifted from the K_{ps} to the K_s term; apart from numerical factors, the results obtained below are the same.

The terms on the R.H.S. linear in the field π represent the effect of the reaction of this field on the K field; they can give also self-energy effects for the K and π particles; unfortunately their elimination is not so simple as in the mathematical model. We shall drop them for the time being and only briefly comment on their possible contribution in the case of pion-nucleon interaction.

Equation (33) can be clearly derived from a non-local, form factor lagrangian in the interacting fields. In order to bring out the connection between this lagrangian and the known ones of the non-local and local theories, we shall consider separately three cases:

A) there are no incoming and outgoing Λ, Σ and Ξ particles;

B) there are no incoming and outgoing N, and Ξ particles;

C) there are no incoming and outgoing N, Λ and Σ particles.

This will be accomplished by taking time ordered vacuum expectation values for the products of the fields quoted and evaluating them in the approximation in which these fields are considered free.

Case A). – The equation (33) becomes:

$$
\begin{aligned}
(34)\qquad (\Box - \mu_\pi^2)\pi_i(x) = ig_\pi \iint \mathrm{d}^4x'\,\mathrm{d}^4x''\,\Delta_k^c(x-x')\,\Delta_k^c(x-x'')\cdot \\
\cdot \Big\{ g_8 g_8' \langle T(\widetilde{\Sigma}_\alpha^{*m}(x')\Sigma_\beta^n(x''))\rangle_0 \langle T[\Xi^\top(x')\tau_2\tau_m\tau_i\tau_n\tau_2\widetilde{\Xi}^*(x''),\gamma_5]_+^{\alpha\beta}\rangle_0 + \\
+ g_7 g_7' T(\widetilde{\Lambda}_\alpha^*(x')\Lambda_\beta(x''))\rangle_0 \langle T[\Xi^\top(x')\tau_2\tau_i\tau_2\widetilde{\Xi}^*(x''),\gamma_5]_+^{\alpha\beta}\rangle_0 + \\
+ g_5 g_5' \widetilde{N}^{*\top}(x')[\langle T(\Lambda(x')\tau_i\widetilde{\Lambda}^*(x''))\rangle_0,\gamma_5]_+ N(x'') + \\
+ g_6 g_6' \widetilde{N}^{*\top}(x')[\langle T((\boldsymbol{\tau}\boldsymbol{\Sigma}(x')(\tau_i(\widetilde{\boldsymbol{\Sigma}}^*(x'')\boldsymbol{\tau}))\rangle_0,\gamma_5]_+ N(x'')\Big\},
\end{aligned}
$$

where T is the time ordering operator ([12]). The first two terms vanish, for the last two one obtains;

$$
[\langle T(\Lambda(x')\widetilde{\Lambda}^*(x''))\rangle_0,\gamma_5]_+ = i[S_\Lambda^c(x'-x''),\gamma_5]_+ = -2i\mu_\Lambda\gamma_5\Delta_\Lambda^c(x'-x'')\,,
$$

$$
[\langle T((\boldsymbol{\tau}\boldsymbol{\Sigma}(x'))\tau_i(\widetilde{\boldsymbol{\Sigma}}^*(x'')\boldsymbol{\tau}))\rangle_0,\gamma_5]_+ = \sum_{j=1}^{3}\tau_j\tau_i\tau_j[\langle T(\Sigma^j(x')\widetilde{\Sigma}^{*j}(x''))\rangle_0,\gamma_5]_+ =
$$

$$
= 2i\mu_\Sigma\gamma_5\tau_i\Delta_\Sigma^c(x-x'')\,,
$$

where S_ν^c is defined by:

$$
(35)\qquad S_\nu^c(x-x') = \left(\gamma_\mu\frac{\partial}{\partial x_\mu} - \mu_\nu\right)\Delta_\nu^c(x-x')\,.
$$

([12]) G. C. Wick: *Phys. Rev.*, **80**, 268 (1950).

We obtain ultimately the following equation for the pion field:

$$(36) \qquad (\Box - \mu_\pi^2)\pi_i(x) = ig_\pi \iint \mathrm{d}^4x'\, \mathrm{d}^4x''\, F_1(x', x, x'')\widetilde{N}^{*\top}(x')\gamma_5\tau_i N(x'')$$

with

$$F_1(x', x, x'') = 2i\,\Delta_k^c(x' - x)\,\Delta_k^c(x - x'')(g_6 g_6' u_\Sigma\,\Delta_\Sigma^c(x' - x'') - g_5 g_5' u_\Lambda\,\Delta_\Lambda^c(x' - x'')) .$$

If we had taken into account also the terms at the R.H.S. of the equation (33) linear in π, we would have obtained, retaining only terms quadratic in g_π, supposing $g' = g$ and dropping self-energy terms:

$$\begin{aligned}(37) \qquad (\Box - \mu_\pi^2)\pi_i(x) = {} & ig_\pi \iint \mathrm{d}^4x'\, \mathrm{d}^4x''\, F_1(x', x, x'')\,\widetilde{N}^{*\top}(x')\gamma_5\tau_i\, N(x'') \; - \\ & - g_\pi^2 \iiint \mathrm{d}^4x'\, \mathrm{d}^4x''\, \mathrm{d}^4x'''\, \Delta_k^c(x' - x)\,\Delta_k^c(x - x'')\,\Delta_k^c(x'' - x''') \cdot \\ & \cdot \Big\{ ig_5^2 \widetilde{N}^{*\top}(x''')\pi_j(x'')\tau_j\tau_i[2\gamma_\mu \nabla_\mu'''\,\Delta_\Lambda^c(x' - x''')]N(x') + \\ & + ig_5^2 \widetilde{N}^{*\top}(x')\pi_j(x'')\tau_i\tau_j[2\gamma_\mu \nabla_\mu'\,\Delta_\Lambda^c(x' - x''')]N(x''') + \\ & - ig_6^2 \widetilde{N}^{*\top}(x''')\pi_j(x'')[4\delta_{ij} - \tau_j\tau_i][2\gamma_\mu \nabla_\mu'''\,\Delta_\Sigma^c(x' \quad x''')]N(x') - \\ & + ig_6^2 \widetilde{N}^{*\top}(x')\pi_j(x'')[4\delta_{ij} - \tau_i\tau_j][2\gamma_\mu \nabla_\mu'\,\Delta_\Sigma^c(x' - x''')]N(x''') \Big\} ,\end{aligned}$$

which can be derived from an interaction lagrangian bilinear in the pion field: similarly one can obtain terms cubic in π and so on. The possible meaning of these terms will be discussed in a future work.

Equation (36) is obtained simply dropping these non-linear terms. This is justified if we are considering only weak interacting fields.

The equation (36) can be thought of as derived from the lagrangian density:

$$(38) \qquad L = L_0 - ig_\pi \iint \mathrm{d}^4x'\, \mathrm{d}^4x''\, F_1(x', x, x')\,\widetilde{N}^{*\top}(x')\gamma_5\boldsymbol{\tau}\, N(x'')\boldsymbol{\pi}(x) ,$$

which is a non-local covariant form factor lagrangian. Thus, for the case A) the linear approximation of the theory is a non-local form factor theory for the pion-nucleon coupling. In appendix we shall compare this lagrangian with those of the non-local, form factor theories and show that if it is taken as a starting point for a theory of pion-nucleon interaction it can render the primitive divergent graphs of the theory convergent.

Case B). – In this case there are no incoming or outgoing N and Ξ particles. From equation (33) we obtain (*):

$$(39)\qquad (\Box-\mu_\pi^2)\pi_i(x)=ig_\pi\iint \mathrm{d}^4x'\,\mathrm{d}^4x''\,\Delta_k^c(x'-x)\Delta_k^c(x-x'')\cdot$$

$$\cdot\Big\{g_5g_6\,\Lambda_\alpha(x')\langle T(\widetilde{N}_\alpha^{*\top}(x')\tau_i\boldsymbol{\tau}N_\delta(x''))\rangle_0\gamma_5^{\beta\delta}\widetilde{\Sigma}_\beta^*(x'')+$$

$$+\,g_5g_6\,\Lambda_\alpha(x')\langle T(\widetilde{N}_\delta^{*\top}(x')\tau_i\boldsymbol{\tau}N_\beta(x''))\rangle_0\gamma_5^{\delta\alpha}\widetilde{\Sigma}_\beta^*(x'')+$$

$$+\,g_7g_8\,\widetilde{\Sigma}^{*m}(x')[\langle T(\Xi^\top(x')\tau_2\tau_m\tau_i\tau_2\widetilde{\Xi}^*(x''))\rangle_0,\gamma_5]_+\Lambda(x'')+$$

$$+\,g_6g_6'\,\Sigma_\alpha^m(x')\langle T(\widetilde{N}_\beta^{*\top}(x')\tau_m\tau_i\tau_n N_\delta(x''))\rangle_0\gamma_5^{\beta\alpha}\widetilde{\Sigma}_\delta^{*n}(x'')+$$

$$+\,g_8g_8'\,\widetilde{\Sigma}^{*m}(x')\langle T(\Xi^\top(x')\tau_2\tau_m\tau_i\tau_n\tau_2\widetilde{\Xi}^*(x''))\rangle_0\gamma_5\Sigma^n(x'')-\text{c. c.}\Big\}$$

all other terms vanish in the approximation considered. After some manipolations one obtains:

$$(40)\qquad (\Box-\mu_\pi^2)\pi_i(x)=ig_\pi\iint \mathrm{d}^4x'\,\mathrm{d}^4x''\cdot\Big\{F_2(x',x,x'')\cdot$$

$$\cdot(\widetilde{\Sigma}^{*i}(x')\gamma_5\Lambda(x'')+\widetilde{\Lambda}^*(x')\gamma_5\Sigma^i(x''))+$$

$$+\,F_2'(x',x,x'')\cdot(\Lambda_\alpha(x'')\gamma_5^{\beta\alpha}\widetilde{\Sigma}_\beta^{*i}(x')+\Sigma_\beta^i(x'')\gamma_5^{\alpha\beta}\widetilde{\Lambda}_\alpha^*(x'))+$$

$$+\,F_3(x',x,x'')\cdot i\widetilde{\boldsymbol{\Sigma}}^*(x')\times\gamma_5\boldsymbol{\Sigma}(x'')\,|_i+F_3'(x',x,x'')\cdot i\boldsymbol{\Sigma}_\alpha(x'')\times\gamma_5^{\beta\alpha}\widetilde{\boldsymbol{\Sigma}}_\beta^*(x')\,|_i\Big\}$$

where the F_2 and F_3 are given by:

$$(41)\qquad \begin{cases} F_2(x',x,x'')=-4\mu_\Xi ig_7g_8\Delta_k^c(x'-x)\Delta_k^c(x-x'')\Delta_\Xi^c(x'-x'') \\ F_2'(x',x,x'')=\;\;4\mu_\mathrm{N}ig_5g_6\Delta_k^c(x'-x)\Delta_k^c(x-x'')\Delta_\mathrm{N}^c(x'-x'') \end{cases}$$

$$(42)\qquad \begin{cases} F_3(x',x,x'')=\;\;4\mu_\Xi ig_8g_8'\Delta_k^c(x'-x)\Delta_k^c(x-x'')\Delta_\Xi^c(x'-x'') \\ F_3'(x',x,x'')=-4\mu_\mathrm{N}ig_6g_6'\Delta_k^c(x'-x)\Delta_k^c(x-x'')\Delta_\mathrm{N}^c(x'-x'')\,. \end{cases}$$

Case C). – Here we have no incoming and outgoing N, Λ and Σ particles. By the usual procedure, we obtain:

$$(43)\qquad (\Box-\mu_\pi^2)\pi_i(x)=ig_\pi\iint \mathrm{d}^4x'\,\mathrm{d}^4x''\,\Delta_k^c(x'-x)\Delta_k^c(x-x'')\cdot$$

$$\cdot\Big\{g_7\sigma_7'\,\Xi_\alpha^\top(x')\tau_2\tau_i\tau_2\langle T(\widetilde{\Lambda}_\alpha^*(x')\gamma_5^{\beta\delta}\Lambda_\delta(x''))\rangle_0\widetilde{\Xi}_\beta^*(x'')+$$

$$+\,g_7\sigma_7'\,\Xi_\beta^\top(x')\tau_2\tau_i\tau_2\langle T(\widetilde{\Lambda}_\alpha^*(x')\gamma_5^{\alpha\beta}\Lambda_\delta(x''))\rangle_0\widetilde{\Xi}_\delta^*(x'')+$$

$$+\,g_8\sigma_8'\,\Xi_\alpha^\top(x')\tau_2\tau_m\tau_i\tau_n\tau_2\langle T(\widetilde{\Sigma}_\alpha^{*m}(x')\gamma_5^{\beta\delta}\Sigma_\delta^n(x''))\rangle_0\widetilde{\Xi}_\beta^*(x'')+$$

$$+\,g_8g_8'\,\Xi_\beta^\top(x')\tau_2\tau_m\tau_i\tau_n\tau_2\langle T(\widetilde{\Sigma}_\alpha^{*m}(x')\gamma_5^{\alpha\beta}\Sigma_\delta^n(x''))\rangle_0\widetilde{\Xi}_\delta^*(x'')\Big\}$$

(*) We shall suppose in this case that $g_7\sigma_8'=g_7'\sigma_8=g_7g_8$ and $\sigma_5\sigma_6'=\sigma_5'g_6=\sigma_5\sigma_6$.

a straightforward calculation gives:

$$(44)\qquad (\Box - \mu_\pi^2)\tau_i(x) = ig_\pi \iint \mathrm{d}^4x'\,\mathrm{d}^4x''\, F_1(x', x, x'')\bar{\Xi}_\alpha(x')\tau_2\tau_i\tau_2\gamma_5^{\beta\alpha}\tilde{\Xi}^*_\beta(x'')\,.$$

with $F_1(x', x, x'')$ given by:

$$(45)\qquad F_1(x', x, x'') = -2i\,\Delta_k^c(x' - x)\,\Delta_k^c(x - x'')\cdot \cdot(\mu_\Sigma g_8 g_8'\Delta_\Sigma^c(x'' - x') - \mu_\Lambda g_7 g_7'\Delta_\Lambda^c(x'' - x'))\,.$$

The equation (44) is derivable from the lagrangian:

$$(46)\qquad L = L_0 - ig_\pi \iint \mathrm{d}^4x'\,\mathrm{d}^4x''\, F_1(x', x, x'')\bar{\Xi}_\alpha^{\top}(x')\tau_2\boldsymbol{\tau}\tau_2\gamma_5^{\beta\alpha}\tilde{\Xi}^*_\beta(x'')\boldsymbol{\pi}(x)\,.$$

4. – Conclusion.

In all three cases considered in the previons paragraph the interaction lagrangian of the pion field with the nucleon-hyperon field is of non-local type, the form factor being the product of three boson propagators. At low energy the interaction lagrangians become identical with the local ones (see Appendix). In this case the lagrangians of cases *A*), *B*) and *C*) are the same as would be obtained, with the same boundary conditions, from the interaction lagrangian (*):

$$(47)\qquad L_I^{(3)} = -ig_1\tilde{N}^{*\top}\gamma_5(\boldsymbol{\tau}\cdot\boldsymbol{\pi})N - ig_2(\tilde{\Lambda}^*\gamma_5\boldsymbol{\pi}\cdot\boldsymbol{\Sigma} + \tilde{\boldsymbol{\Sigma}}^*\cdot\boldsymbol{\pi}\gamma_5\Lambda) - - ig_3(i\tilde{\boldsymbol{\Sigma}}^*\gamma_5\times\boldsymbol{\Sigma})\cdot\boldsymbol{\pi} - ig_4\tilde{\Xi}^{*\top}\gamma_5(\boldsymbol{\tau}\cdot\boldsymbol{\pi})\Xi\,,$$

with (+):

$$(48)\qquad \begin{cases} g_1 = 2ig_\pi(g_6 g_6'\mu_\Sigma C_\Sigma - g_5 g_5'\mu_\Lambda C_\Lambda) \\ g_2 = -4ig_\pi(g_7 g_8'\mu_\Xi C_\Xi + g_5 g_6'\mu_N C_N) \\ g_3 = 4ig_\pi(g_8 g_8'\mu_\Xi C_\Xi - g_6 g_6'\mu_N C_N) \\ g_4 = -2ig_\pi(g_8 g_8'\mu_\Sigma C_\Sigma - g_7 g_7'\mu_\Lambda C_\Lambda)\,, \end{cases}$$

where C_y is the static limit of the Fourier transform of the form factor

$$\Delta_k^c(x' - x)\,\Delta_k^c(x - x'')\,\Delta_y^c(x' - x'').$$

(*) Remember that $(\boldsymbol{\tau}_2\boldsymbol{\tau}_i\boldsymbol{\tau}_2)^{jk} = -(\boldsymbol{\tau}_i)^{kj}$.

(+) For the constant g_2 we have supposed $g_7\gamma_8' = g_7'\gamma_8 = g_7\gamma_8$ and $g_5\gamma_6' = g_5'\gamma_6 = g_5\gamma_6$.

Now the lagrangian $L_I^{(3)}$, added to the lagrangian $L_I^{(2)}$, has been obtained by B. D'ESPAGNAT and J. PRENTKI (see ref. (11) (13)) starting from invariance considerations only. Thus, if the interaction of the pion field with the hyperon-nucleon field goes only through the K fields, the relations (48) between the coupling constants should be valid in the approximation considered.

Concluding we can say that, if the models presented here have some connection with reality, there is the possibility of understanding the origin of the form-factors of the pion-nucleon, pion-hyperon interactions in terms of the existence of heavier mesons, precisely the form-factors should represent the ignorance of their existence in the pure pion-nucleon, pion-hyperon couplings. The advantage of such non-local formulation of the pion-nucleon, pion-hyperon interactions would be to take implicitly into account the effect of the K-nucleon-hyperon phenomenology at intermediate energies.

The limitations of the models presented here lays in the physical over-simplification for the first model and in the mathematical overcomplications and consequent approximations for the second one. Further their validity is anyway confined to the intermediate energy region where one can still hope that theories with the masses of the different fields given a priori make some sense. In spite of this it is to be hoped that some of the consequences presented here, and others which will be investigated in the future will be apt to be tested with experiments allowing thus a clarification of the possible low energy interplay of the various so called elementary particles.

Added Note.

As this work was being accomplished, a paper of J. SCHWINGER has appeared (*Phys. Rev.*, **104**, 1164 (1956)) in which the interaction lagrangian $L_I^{(1)}$ is also postulated. SCHWINGER postulates also a direct interaction between the pion and the nucleon field.

* * *

We are pleased to express our gratitude to Prof. N. DALLAPORTA for helpful discussions on the subject of this paper.

APPENDIX

It may be interesting to compare the lagrangian (38) with those of the non-local theories and to study its ability, if taken as a basis for a theory of pion-nucleon interaction, to eliminate the divergences. In fact the lagrangian

(13) See also: A. SALAM: *Nucl. Phys.*, **2**, 173 (1956).

(38) is formally identical to the form factor lagrangian of the theory of Kristensen and Möller (14). There the form factor could be written as:

$$F(x', x, x'') = (2\pi)^{-8} \int G(l_1, l_3) \exp\left[i(l_1 x' + l_3 x'' - (l_1 + l_3 x)x)\right] \mathrm{d}^4 l_1 \, \mathrm{d}^4 l_3 \tag{49}$$

and for $G(l_1, l_3)$ an invariant algebraic arbitrary function of the 4-vector l_1 and l_3 was chosen. In the lagrangian (38), $F(x', x, x'')$ can be also put in the form (49) with:

$$G(l_1, l_3) = \frac{2 g_\pi i}{(2\pi)^4} \int \frac{\mathrm{d}^4 k}{[(l_1 + k)^2 + \mu_k^2 - i\varepsilon][(l_3 - k)^2 + \mu_k^2 - i\varepsilon]} \cdot \left[\frac{g_5 g_5' \mu_\Lambda}{k^2 + \mu_\Lambda^2 - i\varepsilon} - \frac{g_6 g_6' \mu_\Sigma}{k^2 + \mu_\Sigma^2 - i\varepsilon}\right], \tag{50}$$

which is obviously invariant and of a family of functions wider than the family of the algebraic functions. At low energy the lagrangian (38) becomes identical with the local one as it should. In fact (50) can, after simple manipulations, be put in the form:

$$G(l_1, l_3) = \frac{4 g_\pi i}{(2\pi)^4} \int \mathrm{d}^4 k \int_0^1 \int_0^1 x \, \mathrm{d}x \, \mathrm{d}y \Big\{ g_5 g_5' \mu_\Lambda [k^2 + l_1^2 x(1 - x) + l_3^2 xy(1 - xy) - \\ + 2 l_1 l_3 xy(1 - x) + \mu_k^2 (1 + xy - x) - \mu_\Lambda^2 xy]^{-3} - g_6 g_6' \mu_\Sigma [\Lambda \to \Sigma]^{-3} \Big\}. \tag{51}$$

Supposing that l_1 and l_3 represent 4-momenta of the incoming or outgoing particles and owing to the fact that they appear only as bilinear expressions in (51), the three-dimensional momenta of the incoming or outgoing particles will, in a suitable Lorentz frame, appear only squared in (51). This means that, as these three-dimensional momenta tend to zero, the integral (51) will tend to a constant, while its derivative with respect to these three-dimensional momenta, will tend to zero. This means that at a low relative impulse of the interacting particles, $G(l_1, l_3)$ can be identified with a constant. This is sufficient to identify the theory with the local corresponding one. This can be proved, in detail, following the method given by Kristensen and Möller in the analogous case.

The form factor (50) contains the 4-vector l_1 and l_3 to the power (-2). In the calculation of the primitive divergent graphs of the theory, one of them will be identified with the energy-momentum 4-vector of an internal line and, as the factor G will appear at least to the second power (two vertices), this will mean a power of at least $(+4)$ of the variable of integration in the denominators contributing thus to the convergence of the theory.

The S matrix elements of real processes can be explicitly calculated starting from (38) with the Yang and Feldman method (15). In this case we obtain,

---

(14) P. Kristensen and C. Møller: *Dan. Mat. Fys. Medd.*, **27**, No. 7 (1952).

(15) C. N. Yang and D. Feldman: *Phys. Rev.*, **79**, 972 (1950).

for instance, for the self-energy of the pion of 4-momentum p', in the approximation quadratic in g_π, the following expression:

$$(52) \qquad \delta m^2 = \frac{16 g_\pi^2}{(2\pi)^{11}} \int \mathrm{d}^4k \, \mathrm{d}^4k' \, \mathrm{d}^4k'' \frac{p'k}{p'^2 + 2p'k} \, \delta(k^2 + M^2) \cdot$$

$$\cdot [(k + k')^2 + \mu_k^2 - i\varepsilon]^{-1} [(k + p' + k')^2 + \mu_k^2 - i\varepsilon]^{-1} \left[\frac{g_5 g_5' u_\Lambda}{k''^2 + \mu_\Lambda^2 - i\varepsilon} - \frac{g_6 g_6' u_\Sigma}{k'^2 + \mu_\Sigma^2 - i\varepsilon} \right] \cdot$$

$$\cdot [(k - k'')^2 + \mu_k^2 - i\varepsilon]^{-1} [(k + p' - k'')^2 + \mu_k^2 - i\varepsilon]^{-1} \left[\frac{g_5 g_5' u_\Lambda}{k''^2 + \mu_\Lambda^2 - i\varepsilon} - \frac{g_6 g_6' u_\Sigma}{k''^2 + \mu_\Sigma^2 - i\varepsilon} \right],$$

which is in fact quadratically convergent. Similarly the self-energy of the nucleon in the same approximation, becomes cubically convergent. It is to be noted that the matrix element for the meson-meson scattering is strongly convergent.

Another method which gives equivalent results could be to calculate the S matrix element in the Interaction Representation starting from the lagrangian (29+30) and retaining in the Dyson's series only those terms in which the fields Λ, Σ, Ξ and K are contracted and in which their propagators appear in the combination

$$(53) \qquad \Delta_k^c(x - x') \, \Delta_k^c(x'' - x) \, S_\nu^c(x' - x'')$$

and in this only. If one adopts this method, one can deduce the degree of the divergence, we find for it:

$$(54) \qquad n' = n - 2C \,,$$

where

$$(55) \qquad n = 4 - (\tfrac{3}{2} N_e + M_e)$$

is the degree of the divergence in the local pseudoscalar theory and C is the number of the corners for the diagram considered (here a « corner » is represented by a triangle of three internal boson lines); N_e and M_e are the numbers of the nucleon external lines and pion external lines respectively.

RIASSUNTO

Supponendo che il pione interagisca con il nucleone-iperone solo tramite campi intermedi, si possono ottenere, dopo formale eliminazione di tali campi, modelli covarianti di interazione non locale tra il pione ed il nucleon-iperone. Nella prima parte si studia un semplice modello matematico che ammette soluzioni esatte. Tale modello ha alcuni aspetti formali in comune con la teoria di Pais-Uhlenbeck, ma evita la difficoltà dell'energia non definita per i campi liberi. Nel caso dell'accoppiamento pseudo-

vettoriale il potenziale statico nucleon-nucleone che si ottiene presenta nella parte centrale a piccole distanze repulsione per stati di singoletto-singoletto e tripletto-tripletto ed è priva di divergenza nella parte tensoriale. Al secondo paragrafo si studia la possibilità che il campo interno sia costituito da una coppia di mesoni K di parità opposta. Una approssimazione lineare di questo modello è equivalente ad una teoria non locale alla Kristensen-Møller, la trasformata di Fourier del fattore di forma appartiene tuttavia ad una classe di funzioni più generale di quella delle funzioni algebriche. Una teoria che assuma come punto di partenza tale lagrangiano non locale, presenta caratteri di convergenza piuttosto generali. In questa approssimazione lineare si ottengono relazioni tra le costanti di accoppiamento K-nucleone-iperone e pione-nucleone, pione-iperone.

Further Results on Parity Conservation in π-μ-e Decays.

C. Castagnoli, C. Franzinetti and A. Manfredini

Istituto di Fisica dell'Università - Roma
Istituto Nazionale di Fisica Nucleare - Sezione di Roma

(ricevuto il 5 Febbraio 1957)

Summary. — In a previous note [1] the present authors gave some preliminary results on the angular distribution of the decay products in π-μ-e decays. This research was suggested by Lee and Yang [2] to verify parity conservation in weak interactions. In fact, if parity conservation is violated in both processes (π-μ and μ-e decays) the angular distribution of the electron with respect to the line of motion of the μ-meson in the system in which the π is at rest, is expected to follow the law $f(\omega) = \text{const} \times (1 + \alpha \cos \omega)$. On a total of 1 028 events we obtain now $\alpha = -0.222 \pm 0.067$. The probability of α being zero (isotropic distribution) is found to be $\sim 3 \cdot 10^{-3}$. All the decays have been observed in plates exposed to cosmic rays.

In a recent paper Lee and Yang [2] noticed that the hypothesis of parity conservation in weak interactions (β-decays, meson and hyperon decays, etc.) is not supported by any experimental evidence and that, on the other hand, if parity need not be conserved, θ^+ and τ^+ may be identified as the same particle.

To decide the question they suggested several experiments and in particular the study of the angular distribution of the electron with respect to that of the μ-meson in π-μ-e decays. If parity conservation is violated in both processes, (π-μ decay and μ-e decay) the μ-meson would be polarized in the direction of its motion in the system in which the π is at rest, and the distri-

---

[1] C. Castagnoli, C. Franzinetti and A. Manfredini: *The Avogadro Conference on Fundamental Constants*, Turin, September 1956, Italy (in press on the *Suppl.* of the *Nuovo Cimento*).

[2] T. D. Lee and C. N. Yang: *Phys. Rev.*, **104**, 254 (1956).

bution of the angles ω—this being the angle between the direction of motion of the μ when emitted from its parent π at rest and that of the electron when emitted from the μ-e decay—should be asymmetric with respect to the $\omega = \pi/2$ plane.

A preliminary experimental distribution of ω, obtained on 410 events was shown by the present authors [1] at the Avogadro Conference on Fundamental Constants, held at Turin last September. In view of the importance associated with this the research was continued. Confirmation of the LEE and YANG hipotesis has come, in the meantime, from various experiments [3,4]. In the present note we report on the results obtained on a total of 1028 events which have since been accumulated. All the events have been observed in emulsions exposed to cosmic rays at high altitude.

Experimental method.

We have examined all the π-μ-e decays from π's at rest, which have been observed in 600 μm and 1200 μm thick emulsions exposed to cosmic rays. We have selected 1028 events which satisfied the following conditions:

a) the μ decayed in the same emulsion in which it was created;

b) the projection of the electron track on the plane of the emulsion was $\geqslant 20\ \mu$m;

c) the electron formed an angle with the plane of the emulsion of less than 68°.

The condition *a*) reduced the number of events of about a factor 2, since most of them came from 600 μm emulsions. We did so, however, because we regarded the precision attainable on the measurement of ω too poor for our experiment when it was based on two parts of the same events placed in two different emulsions. With our emulsions the relative position of two adjacent plates at the moment in which the event took place could not be established with the required precision since the plates had been exposed for different experiments and X-ray marking had not been made to establish a unique frame of reference.

If one selects only μ's which are entirely contained in one emulsion, and their track is taken to be a straight segment, the distribution of the angles φ_μ

---

(3) C. S. WU, E. AMBLER, R. H. HAYWARD, D. D. OPPES and R. P. HUDSON, in press.

(4) R. L. GARWIN, L. M. LEDERMAN and M. WEINRICH, in press.

of emission with respect to the plane of the emulsion (Fig 1) is expected to be

$$f(\varphi_\mu) = \text{const} \times (1 - \sin \varphi_\mu) \,. \tag{1}$$

The experimental φ_μ distribution was found to be fairly well represented by this equation. Slight differences, especially noticeable at small values of φ_μ (see Fig. 2), could be explained as due 1) to the fact that the track of the μ is not a straight segment, 2) that the scattering in the initial part of the track introduces an uncertainty in the determination of φ_μ of a few degrees, and tends to make the apparent distribution of φ_μ more isotropic than it is. It can be seen however that both effects do not contribute appreciably to the final estimate of the error.

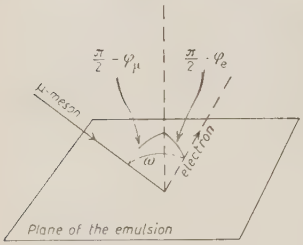

Fig. 1.

Fig. 2.

The condition *b*) was introduced obviously because an electron track can be associated with certainty to the ending of a μ-meson only if the projection of its visible track is not too short. The condition *c*) is due to the fact that if the track is too steep the determination of its direction is made uncertain by the distortion. The graph of Fig. 3—where the distribution is shown of the angles φ_e between the line of motion of the electrons which could be measured and the plane of the emulsion—indicates that for values of φ_e between 0 and 72° the experimental distribution is practically isotropic, while for angles $\varphi_e \geqslant 72°$ many events could not be measured. We feel confident that cutting our statistics at 68° no bias was introduced.

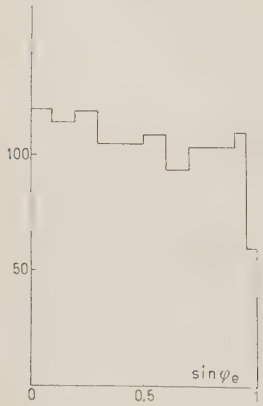

Fig. 3.

Conditions *a*) and *b*) introduce an asymmetric bias in the ω-distribution. Consider for instance the decay of a μ-meson close to the upper surface of the emulsion. If the electron is emitted upwards it may not satisfy the condition *b*); on the other hand if the μ has to satisfy the condition *a*) it can only

come from below with respect to the surface, which means that of the electrons which are rejected the majority are those emitted in the forward direction ($\omega > \pi/2$). It is essential, for the purpose of the research, to know the «loss» due to all the imposed conditions as a function of ω. This has been calculated for both 600 μm (Fig. 4) and 1200 μm emulsions assuming that the φ_μ distribution was given by eq. (1) and that of the φ_e was isotropic (5).

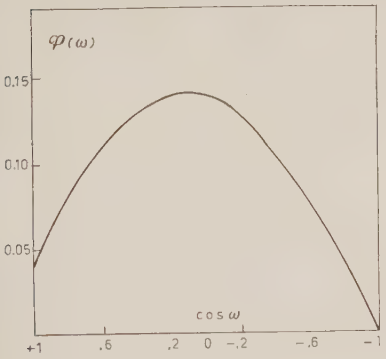

Fig. 4.

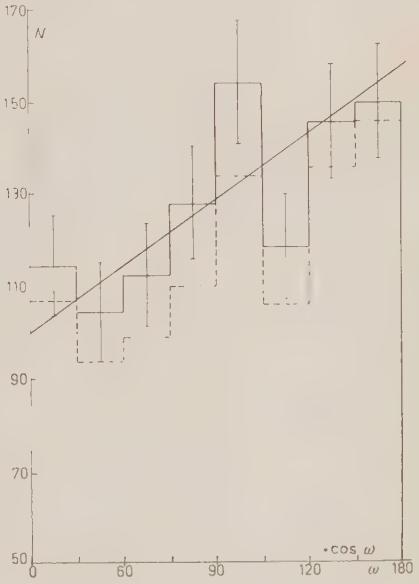

Fig. 5.

Results.

Details of the results are shown in Fig. 5. The dotted lines indicate the observed frequencies and the full line gives the data corrected for geometrical biases.

According to LEE and YANG, the expected angular distribution should be of the type

$$f(\omega) = \text{const} \times (1 + \alpha \cos \omega) .$$

If so, the value of α which fits the experimental plot—as determined by the least square method—is

$$\alpha = -0.222 \pm 0.067 .$$

Using the χ^2-method we find that the probability that the observed data be due to an isotropic distribution is $\sim 3 \cdot 10^{-3}$. From the backward-forward

(5) It must be pointed out that since the ω-distribution has been shown to be not isotropic, this assumption is not strictly valid. It is easy to show however that the alteration on the calculated loss is small and that in any case in proceeding as we did we slightly underestimated the fraction of particles going backwards.

excess, we obtain

$$\alpha = -0.218 \pm 0.066 .$$

* * *

It is our pleasant duty to thank Dr. GATTO foir pointing out to us LEE and YANG's paper and for other stimulating discussions.

RIASSUNTO

In una precedente nota (1) degli stessi autori sono stati dati alcuni risultati preliminari sulla distributions angolare dei secondari nei decadimenti π-μ-e. Questa ricerca è stata suggerita da LEE e YANG (2) per verificare la conservazione della parità in interazioni deboli. Infatti, se la conservazione della parità è violata in entrambi i processi di decadimento (π-μ e μ-e rispettivamente), la distribuzione angolare dell'elettrone rispetto alla linea di volo del mesone μ nel sistema nel quale il π è a riposo deve seguire una legge del tipo $f(w) = (1 + \alpha \cos w) \times \text{cost}$. Su di un totale di 1028 eventi è stato ottenuto per α il valore $\alpha = -0.222 \pm 0.067$. La probabilità che α sia zero (distribuzione isotropa) è di circa $3 \cdot 10^{-3}$. Tutti i decadimenti sono stati osservati in lastre esposte ai raggi cosmici.

IL NUOVO CIMENTO Vol. V, N. 3 1° Marzo 1957

On a Non-Local Relativistic Quantum Theory of Fields (*) - I.

G. Wataghin

Istituto di Fisica dell'Università - Torino

(ricevuto il 9 Febbraio 1957)

Summary. — A new formalism of a relativistic non-local theory of fields is suggested and discussed. In a first approximation special form-factors are introduced and with them a hamiltonian formalism is developed satisfying the claim of macroscopic causality. The problem of the convergency of the perturbation metod in the S-matrix formalism is examined in view of new assumptions concerning the finite life time of the virtual states.

1. – Introductory Remarks.

In this note we want to analyze a new form of a non local theory of fields (**), which is free from infinities and satisfies the claim of macroscopic causality. The fundamental problem of the mass quantization connected with the self-energy calculations will be analysed in another place. Also the discussion of new limitations in the interpretation of physical phenomena, like those concerning the measurability in small domains of space and time and the validity of free particle picture in such domains, will be only briefly mentioned.

A revision of the whole S-matrix formalism will be necessary. We shall illustrate the method on the examples of a collision problem and a self-energy problem in the case of a ps-pv coupling between pions and nucleons, but the same formalism can be applied equally well to the electrodynamics or to coupling of K-mesons and hyperons or to a non linear coupling of the type:

$$M\bar{\psi}(\exp[g\gamma_5\varphi]-1)\psi\,, \tag{1}$$

where the φ represents a pseudo-scalar boson field.

(*) The main results obtained in this work were subject of a communication presented at the International Conference on Fundamental Constants on September 6-th, 1956 in Turin.

(**) Many features of the new formulation were already suggested in previous notes.

Let us start with the analysis of the state of a nucleon having a definite average momentum and energy p. From the theory of the anomalous magnetic moment and of the photo-meson production on nucleons one can deduce that it is possible to represent the state of a « dressed » nucleon (with its meson cloud and with appropriate vacuum polarisation effects) as a linear superposition of states of bare particles:

$$(2) \qquad |n_p\rangle = z_n \psi_n(\boldsymbol{p}) + \sum_{\boldsymbol{p}+\boldsymbol{k}_1=\boldsymbol{p}} c_1(\boldsymbol{p}_1\boldsymbol{k}_1)\psi_n(\boldsymbol{p}_1)q(\boldsymbol{k}_1) + \sum_{\boldsymbol{p}_2+\boldsymbol{k}_2'+\boldsymbol{k}_2''=\boldsymbol{p}} c_2(\boldsymbol{p}_2\boldsymbol{k}_2'\boldsymbol{k}_2'')\psi_n(\boldsymbol{p}_2)q(\boldsymbol{k}_2')q(\boldsymbol{k}_2'') + \dots$$

In a similar way the state of a pion can be represented as follows:

$$(2') \qquad |\pi_k\rangle = z_\pi \varphi_\pi(\boldsymbol{k}) + \sum_{\boldsymbol{p}_1'+\boldsymbol{p}_1''=\boldsymbol{k}} a_1(\boldsymbol{p}_1'\boldsymbol{p}_1'')\psi(\boldsymbol{p}_1')\bar{\psi}(\boldsymbol{p}_1'') + \dots .$$

where $\psi_n(\boldsymbol{p})$, $q(\boldsymbol{k})$ are the eigen-states of the free hamiltonian with non renormalized masses and charges.

The coefficients $z_n c_i a_\pi \dots$ of this expansions can be interpreted as amplitudes of the probability to find the nucleon without mesons, or with one meson, or with two mesons, or, respectively, a bare pion and so on. The creation and destruction of particles must be described by the second quantization method of Dirac. But, in this method the created particle, having a definite momentum and energy, is supposed to be in a stable state and the quantized field is assumed to have negligible interaction with other fields. Thus the created particle should be a « bare » particle, whereas the « bare » state is not a stable state. This argument shows that only an approximate description of states of bare particles is possible with the use of the 2-nd quantization, and will induce us to take into account the finite life time of these states by means of another approximation.

The introduction of relativistic cut-off operators and a new assumption concerning the damping of virtual states will allow us to obtain the conditions of convergency of the perturbation expansion and thus tentatively to explain the succes of the application of perturbation calculations in the electrodynamics.

2. – Definition of the Cut-Off Operators. First Approximation to the Construction of the S-Matrix.

In order to give in a simple way the rules of the new formalism let us consider the collision between particles having known momenta, spins, polarizations etc., and let us represent them as plane wave solutions of the free particle equations (« bare » particles). Let $P_\mu = \sum p_\mu$ be the total energy-momentum 4-vector and let u_μ be the velocity vector of the centre of mass

(C.M.) system of the ingoing particles (*):

$$u_\mu = \frac{1}{m} P_\mu , \qquad \text{where} \qquad m^2 = P_\mu P^\mu > 0 .$$

Taking the scalar product $k_\nu u^\nu$ of any vector k (projection on u^ν), we shall form two invariants

$$I_t = k_\nu u^\nu , \qquad I_s = \sqrt{I_t^2 - k_\nu k^\nu} = I_s(k) ,$$

which we shall call « projections » on the time axis and respectively on the space of the C.M. system, because in the C.M. system one has:

$$I_t = k_0 . \quad I_s = |\boldsymbol{k}| , \quad I_s^2 = k_0^2 - (k_0^2 - k_1^2 - k_2^2 - k_3^2) = k_1^2 + k_2^2 + k_3^2 .$$

The cut-off operators will be functions of these invariants.

Let us now consider all the terms of the S-matrix which transform the above mentioned set of ingoing particles in a given set of outgoing particles (also plane waves). This group of terms will transform covariantly under the Lorentz transformation. Knowing the interaction hamiltonian and applying the usual formalism, we can write down easily the term of n-th order S_n in the momentum representation of the collision matrix S, corresponding to a given Feynman graph. Then we can formulate the rules of the relativistic cut-off method in the following way: *every non degenerated intermediate or final state of a bare particle having the momentum k, has a statistical weight $= G^2(I_s(k))$.* Therefore in the S-matrix formalism in every *internal boson or fermion propagator and in every external line one must insert a factor G.* Such invariant operators obviously conserve the general covariancy of the theory. These statistical weights depend on the particular interaction process considered; for example, the weight of the bare state of a nucleon can be modified by the interaction with another nucleon.

Although a definite choice of the cut-off function $G(I_s(k))$ and of the universal length l cannot be made on the basis of general properties of a non local interaction and will depend probably on the solution of the problem of « mass quantization », some experimental results concerning the mass differences between charged and neutral particles (interpreted as due to the electromagnetic interaction) and the momentum distribution in the C.M. frame of reference of π and K-mesons created in a high energy collision suggest a choice of G

(*) Each of the incident « physical » particles interacts in a definite state as a bare particle or a set of bare particles. We adopt *units*: $c = 1$, $\hbar = 1$.

of the type

$$G(\xi) = \frac{3[\sin\xi - \xi\cos\xi]}{\xi^3} = 3\sqrt{\frac{\pi}{2}}\,\xi^{-\frac{3}{2}} I_{\frac{3}{2}}(\xi), \tag{3}$$

where $\xi = lI_s(k)$.

This choice corresponds to a form-factor $F(I_s(\eta))$ (see the definition below) in «internal» co-ordinates η_ν, which, in the C.M. system, is:

$$F = l^{-1}\delta\left(\frac{\eta_0}{l}\right) f\left(\frac{|\boldsymbol{\eta}|}{l}\right), \tag{3'}$$

where

$$f\left(\frac{|\boldsymbol{\eta}|}{l}\right) = \begin{cases} -(3/4\pi)\, l^{-3}, & \text{if} \quad \boldsymbol{\eta} \leqslant l, \\ 0 \qquad\quad , & \text{if} \quad |\boldsymbol{\eta}| > l. \end{cases}$$

This sharp limitation of the small domain of $|\boldsymbol{\eta}|$ in which F is not vanishing is also required be the claim of macroscopic causality. The statistical weight factors G^2 behave asymptotically for $\xi \to \infty$ as $\sim (\cos^2(\xi))/\xi^4$.

3. Internal Co-ordinates. Definition of a Non-Local Interaction Hamiltonian and of the Modified Propagators.

The simple rules of the calculation of the non local S-matrix in the momentum space given above can be deduced starting from the definition of a non local hamiltonian density in space-time $H'(x)$ and from the assumptions concerning the new rules of calculation of the S-matrix in configuration space.

In order to describe the fundamental uncertainties in the space-time co-ordinates of a particle during the interaction we shall introduce new «internal parameters» for each field.

Besides the coordinates of spin and isotopic spin and strangeness, we shall introduce 4 continuous «internal co-ordinates» $\eta_0\eta_1\eta_2\eta_3$ which will transform as differences of the space-time co-ordinates (obeying the homogeneous Lorentz transformation). Similar co-ordinates were introduced by many authors (Marcov, Yukawa and others) and used in non local or «bilocal» theories (*). Our definitions differ from other insofar as they depend essentially on our definition of relativistic form-factors and as we require that the parameters η_l are commutable with all the momenta (as differences of co-ordinates) and that they are not measurable (as the angular variables canonically conjugated to the spin components).

(*) The equivalence of such relativistic theories with the cut-off method was pointed out many times.

The description of points in the space-time will be made by postulating that every co-ordinate x_ν is to be substituted by $x_\nu - \eta_\nu$, where the domain D_l of possible values of η_ν is limited by means of the value of a universal lenght l. Since η_ν are not measurable, this assumption is compatible with the statement that each space or time interval is uncertain within the limits fixed by the domains D_l. This limitation can be done in a relativistic way by introducing relativistic form-factors in the formalism of field theories. In order to illustrate the method we start by the consideration of a collision process and of the n-th order term S_n of the perturbation expansion of the S-matrix in the usual local theory:

$$S^n = \frac{(-i)_n}{n!} \int_{-\infty}^{\infty} \mathrm{d}^4x_1 \dots \mathrm{d}^4x_n P(H'(x_1) \dots H'(x_n)) \,. \tag{4}$$

We shall illustrate the method assuming that the local hamiltonian H' represents a ps-pv interaction:

$$H'(x) = i \frac{g}{m} (\overline{\psi}(x)\gamma_5\gamma_\nu\tau_\sigma\psi(x)\partial_\nu\varphi_\sigma(x) + \dots) \,. \tag{5}$$

Each field amplitude φ, ψ, $\bar{\psi}$ can be split, as usually, into positive and negative frequency components and can be expanded into Fourier components containing absorption and creation operators of particles with momenta $k' k'' k'''$ (we shall adopt the formalism in which the negative energy states are substituted by the « charge conjugated solutions » representing the antiparticles in the positive energy states and the 2-nd quantization is applied to travelling non stationary waves). For instance in the case (5) we shall have 16 terms of H' with given momenta k', k'', k''' of the 3 interacting fields corresponding to the different sets of creation and annihilation operators of the type $b^*_{k''} b_{k'''} a_{k'}$.

In order to transform (4) and (5) into non-local operators in a covariant way we postulate the following rules: considering a vertex point x and a term of the above Fourier expansion, we substitute in this term the phase factor $\exp[-ik'x]$ belonging to a positive frequency component by $\exp[-ik'(x + \eta')]$ and the phase factor $\exp[ik'''x]$ belonging to a negative frequency by $\exp[ik'''(x - \eta''')]$ and introduce invariant form-factors F operating on the « internal coordinates » η', η'', η'''. These internal co-ordinates will, by definition, transform like differences of co-ordinates obeying the homogeneous Lorentz transformation, and will commute with the momentum operators.

Since simultaneity depends on the Lorentz reference system we shall make the basic assumption that in the definitions and laws which follow the simul-

taneity is defined in the C.M.-system, (e.g. by means of the proper time of the C.M.-system).

In general case of a graph corresponding to the term (4) one shall have at the time x_0 of the vertex x a number of other « boson » and « fermion » lines which do not end or begin in this vertex point. Also each of these lines, let us say the one with momentum k^{IV}, can be considered as an ingoing particle arriving with the phase-factor $\exp[-ik^{\mathrm{IV}}(x^+ + \eta^{\mathrm{IV}})]$ and going out with the phase-factor $\exp[ik^{\mathrm{IV}}(x^- + \eta^{\mathrm{IV}})]$. Since we shall put in further calculations: $x^+ = x^- = x$, the above phase-factor will not modify the values of the matrix-elements (5). In the above example, if the term $b_{k''}b_{k'''}a_{k^{\mathrm{IV}}}$ is considered, and if there is just one more line (k^{IV}) not passing through the vertex x, the total phase-factor will be:

$$(6) \qquad \exp[-i(k' + k'' + k^{\mathrm{IV}})x^+ - i(k'\eta' + k''\eta'' + k^{\mathrm{IV}}\eta^{\mathrm{IV}})] \cdot \cdot \exp[i(k''' + k^{\mathrm{IV}})x^- + i(k'''\eta''' + k^{\mathrm{IV}}\eta^{\mathrm{IV}})] .$$

The invariant form-factors F will be chosen in such a manner as to limit the values of the variables η', η'', η''', η^{IV}, x^+ and x^- to a small domain D_t of space and time containing the vertex-point x. These F's are functions of invariants defined below in a manner similar to those (I_s, I_t) introduced in the cut-off operators in the momentum space. Let ∂_ν^- indicate the derivative $\partial/\partial x_\nu^-$ and $\hat{c}_\nu^-$ the derivative $\hat{c}/\hat{c}x_\nu^-$. Then the form-factors limiting the domains of internal co-ordinates η are defined as functions of the invariant operators $I_s^\pm$ and $I_t^\pm$:

$$(7) \qquad \begin{cases} (I_s^+)^2 = \dfrac{(\eta i^\nu \hat{c}_\nu^+)^2}{|i\hat{c}_\nu^+ \cdot i\partial^{+\nu}|} - \eta^\nu\eta_\nu = (\eta^\nu U_\nu^+)^2 - \eta^\nu\eta_\nu , \\ I_t^+ \quad = \dfrac{\eta^\nu i\hat{c}_\nu^+}{|i\hat{c}_\nu^+ \cdot i\partial^{+\nu}|} = \eta_\nu U_\nu^+ \end{cases}$$

where, after the application of (7) to (6), one obtains

$$U_\nu^+ = \frac{k' + k'' + k^{\mathrm{IV}}}{|k' + k'' + k^{\mathrm{IV}}|} ,$$

in the case of a positive frequency component, whereas they are defined as function of

$$(7') \qquad (I_s^-)^2 = \frac{(\eta^\nu i\hat{c}_\nu^-)^2}{|i\hat{c}_\nu^- i\partial^{-\nu}|} - \eta^\nu\eta_\nu = (\eta^\nu U_\nu^-)^2 - \eta^\nu\eta_\nu ; \qquad I_t^- = \eta^\nu U_\nu^- ,$$

where, applying (7') to (6), one finds

$$U_\nu^- = \frac{k''' + k^{\mathrm{IV}}}{|k''' + k^{\mathrm{IV}}|} ,$$

in the case of a negative frequency component. Here the expression of the invariants $I_s^{\pm}$ and $I_t^{\pm}$ is defined as function of operators $\hat{c}'$, $\hat{c}$ and specified in function of the momenta k', k'', k''' and k^{IV} for the case of the term containing $b_{k''}^{*} b_{k'''} a_{k'}$ and must be substituted by similar expressions in other cases. The vectors U^{+} and U^{-}, and the invariants $I_s^{\pm}$, $I_t^{\pm}$ are obviously analogous to u and I_s, I_t defined in Sect. 2. Also the function $F(I_s, I_t)$ must be of the type (3′) of Sect. 2 in order to have, in the C.M.-reference system in which the $U^{\pm}$ components are $(1, 0, 0, 0)$, the $\delta(\eta_{f0})$ dependence of the time and satisfy the limitation

$$F = \text{const} \neq 0, \quad \text{if} \quad |\boldsymbol{\eta}| \lesssim l,$$

$$F = 0, \quad \text{if} \quad |\boldsymbol{\eta}| > l.$$

The next step in the calculation is the integration over all « internal co-ordinates η', η'', η''', η^{IV}, and this gives us the cut-off operators G $(lI_s(k))$ for each momentum k', k'', k''' and a factor -1 for k^{IV} (because $\int F(\eta_l^{IV})\,\mathrm{d}^4\eta_l^{IV} = -1$). A further step concerns the condition $x^{+} = x^{-} = x$. We can associate $\delta(x^{+} - x)$ and $\delta(x^{-} - x)$ factors and integrate over x^{+} and x^{-}. After this integration remains the phase-factor $\exp[-i(k' - k'' - k''')x]$. Successive integration over x will give us the usual $\delta^4(k' + k'' - k''')$ factor. It is easy to see that one obtains in this way: $U^{+} = U^{-} = u$ in all vertex points, and therefore one has the important result that all the cut-off and form-factors are referred to the same 4-vector u_ν in all vertex-points and this 4-vector u_ν is defined as the velocity-vector of the C.M. system of the incident (and also of the outgoing) particles. Writing each of the field amplitudes as a sum of terms representing respectively absorption and creation of particles, and thus substituting $\varphi(x+\eta)$ by $\varphi^{+}(x^{+}+\eta) + \varphi^{-}(x^{-}+\eta)$, one can put the non-local hamiltonian into the form:

$$\text{const} \int \mathrm{d}^4\eta' \,\mathrm{d}^4\eta'' \,\mathrm{d}^4\eta''' \int \delta(x^{+} - x)\,\delta(x^{-} - x)\,\mathrm{d}x^{+}\,\mathrm{d}x^{-}\,[F(I_s^{+}(\eta') + F(I_s^{-}(\eta'))]\,[\ldots]\cdot$$

$$\cdot [F(I_s^{+}(\eta''')) + F(I_s^{-}(\eta'''))]\,\{[\bar{\psi}^{+}(x^{+}+\eta''') + \bar{\psi}^{-}(x^{-}+\eta''')]\ldots[\varphi_\sigma^{+}(x^{+}+\eta') + \varphi_\sigma^{-}(\varphi^{-}+\eta')]\}\,.$$

The new hamiltonian remains hermitian and in the C.M. system contains only the derivatives $\hat{c}_\nu^{+}$ and $\hat{c}_\nu$ with respect to the space co-ordinates. Since the formfactors, in the C.M. system, do not depend on time co-ordinates $t' - t''$, the well known difficulties connected with the Cauchy problem are eliminated in our case (*).

The remaining part of the calculation of the S_n can be performed applying the usual commutation relations between the creation and annihilation oper-

(*) See also a theorem of V. I. Grigor'ev: *Žu. Éksper. Teor. Fiz.*, **30,** 873 (1955).

ators $a_k a_k^* b_{k''}$ etc., in the momentum space (obviously the commutators, anti-commutators and propagators in space-time are modified by the cut-off). One obtains instead of the usual causal boson propagator $\Delta_c(x-y)$ the following non-local propagator:

$$\Delta_c'(x-y) = \frac{1}{(2\pi)^4}\int_c \frac{G(lI_s(k))\,\exp[-ik_\nu(x^\nu - y^\nu)]}{k^2 - m^2}\,\mathrm{d}^4k\,, \tag{8}$$

and similar expression for $S_c'(x-y)$. If one applies to Δ_c the operator $G(I_s^{\pm})$ where I_s is defined by (7), one obtain Δ_c'. Wherease Δ_c satisfies the inhomogenous equation of the Green function, Δ_c' satisfies a similar equation where the function $\delta(x-y)$ is substituted by $G(I_s^{\pm})\delta(x-y)$, which corresponds to an extended source. Since Δ_c' is an invariant, we can calculate it in the C.M. system where $I_s(k) = |\boldsymbol{k}|$. Then the first integration over k_0 in (8) can be performed with the usual prescription about the contour. In this manner the causality condition of Stückelberg and Feynman [formulated as the condition requiring that for $x^0 - y^0 > 0$ only the pole $k_0 = \sqrt{k^2 + m^2}$ contributes to (8) and for $x^0 - y^0 < 0$ only the pole $k_0 = -\sqrt{k^2 + m^2}$] is fulfilled.

One finds easily that, if $G(lI_s(k))$ is given by (3) one has in the C.M. system (*):

$$\Delta_c'(x-y) = \frac{3}{4l}\int_t^l \left[1 - \left(\frac{\alpha}{l}\right)^2\right]\Delta_c(t,\, r+\alpha)\,\mathrm{d}\alpha\,. \tag{8'}$$

Therefore $\Delta_c'(x-y)$ is regular everywhere and has non vanishing values in the neighbourhood of the light cone $|t-r| < l$. If one considers short range interactions and $m \gtrsim l^{-1}$ (nucleon-pion interactions) and one takes into account that in another vertex point the new interaction is also limited by a form-factor F, then the domain in which Δ_c', S_c' propagate, results limited, in the C.M. system, by $r \lesssim l$ and $t \lesssim l$. In other reference systems this domain appears Lorentz contracted in space and expanded in time.

In the case of particles of vanishing rest-mass, as photons or neutrinos, one has: if $x_0 > 0$; $m = 0$; [in the C.M. system]

$$\begin{aligned}\Delta_c'(x) &= \frac{i}{(2\pi)^3}\int \frac{\mathrm{d}^3k}{2\,|\boldsymbol{k}|}\,G(l\,|\boldsymbol{k}|)\,\exp[-ik_\nu x^\nu] = \\ &= \frac{1}{(2\pi)^2}\,\frac{1}{2r}\int G(lk)\,(\exp[ik(r-t)] - \exp[-ik(r+t)])\,\mathrm{d}k = \\ &= \frac{1}{2(2\pi)^2}\,\frac{1}{lr}\left\{f_1\left(\frac{r}{l}\;\frac{t}{l}\right) - f_1\left(\frac{r+t}{l}\right)\right\},\end{aligned} \tag{9}$$

(*) I thank Dr. T. Regge for indicating to me this relation.

where $r = |\boldsymbol{x}|$; $k = |\boldsymbol{k}|$; $t = x_0 > 0$ and f_1 is:

$$(9') \qquad f_1\left(\frac{\circ}{l}\right) = \int G(\alpha) \exp\left[i\alpha\left(\frac{\circ}{l}\right)\right] \mathrm{d}\alpha$$

$$\begin{cases} \frac{3}{4}\left[1 - \left(\frac{\circ}{l}\right)^2\right], & \text{if } \left(\frac{\circ}{l}\right)^2 \leqslant 1 \qquad (\text{or } |r \pm t| \leqslant l), \\ 0 \qquad , & \text{if } \left(\frac{\circ}{l}\right)^2 > 1 \qquad (\text{or } |r \pm t| > l). \end{cases}$$

One obtains similar results, if $x_0 < 0$.

Since in the non local theory proposed here the particle which emits or absorbs photons can at best be localized with an uncertainty $\sim l$, the use of the propagator (9) is not in contradiction with the claim that no signal propagates with velocity $> c$.

The above formalism of cut-off operators of the type (3) (3′) is compatible with the hamiltonian method if applied in the C.M. system, because of the $\delta(x_{j0}) \quad \delta(t)$ time-dependence of form-factors F. This formalism is not sufficient to avoid the possibility of interaction being transmitted along a space-like direction if many particles are placed at small distance one near another. The interaction having a statistical meaning, we shall assume as a further assumption, that this interaction can take place with nearly constant probability at any moment of a time-interval $\sim l$, and introduce a supplementary uncertainty in time $\Delta t \sim l$.

Such assumption is equivalent to the introduction of a supplementary cut-off operator $g(lI_t(k)_\nu)$ in the momentum representation of the S-matrix in every internal line of the n-th order term S_n. In the C.M. system an operator of the type $(\sin k_0 l)/k_0 l$ or $l^{-1}(k_0 - il^{-1})^{-1}$ can be inserted (where k_0 appears instead of the invariant $(I_t(k_\nu))$. In the case of the self-energy problem and in the cases of short range interactions, we shall make another assumption: *the total duration in the* C.M. *system of the n-th order interaction is also* $\sim l$. This assumption is made plausible by the following property of the propagators (8) and (9): the main contribution of these propagators lies in a small zone: $|t \mp z| \lesssim l$ near the light cone. Thus in a time interval $\Delta t \gg l$ the created particles would fly apart and could not interact again in the next vertex point. One obtains equivalent results inserting in H' instead of $G(lI_s(k))g(lI_t(k))$ the operator: $G' = l^{-2}\xi'^{-2}8J_2(l\xi')$, where $\xi'^2 = I_s^2 - I_t^2$.

But in the following we shall suggest another approach to the same problem.

4. Mean Life of Virtual States. Convergency of the Perturbation Solution.

In the introduction we made a remark concerning the bare state of a particle being not a stable state. Also the states of a nucleon with n mesons in the cloud or of a virtual pair nucleon + antinucleon, which can substitute a pion, are not stable having a finite life-time, determined by the total probability of all transitions from these states. The introduction of the cut-off factors makes the total life-time of each of these states finite.

The process described by a given Feynman diagram of n-th order can be thought of as a chronological sequence of n transitions having each a definite probability.

In order to formulate a new basic assumption concerning the virtual and real states of a physical particle or of a group of interacting particles, let us consider the example of the time dependent Schrödinger equation of a nucleon in the C.M.-system of this nucleon:

$$H|n\rangle = (H_0 + H')|n\rangle = i\hbar \frac{\partial}{\partial t}|n\rangle ,$$

where H' includes all the interactions of the given particle with all other fields. The time dependence of an intermediate virtual state, in which particles with energies ε_p, ε_k, ... are present, can be put in the form:

$$\exp\left[-i(\varepsilon_p + \varepsilon_k + \ldots)t - \frac{\Gamma}{2}t\right],$$

where Γ is the total width of the considered state and t is the proper time of the C.M. system.

We shall assume as a fundamental property of the interaction of fields that the *total life-time of a state measured in the C.M. system cannot be less than a universal time-interval l.*

This assumption is compatible with and is made plausible by the above mentioned properties of the modified propagators.

(The « stable » state of a free, strongly interacting, particle, having $m > 0$, offers an example of continous fluctuations from one virtual state to another, in accord with the representation (2), with an average frequency l^{-1}, if measured in the C.M. system).

Another fundamental assumption, which we consider necessary to introduce as an independent assumption in the present state of the theory, concerns the time-interval (as measured with the proper time in the C.M. system) in which the higher order transitions can take place.

The total life-time of a transition described by the n-th order term S_n of the perturbation expansion of the S-matrix is independent of n and is $\sim l$.

In order to illustrate this assumption, let us notice that on the basis of the above mentioned assumption, giving life-times $\tau \gtrsim l$ for each virtual state, the time-interval of a cronological sequence of n transitions should average $\sim nl$. The probability of n independent transitions taking place in a time-interval l is then reduced by the well known Poisson's factor

$$\sim \frac{1}{n!} \exp\left[-zl^{-1}\tau\right](zl^{-1}\tau)^n ,$$

where $0 < z < 1$ is the average a priori probability of the virtual states (z is roughly an average value of the principal coefficients z_n, c_1 ... in (2)). In our case $l^{-1}\tau \sim 1$.

Thus assuming that the n transitions in an n-th order term S_n are statistically independent, and applying the Poisson's formula, we can discuss conditions of convergency of the perturbation expansion. In a non local theory all the elements of the interaction hamiltonian are finite. The damping terms make finite the transition amplitudes S_n also in the case of resonance. In calculations of S_n in the momentum representation one can establish the existence of an upper limit of the integrals over the propagators modified by the cut-off factors and show that:

$$S_n | < A \sum \frac{L_n}{n!\, n!} ,$$

where $\sum$ is extended to all possible graphs of the n-th order corresponding to a given process and A is a constant depending on the ingoing and outgoing particles. In simple cases the number of these graphs does not increase faster then $n!$ and the series converges. The general demonstration of convergency in non linear theories requires a detailed analysis of every single case of interaction matrix H' and will not be attempted here.

6. – Causality. Concluding Remarks.

In a non local theory we cannot fulfill the claim of microscopic causality in the sense that the commutator of two field components $[A(x'), A(x'')]$ vanishes if $x'_\nu - x''_\nu$ is a space like vector. In the theory suggested here this condition is verified if on a space like surface $|\boldsymbol{x}' - \boldsymbol{x}''| \gg l$, because of the limitation in space of the interaction domains D_l. In earlier formulations of the non local theories some authors, following the suggestion of PEIERLS and

Mc Manus used form factors which are functions only of the 4-dimensional intervals $(x' - x'')^2$. C. Bloch showed that such factors do not always give convergent results and Stückelberg and Wanders showed that these factors give rise to a contradiction with the claim of macroscopic causality.

Our method, based on the use of new invariants (see Sect. 2), is free from both objections, as can be shown easily considering the properties of the propagators Δ_c' and S_c' mentioned above and the limitations in space and time of the interaction domain D_l. Indeed in the C.M. system this domain is a sphere of radius l in space and a time-interval $\Delta t = l$ in time.

Let us now summarize the essential features of the proposed theory. The method of relativistic cut-off contains two essential modifications of the local field theory. First one makes the assumption that the statistical weight of every non degenerated real or virtual state of a bare particle of a given momentum $I_s(k_\nu)$ is $G^2(I_s(k_\nu))$, where G is a function of the type (3) of an invariant $I_s(k_\nu)$. The form factor $F(I_s^2(\eta))$ operates on the internal co-ordinates and is the Fourier transform of G.

The only necessary condition for the introduction of these weight-factors is the possibility of defining a C.M. system in which the total mass $(P_\nu P^\nu)^{\frac{1}{2}} = m \neq 0$. The case $m = 0$ must be treated in a different manner. For example, in the self-energy problem of a photon or of a neutrino our method fails. We think that it is plausible to assume that the free « zero-mass » particles must be considered as free from the vacuum fluctuations as if they were not coupled to other fields. For them only the collision with another particle creates conditions for interaction with all other fields.

This introduction of cut-off operators G conserves the hermitian nature of the hamiltonian and thus the unitarity of the S-matrix. Indeed terms of the hamiltonian containing operators $b_{k''}^* b_k a_k$ and $b_{k''} b_{k''}^* a_k^*$ receive the same real cut-off factors and remain complex-conjugated.

The second assumption concerns the existence of a lower limit of the life-time of intermediate states. This implies the consideration of a non-hermitian hamiltonian and of complex energy values. We think that approximate results can be obtained by introducing appropriate cut-off operators of the type mentioned at the end of Sect. 3.

The elimination of infinities permits to calculate all the self-energies and the anomalous magnetic momenta. The choice G' of Sect. 3 of the cut-off factors with $l^{-1} \sim 4m_\pi$, where m_π is the pion-mass, gives a reasonable value of the electromagnetic self-energy in the case of $\pi^\pm$, π^0 mass-difference and of the neutron-proton mass-difference. Also the anomalous magnetic momenta have the correct order of magnitude. Our method allows also a natural description of the multiple meson production if one introduces non linear coupling of the type mentioned in Sect. 1. The theory of this multiple production and of the mass quantization will be the subject of a next pubblication.

RIASSUNTO

Si propone una nuova teoria non locale dei campi. In prima approssimazione si introducono fattori di convergenza compatibili coll'uso del metodo Hamiltoniano e col principio della causalità macroscopica. Si studiano anche le condizioni di convergenza del metodo perturbativo del calcolo della matrice S e si introducono nuove ipotesi sulle vite medie degli stati virtuali.

NOTE TECNICHE

Risultati di un oscillatore con transistore (*).

M. R. E. Bichara

Johannesburg, South Africa

(ricevuto il 1° Settembre 1956)

Riassunto. — Si esaminano due oscillatori con transistore per poter dedurre statisticamente la loro precisione. Dai risultati si vede che stabilizzando voltaggio d'alimentazione la precisione viene portata da $\pm$ 0.0055% a $\pm$ 0.000 57 % per l'oscillatore la cui frequenza nominale sia di 349 779 Hz e $\pm$ 0.001 07 % per quello di 99 935.8 Hz con limiti di fiducia del 99%.

Descrissi altrove (1) un oscillatore che utilizza un transistore a punte mentre il circuito equivalente è il ponte di Wien.

Tale oscillatore si distingue per il fatto che la sua frequenza varia di solo 0.005 5% quando il voltaggio d'alimentazione varia del 44%. Tale stabilità è ottenuta senza uso di termistori od altri componenti non lineari.

Dato che tale oscillatore avrebbe dovuto funzionare per un periodo ininterrotto di non oltre 48 ore era necessario un esame sulla stabilità della sua frequenza. Diamo qui, per l'appunto, il riassunto di tale esame e le conclusioni dedottene.

L'oscillatore di 350 kHz, cioè quello già descritto e che chiameremo N. 1, fu tenuto sotto controllo per un periodo ininterrotto di 10 giorni. Nessuna precauzione fu presa per diminuire le variazioni di temperatura o le vibrazioni minerarie, sismiche o dovute al traffico. Solo il voltaggio d'alimentazione fu tenuto costante. Il controllo di frequenza fu fatto tre volte al giorno. La Tabella I elenca i valori ottenuti assieme ad altri dati complementari.

Dato che i parametri dei transistori sono profondamente influenzabili dalle variazioni di temperatura $\Delta^{\circ}T$)) è interessante osservare la relazione tra $\Delta^{\circ}T$ e la variazione di frequenza $\Delta(f)$.

(*) Presentato al Congresso di Torino, 6-11 Settembre 1957.

(1) *Compt. Rend. Acad. Sci.*, **240**, 2393 (1955).

TABELLA I.

Ora	Frequenza (f)	Temperatura ($°T$)	Dev. $p/10^6$ (f)
08.30	349 794	22.8	— 17.2
12.35	349 791	23.6	— 25.7
16.30	349 788	24.6	— 34.3
08.25	349 791	20.9	— 25.7
13.10	349 790	22.6	— 28.6
16.30	349 788	24.2	— 34.3
11.45	349 794	23.0	— 17.2
08.15	349 792	21.5	— 22.9
13.50	349 794	24.5	— 17.2
16.25	349 794	24.4	— 17.2
08.30	349 795	21.7	— 14.3
12.45	349 794	23.3	— 17.2
16.30	349 791	23.7	— 25.7
08.20	349 794	21.5	— 17.2
12.50	349 795	22.7	— 14.3
16.20	349 792	24.4	— 22.9
08.25	349 794	21.5	— 17.2
13.55	349 791	23.0	— 25.7
16.30	349 788	23.7	— 34.3
08.20	349 798	21.4	— 5.7
13.05	349 792	22.6	— 22.9
16.15	349 791	23.6	— 25.7
08.35	349 794	21.1	— 17.2
12.45	349 794	21.1	— 17.2
17.05	349 790	25.2	— 28.6
08.25	349 794	22.0	— 17.2

Per mezzo del metodo dei « minimi quadrati » si può definire una linea retta tra i punti ottenuti, e la sua equazione è:

$$\Delta f = -2.867\,°T + 43.794. \tag{1}$$

La distribuzione dei punti attorno alla retta è alquanto ampio, però se l'equilibrio del ponte di Wien venisse distrutto si ricaverebbe, dai nuovi valori ottenuti, un'altra equazione. Tali valori sono elencati nella tavola seguente:

Tabella II.

Frequenza	Temperatura	Dev. $p/10^6$
378 000	22	80 000
415 000	30	186 000
436 000	35	246 000
467 000	40	334 000

mentre l'equazione ricavata è:

$$\Delta f = 13\,641\ ^\circ T - 221\,602\ . \tag{2}$$

Si nota chiaramente che le due pendenze delle equazioni (1) e (2) non sono dello stesso ordine di grandezza.

Ora resta a vedere a chi attribuire la stabilità di frequenza. Perciò fu costruito un secondo oscillatore che chiameremo N. 2. Fu usato lo stesso procedimento teorico di progettazione del N. 1 mentre, invece, furono alterate tutte le caratteristiche fisiche del circuito per poter trovare se la stabilità fosse dovuta al progetto oppure ad una felice combinazione tra componenti circuitali. Al nuovo oscillatore furono cambiati: 1) il modello del transistore, 2) il taglio del quarzo, 3) il fattore di merito del quarzo e 4) la frequenza. I valori di tali cambiamenti sono come segue:

	Osc. N. 1	Osc. N. 2
1)	0C51	0C50
2)	*CT*	*X*
3)	14000	429
4)	350 kHz	100 kHz

L'esame fu, naturalmente, identico al primo e la Tabella III ne elenca i risultati.

Tracciandi di nuovo una retta, col solito sistema, tra i punti ottenuti ricavammo:

$$\Delta f = -4.41\ ^\circ T + 81.64\ . \tag{3}$$

Paragoniamo ora i risultati dal punto di vista statistico.

Togliendo, statisticamente, gli effetti della temperatura vedremo che i due oscillatori si comportano allo stesso modo, mentre lo sparpagliamento dei punti, lungo la media, si restringe di ben poco.

Da quanto detto si può concludere che:

1) la stabilità è ottenuta dal sistema di progettazione e non dalla qualità nè delle combinazione dei singoli elementi;

2) la variazione di temperatura ha una minore influenza sul quarzo quando è inserito nel circuito che non da solo;

3) la differenza del fattore di merito è appena percettibile;

Tabella III.

Ora	Frequenza (f)	Temperatura (°T)	Dev. $p/10^6$ (Δf)
11.00	99 936.7	21.3	$\geqslant$ 3
08.30	99 936.7	20.3	— 3
13.55	99 935.3	22.7	— 17
16.30	99 934.1	23.4	— 29
08.45	99 935.3	20.1	— 17
14.00	99 935.3	22.2	— 17
16.30	99 936.7	21.8	— 3
08.30	99 938.2	18.8	+ 12
13.00	99 936.7	21.2	— 3
16.25	99 935.3	22.4	$\geqslant$ 17
08.30	99 935.3	19.6	— 17
14.00	99 938.2	20.0	+ 12
16.20	99 936.7	20.4	$\geqslant$ 3
08.35	99 937.5	19.1	+ 5
13.15	99 935.3	21.5	— 17
16.30	99 935.2	23.3	— 18
08.45	99 936.0	20.5	— 10
08.25	99 935.3	20.6	— 17
13.15	99 934.5	23.6	— 25
16.30	99 934.1	24.7	— 29
08.40	99 936.6	21.2	— 4
13.50	99 934.5	21.9	— 25
16.20	99 936.7	21.9	— 3
08.25	99 955.5	18.8	— 15
16.30	99 934.5	21.8	— 25
08.17	99 934.2	19.9	— 28

4) la variazione di frequenza è dovuta ad altre ragioni che non la temperatura;

5) l'ampiezza delle variazioni di frequenza è direttamente proporzionale alla differenza tra temperatura di lavoro e quella ottima del cristallo.

Effettivamente sia nel quarzo a taglio CT che in quello X, la funzione $\Delta f = g(°T)$ è di forma parabolica e per conseguenza la df/dT aumenta a mano a mano che ci si allontana dall'asse di simmetria.

	Osc. N. 1	Osc. N. 2		Osservazioni
$S = \sqrt{\frac{1}{n-1}\sum_{i=1}^{n}(f_i - \bar{f})^2}$	1.334	0.229	—	—
$F = \left.\frac{\sum_{i=1}^{n}(f_{i_1} - \bar{f}_1)^2}{\sum_{i=1}^{n}(f_{i_2} - \bar{f}_2)^2}\right\|_{n_1 = n_2}$	—	—	33.97	differente
$\sigma^2 = \frac{1}{n-2}\sum(\Delta f_i - aT_i - b)^2$	37.82	101.51	—	—
$F = \left.\frac{\sum_{i=1}^{n}(\Delta f_{i_1} - \Delta\bar{f}_1)^2}{\sum_{i=1}^{n}(\Delta f_{i_2} - \Delta\bar{f}_2)^2}\right\|_{n_1 = n_2 = 24-1}$	—	—	2.68	senza signif. al livello dell'1% per $\Delta f/T$
$\hat{b}$	2.867	4.41	—	—
var $\hat{b}$	1.016	1.728	—	—
$t = \frac{\hat{b}_1 - \hat{b}_2}{\sqrt{\text{var}(\hat{b}_1) + \text{var}(\hat{b}_2)}}$	—	—	0.93	senza signif. al livello dell'1%
$t = \frac{\overline{T}_1 - \overline{T}_2}{\sqrt{\frac{s^2_{T_1} + s^2_{T_2}}{n}}}$	—	—	4.48	signif. al livello dell'1%

* * *

Desidero ringraziare la dott. B. S. Hobson dei Laboratori di Ricerche del Transvaal & Orange Free State Chamber of Mines, Johannesburg, South-Africa, per il suo lavoro nel calcolo statistico.

SUMMARY (*)

Two oscillators with transistor are examined in order to deduce statistically their precision. From the results one gathers that stabilizing their input voltage the precision is varied from $\pm 0.0055\%$ to $\pm 0.00057\%$ for the oscillator the nominal frequency of which is 349 779 Hz and $\pm 0.00107\%$ for the one of 99 935.8 Hz frequency with precision limits of 99%.

(*) *Editor's translation.*

IL NUOVO CIMENTO Vol. V, N. 3 1° Marzo 1957

A Geiger Counter Design Giving a Definite Counting Length.

P. J. Grouse and H. D. Rathgeber

The F.B.S. Falkiner Nuclear Research and Adolph Basser Computing Laboratories, School of Physics (*), *The University of Sydney - Sydney, N.S.W., Australia*

(ricevuto l'11 Dicembre 1956)

Summary. — A design of Geiger counter is described which is simple to make and the effective length of which is readily obtainable from its geometry and operating voltage. The results of field calculations and measurements agree. The operating voltage is chosen such that variations of effective length due to voltage fluctuations are minimized.

1. – Introduction.

In many measurements using Geiger counters such as those concerned with absolute rates or with beams which must be limited exactly, it is essential to know the effective length of the counting volume. In the study of time variations it is further essential to keep the variations due to length fluctuations much smaller than the variations in the counting rate.

The effective length of different types of counters has been measured ([1-4]), however, only a few reports have been published concerning the variation of effective length with working voltage ([5,6]).

One design has been described in which the effective length is limited by field tubes and is independent of working voltage ([7]). This design cannot be

(*) Also supported by the Nuclear Research Foundation within the University of Sydney.

([1]) K. Greisen and N. Nereson: *Phys. Rev.*, **62**, 316 (1942).

([2]) A. G. Engelkemeir and W. F. Libby: *Rev. Sci. Instr.*, **21**, 550 (1950).

([3]) D. Blanc: *Nuovo Cimento*, **1**, 1280 (1955).

([4]) A. M. Baptista and J. P. Galvão: *Nuovo Cimento*, **3**, 647 (1956).

([5]) A. Rogozinsky and A. Voisin: *Compt. Rend. Acad. Sci.*, **225**, 409 (1947).

([6]) Ryumyo Ito: *Journ. Phys. Soc. Japan*, **7**, 256 (1952).

([7]) A. L. Cockroft and S. C. Curran: *Rev. Sci. Instr.*, **22**, 37 (1951).

improved upon for precise definition of effective length. It is, however, relatively difficult to make.

The present investigation arose from the desire to develop a counter fulfilling the following conditions, namely, that it is relatively simple to make, that its effective length is calculable in advance, that the factors governing this effective length are controllable, and finally that the variation of effective length with working voltage is calculable and is sufficiently small for most purposes.

2. – Design.

Since the effective length is governed by the field on the centre wire which in turn depends upon boundary potential conditions, it is to be expected that in counters in which an appreciable area of good insulator is visible from the wire, uncontrollable surface charges may have serious effects. Such conditions occur when insulating glass sleeves are used as length limiters ([2,8]). In order to satisfy the third condition above, the potential of all inside surfaces of the counter must be well defined.

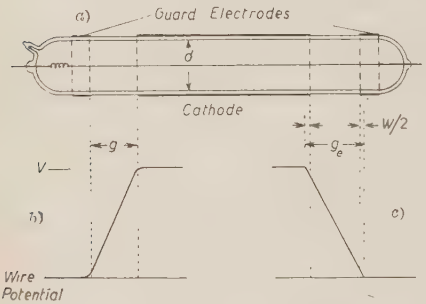

Fig. 1. – *a*) Design of Geiger counter; *b*) Actual potential distribution on inside of counter: *c*) Potential distribution approximation for calculations.

In the Maze type of counter ([9]) the conductivity of the glass envelope ensures this condition. In his original design Maze limited the effective length by small diameter metal tubes which held the wire. From measurements on proportional counters ([10]) it is known that the influence of such metal sleeves on the field at the wire extends for several cm along the wire. We have concluded that this type of length limitation would cause rapid variation of effective length with applied voltage. After considering the various factors, we chose to study the design shown in Fig. 1 (*a*) and which is similar to one previously described ([8]). This incorporates a pair of guard electrodes separated from the cathode by a gap of length g. Both guard electrodes and cathode are of colloidal graphite painted onto the outside of the glass envelope. While the guard rings are held at the potential of the centre wire it was nevertheless considered inadvisable to extend them to the wire in order to keep down the capacity to ground of the circuit input, and the coupling between counters.

([8]) D. Blanc and M. Scherer: *Compt. Rend. Acad. Sci.*, **228**, 2018 (1949).

([9]) R. Maze: *Journ. Phys. Rad.*, **7**, 164 (1946).

([10]) B. B. Rossi and H. H. Staub: *Ionization Chambers and Counters*. National Nuclear Energy Series (New York, 1949), p. 91.

3. – Calculations.

The end position of the counter under discussion is defined to be that point at which the field strength at the centre wire drops below the minimum field strength required to produce a pulse capable of detection by the associated circuitry. We may assume that this critical field exists inside an infinitely long counter when operated at its starting voltage V'. It may further be assumed that the effective volume is limited lengthwise by a surface normal to the equipotential surfaces and containing the point on the wire at starting field strength. The boundary conditions on the inside of the counter will determine the position of this point. For the design chosen the lengthwise potential distribution on the inside surface is of the shape shown in Fig. 1 (*b*). This curve typifies the results obtained from our investigations with a dry electrolytic tank ([11]). As it has been pointed out by BLANC ([12]) this potential distribution is altered for high counting rates due to the resulting higher current through the glass envelope. No indication of such an effect was found for the counting rates used which were as high as 25 s^{-1}. For the purpose of analysis, the conditions represented by this curve are approximated to by infinitely long guard rings with a linear potential drop to the cathode potential as in Fig. 1 (*c*). The effective gap g_e is taken as $g - w$ where w is the wall thickness. The midpoint of the effective gap coincides with that of the painted gap. This is sufficiently accurate for $w < g/4$.

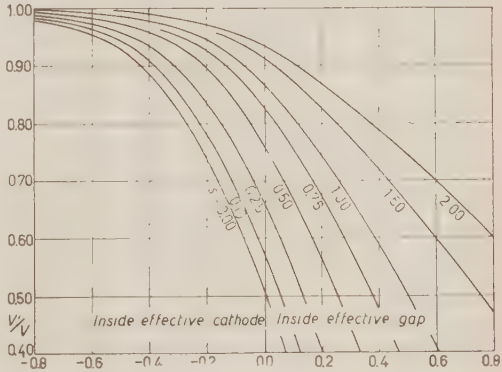

Fig. 2. Calculated end of effective volume on axis of Geiger counter. $s = g_e/d$ normalized gap length: V' starting voltage; V working voltage.

It is possible to obtain an analytical solution of the Laplace equation in terms of Bessel functions. An outline of this analysis will be found in the mathematical appendix. The relevant numerical results obtained with SILLIAC, the electronic digital computer of the Physics School of the University of Sydney are given in Fig. 2. In this figure $s = g_e/d$ and V is the working voltage. The parts of the curves not shown are centersymmetric about their intersection with $V'/V = 0.5$.

4. – Measurements.

The effective length of a counter as described was measured for various operating voltages. The counter had the following dimensions: overall length

([11]) C. T. MURRAY and D. L. HOLLWAY: *Journ. Sci. Instr.*, **32**, 481 (1955).
([12]) D. BLANC: *Journ. Phys. Rad.*, **16**, 681 (1955).

22 cm, gap 2.44 cm, external diameter 1.9 cm, wall thickness 0.5 mm. The measurements were made by passing magnetically separated 1.4 to 1.6 MeV β-particles from a ^{90}Sr ^{90}Y source in a 1 mm wide beam through the counter and normal to its axis. β-rays were chosen to avoid the uncertainty found in measurements with γ-rays ([5]) and to obtain a higher rate than that possible with cosmic rays. After passing through the counter the beam was further defined by a lead slit 1 mm wide and again detected by a thin window counter in coincidence with the first. The coincidence rate was recorded for various positions of injection into the counter. The removal of the low energy β-particles from the beam minimizes the current through the glass due to particles which fire only the first counter.

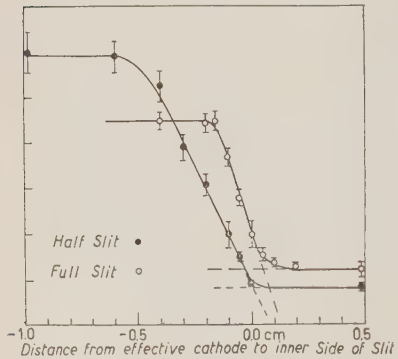

Fig. 3. Counting rate against beam position. Starting voltage V' 1040 V; working voltage V 1180 V. Errors shown are standard deviations.

The first measurements were made with quenching circuits giving 250 V pulses. When the difference between working and starting voltage became greater than the quench pulse the results became erratic. Good reproducible results were obtained for the high voltage points by using a quench pulse of 300 μs duration of height equal to the working voltage.

Measurements were made both with a 1 mm wide slit and with a « half » slit, the latter being completely open on the guard ring side. Fig. 3 shows a typical result for each slit at the same working voltage.

5. – Discussion.

The curves of coincidence rate against injection position in Fig. 3 have a common characteristic shape, namely a plateau followed by a linear falling off which then tails off gradually to a constant background level. The effective end position is obtained by extrapolating the linear fall-off to the background level and adding half the beamwidth for the full slit; the latter correction having been shown necessary by an analysis of the relationship of the counting curves with the geometry of the end surface of the effective volume and the two beams. Since it was found that the results from the half and full slit were in agreement, the remaining runs were all carried out using the half slit as a much higher coincidence rate was obtained. The comparison between the measurements and the calculated values are shown by the graph in Fig. 4. It is evident that they are in good agreement, thus justifying the assumption made for the calculations.

The linear drop in the counting rate in Fig. 3 takes place over 2 mm for the full slit. Since the run was made with a 1 mm slit, it may be assumed that in this case the longitudinal extension of the end surface is about 3 mm. This agrees within the errors with the value obtained from field plotting.

The tail in the curve is explained by diffusion of the primary electrons ([6]) which is calculated to be less than 1 mm and by δ-rays and knock on electrons produced by particles passing outside the sensitive volume. Assuming this to be so we can deduce from the extension of the tail that particles passing further than 1 to 2 mm from the sensitive volume do not contribute measurably to the counting rate.

Such an effect would not be expected at the initial falling off in the rate since particles producing countable δ-rays are themselves counted.

As far as the results of our calculations are concerned it is important to point out that the minimum variations in effective length with voltage fluctuations occur for $s < 0.5$ and $V'/V < 0.6$. It is also evident that the plateau slope of counting rate curves which is due to the increase in effective length decreases with decreasing s.

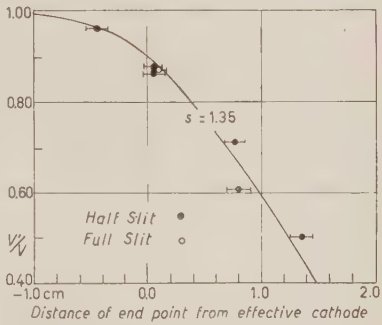

Fig. 4. – Measured and calculated end of effective volume. Errors shown are estimated errors of curve fitting.

Our results also explain the apparently conflicting measurements of BLANC ([3]) and of BAPTISTA and GALVAO ([4]). The first using relative gaps $s > 1$ finds that the endpoints of his Maze counters fall inside the gap. The second with a gap $s \sim 0.2$ obtain an effective length shorter than the cathode. Referring to our Fig. 2 and assuming that the working voltage is chosen as usual i.e. $V'/V = 0.8$ to 0.9 we see that within the limits of the information given in the papers the measurements agree with our calculations: namely that in the first case the end point falls inside the gap and in the second inside the cathode.

6. – Rules for Design.

The conditions for minimum variation of effective length considered above require a voltage ratio V'/V which is impractical in most circumstances due to either the upper limit of the plateau or the large quenching voltage required. The practical voltage ratio lies between 0.8 and 0.9. Fig. 2 shows that for $s \leqslant 0.5$ the variation of effective length is still quite acceptable. Conduction in the gap and breakdown, on the surface of the glass make it inadvisable to make the gap too small. The above conditions put the end points between 0.1 and 0.3 diameters inside the effective cathode. Variations in the diameter of the wire and its eccentricity may give rise to variations in the starting voltage along the centre wire and thus affect the design values. Consideration must also be given to possible variations in V'/V due to fluctuations in the H.T. supply or to the ageing of the counter. The maximum value which V'/V is likely to reach should be used in the above calculation.

Finally we wish to point out that all types of counters except those with field tubes are subject to the effects discussed in this paper by varying amounts.

The advantage of the present design is that the effects are known exactly and can be predicted.

* * *

We should like to thank Professor H. MESSEL for providing the excellent laboratory facilities and financial support. We are also indebted to Mr. C. MURRAY of the Department of Electrical Engineering in the University of Sydney for his help with the electrolytic tank measurements.

The work was supported by the Nuclear Research Foundation within the University of Sydney and by the Research Committee of the University of Sydney who provided a research studentship for one of us.

APPENDIX

Method of approach:

(i) Solution of the Laplace equation.
(ii) Evaluation of E at the centre wire.
(iii) Solution for the end point.

Determination of the Potential.

Since the boundaries are axially symmetric we may express Laplace's equation in the form

$$\left(\frac{\partial^2}{\partial z^2} + \frac{\partial^2}{\partial r^2} + \frac{1}{r}\frac{\partial}{\partial r}\right)\varphi = 0, \tag{1}$$

where r and z are the usual cylindrical co-ordinates.

By assuming a potential of the form

$$\varphi = \int_{-\infty}^{\infty} \mathrm{d}k\, Z(z, k)\, R(r, k)\, a(k) \tag{2}$$

it is possible to perform a separation and obtain

$$Z(z, k) = A \exp [ikz] + B \exp [-ikz] \tag{3}$$

$$R(r, k) = CJ_0(ikr) + DN_0(ikr) = Z_0(ikr) \tag{4}$$

where J_0 and N_0 are zero order Bessel functions of the first and second kinds respect-

ively. Thus

$$\varphi(r, z) = \int_{-\infty}^{\infty} dk \exp [ikz] Z_0(ikr)\, a(k) , \tag{5}$$

$a(k)$ is obtained from the boundary conditions

$$\begin{cases} \varphi(r_1, z) = 0 \\ \varphi(r_2, z) = f(z) , \end{cases} \tag{6}$$

where $f(z)$ is the potential distribution along the inside of the envelope and is plotted in Fig. 1*c*. r_1 and r_2 are the radius of the inner wire and the inside radius of the glass envelope respectively. We shall assume the boundary potential $f(z)$ to correspond to that of a semi-infinite cathode separated from a semi-infinite guard ring by a distance g_e, i.e.

$$\begin{cases} f(z) = V & -\infty < z < 0 \\ f(z) = V\left(1 - \dfrac{z}{g_e}\right) & 0 < z < g_e \\ f(z) = 0 & g_e < z < \infty . \end{cases} \tag{7}$$

The radial field component is given by

$$E_r(r, z) = -\int_{-\infty}^{\infty} dk \exp [ikz] a(k)\, Z_0(ikr) . \tag{8}$$

Defining

$$R(x, y) = J_0(ix)\, N_0(iy) - N_0(ix)\, J_0(iy) \tag{9}$$

and

$$F(k) = \int_{-\infty}^{\infty} dz \exp [-ikz] f(z) = V\{\pi\, \delta(k) + (1 - \exp [-ikg_e])/k^2 g_e\} , \tag{10}$$

Evaluation of $a(k)$ results in

$$E_r(r, z) = -\frac{1}{2\pi} \int_{-\infty}^{\infty} dk\, F(k) \exp [ikz] R'(kr, kr_1)/R(kr_2, kr_1), \tag{11}$$

where the prime indicates differentiation with respect to r.

Substituting for $F(k)$, and making use of the symmetry of $R(kx, ky)$ about $k = 0$,

this reduces at $r = r_1$ to

$$E_r(r_1, z) = E_r^{(1)}(r_1, z) + E_r^{(2)}(r_1, z)\,, \tag{12}$$

where

$$E_r^{(1)}(r_1, z) = -V/2r_1 \ln (r_2/r_1) \tag{13}$$

and

$$E_r^{(2)}(r_1, z) = -\frac{V}{l\pi^2 r_1}\int_{-\infty}^{\infty} \mathrm{d}k\, \frac{\sin k(z-l)\sin kl}{k^2 R(kr_2, kr_1)}\,, \tag{14}$$

with

$$l = g_e/2\,. \tag{15}$$

Futher since $r_1 \ll r_2$, we have to a good approximation

$$E_r^{(2)}(r_1, z) = VhI(u, s)/2\pi l \ln h\,, \tag{16}$$

where

$$\left\{\begin{aligned} u &= (z-l)/r_2 \\ s &= l/r_2 \\ h &= r_2/r_1 \\ x &= kr_2 \end{aligned}\right. \tag{17}$$

$$I(u, s) = \int_{-\infty}^{\infty} \mathrm{d}x\, \frac{\sin ux \sin sx}{x^2 I_0(x)}\,. \tag{18}$$

$I_0(x) = J_0(ix)$ is the zero order cylindrical Bessel function of the first kind. Evaluation of $I(u, s)$ by contour integration gives

$$I(u, s) = C(s) - 2\pi\sigma(u, s)\,, \tag{19}$$

where

$$\sigma(u, s) = \sum_{\alpha_r} \frac{\exp[-u\alpha_r]/\sinh(s\alpha_r)}{\alpha_r^2 J_1(\alpha_r)}\,; \tag{20}$$

α_r are the zeros of $J_0(x)$. The expansion for σ converges only for $u \geqslant s$ in which case as

$$\operatorname*{Lim}_{u\to\infty} \sigma(u, s) = 0$$

$$\operatorname*{Lim}_{u\to\infty} I(u, s) = C(s),$$

but from (14)

$$\lim_{u\to\infty} E_r^{(2)}(r_1, z) = V/2r_1 \ln h$$

$$\therefore C'(s) \quad \pi s$$

and

(21) $$I(u, s) \quad \pi[s \quad 2\sigma(u, s)] \qquad \text{for } u \quad s.$$

In the case $|u| < s$ we can interchange u and s without affecting the form of I and get

(22) $$I(u, s) = \pi[u - 2\sigma(s, u)] \qquad \text{for } |u| < s$$

and in the case of $u < -s$ we may use

$$I(u, s) \quad I(\quad u, s)$$

i.e.

(23) $$I(u, s) = -\pi[s - 2\sigma(-u, s)] \qquad \text{for } u < -s.$$

By writing

(24) $$\sigma(u, s) = \lambda(u - s) - \lambda(u+s)\,,$$

where for $p \geq 0$,

(25) $$\lambda(p) = \frac{1}{2}\sum_{\alpha_r} \frac{\exp[-p\alpha_r]}{\alpha_r^2 J_1(\alpha_r)}$$

and

(26) $$\lambda(-p) = \lambda(p) + p/2$$

we have, for all u

(27) $$\begin{cases} E_r^{(2)}(r_1 z) = (Vh/l \ln h)\left(\dfrac{s}{2} - \lambda(u - s) + \lambda u + s\right) \\ \therefore E_r(r_1, z) = -V(h/l \ln h)(\lambda(u - s) - \lambda(u + s))\,. \end{cases}$$

From the assumption that the end of the counting length is given by the position for which the field at the centre wire falls just below the minimum field strength E' capable of forming a pulse, we obtain

(28) $$E' = -V'hs/l \ln h\,,$$

where V' is the starting voltage. This follows from the fact that the field is E' when

$V = V'$ at $u = -\infty$

$$\therefore \frac{V'}{V} = \frac{\lambda(u-s) - \lambda(u+s)}{s} = \frac{\sigma(u, s)}{s} . \tag{29}$$

Solving for u gives the end point. The values of $\lambda(p)$ were evaluated using the SILLIAC.

The form of $\sigma(u, s)/s$ may be seen from Fig. 2 in which the function is plotted for various values of s.

RIASSUNTO (*)

Si espone il progetto di un Geiger di semplice costruzione e la cui lunghezza effettiva si può facilmente desumere dalla geometria e dalla tensione di funzionamento dell'apparecchio. I risultati dei calcoli e delle misure di campo si accordano. La tensione di funzionamento è scelta in modo da render minime le variazioni della lunghezza effettiva per effetto delle oscillazioni della tensione.

(*) *Traduzione a cura della Redazione.*

Interferometro per misure di precisione della velocità degli ultrasuoni nei liquidi.

A. Barone

Istituto Nazionale di Ultracustica «O. M. Corbino» - Roma

(ricevuto il 7 Gennaio 1957)

Riassunto. — Si descrive un nuovo tipo di interferometro per misure della velocità degli ultrasuoni nei liquidi. Pur valendosi di un metodo di rivelazione ottico, questo apparecchio consente la misura della velocità anche in liquidi non trasparenti. Da una discussione sulle varie cause di errore che possono influire sulla precisione delle misure, risulta che il massimo errore relativo che si può commettere è di circa $2 \cdot 10^{-4}$. Come conferma della precisione dell'interferometro, si riferisce brevemente sulle misure di velocità effettuate in alcuni liquidi.

1. – Introduzione.

L'interferometria ultracustica ha una posizione preminente nel campo della metrologia degli ultrasuoni, poichè molti dispositivi usati per la misura precisa della velocità di propagazione degli ultrasuoni nei fluidi, si basano sui fenomeni di interferenza fra due o più onde elastiche. Essi derivano, in linea di principio, dal classico tubo di Kundt.

Sostanzialmente si tratta di determinare la velocità c delle onde elastiche di frequenza f, mediante una misura esatta della lunghezza d'onda λ che è legata alle grandezze precedenti dalla ben nota relazione:

$$c = \lambda \cdot f \,.$$

Generalmente viene stabilito nel mezzo in esame un sistema di onde stazionarie dovuto all'interferenza fra due gruppi di onde piane progressive di egual direzione, procedenti in verso contrario. Tale sistema di onde prende origine nel mezzo interposto fra una sorgente ultrasonora — di solito una piastra di quarzo piezoelettrico — ed un riflettore ad essa affacciato, quando

quest'ultimo è situato ad una distanza D pari ad un numero intero n di semilunghezze d'onda:

$$D = n\lambda/2 .$$

Se il mezzo di propagazione è un liquido otticamente trasparente, visualizzando il campo ultrasonoro secondo il metodo di Hiedemann [1], si ottiene, su uno schermo di proiezione, l'immagine delle onde stazionarie. Questa si presenta sullo schermo come mostra la fotografia di Fig. 1.

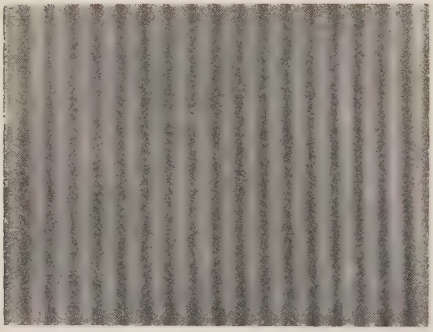

Fig. 1. Immagine di onde stazionarie in un liquido.

Le linee chiare su fondo scuro corrispondono ai massimi di variazione di pressione dell'onda stazionaria che nel liquido sono distanziati di mezza lunghezza d'onda gli uni dagli altri.

Si può allora determinare la lunghezza d'onda spostando nella direzione di propagazione il recipiente che contiene il liquido percorso dalle onde e traguardando su una linea di riferimento, tracciata sullo schermo, un certo numero n di immagini delle onde stazionarie. Il corrispondente spostamento S può essere misurato con buona precisione e la lunghezza d'onda sarà data da: $\lambda = 2S/n$.

Un utile perfezionamento di questo metodo introdotto da A. Giacomini [2] consiste nella sostituzione del sistema di onde stazionarie — ottenuto mediante il riflettore — con due fasci di onde progressive di egual frequenza ed intensità moventi in senso opposto ed aventi gli assi paralleli, ma non coincidenti. In tal modo essi sono attraversati dalla luce, uno dopo l'altro, ma gli effetti ottici che ne derivano danno luogo ad immagini di interferenza perfettamente identiche a quelle ottenute con le onde stazionarie [3]. Si elimina così la difficoltà di ricercare la particolare posizione del riflettore che dia luogo al regime stazionario.

Se poi il mezzo in esame non è trasparente, si ricorre allo spostamento del riflettore in direzione della sorgente ultrasonora in modo da stabilire successivamente le condizioni adatte alla formazione delle onde stazionarie [4]. Queste vengono indicate dalle variazioni della corrente di alta frequenza che alimenta il quarzo, dato che l'onda stazionaria reagisce fortemente sulla sorgente ultrasonora.

I dispositivi a rivelazione ottica sono più sensibili degli altri, ma, in generale, la precisione dei vari metodi citati non supera l'uno per mille.

[1] C. H. Bachem, E. Hiedemann e H. R. Aslach: *Zeits. f. Phys.*, **87**, 734 (1934).
[2] A. Giacomini: *Rend. Acc. Naz. Lincei*, **2**, 791 (1947).
[3] R. Bär: *Helv. Phys. Acta*, **9**, 678 (1936).
[4] G. W. Pierce: *Proc. Am. Acad.*, **60**, 269 (1925); J. C. Hubbard e A. L. Loomis: *Phil. Mag.*, **5**, 1177 (1928); E. Klein e W. D. Hershberger: *Phys. Rev.*, **37**, 760 (1931).

Il metodo che si vuole qui illustrare si vale anch'esso dei fenomeni di interferenza che accompagnano la propagazione di due onde ultrasonore, ma si discosta sensibilmente da quelli fondati sui principi già descritti, sia per il particolare tipo di interferenza, sia per il metodo di rivelazione. Esso inoltre appare atto a conseguire una precisione di misura di qualche unità su diecimila.

2. – Principio di funzionamento.

Due fasci di onde ultrasonore piane, di egual frequenza ed intensità, che si propagano nello stesso verso secondo due direzioni formanti un piccolo angolo α tra loro, danno luogo a nette righe di interferenza rettilinee e parallele, orientate secondo la direzione della bisettrice dell'angolo formato dai due fasci. La distanza D fra una riga e l'altra è determinata dall'angolo α e dalla lunghezza d'onda λ dell'ultrasuono nel mezzo, secondo la relazione:

$$D = \lambda/2[\sin(\alpha/2)]^{-1}. \tag{1}$$

Tale situazione è posta in chiara evidenza nella Fig. 2. I due fasci ultrasonori procedono nelle direzioni a e b. L'insieme di linee continue e tratteggiate rappresenta le sezioni dei fronti d'onda rispettivamente nelle due fasi opposte di massima e di minima pressione. Nelle intersezioni fra un fronte d'onda di massima ed un fronte d'onda di minima pressione ha luogo l'interferenza che annulla gli effetti delle due onde ultrasonore. La traccia di tali zone di interferenza è indicata in figura dalle linee doppie congiungenti i punti di intersezione fra le tracce dei fronti d'onda di fase opposta.

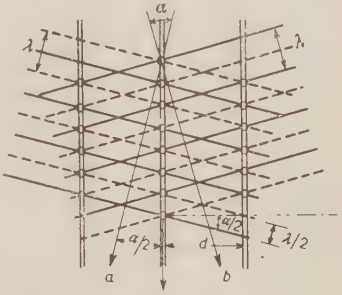

Fig. 2. - Schema delle interferenze.

È evidente che la posizione delle righe di interferenza permane invariata nel tempo, poichè, nel propagarsi, le due onde mantengono costanti in ogni punto le relazioni fra le fasi e quindi anche le opposizioni restano localizzate sempre nelle medesime regioni. Ciò peraltro non avviene nel caso in cui le onde, pur propagandosi in direzioni eguali alle precedenti, abbiano verso opposto.

Con il metodo delle strie che consiste, come è noto, nell'utilizzare la luce diffratta dal campo ultrasonoro per ottenere una immagine di questo, si possono rendere chiaramente visibili le figure di interferenza. Naturalmente la propagazione deve avvenire in un liquido trasparente e il piano individuato dagli assi dei due fasci ultrasonori deve risultare perpendicolare all'asse del sistema ottico di visualizzazione.

La Fig. 3*a* riporta un'immagine fotografica di questo genere. Nella Fig. 3*b* è lo schema della disposizione sperimentale. I due quarzi (Q_1) e (Q_2), immersi in un liquido trasparente e isolante, sono disposti uno di fronte all'altro con le superficie emittenti leggermente inclinate nel piano della figura. Essi sono alimentati alla stessa frequenza e ciascuno è libero di emettere dalle due facce opposte due fasci di ultrasuoni.

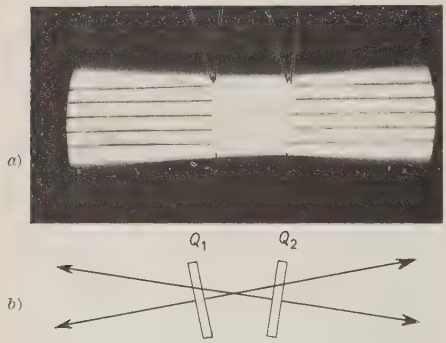

Fig. 3. – *a*) Righe di interferenza ottenute con due quarzi. *b*) Schema della disposizione sperimentale.

Nelle regioni che si trovano ai lati della coppia di quarzi, i due fasci ultrasonori si incontrano proprio nelle circostanze adatte alla manifestazione dei particolari fenomeni di interferenza sin qui esaminati.

Una disposizione più semplice può essere attuata con un solo quarzo generatore di ultrasuoni (Q), disponendo di fronte ad esso il riflettore (R) che invii il fascio riflesso verso la parte opposta del quarzo per interferire con l'altro fascio ultrasonoro emesso ivi direttamente. L'immagine delle figure di interferenza ed il relativo schema sono riportati rispettivamente nelle Fig. 4*a* e 4*b*.

Su questa ultima disposizione sperimentale è basato il funzionamento dell'interferometro. Se infatti il riflettore, mantenendo costante il proprio orientamento, viene spostato lungo l'asse centrale del quarzo, le linee di interferenza nella regione a destra di questo, si spostano parallelamente a loro stesse in un verso o nell'altro, a seconda che il riflettore si avvicini al quarzo o se ne allontani. Ogni qualvolta però il fascio riflesso risulta spostato di una lunghezza d'onda, le interferenze assumono di nuovo le medesime posizioni poichè la fase relativa è variata di 2π. Così, spostando il riflettore di mezza l'unghezza d'onda, le righe di interferenza riprendono la stessa posizione.

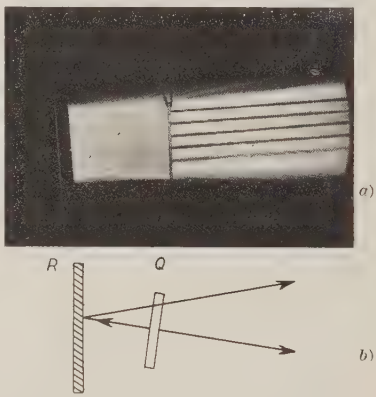

Fig. 4. – *a*) Righe di interferenza ottenute con un solo quarzo. *b*) Schema della disposizione sperimentale.

Siffatto comportamento del campo ultrasonoro, consente la misura della lunghezza d'onda nel mezzo interposto fra quarzo e riflettore e quindi della velocità quando sia nota la frequenza dell'ultrasuono.

La semilunghezza d'onda nel liquido in esame è data infatti dal valore dello spostamento del riflettore cui corrisponde, nella figura di interferenza, il passaggio da una riga alla successiva.

3. – Descrizione.

La Fig. 5 riporta la sezione schematica dell'interferometro. La lamina di quarzo (Q) costituisce il fondo del recipiente superiore che contiene il liquido da esaminare (X). Nell'interno del recipiente è situato il riflettore (R) sposta-

bile in direzione del quarzo mediante una vite (*S*). Un micrometro-comparatore di precisione (*M*) il cui gambo è appoggiato sull'asse (*D*) del riflettore, ne misura lo spostamento.

La superficie riflettente di (*R*) può essere inclinata di un piccolo angolo mediante un'altra vite (*V*) manovrata dall'esterno. Il recipiente sottostante contiene, fino ad un livello tale da bagnare la faccia inferiore del quarzo, un liquido trasparente (*Y*) nel quale il fascio di ultrasuoni emesso dalla faccia inferiore del quarzo interferisce con quello riflesso da (*R*). Quest'ultimo attraversa senza sensibile attenuazione la lamina di quarzo, essendo essa perfettamente trasparente all'onda elastica per via del suo spessore che, ovviamente, è pari a mezza lunghezza d'onda.

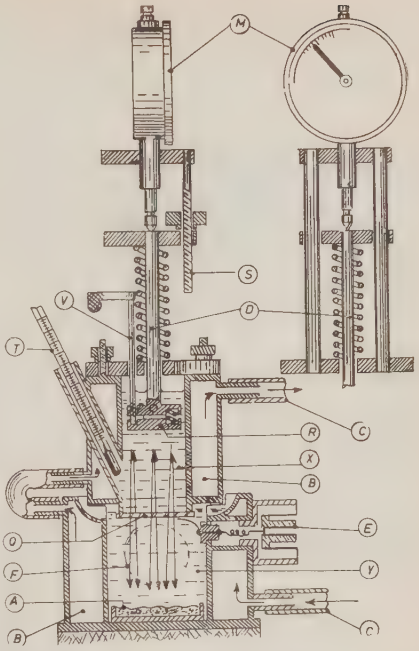

Fig. 5. Sezione schematica dell'interferometro.

Per rendere visibili le righe di interferenza che prendono origine nel liquido situato al disotto del quarzo, ci si vale, come si è detto, del metodo delle strie. A tale scopo il recipiente inferiore porta due finestre di vetro affacciate che consentono il passaggio di un fascio di luce parallela in direzione ortogonale al piano individuato dai due fasci ultrasonori interferenti.

La traccia di queste finestre è rappresentata nella figura dal cerchio tratteggiato (*F*). Sul fondo del recipiente è disposto uno strato (*A*) di materiale assorbente delle onde ultrasonore — lana di vetro o lana minerale — avente

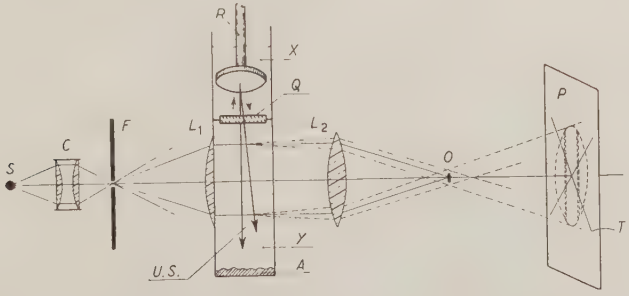

Fig. 6. - Schema della disposizione ottica di visualizzazione: *S* sorgente, *C* condensatore. *F* diaframma, L_1 L_2 lenti convergenti, *X* liquido in esame, *Y* liquido di visualizzazione, *R* riflettore. *Q* quarzo, *U.S.* fasci ultrasonori, *A* assorbitore, *O* ostacolo per la luce non diffratta, *P* schermo di proiezione, *T* traguardo.

lo scopo di eliminare le riflessioni degli ultrasuoni che potrebbero deformare l'immagine delle righe di interferenza.

Lo schema di Fig. 6 riporta la disposizione ottica di visualizzazione secondo il principio sopra menzionato. L'immagine che si ottiene, si presenta sullo schermo come nella fotografia di Fig. 7. Traguardando un certo numero n di queste righe attraverso una linea di riferimento tracciata sullo schermo, si ottiene il valore della velocità degli ultrasuoni:

Fig. 7. – Immagine delle righe di interferenza generate nell'apparecchio.

$$c = \lambda f = \frac{2Sf}{n}, \qquad (2)$$

essendo f il valore della frequenza usata. S è in questo caso lo spostamento totale del riflettore.

Il piccolo spessore delle righe paragonato con la distanza fra due righe successive, può dare un'idea della maggior sensibilità di questo metodo rispetto agli altri metodi ottici.

Lo spessore delle righe dipende, in larga misura, dall'intensità degli ultrasuoni emessi dalla sorgente sicchè, entro certi limiti, possiamo ottenere delle righe sottilissime.

Poichè il controllo della temperatura è fondamentale nelle misure della velocità degli ultrasuoni, tutto l'interferometro è mantenuto alla temperatura voluta mediante circolazione di acqua proveniente da un termostato esterno munito di adeguati controlli termici.

Il liquido termostatico circola attraverso i condotti (C) (vedi Fig. 5) in una intercapedine (B) compresa fra le due pareti che costituiscono l'involucro esterno dell'interferometro.

La temperatura del liquido in esame è misurata da un termometro a mercurio (T) il cui gambo, passando per un condotto praticato nella doppia parete superiore, risulta immerso direttamente in questo liquido.

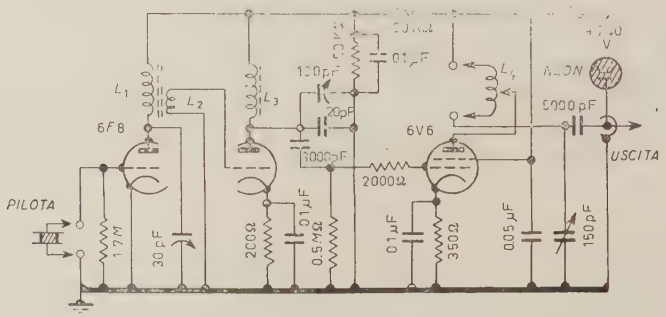

Fig. 8. – Schema del circuito elettrico del generatore.

La tensione di alta frequenza che alimenta, attraverso la presa schermata (E), la piastra di quarzo, è fornita da un generatore elettrico il cui schema è riprodotto in Fig. 8. È un oscillatore pilotato da un cristallo di quarzo, seguito da due stadi di amplificazione accordati. In tal modo resta garantita la stabilità

Fig. 9. Fotografia dell'interferometro.

della frequenza che, d'altra parte, è anche perfettamente nota. Nel modello descritto, la frequenza è di 4 MHz, ma l'apparecchio può funzionare egualmente in una vasta gamma, da ca. 1 MHz fino a frequenze di alcune decine di MHz.

Il limite inferiore di frequenza è imposto dal metodo di visualizzazione mentre il limite superiore dipende dall'assorbimento dei liquidi attraversati dagli ultrasuoni che può raggiungere valori eccessivi a frequenze molto elevate.

La fotografia di Fig. 9 mostra l'aspetto esteriore dell'interferometro.

4. – Precisione delle misure.

Una delle principali caratteristiche di questo interferometro è quella di poter fruire di un metodo ottico, notoriamente molto sensibile, per misure di velocità anche in liquidi non trasparenti. Inoltre le immagini delle righe di interferenza sono nitide e sottili e possono essere mantenute sufficientemente distanti fra loro alle più alte frequenze, cosa impossibile ad ottenersi se si utilizzano invece le onde stazionarie.

In generale la precisione dei metodi interferometrici dipende:

1) dal numero di semilunghezze d'onda contate e quindi dallo spostamento totale del riflettore;

2) dalla precisione meccanica del dispositivo di misura dello spostamento;

3) dal rapporto fra la larghezza di ogni singola riga di interferenza e la distanza che separa fra loro le righe;

4) dalla perfezione dei controlli termici e dalla influenza che ogni eventuale variazione incontrollata di temperatura può avere sul risultato finale della misura.

Riferendoci all'attuale interferometro ci si propone di indicare brevemente l'entità di possibili errori dovuti alle cause sopra elencate.

Per quanto riguarda le prime tre cause, l'errore può essere introdotto da imprecisione (ΔS) nella valutazione dello spostamento S del riflettore e da incerto puntamento, attraverso la linea di riferimento sullo schermo, della prima ed ultima riga di interferenza.

Tale incertezza introduce un errore Δn nel numero n delle righe contate.

Così dalla (2) risulta un errore assoluto per la velocità pari a:

$$\Delta c = \frac{2f}{n^2}(n\,\Delta S \mp S\,\Delta n)\,,$$

dove la frequenza f è considerata costante e nota.

L'errore relativo sarà quindi:

$$\frac{\Delta c}{c} = \frac{\Delta S}{S} \mp \frac{\Delta n}{n}\,. \tag{3}$$

I due segni, negativo e positivo, tengono conto della eventualità che i due errori siano alternativamente in eccesso e in difetto, ovvero concomitanti.

Nel nostro apparecchio, la corsa utile S del riflettore è 2 cm. L'errore ΔS è inferiore a $\pm$ 1 μ poichè il quadrante del comparatore centesimale, per la sua notevole dimensione, permette di valutare facilmente il quarto di divisione (2.5 μ). D'altra parte, alla frequenza usata di 1 MHz, per liquidi in cui la velocità è compresa fra ca. 1000 e 1500 m/s, il numero di semilunghezze d'onda contenuto nella corsa del riflettore, è certamente $n > 100$. Inoltre il possibile scarto Δn dovuto all'inesatto puntamento della riga, può essere compreso, come si può constatare dalla Fig. 7, entro 1/100 della distanza fra due righe.

Sostituendo allora questi valori nella (3) si ha per l'errore relativo della velocità:

$$\frac{\Delta c}{c} = 10^{-4} \mp 10^{-4} .$$

Al massimo, quindi, l'errore sarà di $2 \cdot 10^{-4}$.

Occorre adesso tener conto della quarta causa di errore, cioè della fluttuazione di temperatura che può aver luogo durante le operazioni di misura. Essa produce effetti sulla propagazione delle onde, sia nel liquido sottoposto a misura, sia in quello di visualizzazione, dando origine ad uno spostamento delle righe di interferenza.

Consideriamo gli effetti separatamente nei due liquidi. In quello di visualizzazione, il coefficiente di temperatura per la velocità x è noto. Ad ogni incremento $d\tau$ della temperatura corrisponderà un incremento di velocità degli ultrasuoni: $dc = x\, d\tau$.

Se x è costante, la velocità c viene espressa, in funzione della temperatura, dalla relazione:

$$c = x\tau + c_0 ,$$

ottenuta per integrazione. c_0 rappresenta la velocità alla temperatura cui viene riferito il valore di τ.

La distanza D fra due successive righe sarà allora $D = A + B\tau$, con A e B costanti e per la (1):

$$A = \frac{c_0}{2f \sin(\alpha/2)} , \quad B = \frac{x}{2f \sin(\alpha/2)} .$$

Qualora la temperatura non si mantenga costante ad ogni passaggio di riga, potremo porre $\tau = \varphi(i)$, essendo i il numero d'ordine della riga d'interferenza traguardata. D'altra parte lo spostamento totale S del riflettore misurato dal comparatore, è proporzionale alla somma delle successive distanze fra le righe: $S = k \sum_{i=0}^{n} D_i$, dove $D_i = A + B\varphi(i)$, e k dipende dall'ingrandimento ottico del sistema di visualizzazione.

Se durante le operazioni di misura la temperatura varia linearmente con i, come del resto è lecito supporre data la uniformità di spostamento del riflettore e la regolarità di funzionamento del termostato, il valore di $\sum$ sarà eguale al valor medio di D moltiplicato per il numero totale n delle righe traguardate.

Da cui:

$$S = kn\left(A + B\frac{\tau_n}{2}\right),$$

essendo τ_n la variazione di temperatura fra l'inizio e la fine della misura.

Indicando con $S_0 = knA$ lo spostamento totale del riflettore nel caso in cui la temperatura non fosse cambiata, la variazione relativa dello spostamento per uno scarto di temperatura τ_n sarà:

$$\frac{S - S_0}{S_0} = \frac{\Delta S}{S_0} = \frac{x\tau_n}{2c_0},$$

ovvero

$$S_0 = S\left(\frac{x\tau_n}{2c_0} + 1\right)^{-1}. \tag{4}$$

Per ogni eventuale variazione di temperatura, la (4) fornisce il fattore di correzione per lo spostamento misurato S.

Peraltro, non tenendo conto di questa correzione, l'errore relativo $\Delta S/S_0$ che si potrebbe commettere nella determinazione dello spostamento del riflettore, risulterebbe circa $3.5 \cdot 10^{-5}$, avendo assunto

$$\frac{x}{c_0} \approx 1.4 \cdot 10^{-3}\ °C^{-1}, \qquad \tau_n \approx 0.05\ °C.$$

Per quanto riguarda la determinazione dell'errore dovuto agli effetti della variazione di temperatura nel liquido in esame, vi è la difficoltà che in questo caso il coefficiente di temperatura per la velocità non è noto.

Una correzione diretta dei risultati non è quindi possibile, ma l'ordine di grandezza dell'errore potrebbe essere facilmente dedotto assegnando i limiti approssimati entro i quali è compreso il coefficiente di temperatura dei liquidi in generale.

In tal caso, per velocità di ca. $1\,000 \div 1\,500\ m \cdot s^{-1}$ uno scarto di temperatura di 0.05 °C darebbe luogo ad un errore relativo non superiore a 10^{-4} qualora si fosse assunta come temperatura del liquido la media fra i valori all'inizio e al termine di ogni misura. Tale errore andrebbe aggiunto a quello calcolato per il liquido di visualizzazione.

Queste considerazioni danno un'idea degli errori massimi che si possono commettere con una sola operazione di misura, ma è facile constatare che l'apparecchio è in grado di fornire una precisione maggiore perchè, con due o più operazioni di misura, si possono ottenere risultati pressochè indipendenti dalle variazioni di temperatura.

Con più di una determinazione il puntamento sia della prima che ultima riga di interferenza può essere infatti riferito alla medesima temperatura.

In generale la temperatura del liquido aumenta quando il riflettore si allontana dalla sorgente perchè la capacità termica della parte interna dell'interferometro diminuisce mentre il calore rifornito rimane all'incirca costante.

Pertanto, quando la prima riga traguardata è quella che corrisponde alla

posizione del riflettore più vicina alla sorgente, il puntamento dell'ultima riga (n-ma) risulterà effettuato ad una temperatura leggermente più alta.

Se ora il puntamento della prima riga, anzichè ad una sola temperatura viene fatto a due temperature diverse (variando le condizioni di termostatazione), sarà facile ottenere per interpolazione o estrapolazione, la posizione che questa riga occuperebbe alla temperatura alla quale è stata tragnardata la riga n-ma.

Per lo studio delle proprietà molecolari di un liquido occorre di solito che le misure di velocità delle onde elastiche siano fatte in un ampio intervallo di temperatura sicchè il procedimento descritto non introduce nuove difficoltà nel metodo di misura.

Altra causa d'errore potrebbe aversi nell'eventuale presenza d'un gradiente termico in seno alla massa liquida percorsa dalle onde ultrasonore. Una valutazione quantitativa appare difficile, ma l'effetto può considerarsi trascurabile di fronte agli altri errori quando si abbia cura di iniziare le misure dopo un certo tempo che l'apparecchiatura è in funzione, in modo da ritenere che l'equilibrio termico di ogni parte dell'interferometro sia adeguatamente raggiunto.

Riassumendo le precedenti considerazioni, possiamo concludere che la causa principale di errore resta ancora legata alla sensibilità del dispositivo di misura dello spostamento del riflettore. Come si è visto, essa può introdurre nella velocità misurata un errore relativo massimo di ca. $2 \cdot 10^{-4}$. Tutti gli altri possibili errori presi insieme, danno origine ad un effetto del secondo ordine rispetto a questo valore.

5. – Conferme sperimentali.

Una diretta conferma di quanto è stato detto sulla precisione di questo metodo, si è avuta nei risultati sperimentali.

Si è potuto, ad esempio, mettere in evidenza una anomalia nella velocità di propagazione degli ultrasuoni in alcuni liquidi sopraffusi ([5]). Il coefficiente di temperatura per le velocità è, nella regione di sopraffusione, leggermente superiore al normale. In generale, in questa regione, le deviazioni della velocità dai valori previsti dalla legge di linearità valevole al disopra del punto di fusione, sono, in un ampio intervallo di temperatura, inferiori all'1‰. L'anomalia è stata attribuita alla formazione di associazioni molecolari.

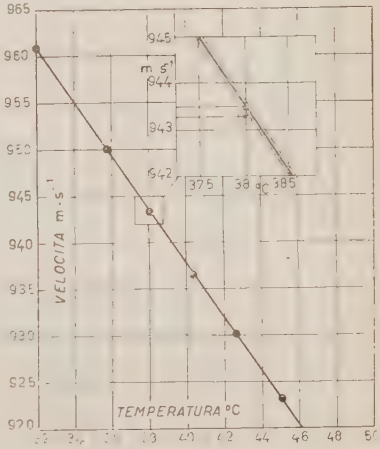

Fig. 10. Velocità degli ultrasuoni in un silicone (frequenza 4 MHz).

([5]) A. Barone, G. Pisent e D. Sette: *Ultrasonic Velocity in Supercooled Liquids*, Relazione presentata al II Congresso Internazionale di Acustica, Cambridge, Mass., Giugno 1956.

Inoltre è stata iniziata una ricerca su alcuni polimeri liquidi, che ci si propone di portare a termine fra breve e, come ulteriore esempio dimostrativo delle possibilità dell'interferometro, riportiamo le misure di velocità in un dimetil polisiloesano (silicone) (*), in funzione della temperatura.

Come si vede nel grafico di Fig. 10, la dispersione dei valori misurati è molto piccola. Per precisarne l'entità, nel particolare riportato in un lato della figura, sono state espanse fortemente le due scale degli assi coordinati intorno ad un punto che presenta il maggiore scarto rispetto alla retta tracciata mediando i valori della velocità.

Si nota che lo scarto è di circa $0.20\,\mathrm{m}\cdot\mathrm{s}^{-1}$. L'errore relativo è quindi in accordo con quanto era stato previsto nelle considerazioni generali sulla precisione delle misure.

(*) Fluido DC 200/10 della Dow Corning Co.

SUMMARY (*)

Presentation of a new type of interferometer for the measurement of the velocity of ultrasounds in liquids. Although it employs an optical method of revelation this apparatus allows to measure velocity also in non-transparent liquids. From a discussion on the different causes of error which may affect the precision of measurement results that the greatest relative error which can be made is about $2\cdot10^{-4}$. As a proof of the precision of the interferometer a short report is given on velocity measures performed in some liquids.

(*) *Traduzione a cura della Redazione.*

LETTERE ALLA REDAZIONE

(La responsabilità scientifica degli scritti inseriti in questa rubrica è completamente lasciata dalla Direzione del periodico ai singoli autori)

On the Spin of the $K_{\mu 3}$ Meson.

L. A. Radicati and S. Rosati

Istituto di Fisica dell'Università - Pisa

(ricevuto il 19 Dicembre 1956)

The information about the spins and parities of the K-mesons, is, at present, restricted to the τ- and θ-mesons. Though the experimental evidence is not yet absolutely conclusive, it seems fairly likely that the spin of the τ-meson should be zero and its parity odd; under the simplest assumptions, the spin of the θ-meson is zero with even parity.

It would be interesting to know if also the K-mesons that undergo a light particle decay, have spin zero, to ascertain if they represent alternative modes of decay of unique spin zero particle, which would either decay by processes violating parity conservation [1], or would exist in two states with opposite parity [2].

The purpose of this letter is to present the results of our calculation on the momentum spectrum of the μ-meson which results from the decay mode

$$K_{\mu 3} \to \pi + \mu + \nu \,. \tag{1}$$

The measurement of this spectrum would allow in principle to determine the spin of the $K_{\mu 3}$ meson, without telling however anything about its parity.

To calculate the momentum spectrum we shall assume that only one coupling is effective. Moreover we shall assume that the same coupling is also responsible for the $K_{\mu 2}$ decay. Under these assumptions the matrix element for the decay at rest of a K-meson with spin j is

$$M = g \cdot \overline{\psi}(p) \cdot 0 \cdot \varphi(q) \cdot \Phi(p+q) \cdot f_l(p+q) \,, \tag{2}$$

where $\psi(p)$, $\varphi(q)$ and $\Phi(p+q)$ are the lepton and π-meson field operators; 0 and f_l are tensors whose rank depends on j and on the type of coupling; g is the coupling constant; finally p and q are the momenta of the light particles.

We shall assume in the following that the operator 0 depends only on the Dirac matrices, excluding in this way, amongst other possibilities, also the existence of derivative couplings. This assumption is based on the analogy with the β-decay interaction, but cannot be justified on any a priori arguments.

By using standard methods, one can calculate the momentum spectrum of the μ-meson: the result is of the form

$$P(p)\,\mathrm{d}p = F_l^{(j)}(p) + \lambda G_l^{(j)}(p) \,,$$

where $F_l^{(j)}$ and $G_l^{(j)}$ are complicated functions depending on the spin j of the

(1) T. D. Lee and C. N. Yang: *Phys. Rev.*, **104**, 254 (1956).

(2) T. D. Lee and C. N. Yang: *Phys. Rev.*, **102**, 290 (1956).

K-meson and on the rank of the tensor $f_l(p+q)$; λ is a number which depends on the type of coupling: its values are well known from the β-decay theory.

Instead of giving the explicit expressions for $F_l^{(j)}$ and $G_l^{(j)}$ we have drawn a fairly accurate determination of the spectrum.

The experimental knowledge of the momentum spectrum is still very scanty. The analysis of RITSON *et al.* [3], seems to show that the number of low momentum μ-mesons is larger than predicted by the statistical factor alone.

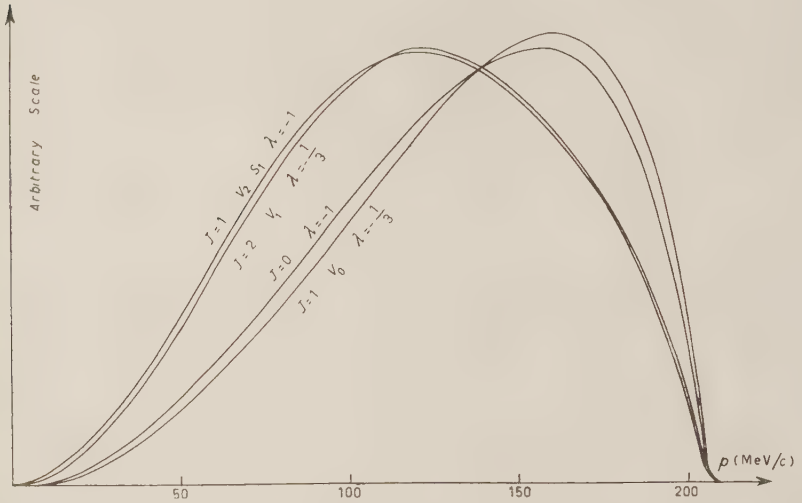

Fig. 1. – Momentum spectrum of the μ meson. V_0, V_1, V_2, S_1 mean vector and scalar interactions with $l = 0, 1, 2$. The mass of the $K_{\mu 3}$ mesons has been taken equal to 966 m_e.

In Fig. 1 the momentum spectrum of the μ-meson which obtains for spin zero and one.

In Fig. 2 the spectrum corresponding to spin zero, is compared with the statistical factor.

For spin two, only the curve corresponding to vector coupling with $l=1$ is reported (see Fig. 1).

The other couplings give rise to spectra whose maxima are deplaced towards the low momentum and are therefore even more different from the one corresponding to spin zero.

It thus appears possible in principle to determine whether the spin of the $K_{\mu 3}$-meson, is zero. In practice, however, the distinction between spin zero and spin one with vector coupling, requires

If this result were confirmed, it would be an indication that the spin of the $K_{\mu 3}$-meson is larger than zero [4]. Spin one with vector coupling and $l=0$ would be also excluded. It would still require fairly accurate measurements to decide between spin one and two and between the different couplings.

Amongst the possible couplings corresponding to spin one, the vector coupling with $l = 2(V_2)$ can perhaps be

[3] D. M. RITSON *et al.*: *Phys. Rev.*, **101**. 1085 (1956).

[4] This is true as long as the assumptions on which (2) is based are valid. In particular it is no longer true if one allows for the possibility of a tensor coupling.

ruled out on the basis of the essential equality between the lifetimes of the $K_{\mu 3}$ and $K_{\beta 3}$ decays [5].

Indeed one can easily prove by an

It must be borne in mind, however, that this argument rests on the assumption that the coupling between K-mesons and electrons or μ-mesons,

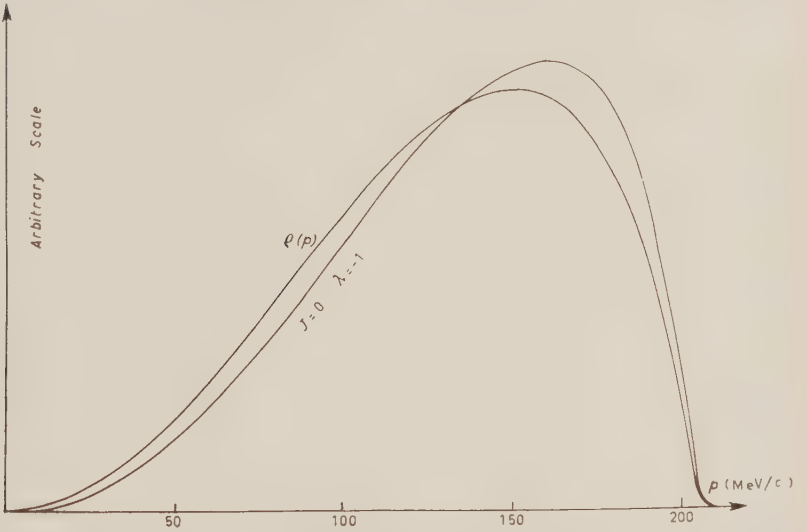

Fig. 2. – Comparison between the statistical factor $\varrho(p)$ and the momentum spectrum for $J = 0$.

argument which closely parallels the discussion of MYAZAWA and OEHME for the two body decay of a spin zero boson [6], that for vector and pseudovector couplings, the ratio between the two lifetimes is

$$\frac{\tau^{K}_{\beta 3}}{\tau_{K\mu 3}} \sim \left(\frac{\text{electron mass}}{\mu\text{-meson mass}}\right)^2 .$$

should be the same: whether this assumption is true, remains still an open question.

More detailed calculations will be published shortly, along with the angular correlations between the direction of emission of the μ-meson and the charged light particle. These angular correlation curves may be of interest especially for the decay of the neutral $K_{\mu 3}$ and $K_{\beta 3}$ of which a few cases have recently been reported in the literature.

[5] T. F. HOANG, M. F. KAPLON and G. YEKUTIELI: Private communication.

[6] H. MIYAZAWA and R. OEHME: *Phys. Rev.*, **89**, 316 (1955).

Electromagnetic Properties of Nucleons and Barion-Heavy Meson Interactions.

B. Vitale

Istituto di Fisica dell'Università - Catania
Centro Siciliano di Fisica Nucleare - Catania

(ricevuto il 19 Dicembre 1956)

The electromagnetic (e.m.) properties of the pion cloud of physical nucleons, calculated by fixed source techniques, do not fully justify the observed « anomalous » e.m. properties of nucleons (anomalous magnetic moment, intrinsic interaction constant ε_1) ([1,2]). The contribution of the pion cloud to the anomalous magnetic moment results of the right sign both for proton and for neutron but slightly greater than the experimental value; the low energy neutron-electron (n-e) interaction, described through a conventional potential V^0 with radius equal to the classical electron radius, results at least 20 times too large.

Fixed source calculations are made on a model where the core of the physical nucleon is assumed to be a Dirac particle without « anomalous » interactions. As we have no reasons to assume so, results previously quoted cannot be supposed to indicate shortcomings of the fixed source theory; we know that nucleons interact with heavy mesons and that this interaction will determine a structure of the core that can modify the e.m. properties both of the pion cloud and of the core. It seems therefore more consistent with our knowledge to consider the core as a complex system bearing some intrinsic anomalous magnetic moment and ε_1; we have then two constants more to introduce into our phenomenological description.

Sandri gave the first indication that a K-meson cloud forming a sort of internal shell around the core can contribute to the n-e interaction and add its contribution with opposite sign to the pion cloud contribution ([3]). The latter is supposed to be not modified by the presence of the K-meson cloud; using a coupling constant for K-nucleon interaction not in disagreement with our scant information on K-nucleon scattering he found that the total n-e interaction can be brought to a better agreement with experiments.

It seems doubtful that the nucleon can be described as a set of independent shells with a central Dirac particle with no « anomalous » interactions; the problem

([1]) For the anomalous magnetic moment: H. Miyazawa: *Phys. Rev.*, **101**, 1564 (1956); S. Fubini: *Nuovo Cimento*, **3**, 1425 (1956).

([2]) For the intrinsic n-e interaction: G. Salzman: *Phys. Rev.*, **99**, 973 (1955); S. B. Treiman and R. G. Sachs: *Phys. Rev.*, **103**, 434 (1956).

([3]) G. Sandri: *Phys. Rev.*, **101**, 1616 (1956).

of the e.m. properties of the nucleon, when barion-heavy meson interactions are present, has to be analysed therefore in the spirit of a more realistic model. We can picture this model in the following way.

The pion field is coupled to a heavy particle that interacts with an external e.m. field as a « Foldy » particle ([4]); an anomalous magnetic moment (together with the Dirac magnetic moment for the charged case) and an intrinsic ε_1 shall be associated with this particle that we shall call in the following C. C determines through its properties and the characteristics of its interaction with the pion field the structure of the associated pion cloud. The « anomalous » constants of C could be found out either by analysing simple models for the structure of C, or by taking the difference between the experimental values and those corresponding to the pion cloud contributions.

The first method has been the one used by SANDRI ([3]); the second one does not seem very useful in practice, as it shifts the problem from a known structure (pion cloud) to an unknown one (K-meson cloud) and substitutes to our ignorance two empirically determined parameters. It could be however of interest to verify if the modifications of the e.m. properties of the pion cloud due to the presence of hyperons and K-mesons in C can take into account alone the observed discrepancies between fixed source results and experimental data. It if turns to be so we shall be able to conclude that the contributions of the structure of C (K-meson cloud anomalous properties of hyperons, and so on) to the e.m. properties of the physical nucleon are small enough to be disregarded.

In order to calculate the exact nature of the modifications to be expected in the pion cloud we should have much wider knowledge on the nature and interactions of K-mesons and hyperons than we have; we lack in particular any information about pion-hyperon interaction. We shall try and guess the order of magnitude of such modifications in the extreme assumption:

$$f^2_{B-\pi} \gg f^2_{B-K}\,, \tag{1}$$

where the f^2 are coupling constants and B refers to barions.

We suppose therefore that the number of elementary processes of pion emission and absorption between two processes of emission or absorption of a K is so high that we can speak in each case (nucleon and hyperon) of an equilibrium cloud around the barion. We shall disregard in the following processes connecting different types of barions.

Because of the finite rest mass of K-mesons, virtual K-hyperon states have a very short life, of the order of 10^{-24} s; of the same order of magnitude, therefore, as the time of flight of a pion through the interaction volume, rising doubts on the equilibrium hypothesis. On the other hand we have some indication that the coupling of K with barions is smaller than that of pions with barions; the model previously described can perhaps give some indications that would not be qualitatively altered by a more realistic approach.

As a consequence of (1), states with more than one K can be disregarded as very improbable; then K, that can be present in the K-cloud only with an equal or greater number of K's, will not contribute at all. Only K^+ and K^0 will contribute and the physical states between which expectation values have to be taken are

([4]) L. L. FOLDY: *Phys. Rev.*, **87**, 688 (1952).

limited to positive and neutral hyperon states (for physical proton) and to neutral and negative states (for physical neutron). The relative proportions of charged and neutral hyperons will be determined assuming isobaric spin (i-spin) conservation in barion-heavy meson interactions.

Let us now disregard for simplicity Λ^0 hyperons; intermediate hyperons will be only Σ particles. If we disregard also pair production from pions and heavy mesons conservation of barions limits to zero or one the number of Σ present in C. We assume the Σ to have spin $\frac{1}{2}$, without assigning their parity with respect to nucleons: if K-mesons are emitted and absorbed in and from states with the lowest orbital momentum compatible with parity and angular momentum conservation, intermediate Σ particles will have spin parallel or antiparallel to the nucleon spin. heavy mesons involving a mixture of scalar particles (ϑ) and pseudoscalar ones (τ). Besides, in a fixed source theory any elementary process involving Σ and pions can take place only from pions in a p-state.

Formally, therefore, pion-Σ interaction seems to be analogous to nucleon-pion interaction in the static approximation; results obtained with the fixed source methods shall preserve their validity, when the Σ i-spin matrices and physical states are substituted to the corresponding nucleon operators and states. But expectation values between states of physical nucleon can be determined at all orders as functions of the renormalized coupling constant $f^2_{N-\pi}$ and of the experimental cross-sections for pion-nucleon scattering ([1]); an analogous calculation is not possible for the expectation values between Σ states, because of the absence of any information about π-Σ scattering. The terms containing integrals over the cross-section represent however only corrections on results obtained at the lowest order (with renormalized f^2) and such corrections, calculated for both μ_π and ε_1 ([1,2]) do not change for more than about 20% the lowest order results. Because of the rough type of our model we are then allowed to use fixed source techniques at the lowest order, for both nucleon and hyperon contributions.

If P_K represents the probability of finding a virtual K in C, the results will depend on two more parameters: P_K and $f^2_{\pi-\Sigma}$; and our model gives the following results:

1) For the anomalous magnetic moment associated with the pion cloud:

$$\mu'_\pi = (1 - P_K)\mu'^{(N\uparrow)}_\pi + (P_{K'} + \tfrac{1}{3}P_{K''})\mu'^{(\Sigma\uparrow)}_\pi + \tfrac{2}{3}P_{K''}\mu'^{(\Sigma\downarrow)}_\pi , \tag{2}$$

where $P_{K'}$ and $P_{K''}$ represent the probabilities that a K of type K′ or K″ is present in C ($P_K = P_{K'} + P_{K''}$); attribution of type K′ or K″ to ϑ and τ is made according to the assumed parity of Σ.

From (2) we get, using the results of ([1]):

$$\mu'^p_\pi = 22.5\,[f^2_{\pi-N}(1 - P_K) + \tfrac{2}{3}\cdot f^2_{\pi-\Sigma}(P_{K'} - \tfrac{1}{3}P_{K''})] , \tag{3}$$

$$\mu'^n_\pi = -\mu'^p_\pi , \tag{4}$$

where the f^2 represent renormalized coupling constants.

Let us assume $f^2_{\pi-N} = f^2_{\pi-\Sigma} = 0.105$; we get from (3):

$$\mu'^p_\pi = 2.36\,(1 - P_K) + 1.57\,(P_{K'} - \tfrac{1}{3}P_{K''}) , \tag{5}$$

that has to be compared with the experimental value: $\mu^{an} = 1.90$.

If $P_{K'} = P_{K''}$ this gives: $P_K \sim 0.2$; a good agreement with experiment can therefore be obtained with a rather small value for P_K; and moreover P_K does not seem to depend much on the hypothesis made on the relative frequencies of K′ and K″ type mesons.

2) For the n-e interaction conventional potential:

$$V^0 = 155\,[f^2_{\pi-N}(1 - P_K) + f^2_{\pi-\Sigma}\cdot\tfrac{2}{3}\cdot P_K]\ \text{keV}\,, \tag{6}$$

(we used in (6) the numerical results of [2]). For the same value as before for the coupling constants and $P_K = 0.2$, this gives:

$$V^0 = 13.8\ \text{keV}\,. \tag{7}$$

Variations on the assignment of P_K do not alter the conclusion that the modifications of the pion cloud fail to adjust alone theory to experiment. It seems therefore that the contribution to ε_1 coming from intrinsic « anomalous » interactions of C cannot be disregarded.

Introduction of Λ^0 could improve the situation, giving raise to more neutral intermediate hyperon states whose pion cloud does not contribute to the intrinsic interaction. Besides, much of the conclusion reached so far is bound to the hypothesis that the coupling constants of pions to nucleons and hyperons are of the same order of magnitude; if this is not so, how previous results have to be altered cannot be foreseen at present.

On the ground of the results of our rough model, it seems reasonable to foresee that many of the results obtained with fixed source techniques as applied to nucleon-pion systems have to be modified, in order to take into account the modification of the pion cloud and the intrinsic « anomalous » interactions of C. Relations obtained by means of i-spin conservation can be altered too, because of the intermediate hyperon states having different i-spin; in particular relations derived on the ground of rigorous charge independence between pions and nucleons can lose part of their validity, as can be seen easily from the following example.

The cross-sections for the processes: *a*) $(\pi^+ p\,|\,\pi^+ p)$; *b*) $(\pi^- p\,|\,\pi^- p)$; *c*) $(\pi^- p\,|\,\pi^0 n)$ in the assumption of only $T = \frac{3}{2}$ interaction have relative ratios given by:

$$a) : b) : c) :: 9 : 1 : 2\,. \tag{8}$$

But interaction can go also through a different channel, with a probability P_K; the proton can give Σ and K, the π can scatter on Σ, and at last the Σ can absorbe again the K and give back a nucleon. If we take into account the necessary conservation of charge and i-spin in all of these processes we can find the relative ratios of *a*), *b*) and *c*) in terms of the three scattering amplitudes A_0, A_1 and A_2 (corresponding to the three i-spin states of π-Σ system).

Our model is of course too crude to allow us to foresee how much intermediate hyperon states modify (8); a suitable choice of the A's can lead to results not very different from (8) (using $P_K = 0.2$). But any deviation from a rigorous charge independence can alter considerably the structure of dispersion relations describing, for instance, pion-nucleon scattering. Contributions of the type previously described can add to other non charge independent effects and alter the dispersion relation

results. An indication that dispersion relations can be altered in some way by non charge independent interaction was given recently by the Bologna group [5].

We have been concerned so far with consequences of assumption (1); in the extreme opposite assumption:

$$f^2_{B-\pi} \ll f^2_{B-K} \,. \tag{9}$$

we cannot speak any more of equilibrium clouds of pions. We should consider C as a complex particle with different states of charge, spin, i-spin and parity. This requires different pion interaction and therefore modifies in some radical way the pion cloud and can give raise, for instance, to s-wave scattering. As we know that fixed source results are in no qualitative disagreement with experiments, assumption (9) seems to be less realistic than (1). Another process that could radically alter the fixed source picture will be any direct pion-K interaction, as postulated by SCHWINGER [6]; but we have no experimental confirmation of the existence of such an interaction.

In conclusion, the previous analysis allows us to believe that barion-K interactions do not only alter the e.m. properties of the core but modify also the e.m. properties of the pion cloud; and that the introduction of virtual intermediate hyperon states can give raise to contributions to non charge independent effects in pion-nucleon scattering.

* * *

I should like to thank Proff. R. PEIERLS and M. CINI for useful advices and critical discussions.

[5] G. PUPPI: *CERN Symposium*, **2**, 182 (1956) and private communication.
[6] J. SCHWINGER: to be published.

Observation on the Energy Spectra of Multiply Charged Nuclei in the Cosmic Radiation.

C. J. WADDINGTON

H. H. Wills Physical Laboratory - Bristol

(ricevuto il 31 Dicembre 1956)

The integral energy spectrum of the multiply charged nuclei in the primary cosmic radiation is frequently represented by an expression of the form

$$N(>E) = \frac{C}{(m_0c^2 + E)^n},$$

where N is the number of nuclei with a kinetic energy greater than E, (m_0c^2+E) is the total energy in GeV per nucleon and C and n are constants. In a recent publication [1] it was shown that this expression is a good representation for energies between 0.33 and 800 GeV per nucleon. Further, in a sample of nuclei composed of 150 α-particles and 50 heavier nuclei having a mean charge of 7.4, n was found to be 1.50 ± 0.18 for energies between 1.8 and 3.0 GeV per nucleon.

The calculation of this value of n depends on the assumption that n is independent of Z, the charge of the nuclei, for all charge components of the cosmic radiation other than protons. This assumption is commonly made, although the experimental evidence in favour of it has never been very strong. In a recent review article SINGER [2] has suggested that n increases with increasing charge. He has tentatively proposed the following values; for α-particles, $n = 1.5$; for nuclei with $6 \leqslant Z \leqslant 9$, $n = 2.0$; and for nuclei with $Z \geqslant 10$, $n = 2.3$. These values are derived from a consideration of the variation of flux with geomagnetic cut-off energy. They depend on the somewhat doubtful flux measurements made near the equator, and on the ill-defined relationship between geomagnetic latitude and cut-off energy. In addition, the flux measurements considered were made over a period of several years, and thus the influence of possible long term time variations cannot be neglected.

For these reasons it was decided to study these spectra by observing the directly measured energies. The method chosen compared the integral energy spectrum of α-particles observed in a particular stack of photographic emulsions with the spectrum obtained from higher charged nuclei observed in the *same* emulsions. This method has the

(1) F. H. FOWLER and C. J. WADDINGTON: *Phil. Mag.*, **1**, 637 (1956).

(2) S. F. SINGER: *Progress in Elementary Particle and Cosmic Ray Physics*, **4**, (New York 1957), in press.

advantage that the systematic errors in the energy determinations which may be introduced in emulsions will tend to cancel when the two spectra are compared.

In this initial investigation the previous experimental work [1] was used as a basis, and the reader is referred to it for experimental details. Energy determinations were made on the tracks of ten additional nuclei with charges greater than that of Boron satisfying the geometrical conditions previously defined. The experimental values of n obtained for the α-particle spectrum, n_α, and for the spectrum of those nuclei with a charge greater than five, n_A, were:

$$n_\alpha = 1.7 \pm 0.2, \quad n_A = 1.2 \pm 0.3 ,$$

for energies between 1.8 and 3.0 GeV per nucleon. Energy determinations were made on 150 α-particles and 52 heavy nuclei with a mean charge of eight.

The ratio n_A/n_α, R, was found to be 0.7 ± 0.2, whereas the value predicted by Singer is at least 1.33, and the commonly accepted value is 1.0. It can be seen that the probability of R being as great as 1.33 is less than 1%, while the probability of it being as great as 1.0 is about 7%. Therefore, provided that the possibility of R being less than 1.0 is neglected as being physically unlikely, it is probable, at least over the restricted energy range considered, that the spectra of the various multiply charged components of the primary cosmic radiation are closely similar. Further experiments of the type described here, but of greater statistical weight, would enable a final conclusion to be drawn.

* * *

The author thanks the Royal Society for the award of a Mackinnon Research Studentship.

Propagation Kernels as Functions of the Masses.

E. R. Caianiello (*)

Department of Physics, University of Washington - Seattle

(ricevuto il 5 Gennaio 1957)

In this note we present, for future reference, a few results on propagation kernels which have proved of importance in a mathematical investigation of renormalization theory (to be published in this Journal); we think it convenient to discuss them apart, because they may be of practical use in cases where the usual perturbative expansions do not seem appropriate, e.g. in some of the current non-covariant meson theories.

The kernel K_{N_0,P_0} ($2N_0$ ext. fermion lines, P_0 ext. boson lines) admits the formal perturbative expansion (1):

$$(1) \qquad K_{N_0,P_0} = K\begin{pmatrix} x_1 \dots x_{N_0} & t_1 \dots t_{P_0} \\ y_1 \dots y_{N_0} & \end{pmatrix} = \sum_{N(P_0)} \frac{\lambda^N}{N!} \int \sum \gamma^1 \dots \gamma^N \begin{pmatrix} x_1 \dots x_{N_0} \; \xi_1 \dots \xi_N \\ y_1 \dots y_{N_0} \; \xi_1 \dots \xi_N \end{pmatrix} [t_1 \dots t_{P_0} \; \xi_1 \dots \xi_N] \, \mathrm{d}\xi_1 \dots \mathrm{d}\xi_N \, .$$

We remind that in (1) $\sum_{N(P_0)}$ means sum over all N having same parity as P_0; $\begin{pmatrix} \alpha_1 \dots \alpha_n \\ \beta_1 \dots \beta_n \end{pmatrix}$ is the Sylvester notation for the determinant of elements $(\alpha_h \beta_k)$, where:

$$(2) \qquad (\gamma \partial_x + m_f)(xy) = i\delta(x-y) \, .$$

$(xy) = \frac{1}{2} S^{\mathrm{F}}(x-y)$ is the free fermion causal propagator, *defined* so that $(xx) = 0$. Likewise, $[\alpha_1 \dots \alpha_{2m}]$ is the hafnian (1) of elements $[\alpha_h \alpha_k]$ where:

$$(3) \qquad (\Box_x - m_b^2)[xy] = i\delta(x-y) \, ,$$

and again we *define* the free boson causal propagators $[xy] = [yx]$ so that $[xx] = 0$.

(*) On leave from the Istituto di Fisica Teorica Università di Napoli, Napoli.

(1) E. R. Caianiello: *Nuovo Cimento*, **10**, 1634 (1953); **11**, 492 (1954).

In this notation, spinor and vector indices and operations on them are not explicitly indicated.

Therefore, as is well known [2]:

$$\frac{\partial(xy)}{\partial m_f} = i\int \mathrm{d}\xi\,(x\,\xi)(\xi y)\,, \tag{4}$$

$$\frac{\partial[xy]}{\partial(m_b^2)} = -\,i\int \mathrm{d}\xi\,[x\,\xi][\xi y]\,. \tag{5}$$

We point out that any operator independent of the masses can be substituted for $\gamma\delta_x$ and $\Box_x$ in (2) and (3), without altering (4) and (5): these formulae are therefore valid in covariant as well as in non-covariant theories.

From (4) we have:

$$\frac{\hat{c}}{\hat{c}m_f}\begin{pmatrix}\alpha_1 \dots \alpha_n\\ \beta_1 \dots \beta_n\end{pmatrix} \sum_{h,k=1}^{n} \frac{\partial(\alpha_h\beta_k)}{\partial m_f}\,\frac{\hat{c}}{\partial(\alpha_h\beta_k)}\begin{pmatrix}\alpha_1 \dots \alpha_n\\ \beta_1 \dots \beta_n\end{pmatrix} = -\,i\int \mathrm{d}\xi\begin{pmatrix}\xi\alpha_1 \dots \alpha_n\\ \xi\beta_1 \dots \beta_n\end{pmatrix}. \tag{6}$$

and from (5):

$$\frac{\partial}{\partial(m_b^2)}[\alpha_1 \dots \alpha_{2m}] = \sum_{h<k}^{1\dots 2m} \frac{\partial[a_h a_k]}{\partial(m_b^2)}\,\frac{\partial}{\partial[a_h a_k]}[a_1 \dots a_{2m}] = \frac{1}{2}\sum_{h\neq k}^{1\dots 2m} \dots = -\frac{1}{2}\int \mathrm{d}\xi\,[\xi\xi\alpha_1 \dots \alpha_{2m}]\,. \tag{7}$$

We conclude:

$$\frac{\partial}{\partial m_f} K\begin{pmatrix}x_1 \dots x_{N_0}\\ y_1 \dots y_{N_0}\end{pmatrix} t_1 \dots t_{P_0}\Big) = -\,i\int \mathrm{d}\xi\, K\begin{pmatrix}\xi x_1 \dots x_{N_0}\\ \xi y_1 \dots y_{N_0}\end{pmatrix} t_1 \dots t_{P_0}\Big). \tag{8}$$

$$\frac{\partial}{\partial(m_b^2)} K\begin{pmatrix}x_1 \dots x_{N_0}\\ y_1 \dots y_{N_0}\end{pmatrix} t_1 \dots t_{P_0}\Big) = -\,\frac{i}{2}\int \mathrm{d}\xi\, K\begin{pmatrix}x_1 \dots x_{N_0}\\ y_1 \dots y_{N_0}\end{pmatrix} \xi\xi t_1 \dots t_{P_0}\Big). \tag{9}$$

(8) and (9) are the formulae we proposed to exhibit; their structure makes perhaps already apparent their importance in a graph-independent formulation of renormalization. Clearly the validity of (8) and (9) is quite general, since they can be deduced, as easily, in several other ways, e.g. through variational differentiations.

Compare them with:

$$\frac{\partial}{\partial\lambda} K\begin{pmatrix}x_1 \dots x_{N_0}\\ y_1 \dots y_{N_0}\end{pmatrix} t_1 \dots t_{P_0}\Big) = \int \mathrm{d}\xi\gamma^\xi K\begin{pmatrix}x_1 \dots x_{N_0}\xi\\ y_1 \dots y_{N_0}\xi\end{pmatrix} \xi t_1 \dots t_{P_0}\Big). \tag{10}$$

The last formula is the source of all standard perturbative expansions in powers of the interaction strength λ. This shows the possible rôle of (8) and (9) in cases where expansions of this sort are not reliable: whenever an asymptotic estimate of the values of the kernels when one (or both) of the masses becomes zero (or infinite) is available (estimates of this kind have been attempted in several cases with success in the literature), then (8) and (9) can be used to obtain perturbative expansions

[2] Y. Takahashi and H. Umezawa: *Prog. Theor. Phys.*, **6**, 543 (1952).

where the expansion parameter is a mass, or its inverse, or both masses or their inverse. Finally, it is clear that (8), (9) and (10) can be used to check the consistency of particular methods, e.g. strong-coupling approximations.

* * *

The author takes pleasure in extending his sincere thanks to Prof. J. H. MANLEY and to the members of the Physics Department of the University of Washington for their warm hospitality.

On the Σ Hyperon-Nucleon Interaction Cross-Section.

N. Dallaporta and F. Ferrari

Istituto di Fisica dell'Università - Padova
Istituto Nazionale di Fisica Nucleare - Sezione di Padova

(ricevuto il 14 Gennaio 1957)

Recent experimental results have given some indications about the Λ_p/Σ_p ratio of the production probabilities of Λ and Σ hyperons in the capture of K^- mesons at rest by nucleons.

Haskin *et al.* [1] have analyzed seventy events of K^- capture at rest in emulsion stacks. The above ratio is estimated by considering the energy distributions of emitted pions in the reactions:

$$K^- + N \rightarrow Y + \pi \tag{1}$$

where the hyperon may be either a Σ, with all possible charge values, or a Λ. Two peaks are expected for the pion energies of 90 and 150 MeV, corresponding to Σ and Λ reactions respectively. However the spread due to the Fermi motion of the nucleons of the target nucleus and the secondary interactions of the pions can greatly distort these distributions, so that the estimate $\Lambda_p/\Sigma_p \sim 0.5$ can be only very rough.

A much better and more direct estimation has recently been obtained by Solmitz *et al.* [2] in a hydrogen bubble chamber. From direct observation the Λ_p/Σ_p ratio turns out in this case to be about $\frac{1}{7}$, taking into account also the production of Σ^0 and the K_ϱ. Further, if we use the limiting values of the relative amplitudes of the different isotopic spin states given in [2] we can calculate the extreme values of the Λ_p/Σ_p production ratio for neutrons and finally the expected value of Λ_p/Σ_p for emulsion nuclei, which turns out to be between $\frac{1}{3}$ and $\frac{1}{5}$.

These figures are in clear contrast to those obtained from direct observation of the hyperons emitted in K^- captures from the nuclei of emulsion stacks [3]; in

[1] D. M. Haskin, T. Bowen and M. Schein: *Phys. Rev.*, **103**, 1512 (1956); S. Goldhaber: *Proc. Sixth Annual Rochester Conference*, 1956.

[2] F. T. Solmitz, L. W. Alvarez, H. Bradner, P. Falk, J. D. Gow, A. H. Rosenfeld and R. D. Tripp: *Bull. Am. Phys. Soc.*, December 1956: we are grateful to the Berkeley group for having let us know their bubble chamber data before publication.

[3] W. Fry: *Phys. Rev.*, **100**, 950 (1955): D. W, Falla, M. W. Friedlander, F. Anderson, W. D. B. Greening, S. Limentani, B. Sechi Zorn, C. Cernigoi, G. Jernetti and G. Poiani: *Parent Stars of* K-*mesons* (in course of publication).

this case Λ_n/Σ_n turns out to be ~ 2. It is possible to reconcile these values only by assuming that there is probably a rather large cross-section for the process

$$\Sigma + N \to \Lambda + N + Q \qquad Q \simeq 70 \text{ MeV} \tag{2}$$

which transforms, inside the nuclear matter, a large numbers of Σ's into Λ's. Of course, the comparison of these two different values of the ratios Λ_p/Σ_p and Λ_n/Σ_n gives us a possibility of determining the order of magnitude of the scattering cross-section of Σ hyperons by nucleons.

With this aim in view, let us consider a K^- which is captured at a point P distant ϱ from the center of the nucleus and let $\varphi(\varrho)$ be the probability of such a capture occuring. It is to be noted that, owing to its small kinetic energy, a Λ produced according to the reaction (1) will never have enough energy to become a Σ, even if we take into account the momentum distributions of the nucleons (the threshold energy is about 70 MeV). This fact greatly simplifies the situation because it will be sufficient for our problem to consider beside (2) only the scattering reaction

$$\Sigma + N \to \Sigma + N\,. \tag{3}$$

If we now indicate respectively with $\sigma_{\Sigma\Lambda}$, $\sigma_{\Sigma\Sigma}$ the cross-sections for the reactions (2) and (3) and with $\lambda_{\Sigma\Lambda}$, $\lambda_{\Sigma\Sigma}$ the corresponding mean free paths, the probability that a hyperon generated at a point P by a capture event, will escape from the nucleus as Σ or Λ, will be given by the following relations, if we consider the possibility of only one scattering:

$$\pi_\Sigma = \int_{R-\varrho}^{R+\varrho} W(R, \varrho, t) \left\{ \Sigma_p \left[\exp\left[-t/\lambda_{T\Sigma}\right) + \frac{\lambda_{T\Sigma}}{\lambda_{\Sigma\Sigma}} \left(1 - \exp\left[-t/\lambda_{T\Sigma}\right]\right) \right] \right\} \mathrm{d}t\,, \tag{4}$$

$$\pi_\Lambda = \int_{R-\varrho}^{R+\varrho} W(R, \varrho, t) \left\{ \Sigma_p \frac{\lambda_{T\Sigma}}{\lambda_{\Sigma\Lambda}} \left(1 - \exp\left[-t/\lambda_{T\Sigma}\right]\right) + \Lambda_p \right\} \mathrm{d}t\,. \tag{5}$$

In these formulas $W(R, \varrho, t)$ is the probability, as defined by CLEMENTEL and PUPPI [4], that a particle produced (isotropically) at a point P travels a distance t in the nuclear matter; $\lambda_{T\Sigma}$ is the total mean free path of the Σ hyperon and $R = r_0 A^{\frac{1}{3}}$ is the nuclear radius. The Λ_n/Σ_n ratio for nuclei of emulsion stacks will be consequently obtained by means of the formula

$$\frac{\Lambda_n}{\Sigma_n} = \frac{\int_0^R \varphi(\varrho)\,\mathrm{d}\varrho \int_{R-\varrho}^{R+\varrho} \mathrm{d}t\, W(R, \varrho, t) \left\{ \eta \left(1 - \exp\left[-t/\lambda_{T\Sigma}\right]\right) + \dfrac{\Lambda_p}{\Sigma_p} \right\}}{\int_0^R \varphi(\varrho)\,\mathrm{d}\varrho \int_{R-\varrho}^{R+\varrho} \mathrm{d}t\, W(R, \varrho, t) \left\{ \eta \left(\exp\left[-t/\lambda_{T\Sigma}\right] - 1\right) + 1 \right\}} \tag{6}$$

in which $\eta = \lambda_{T\Sigma}/\lambda_{\Sigma\Lambda}$.

(4) E. CLEMENTEL and G. PUPPI: *Nuovo Cimento*, **10**, 197 (1953).

We have supposed that the K^- is captured in a k-orbit (mean life of capture $\tau_k \simeq 10^{-18}$ s). Therefore we have assumed for the probability function $\varphi(\varrho)$ the gaussian shape $\exp[-(R-\varrho)^2]$ for heavy nuclei ($A=100$) and the exponential shape $\exp[-(R-\varrho)]$ for light nuclei ($A=14$).

Finally, the observed ratio Λ_n/Σ_n will be given by

$$\frac{\Lambda_n}{\Sigma_n} = p\left(\frac{\Lambda_n}{\Sigma_n}\right)_l + (1-p)\left(\frac{\Lambda_n}{\Sigma_n}\right)_h . \tag{7}$$

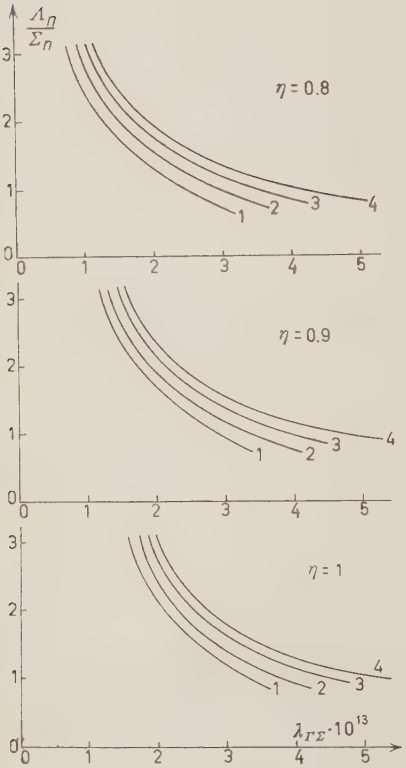

Fig. 1.

In these p is the percentage of captures in light nuclei and has been assumed ~ 0.39 as suggested by the corresponding values of the μ captures [5]; $(\Lambda_n/\Sigma_n)_l$ and $(\Lambda_n/\Sigma_n)_h$ are the values calculated by means of the formula (6) of the ratios for the light and heavy nuclei.

The results are plotted in Fig. 1 (with $r_0 = 1.4\cdot 10^{-13}$ cm) for several values for Λ_p/Σ_p and η (the curves 1, 2, 3, 4 correspond to the values 0.1, 0.2, 0.3, 0.4 of Λ_p/Σ_p). Λ_n/Σ_n is given as function of $\lambda_{T\Sigma}$.

It is seen that for a given experimental value of Λ_p/Σ_p and Λ_n/Σ_n different $\lambda_{T\Sigma}$ may be obtained for different η. It may be seen that η cannot be less than a limit value, which from our figures is about 0.55. It is however probable that in our case η is not very different from 1, because according to phase space considerations at low energies, reaction (2) will predominate over reaction (3). Moreover, as FRY [6] pointed out to us, a large fraction of the Σ are observed in K^- capture reactions emerging from stars without other prongs and this can be interpreted as an indication that in the cases in which the Σ is able to escape from the nucleus (either no interaction or interaction (3)), no secondary interactions generally do occur, so $\lambda_{\Sigma\Sigma}$ has to be much greater than $\lambda_{\Sigma\Lambda}$. Further the ratio Λ_n/Σ_n observed in plates is about the same as that of heavy to light nuclei and this may be also interpreted, owing to the small value of Λ_p/Σ_p at production, that Σ produced in light nuclei could generally escape from the nucleus, while those produced in a heavy nucleus would be generally transformed in a Λ.

[5] W. FRY: *Nuovo Cimento*, **10**, 490 (1953) A. BONETTI and G. TOMASINI: *Nuovo Cimento* **9**, 693, (1951).

[6] W. FRY: Private communication.

On the basis of these considerations, assuming $\eta = 1$ and therefore $\lambda_{T\Sigma} = \lambda_{\Sigma\Lambda}$ and taking $\Lambda_n/\Sigma_n = 2$, Λ_p/Σ_p either $\frac{1}{3}$ or $\frac{1}{5}$ we obtain $\lambda_{T\Sigma} \simeq 2.5 \cdot 10^{-13}$ respectively $2.3 \cdot 10^{-13}$ and a reaction cross section $\sigma_{T\Sigma} = \sigma_{\Sigma\Lambda} \sim$ between 0.45 mb and 0.50 mb. This value is of the same order of magnitude as the geometric scattering nucleonic cross-section; this order of magnitude does not change when we chose other reasonable values of the ratio η. Moreover the preceeding discussion and the results obtained for the total Σ-nucleon scattering cross-section supports a posteriori that to consider one scattering only was a reasonable assumption and that corrections due to successive scatterings of the hyperon before escaping from the nucleus should be small.

* * *

We are indebted to Prof. W. FRY for a helpful discussion on the problem.

Note added in proof.

We are informed by Prof. W. FRY that, from a study of stopped negative K-mesons, the ratio of Λ to Σ hyperons emitted from nuclei is $\Lambda_n/\Sigma_n = 4.1 \pm 0.6$. With this value and taking $\Lambda_p/\Sigma_p = 0.3$ one then finds that $\sigma_{\Lambda\Sigma} = 0.72$ mb.

The Mass Difference Between the Σ^+ and Σ^- Hyperons.

R. C. Kumar, W. B. Lasich and F. R. Stannard
Physics Department, University College - London

(ricevuto l'8 Gennaio 1956)

The mass difference between the Σ^+ and Σ^- hyperons can be studied through the interactions:

$$(1) \qquad K^- + P \to \Sigma^+ + \pi^- + Q_1 ,$$

and

$$(2) \qquad K^- + P \to \Sigma^- + \pi^+ + Q_2 .$$

In investigations with photographic emulsions, a few events have been obtained ([1,2]) which have been attributed to the capture of a K^--meson at rest by an unbound proton. These are characterised by a star consisting of two collinear prongs, one being identified as a Σ hyperon and the other a π-meson.

In the course of studying a stack of 600 μm plates exposed to the K^- beam of the Bevatron, we have so far found 50 K^- stars by «along the track scanning». Of these, three emit a Σ and a π and no other charged particle, and one of these cases satisfies the condition of collinearity to (0.3 ± 1.0) degree. The projected angle was found to be $(180.0 \pm 0.5)°$. The event is well situated in the emulsion and the Σ comes to rest in the same pellicle giving rise to an Auger electron. The angle of dip of the tracks is 25° in unprocessed emulsion. The measured range of the Σ is (714 ± 7) μm, where the quoted error is due primarily to the uncertainty in the determination of the shrinkage factor. From measurements on the ranges of μ-mesons from $\pi \to \mu$ decays this was found to be 2.05 ± 0.10.

Confirmation is lent to the interpretation by integral gap length measurements which give about protonic mass for the hyperon and, in addition, range and scattering lead to a mass of $2\,700^{+2000}_{-1000}\ m_e$. The π-meson could be followed for several plates and scattering gave a value for $p\beta$ of 135^{+40}_{-25} MeV/c. The measured grain exponent, g^*, of this track was (1.16 ± 0.06) times that for the 150 MeV. π-mesons of the beam near the event. This leads to an energy for the π of 90^{+30}_{-15} MeV, compared with 80^{+30}_{-15} MeV from scattering.

Including this event, four observations of the collinear production of a Σ^- and a π^+ in emulsion have now been reported. The Σ^- ranges are summarised

([1]) *Proceedings of 6th Annual Rochester Conference on High-Energy Physics.* Report by S. Goldhaber.

([2]) W. F. Fry, J. Schneps, G. A. Snow, M. S. Swami and D. C. Wold: *Phys. Rev.*, **104**, 270 (1956).

in the following table. The errors include straggling (3).

TABLE I. – *Ranges of* Σ^- *hyperons.*

Range (μm)	Source	Weight
695 ± 25	Berkeley (1)	2
691 ± 45	M.I.T. (1)	1
670 ± 21	Wisconsin (2)	2
714 ± 18	Described above	2
693 ± 12	Weighted Mean	—

If it can be assumed that the K-meson responsible for the interaction has τ-mass, $(966.1 \pm 0.7)\ m_e$, then on the basis of the Fay, Gottstein and Hain range-energy tables (4), the Q-value found from the mean range becomes $(96.8 \pm \pm 0.7)$ MeV. The energy of the Σ^- is (12.78 ± 0.15) MeV, that of the π-meson (84.0 $\pm$ 0.7) MeV, and the corresponding mass of the Σ^- is $2\,339.6 \pm 1.6\ m_e$.

Comparison between the ranges of the Σ^- and Σ^+ from the capture of K^--mesons by free protons provides a means of determining the mass difference, $M_{\Sigma^-} - M_{\Sigma^+}$, which is insensitive to the particular range-energy relation used, and the mass assumed for the K-meson.

Two Σ^+ hyperon events have been reported, one from Berkeley of range (809 ± 40) μm (1) and the other from Wisconsin of range (804 ± 16) μm (2) (where the quoted errors include straggling). These give a weighted mean of (805 ± 15) μm. Combining this result with the mean range found for the Σ^- one arrives at a mass difference of

$$M_{\Sigma^-} - M_{\Sigma^+} = (14.1 \pm 2.3)\ m_e .$$

This is in good agreement with the value of $(16 \pm 5.4\ m_e)$ found by BUDDE *et al.* (5) from the decay of a Σ in a bubble chamber.

* * *

We wish to thank the staff of the Radiation Laboratory, Berkeley, Calif., who exposed the plates for us, thus making the experiment possible; and Professor C. F. POWELL for the facilities he has laid at our disposal at Bristol for the processing of the plates. We also wish to thank Dr. E. H. S. BURHOP for his interest in this work and Mr. D. DAVIS and Mr. N. N. RAINA for assistance in the measurements.

(3) P. H. FOWLER and D. H. PERKINS: *Proceedings of the Bristol Symposium* (March 1950), p. 341.

(4) H. FAY, K. GOTTSTEIN and K. HAIN: *Suppl. Nuovo Cimento*, **11**, 234 (1954).

(5) R. BUDDE, M. CHRÉTIEN, J. LEITNER, N. P. SAMIOS, M. SCHWARTZ and J. STEINBERGER: *Phys. Rev.*, **103**, 1827 (1956).

Improvements on a Multichannel Pulse Analyzer.

S. Colombo (*), C. Cottini and E. Gatti

Laboratori CISE - Milano

(ricevuto il 15 Gennaio 1957)

A new multichannel analyzer has been built which is a development of one described by E. Gatti [1], to which the reader is referred. The working experience about this mentioned instrument has suggested some changes which led to better characteristics.

The electrical scheme of the instrument is given in Fig. 1 (output discriminators and coincidences are not shown).

In this instrument after having stretched the input pulse, its leading edge is not substituted by a new standard one, as was done in the former instrument: the original leading edge is maintained and its eventual influence on the threshold level of the discriminator circuits is nullified through the addition, after about $\frac{1}{2}$ μs from the end of the leading edge, of a first calibrated step to the flat top of the lengthened pulse; this addition is followed by the addition of a second calibrated step pulse which, as in the old instrument, fixes the width of the channels (Fig. 2).

By this way of forming the input pulse, if we can suppose that at the instant of application of the first calibrated step the discriminator circuits have recovered to the static threshold (eventually disturbed in previous instants by the influence of the leading edge of the pulse) we can also state that the discriminators are driven by the same pulse shape and amplitude irrespective of the amplitude of the input pulse to be classified; this assures, even more strongly than in the old instrument, the identical width of all channels.

The lengthening circuit of Kelley whose good performance depends critically in our application upon the inverse resistance of the lengthening diodes has been substituted with the Chase lengthener [2] whose lengthening proprieties do not depend upon crital parameters.

The first calibrated step has also allowed to widen the measuring range to the low levels (until 2 volt) because

(*) SELO, Milano.

(1) E. Gatti: *Nuovo Cimento*, **11**, 153 (1954).

(2) R. L. Chase: *Brookhaven National Laboratory Report*, 263 (T-42, 1954).

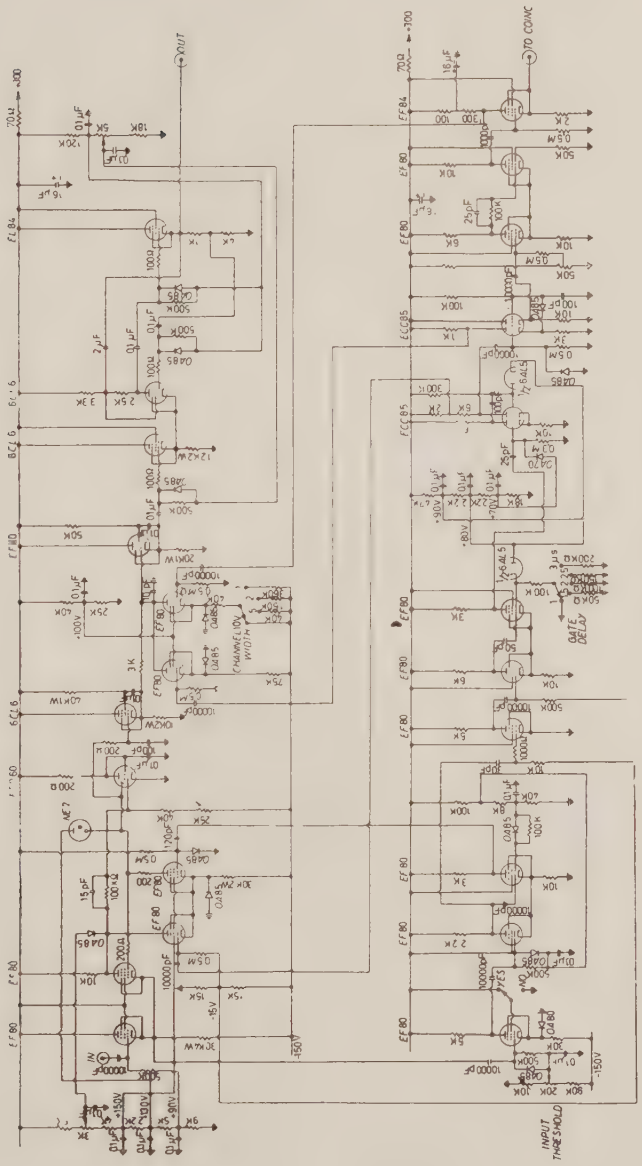

Fig. 1. – Electrical scheme of the pulse shaper.

small pulses appear added to the first calibrated step an therefore are larger

Fig. 2. – Shaped pulse.

than the hysteresis voltage of the output discriminators.

Output discriminators are constructed with two penthodes instead of two triodes in order to minimize feedback of spurious pulses at their input when triggered.

When very high resolution is desired the instrument is connected with a window amplifier which was built folloving the Hutchinson design ([3]) with obvious changes in order to have a gain of 10 and an upper limitation of output pulses to 60 V and power supplies of + 300 V and — 150 V.

([3]) G. W. HUTCHINSON: *Rev. Scient. Instr.* **27**, 592, (1956).

Spin-Echoes with any Number of Pulses.

T. Ghose, S. K. Ghosh and D. K. Roy
Institute of Nuclear Physics - Calcutta, India

(ricevuto il 9 Gennaio 1957)

Extending the application of the vector model developed by Banerjee *et al.* [1] to explain the formation of primary and stimulated echoes for two and three pulse systems to the case of four and more pulses, it can be shown that the total number of echoes formed with n rf-pulses is given by:

$$y_n = \tfrac{1}{4}(3^n - 2n - 1) .$$

This has been experimentally verified for n up to 5. The analysis shows that the formation of all the echoes with any number of pulses can be explained by considering only the following three basic mechanisms: (i) primary echo mechanism, (ii) stimulated echo mechanism and (iii) « virtual » stimulated echo mechanism. The first two mechanisms have been thoroughly dealt with by Hahn [2] and Das and Saha [3]. But the « virtual » stimulated echo, in spite of its occurrence as a term in the mathematical analysis, was disregarded by them on account of its physical non-existence. The general relation for the number of echoes with n pulses thus given by Das and Roy [4] on extending the analysis [3] to more pulses, fails to give correct results as n exceeds 4. The significance of the « virtual » echo was first recognized by Bloom [5] and Crawford [6] when explaining the occurrence of a particular echo with $n = 4$, which otherwise could not be explained only on the basis of primary and stimulated echo mechanisms. Bloom has treated the general case as well — but his general formula fails experimentally as he overlooked the superpositions of certain real echo terms which occur irrespective of the time sequence of the applied r.f. pulses.

The model that has been developed brings out the full significance of the formation of the « virtual » echoes as well as the part played by these in the formation of subsequent real echoes. It has been made clear that apart from their physical non-existence, the « virtual » echoes — each of which corresponds to one stimulated echo — behave

(1) B. M. Banerjee, S. K. Ghosh and A. K. Saha: to be published in the *Ind. Journ. Phys.*

(2) E. L. Hahn: *Phys. Rev.*, **80**, 580 (1950).

(3) T. P. Das and A. K. Saha: *Phys. Rev.*, **93**, 749 (1954).

(4) T. P. Das and D. K. Roy: *Phys. Rev.*, **98**, 525 (1955).

(5) A. L. Bloom: *Phys. Rev.*, **98**, 1105 (1955).

(6) G. J. B. Crawford: *Phys. Rev.*, **99**, 600 (1955).

just like real echoes in forming echoes with subsequent pulses by primary and stimulated echo mechanisms, both real and « virtual ». It can, however, have no effect on the pulse responsible for its occurrence — which is also equally true for real echoes. Thus in the spin echo analysis with any number of r.f. pulses, we need consider only: (1) the primary echo mechanism between two r.f. pulses or between a first echo pulse either real or « virtual » — and a second r.f. pulse, and (2) the stimulated echo mechanism between three r.f. pulses or between an echo pulse either real or « virtual » — and two subsequent r.f. pulses. On this basis the following relations are obtained:

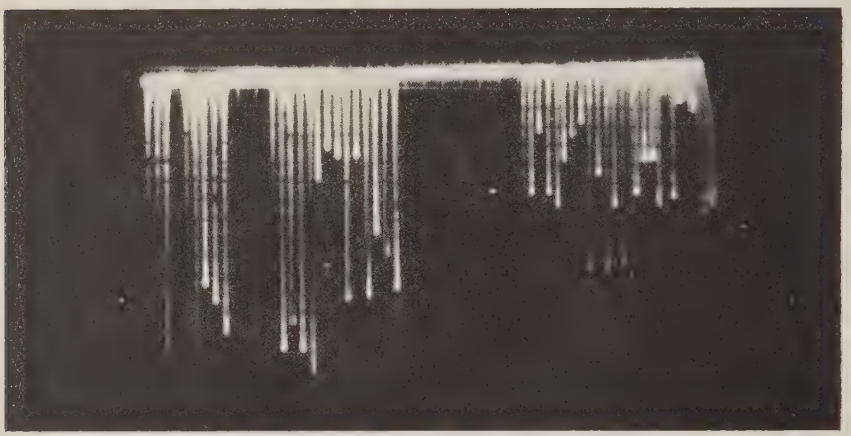

Fig. 1 *a*).

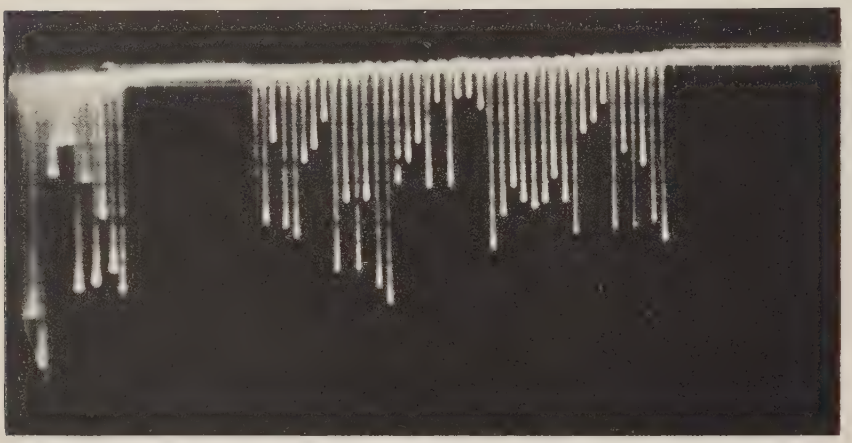

Fig. 1 *b*).

$$y_n = \tfrac{1}{4}(3^n - 2n - 1),$$

and

$$y_n' = \tfrac{1}{4}(3^{n-1} - 2n + 1),$$

giving respectively the total number of real and « virtual » echoes with n r.f. pulses. It is to be noted that the total number of echoes appearing after the n^{th} pulse is given by.

$$y_n - y_{n-1} = \tfrac{1}{2}(3^{n-1} - 1) \qquad y_{n-1}' - y_n' .$$

For experimental observation of all the echoes it is necessary that: (*a*) the r.f. pulses should be other than 90° or 180° except the first pulse which can be chosen to be of 90°; (*b*) pulse separations be properly adjusted to avoid any superposition of echoes, and (*c*) proper samples be chosen corresponding to the pulse separations used, in order to minimize relaxation and diffusion damping.

The validity of the above equations is evident from the Figs. 1 *a* and 1 *b* which are the photographs of the echoes with five r.f. pulses — the first one showing the sweep before and the second one showing that after the fifth pulse. It is obvious that the minimum separations between the pulses satisfying the condition (*b*) is governed by the relation:

$$\tau_{n-1} = (y_n - y_{n-1})\tau_1 .$$

where τ_1 and τ_{n-1} are the times of occurrence of the second and the n^{th} pulses. This enables one to get groups of equispaced echoes, because then between the n^{th} and the $(n+1)^{\text{th}}$ pulses the interval is $(2y_n - 2y_{n-1} + 1)\tau_1$ and the $(y_n - y_{n-1})$ real echoes occur in a group at intervals of τ_1 after the n^{th} pulse, whereas the blank space $(y_n - y_{n-1})\tau_1$ before the $(n+1)^{\text{th}}$ pulse corresponds to the place that would have been occupied by the similarly spaced $(y_{n-1}' - y_n')$ virtual echoes.

* * *

The authors express their thanks to Prof. A. K. Saha and Mr. B. M. Banerjee for their encouragement during the progress of the work.

Parity Conservation and the Mass of the Neutrino.

B. F. Touschek

Istituto di Fisica e Scuola di Perfezionamento in Fisica Nucleare dell'Università - Roma
Istituto Nazionale di Fisica Nucleare - Sezione di Roma

(ricevuto il 26 Gennaio 1957)

In the frame of the special theory of relativity there are two particles of zero mass: the photon and the neutrino. Whereas the photon mass is fixed to be zero by the principle of gauge invariance no similar principle is known for the neutrino. It is however, quite clear that the mass of the neutrino can be defined to be 0 by the requirement that the equations of motion—and with them the Lagrangian—of the free neutrino field are invariant under the transformation

$$\nu' = \exp[i\gamma_5\alpha]\nu\,. \tag{1}$$

Here ν is the waveoperator of the neutrino and α is a real number. Since γ_5 is a Hermitian matrix we have for $\bar{\nu} = \nu^+\gamma_4$:

$$\bar{\nu}' = \bar{\nu}\exp[i\gamma_5\alpha]\,.$$

If the neutrino is allowed to interact with other particles the operators describing these particles must undergo a corresponding transformation and we may choose in particular

$$\psi' = \exp[i\alpha]\psi, \qquad \bar{\psi}' = \bar{\psi}\exp[-i\alpha], \tag{2}$$

for every spinor field ψ and $\varphi = \varphi'$ for every Bose field. If the system of Fermions (other than the neutrino) and Bosons is not coupled to the neutrino field the invariance requirements (1) and (2) ensure that the neutrino mass be zero and that the sum of all Fermi particles minus the sum of all anti-Fermions remains constant. The latter is a property of all known strong interactions. A peculiar situation arises if one tries to construct a Lagrangian in which neutrinos can be singly produced or annihilated. For if one assumes that this Lagrangian is of the usual form

$$\mathcal{L}' = f(\bar{\nu}\Gamma'\psi_1)(\bar{\psi}_2\Gamma\psi_3) + \text{herm. Conj.} \tag{3}$$

where $\psi_1\psi_2\psi_3$ are three not necessarily different spinor field of mass $\neq 0$, invariance under proper Lorentz transformation requires that

$$\Gamma' = (\varepsilon + \eta\gamma_5)\Gamma, \tag{4}$$

in which ε and η are arbitrary numbers. According to the « type » of the Fermions involved conventional theories give either $\varepsilon = 0$ or $\eta = 0$. If we now require that (3) be invariant under (1) and (2) we obtain immediately

$$\exp[i\gamma_5\alpha](\varepsilon + \eta\gamma_5) = \exp[-i\alpha](\varepsilon + \eta\gamma_5)$$

and therefore $\varepsilon + \eta = 0$. The Lagrangian (3) must therefore be of the form

$$\mathcal{L}' = f(\bar{\nu}(1-\gamma_5)\Gamma\psi_1)(\bar{\psi}_2\Gamma\psi_3) \tag{5}$$

and it is obvious that this Lagrangian is invariant under proper Lorentz transformations but is no longer invariant under space reflections.

It has recently been suggested by LEE and YANG [1] that the evidence on the decay of the K-meson could be interpreted to mean that parity is not conserved in « weak » reactions and this suggestion has recently been brilliantly confirmed by experiments carried out by Miss WU [2] at Columbia University. Though it is difficult to see on the basis of the suggested invariance property how the nonconservation of parity in K-decay can be explained it nevertheless seems to suggest a formalism in which parity is not necessarily conserved and in which the loss of one conservation law may be perhaps compensated by the appearance of another.

[1] C. N. YANG, T. D. LEE: *Phys. Rev.*, **104**, 254 (1956).

[2] *Time*; Jan. 28 (1957), p. 39.

Note added in proof.

Instead of (2) a more general complementary transformation can be chosen, viz:

$$(2') \qquad \psi'_i = \exp\,[in_i\alpha]\psi_i\,,$$

valid for all fields excluding that of the neutrino and in which n_i is a number characteristic of the i-th field. One then has the selection rules $\Delta n = \pm 1$ for one-neutrino decay and $\Delta n = \pm 2$ or 0 for two neutrino decay. Also, for $\Delta n = \pm 2$ parity cannot be conserved.

Angular Distribution of the μ-Decay as Test of Parity Conservation.

N. N. Biswas, M. Ceccarelli (*) and J. Crussard (+)
Max-Planck-Institut für Physik - Göttingen

(ricevuto il 4 Febbraio 1957)

It has been shown by Lee and Yang [1] that if parity is not conserved in weak interactions, angular asymmetries may arise in some decay processes. For instance, in the π-μ decay, as a result of the non-conservation of parity, the muon could be polarized parallel to its direction of motion; in the subsequent decay the distribution of the angle θ of the electron with this direction, chosen as polar axis, is then predicted to be asymmetric.

In order to detect such an effect, an experiment using π-μ-e events in nuclear emulsions is in progress in which the spatial angle θ between the directions of emission of the μ-meson and of the electron is measured. The 1000 μm thick emulsions have been exposed to the π^+ beam of the Chicago synchrocyclotron. The plates were shielded from external magnetic field, which, as pointed out by Friedman and Telegdi, would cause Larmor precession of the muon, thus destroying the possible polarization [2]. Special care has been taken to avoid systematic errors in the angular distribution, which may originate from a biased selection of the events or from the systematic loss of electrons emitted in a particular direction. The first cause of errors has been practically eliminated by scanning the plates under low magnification only for π-μ and not for μ-e events. The second source of errors may arise from the cases: *a*) no visible electron track at the end of the μ-meson; *b*) misinterpretation of crossing minimum tracks. Both *a*) and *b*) were reduced by discarding all events in which the μ-meson stopped at less than 50 μm from the surfaces of the emulsions. *a*) is then negligible, as only in 8 out of 2011 cases a minimum secondary was not observed. The bias introduced by *b*) is difficult to be estimated but believed to be also quite small. In the central region of the emulsion both *a*) and *b*) may slightly favour small values of θ, due to the presence of the ending μ track.

In Fig. 1 is given the observed distribution of θ for a total number of 2003 events. The best fit to the points is

(*) On leave from Padua University.

(+) On leave from the Laboratoire de Physique de l'Ecole Polytechnique Paris.

(1) T. D. Lee and C. N. Yang: *Phys. Rev.*, **104**, 236 (1956).

(2) Our plates have been exposed together with those used by Friedman and Telegdi in a similar experiment. For details on the exposure and on the possible influence of the magnetic field, see ref. (3).

(3) J. I. Friedman and V. L. Telegdi: submitted to *Phys. Rev.* in January 1957.

given by the expression $1 - 0.095 \cos \theta$; the backward-forward excess is of $0.044 \pm \pm 0.022$.

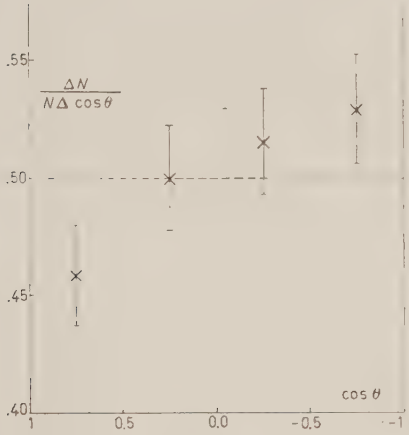

Fig. 1.

From this preliminary result the existence of an asymmetry in the π-μ-e decay cannot be concluded with certainty. However, it is worth mentioning that a backward excess in this decay has now already been observed in three experiments, including the present one: FRIEDMAN and TELEGDI [3] using emulsions exposed in the same conditions as ours have found a backward excess of 0.062 ± 0.027, and the Columbia University group [4] has also obtained a similar result using electronic techniques.

These combined evidences seem to indicate strongly that the Lee and Yang asymmetry effect in the π-μ-e decay really exists.

* * *

We are greatly indebted to Prof. V. L. TELEGDI for having kindly supplied us with the exposed and processed emulsions. Our thanks are also due to Mrs. BAUMBACH, Miss BETTE and Mrs. FAY who helped us in the measurements.

[3] R. L. GARWIN and L. M. LEDERMAN: privately communicated to us by Prof. TELEGDI.

Change of Isotopic Spin in the $K_{\pi 2}$ Decay.

M. Gell-Mann

Department of Physics, California Institute of Technology
Pasadena, California

(ricevuto il 19 Febbraio 1957)

In the slow decays of hyperons and K-mesons into other strongly interacting particles, isotopic spin I is defined before and after the decay but is not conserved. In fact I changes by half-integers. For all such decays that are known, the rule $\Delta I_z = \pm\frac{1}{2}$ (or $\Delta S = +1$, where S is strangeness) seems to obtain [1]. In particular, the apparent absence of the process $\Xi^- \to \pi^- + \mathrm{N}$ is attributed to this rule.

It has been suggested [1,2] that these weak decays have the further property that $|\underset{\sim}{\Delta I}| = \frac{1}{2}$ (at least in the absence of electromagnetic corrections), i.e., that the weak coupling Hamiltonian has the transformation properties of $I = \frac{1}{2}$. Let us call this rule A.

Another suggestion has been made [3], inspired by the notion that the basic coupling involved in these decays may be a four-fermion contact interaction [4] of proton and neutron with proton and Λ^0, analogous to the β-decay coupling (or else a weak coupling [5] of the charged pion to the proton and Λ^0, reminiscent of the process $\pi \to \mu + \nu$). According to these ideas, the rule should be a weaker one than above, viz: $|\underset{\sim}{\Delta I}| = \frac{1}{2}$ or $\frac{3}{2}$. We shall refer to this as rule B (*).

For hyperon decays, rule B has scarcely any consequences, while rule A imposes severe restrictions on the charge ratios. Recently some experimental evidence [6] on hyperons has been adduced against A. Let us proceed, however, to a discussion of the process $\mathrm{K} \to 2\pi$, where it may be possible to test rule B as well.

Since parity is not conserved in weak decays [7], we are not obliged to con-

(1) M. Gell-Mann and A. Pais: *Proceedings of the Glasgow Conference* (1954).

(2) G. Wentzel: *Phys. Rev.*, **101**, 1214 (1956); G. Takeda: *Phys. Rev.*, **101**, 1547 (1956); R. Gatto: *Nuovo Cimento*, **3**, 318 (1956).

(3) M. Gell-Mann: *Proceedings of the Rochester Conference* (1956).

(4) N. Dallaporta: *Nuovo Cimento*, **1**, 962 (1955).

(5) K. Iwata, S. Ogawa, H. Okonogi, B. Sakita and S. Oneda: *Progr. Theor. Phys.*, **13**, 19 (1955).

(*) A discussion of rules A and B is given by S. Oneda: *Nuclear Physics* (in press).

(6) L. W. Alvarez, H. Bradner, P. Falk, J. D. Gow, A. H. Rosenfeld, F. Solmitz and R. D. Tripp: to be published.

(7) T. D. Lee and C. N. Yang: *Phys. Rev.*, **104**, 254 (1956); R. L. Garwin, L. M. Lederman and M. Weinrich: to be published; C. S. Wu, E. Ambler, R. W. Hayward, D. D. Hoppes and R. P. Hudson: to be published.

sider the K^+ meson, say, as more than one particle. We shall assume, therefore, that there are just four states of the K-particle- K^+, K^0, $\overline{K}^0$ and K^-; or, alternatively ([8]), K^+, K_1^0, K_2^0, and K^-. The non-conservation of parity and charge conjugation does not affect ([9]) the K_1^0-K_2^0 picture unless time reversal symmetry is violated. Even in that case ([10]), the changes required are not very violent, and we shall assume that the situation is substantially as described in reference ([8]).

The lifetime of the K^+ meson is observed ([11]) to be about $1.2 \cdot 10^{-8}$ s and the decay gives $\pi^+ + \pi^0$ roughly one-third of the time ([11]). We may thus take about $3 \cdot 10^7$/s for the probability Γ_+ per unit time of $K^+ \to \pi^+ + \pi^0$. The lifetime of the K_1^0 meson ([11]) is about $1.5 \cdot 10^{-10}$ s. In the absence of information to the contrary, we assume that its decay yields two pions nearly all the time. Then the probability Γ_0 per unit time of $K_1^0 \to 2\pi$ is about $6 \cdot 10^9$/s, and $\Gamma_+/\Gamma_0 \sim 1/200$. We will denote by f the fraction of K_1^0 that decay into two neutral pions.

If the spin of the K meson is odd, then f is zero. For the ratio Γ_+/Γ_0, rule A predicts in this case ([2]) the value 1 and is obviously excluded by the experiments. Rule B allows any value of the ratio, but gives no explanation of its smallness.

If the spin of the K meson is even, the situation is very different. Rule A gives ([2]) $\Gamma_+/\Gamma_0 = 0$, and the electromagnetic corrections must change this to a small finite value. It has been objected ([3]), however, that these corrections are of the order e^4 and may be too small ([12]) to give $\Gamma_+/\Gamma_0 \approx 1/200$. If, in spite of this difficulty, rule A can be made to work, it predicts that the decay $K \to 2\pi$ takes place almost entirely to an $I = 0$ state of the two pions, and therefore that f must be very close to $\frac{1}{3}$.

Rule B allows any value $\leqslant \frac{3}{4}$ for the ratio Γ_+/Γ_0 when the spin of the K-meson is even. However, if we use the experiments to impose the condition $\Gamma_+/\Gamma_0 \approx \approx 1/200$, then rule B also predicts that the pions are mostly in the $I = 0$ state and requires f to lie ([13]) between .26 and .41.

A third proposal along different lines has been made by OKUBO and MARSHAK ([14]), who suggest that the small ratio Γ_+/Γ_0 is due to a strong attractive interaction between two pions with $I = 0$ and $J = 0$, which enhances greatly the amplitude for decay into this state. In their model, too, it follows that f must be close to $\frac{1}{3}$.

If it should turn out that the spin of the K-meson is even, but that the fraction f of decays into neutral pions is much less than $\frac{1}{3}$, all of these theories would have to be discarded (*). The small value of Γ_+/Γ_0 could then be accounted for only with appreciable contributions from $|\underset{\sim}{\Delta I}| = \frac{5}{2}$. The idea of a four-

([8]) M. GELL-MANN and A. PAIS: *Phys. Rev.*, **97**, 1387 (1955).

([9]) One merely replaces the charge conjugation operator C of reference ([8]) by CP, where P is the parity operator. In a time-reversible theory, CP is conserved.

([10]) T. D. LEE, R. OEHME and C. N. YANG: to be published.

([11]) *Proceedings of the Rochester Conference* (1956). Session V.

([12]) In fact the process $K^+ \to \pi^+ + \pi^0 + \gamma$ is only of order e^2 in this model and might compete favorably with $K^+ \to \pi^+ + \pi^0$.

([13]) The formula is

$$f \cong \frac{1}{3}\left(1 \pm \sqrt{\frac{32}{3}\,\frac{\Gamma_+}{\Gamma_0}}\cos\varphi\right),$$

for small Γ_+/Γ_0. If time-reversal symmetry applies, then $\varphi = \delta_2 - \delta_0$; where δ_I is the appropriate π-π phase shift in the state with isotopic spin I.

([14]) S. OKUBO and R. MARSHAK: *Phys. Rev.*, **100**, 1809 (1955).

(*) Preliminary experimental results of J. STEINBERGER *et. al.* seem to indicate that f is much less than $\frac{1}{3}$ but not zero. (Private communication from Dr. A. H. ROSENFELD).

fermion interaction could be retained only if the Σ particle is involved.

If the K-meson is spinless, the $K_{\pi 3}$ decay provides another test [2,3] of rules A and B. To the extent that the final state wave function is reasonably smooth (as the experimental spectrum of $K_{\pi 3}$ decay indicates), it is totally symmetric in the three pions, and the final isotopic spin is 1 or 3. According to either A or B the state $I=3$ is inaccessible and the isotopic spin is 1. The predicted branching ratio

$$K^- \to \pi^+ + 2\pi^0 / K^- \to 2\pi^- + \pi^+$$

is then $\frac{1}{4}$, which is not in disagreement with observations [11].

On the Conservation of Nucleons.

B. Ferretti (*)
CERN - Genève

(ricevuto il 21 Febbraio 1957)

During a first research into this question it was found that it was not possible to measure the nucleonic four-current independently from the equation of motion by means of a field only, unless the source of the field was not the four-current itself [1]. This conclusion had some bearing on the problem of the conservation of «nucleons». I have now found that this difficulty might be overcome if, instead of using one field only, one uses two different fields. The idea is roughly the following.

If the «nucleons» do generate two fields Φ and φ, which might even interact with other particles, say X and Y, and if we indicate with $S_\Phi(N)$ the nucleon source of the field Φ, and with $S_\varphi(N)$ the nucleon source of the field φ, and in a like manner with $S_\Phi(X)$, $S_\varphi(Y)$ the sources related to the particles X and Y, provided that on two points $\boldsymbol{x}$, $\boldsymbol{x}'$ such that $\boldsymbol{x}-\boldsymbol{x}'$ is a spacelike or zero vector $[S_\Phi'(X)\, S_\varphi(Y)]_- = 0$, the commutator $[S_\Phi, S_\varphi]_-$ will depend only on the nucleons ($S_\Phi = S_\Phi'(N) + S_\Phi'(X)$.) Now, it is very easy to form with such a commutator expressions which are identical to the nucleonic four-current components. For instance, if we assume that Φ is a scalar and that φ is a «neutrino field», coupled, by means of the anti-symmetrical tensor coupling to the nucleonic field, one can immediately construct, by means of an integration on a spacelike surface, the three first components of the nucleonic four-current, and then an infinitesimal Lorentz transformation will give the fourth component.

Of course, other examples of this kind might be found and, therefore, it seems possible to express the nucleonic four-current by means of the fields created by the nucleons, even if these fields interact with other particles. The bearing of these remarks in respect to the nucleon conservation law is under investigation.

(*) On leave of absence from Istituto di Fisica dell'Università, Bologna.

(1) B. Ferretti: *Nuovo Cimento*, **4**, 951 (1956).

LIBRI RICEVUTI E RECENSIONI

A. S. THOMPSON and O. E. RODGERS – *Thermal Power from Nuclear Reactors*, pp. 229, John Wiley Sons., Inc., New York, 1956.

I problemi di progetto e di conduzione di una centrale utilizzante un reattore nucleare come sorgente di energia sono necessariamente diversi da quelli che si presentano in un impianto convenzionale, ma la loro distribuzione logica è uguale nei due casi, talchè non è difficile confrontarli ed avvicinarli uno ad uno e parlarne con lo stesso linguaggio. Gli Autori si sono proposti di porre in risalto la possibilità di trattare l'argomento reattori nucleari dal punto di vista dell'ingegnere meccanico.

Dopo una breve introduzione, che presenta con estrema semplicità alcuni termini e concetti propri della fisica nucleare, un primo capitolo è dedicato a considerazioni e notizie sulla fisica dei nuclei atomici ed in particolare dei neutroni, in vista dello studio dei reattori nucleari. Vi si tratta cioè specialmente di scattering e di cattura di neutroni da parte dei nuclei e di fissione: il tutto senza molto rigore fisico, ma con una discreta efficacia descrittiva.

Un'ampia parte del libro è poi dedicata al progetto ed alla teoria del funzionamento dei reattori, in condizioni stazionarie o transitorie, cioè al problema della determinazione della massa critica del reattore e della distribuzione in esso dei neutroni ed a quello del controllo. La teoria sviluppata dagli autori è quella ormai classica detta della diffusione, basata su un modello semplificato del moto dei neutroni all'interno del reattore, rinunciando volutamente all'esposizione della teoria più complessa cosiddetta del trasporto che, tenendo conto della asimmetria dello scattering dei neutroni contro i nuclei, dà risultati meglio approssimati. Fra gli esempi di interpretazione della teoria della diffusione dei neutroni, interessante e nuova è una analisi dimensionale delle equazioni relative ad un reattore termico ideale: la creazione di gruppi adimensionali rende particolarmente chiare alcune correlazioni fra i parametri fisici e geometrici relativi al reattore. Lo studio del comportamento del reattore in regime transitorio è eseguito con chiarezza, e, per quanto si riferisca a casi ideali, malgrado molte limitazioni semplificative, lascia intravvedere i possibili modi di considerare il problema pratico del controllo.

Una esposizione del problema dello schermaggio del reattore, comprendente anche indicazioni per il calcolo dello schermo biologico ed una breve descrizione dei materiali usati nei reattori nucleari completano la parte del libro dedicata alla fisica del reattore.

Seguono alcuni capitoli, in cui sono trattati i problemi della estrazione del calore dal reattore, delle sollecitazioni termiche accompagnate alla generazione

di potenza e dei cicli termici realizzabili in un impianto nucleare. La esposizione alquanto sommaria di questi problemi, con richiami a concetti troppo noti a chi si occupi di questioni termiche, non sembra essenziale e vuol essere probabilmente soltanto indicativa delle difficoltà di tipo meccanico e termico che intervengono ove si vogliano considerare impianti nucleari reali.

In conclusione il libro non è rivolto a lettori specializzati, nè può essere usato come base per lo studio della ingegneria nucleare, ma è tuttavia una opera utile, in quanto mostra da un lato come l'interessamento dell'ingegnere ai problemi fisici dei reattori nucleari può portare buoni frutti e dall'altro come sia essenziale e insostituibile l'opera dell'ingegnere meccanico nel progetto di impianti nucleari.

Ogni capitolo è corredato di una buona ed autorevole bibliografia, ed il testo è dotato di un indice analitico.

S. FINZI

Proceedings of the International Conference on the Peaceful Uses of Atomic Enery. Geneva, 8-20 August 1955, vol. 7. *Nuclear Chemistry and Effects of Irradiation.* United Nations, New York, 1956.

La conferenza internazionale sull'uso pacifico dell'energia atomica tenutasi in Ginevra nell'agosto del 1955 ha costituito un punto di incontro per gli scienziati di tutto il mondo che hanno avuto modo di scambiarsi notizie sullo stato degli studi e delle ricerche. Sono stati comunicati a Ginevra dei dati che non erano prima ufficialmente noti o sui quali non era facile ottenere una esauriente documentazione. Non si deve credere, d'altra parte, che le relazioni presentate a Ginevra rappresentino una completa ed esauriente messa a punto di tutti i numerosi argomenti trattati: è evidente intanto che una parte delle conoscenze sino ad oggi acquisite si trova tuttora sotto il vincolo del segreto; le comunicazioni sono poi molto spesso dei riassunti generali, i quali non rispecchiano che indirettamente i contributi originali, e non sempre sono accompagnati da una adeguata documentazione. Ne consegue che, quando si tenti di sintetizzare e riassumere l'insieme di tutti i dati forniti su un determinato argomento vi si trovi qualche imperfezione e lacuna.

Nonostante tutto questo, i 16 volumi degli atti di questo grandioso convegno, pubblicati in quattro lingue a cura delle Nazioni Unite, costituiscono un poderoso complesso di informazioni nei campi più svariati.

Il settimo volume contiene le relazioni presentate sugli argomenti della Chimica nucleare e degli effetti delle radiazioni sui solidi e sui liquidi.

Il volume è diviso in dieci parti corrispondenti ad altrettante sessioni della conferenza, ciascuna delle quali è seguita dai resoconti delle sedute, comprendenti le discussioni.

Nella prima parte quattro lavori sono dedicati ai processi di fissione, osservati particolarmente dal punto di vista chimico; vi si trovano liste dei prodotti di fissione con la loro quantità percentuale misurata con i vari metodi, note sulla fissione spontanea ecc.

L'argomento della seconda parte è di grande interesse pratico in quanto riguarda l'attrezzatura dei laboratori in cui si lavora con materiali altamente radioattivi: vengono descritti vari tipi di laboratorio come quello di chimica analitica, quello metallografico ecc. Presenta particolare interesse la possibilità di confronto tra i paesi maggiormente sviluppati in questo settore.

La chimica delle sostanze radioattive viene poi trattata in cinque delle seguenti sezioni: procedimenti di lavorazione, ed in particolare di estrazione, applicati ai prodotti della pila, chimica dei prodotti

di fissione, chimica degli elementi transuranici e pesanti e metodi di separazione.

Le ultime tre sezioni sono dedicate agli effetti della radiazione sulla materia: sui liquidi si tratta ancora prevalentemente di effetti chimici come le reazioni ridotte nelle sostanze organiche, la radiolisi dell'acqua ecc.; quanto viene discusso nelle due parti dedicate ai solidi ha invece con la chimica solo qualche punto di contatto, ma presenta il massimo interesse per gli studiosi di fisica dei solidi e per gli ingegneri, che si preoccupano delle alterazioni delle proprietà dei materiali strutturali esposti all'intenso flusso dei neutroni ed altre radiazioni presenti nei reattori nucleari.

In effetto lo studio delle modificazioni del materiale strutturale dei reattori è stato forse, dal punto di vista storico, il primo movente delle ricerche in questo campo. Queste ricerche si sono poi sviluppate secondo due direttive principali: quella prevalentemente empirica e applicativa che si preoccupava principalmente dei nuovi sviluppi della tecnica dei materiali e quella più propriamente scientifica che scopriva nello studio degli effetti delle radiazioni, un potente mezzo di indagine sui difetti dei solidi cristallini e sulle loro relazioni con le proprietà fisiche dei solidi stessi. Questi studi, che sono tuttora in pieno sviluppo e ben lungi da una definitiva sistemazione, hanno permesso un notevole progresso alla fisica dei solidi.

La suddivisione della materia nelle due sessioni della conferenza di Ginevra dedicata a questi argomenti rispecchia appunto questi due orientamenti. La sessione che tratta degli effetti sui materiali del reattore è formata principalmente da articoli riassuntivi ad opera di Autori americani, inglesi e russi. Il quadro un po' schematico che ne risulta non può dirsi completo, specialmente per ciò che riguarda lo studio sui metalli nei quali i fenomeni sono di altissimo interesse ma, in condizioni di pratico impiego, le modificazioni delle proprietà macroscopiche difficilmente assumono valori preoccupanti dal punto di vista della ingegneria. Sembra invece di un certo rilievo l'interesse che viene dedicato alle modificazioni subite dai materiali fissionabili e dalla grafite, le quali assumono in certi casi aspetti assai vistosi ed assolutamente non trascurabili.

La parte del volume di maggiore interesse per quanto riguarda la fisica dei solidi è l'ultima: essa contiene due importanti articoli sugli aspetti teorici dei problemi del « Radiation Damage » ad opera di Seitz l'uno e di Dienes l'altro. In questi articoli sono esposti alcuni dei più recenti contributi alla teoria.

Gli altri lavori forniscono un riassunto di risultati sperimentali e delle interpretazioni degli effetti prodotti dalle radiazioni specialmente su cristalli ionici di materiali non metallici; il problema degli effetti sulla grafite viene ripreso in questa sezione, in senso interpretativo, ad opera di G. R. Henning e J. E. Hove.

F. A. Levi

Direttore responsabile: G. POLVANI Tipografia Compositori - Bologna

Questo fascicolo è stato licenziato dai torchi il 25-II-1957